INVESTIGATING MOLECULAR STRUCTURES: RAPIDLY EXAMINING MOLECULAR FINGERPRINTS THROUGH FAST PASSAGE BROADBAND FOURIER TRANSFORM MICROWAVE SPECTROSCOPY

Garry Smith "Smitty" Grubbs II, B.S.

Dissertation Prepared for the Degree of

DOCTOR OF PHILOSOPHY

UNIVERSITY OF NORTH TEXAS

May 2011

APPROVED:

Stephen Cooke, Major Professor

Jeff Kelber, Committee Member

Paul Marshall, Committee Member

Mohammad Omary, Committee Member

Guido Verbeck, Committee Member

William E. Acree, Jr., Chair of the Chemistry Department

James Meernik, Acting Dean of the Toulouse Graduate School

ProQuest LLC.
789 East Eisenhower Parkway
P.O. Box 1346
Ann Arbor, MI 48106 - 1346

Grubbs II, Garry Smith "Smitty." Investigating Molecular Structures: Rapidly Examining Molecular Fingerprints Through Fast Passage Broadband Fourier Transform Microwave Spectroscopy. Doctor of Philosophy (Chemistry), May 2011, 235 pp., 48 tables, 24 illustrations, bibliography, 155 titles.

Microwave spectroscopy is a gas phase technique typically geared toward measuring the rotational transitions of molecules. The information contained in this type of spectroscopy pertains to a molecules structure, both geometric and electronic, which give insight into a molecule's chemistry. Typically this type of spectroscopy is high resolution, but narrowband $\leq$1 MHz in frequency. This is achieved by tuning a cavity, exciting a molecule with electromagnetic radiation in the microwave region, turning the electromagnetic radiation off, and measuring a signal from the molecular relaxation in the form of a free induction decay (FID). The FID is then Fourier transformed to give a frequency of the transition. "Fast passage" is defined as a sweeping of frequencies through a transition at a time much shorter ($\leq$10 μs) than the molecular relaxation ($\approx$100 μs). Recent advancements in technology have allowed for the creation of these fast frequency sweeps, known as "chirps", which allow for broadband capabilities. This work presents the design, construction, and implementation of one such novel, high-resolution microwave spectrometer with broadband capabilities. The manuscript also provides the theory, technique, and motivations behind building of such an instrument.

In this manuscript it is demonstrated that, although a gas phase technique, solids, liquids, and transient species may be studied with the spectrometer with high sensitivity, making it a viable option for many molecules wanting to be rotationally studied. The spectrometer has a relative correct intensity feature that, when coupled with theory, may ease the difficulty in transition assignment and facilitate dynamic chemical studies of the experiment.

Molecules studied on this spectrometer have, in turn, been analyzed and assigned using common rotational spectroscopic analysis. Detailed theory on the analysis of these molecules has been provided. Structural parameters such as rotational constants and centrifugal distortion constants have been determined and reported for most molecules in the document.

Where possible, comparisons have been made amongst groups of similar molecules to try and get insight into the nature of the bonds those molecules are forming. This has been achieved the the comparisons of nuclear electric quadrupole and nuclear magnetic coupling constants, and the results therein have been determined and reported.

ACKNOWLEDGMENTS

I would like to thank, first and foremost, Professor Stephen Cooke for all of his guidance, mentorship, patience and understanding on everything mentioned in this body of work. His teaching and ideas have greatly fueled any success I may have or had as a student. Secondly, I would like to thank the Toulouse Graduate School and Department of Chemistry at the University of North Texas, the Robert A. Welch Foundation, the National Science Foundation, and the United States Department of Energy for financial support both personally and on the projects described in this work. I also would like to thank Dr. Brooks Pate and his group from the University of Virginia for all of their insightful comments and help pertaining to the construction and development of the chirped pulse spectrometer. I want to acknowledge Professors Sean Peebles and Bill Bailey for their collaborations, insightful comments, and other contributions to this work as well as work not mentioned in this document. I would also like to acknowledge all my coworkers in Dr. Cooke's research group that contributed and continue to contribute their help and insight into the ongoing development of this project. Finally, I would like to acknowledge and thank my wife, Laura, and my family for their love, encouragement, support, and kindness throughout my graduate career as well as my life. They truly inspire me in all aspects of life.

TABLE OF CONTENTS

LIST OF TABLES

LIST OF ILLUSTRATIONS

CHAPTER 1

INTRODUCTION

1.1. General Microwave Spectroscopy and Molecules Studied

A molecule's chemistry is closely related to its geometric and electronic structure. Connectivity, bond lengths, conformation, and electron distribution are all relevant when discussing the chemistry and reactivity of the molecule. Microwave spectroscopy has the capability to determine this information with great precision and accuracy. In fact, microwave spectroscopy is the only available technique to provide all of this insight in a single experiment.

Generally speaking, microwave spectroscopy is a gas phase technique used to observe the transition energies of rotating molecules. These rotations may be induced by the interaction of a sample's molecular dipole moment with a microwave pulse. (The resulting signal produced by the molecule is amplified and detected.) The observed spectra produced by the experiment can then be analyzed to give rotational and other molecular electronic constants.[1, 2]

As the technique has advanced, microwave spectroscopy has seen certain advancements in molecular sampling, sensitivity, and accuracy. Advancements key to this work involve (i) the invention of a pulsed sample narrowband cavity technique[3], (ii) the implementation of a laser ablation source[4], and (iii) the invention of a broadband microwave spectrometer.[5, 6, 7] At the heart of all of these techniques, and this work, is the idea of fast passage spectroscopy.[8] Fast passage is defined as a sweeping of frequencies through a transition in a time shorter than the molecular relaxation. Fast passage technology allows for the study of molecules in the time domain which increases resolution, sensitivity, and bandwidth capabilities. How this is achieved is covered later in this work.

The study of heavier molecules, both inorganic and organic in nature, have recently been a focus of rotational spectroscopy. Smaller molecules are usually of interest because the bonding and structure in these molecules are important to understanding and possibly modeling larger systems involving the same structural motifs. Also, understanding the chemistry as one passes from a light molecule to a heavier molecule by atomic substitution is of interest. This is achieved in the following chapters by successively or entirely perfluorinating a molecule (replacing hydrogens with fluorines) and studying the geometric and electronic effects.

Heavier molecules are not usually gases and are, therefore, more difficult to study due to the inherent problems of getting the sample into the gas phase. This, coupled with their small rotational constants can provide population difficulties in the microwave region. Because of these problems, instrumental sampling techniques must be considered to monitor these molecules in the gas phase. In this work, we describe the construction and implementation of a novel broadband microwave spectrometer utilizing a gas, liquid, and laser ablation-equipped sampling techniques capable of collecting spectra on many heavy organic and inorganic molecules.

1.2. Introduction to Theory and Background

The field of experimental rotational spectroscopy may be seperated into two unique areas, (i) the rotational quantum theory and (ii) instrumental theory. We have done this.

The first section, Rotational Quantum Theory and Background, begins by introducing the transition matrix, rigid rotor approximation and the rotational Hamiltonian for a simple diatomic. This model is then expanded for more complicated systems such as symmetric and asymmetric rotors (tops). As the section continues, the quantum chemical principles behind allowed transitions and nuclear quadrupole coupling are briefly covered.

The second section, Instrumental Theory and Background, begins by introducing the idea and math of a polarizing microwave pulse in a brief overview of the Bloch equations.[9] Then the idea of high resolution is covered along with the mathematics involved in signal detection. More practical aspects and application of the spectrometer are discussed in

chapters 2 and 3.

1.3. Rotational Quantum Theory and Background

In any given molecule, there are a specific number of ways that it can move. These movements are translational, rotational, and vibrational. For these motions, the molecule has $3n$ degrees of freedom for the motion where n is the number of atoms.[10] Since a molecule has three dimensions, it can rotate about three different molecular axes, giving any nonlinear, polyatomic molecule three rotational degrees of freedom. Linear molecules have two axes equivalent giving the molecule 2 rotational degrees of freedom.

The field of rotational spectroscopy divides molecules into three unique, but similar types of rotors: linear, symmetric, and asymmetric tops.[1, 2] There is a fourth, spherical top but microwave spectra are not measureable for this symmetry because it has no dipole moment (to be covered later). These rotors all depend on the distribution of masses throughout the molecule. A symmetric rotor is defined as any molecule having a threefold axis of symmetry, or higher. An asymmetric top is the most general type of top; i.e. non-linear with a less than 3-fold symmetry axis.[1]

Molecular energy levels may be obtained by solutions of the Schrödinger equation:

$$\mathbf{H}\Psi = E\Psi \tag{1}$$

where Ψ is a wavefunction, E is the quantized energies of the system, and $\mathbf{H}$ is a Hamiltonian operator. Operation of the Hamiltonian operator on a wavefunction returns a set of quantized energies along with the original function. The quantized energies are also known as the eigenvalues of the equation, making the Schrödinger equation an eigenvector problem. Spectroscopy enters to assist in solving the Schrödinger equation by measuring specific energetic components of these quantized systems, in other words, solving for E. A Hamiltonian may then be built for a system and become a predictive tool for future unknown transitions.

Any given Hamiltonian matrix for a molecule can be generally defined as:

$$\mathbf{H} = \mathbf{H_{elec}} + \mathbf{H_{vib}} + \mathbf{H_{rot}} \tag{2}$$

where $\mathbf{H_{elec}}$, $\mathbf{H_{vib}}$, and $\mathbf{H_{rot}}$ are the electronic, vibrational, and rotational Hamiltonians, respectively. Later on we will break up the rotational Hamiltonian into smaller contributors, but we will leave the rest alone for now.

At this point, it is useful to know that a Hamiltonian is broken down into two components, potential and kinetic energy operators. The Hamiltonian is simply these two operators summed together and prepared to operate on the wavefunction. It is from the quantum mechanical operators pertaining to these two values that the energies pertaining to a particular system may be obtained.

1.3.1. The Transition Matrix

Every spectroscopic transition, be it electric, vibrational, or rotational, is governed by a transition matrix containing a upper and lower state of a two-state system. Each one of these systems contains an allowed or forbidden transition based upon the states involved and some operator. For a rotational system, the operator for dipole allowed transitions is a function of the dipole moment. In a waveguide technique, the operator is the dipole moment and, in a resonance technique, the one covered extensively in this work, goes as the dipole moment squared. If the overall value of the transition matrix is an even function, then the transition is allowed, if odd, then it is forbidden. A prototypical rotational transition matrix in Dirac notation for a diatomic dipole allowed transition is:

$$\langle \Psi_{J''} \mid \mu \mid \Psi_{J'} \rangle \tag{3}$$

where $\Psi_{J''}$ is the wavefunction of the lower rotational state and $\Psi_{J'}$ is the wavefunction of the upper rotational state and μ is the dipole moment. As stated, a transition is allowed if this matrix has a nonzero value. There exists certain beginning and ending states where the overall transition matrix will produce a nonzero element. In transition types where this is

the case, then a selection rule for the transition type is formed. Selection rules are discussed in the following subsections starting with the simplest case, The rigid rotor for diatomic and linear polyatomic molecules.

1.3.2. The Rigid Rotor for Diatomic and Linear Polyatomic Molecules

Quantization emerges when bonded (or complexed) atoms rotate in free space. If the bond is assumed rigid, the bonded, rotating system has a distinct mass distribution bringing about a definite moment of inertia (see Figure 1.1 below).

FIGURE 1.1. Graphic of atoms bound and not bound going through a rotation. The mass on the ends of the bound system create a larger moment of inertia. Axis of rotation is through the center of the rotation coming out of the page.

Mathematically the moment of inertia for a two body system is:

$$I = \mu r^2 \tag{4}$$

where μ is the reduced mass, $\frac{m_1 m_2}{m_1+m_2}$, and r is the bond length. In general, however, the moment of inertia is a tensor, $\mathbf{I}$, represented by[2]:

$$\begin{vmatrix} I_{xx} & I_{xy} & I_{xz} \\ I_{yx} & I_{yy} & I_{yz} \\ I_{zx} & I_{zy} & I_{zz} \end{vmatrix} \tag{5}$$

where each element above is defined by:

$$
\begin{aligned}
I_{xx} &= \sum m(y^2+z^2) \\
I_{yy} &= \sum m(z^2+x^2) \\
I_{zz} &= \sum m(x^2+y^2) \\
I_{xy} = I_{yx} &= -\sum mxy \\
I_{zx} = I_{xz} &= -\sum mxz \\
I_{yz} = I_{zy} &= -\sum myz
\end{aligned} \tag{6}
$$

This, however, is a space-fixed orientation matrix. Rotational spectroscopy, however, is performed in the molecule-fixed orientation with axes labeled a, b, and c. This is just a rotation of the space-fixed orientation giving tensor components I_a, I_b, and I_c which are put in order such that $I_a \leq I_b \leq I_c$. These values may be obtained by diagonalizing the above inertia tensor.

Angular momentum, $\mathbf{P}$, can be described by[2]:

$$
\begin{aligned}
P_a &= I_a\omega_a \\
P_b &= I_b\omega_b \\
P_c &= I_c\omega_c
\end{aligned} \tag{7}
$$

where I is the moment of inertia about each axis and ω is the angular velocity of rotation. Classically, the kinetic energy of the system is:

$$E_k = \frac{1}{2}mv^2 \tag{8}$$

giving[2]:

$$E_r = \frac{1}{2}\boldsymbol{\omega}\cdot\mathbf{I}\cdot\boldsymbol{\omega}$$

$$E_r = \frac{1}{2}\left(\frac{P_a^2}{I_a}+\frac{P_b^2}{I_b}+\frac{P_c^2}{I_c}\right) \tag{9}$$

In a rigid rotor approach the general rotational Hamiltonian comes from Equation 9 above. In a linear polyatomic or diatomic molecule I_b=I_c=I and I_a≈0 and P^2=P_a^2+P_b^2+P_c^2. Since P^2, therefore, would be independent of any coordinate system, it is useful/easier to then describe the system in terms of the molecular-fixed axis. The Hamiltonian, using these assumptions and plugging into Equation 9 becomes[2]:

$$\mathbf{H_{rot}} = \frac{P^2}{2I} \tag{10}$$

The allowed energetic states of rotation that solve the Schrödinger equation then, are[1]:

$$E_r = \frac{h^2}{8\pi^2 I}J(J+1) \tag{11}$$

and if B=$\frac{h}{8\pi^2 I}$ (or more appropriately B=$\frac{h}{8\pi^2 I_b}$), then Equation 11 becomes[2]:

$$E_r = hBJ(J+1) \tag{12}$$

According to references [1] and [2], transitions will occur according to the equation:

$$\nu = \frac{E_{J+1}-E_J}{h} = B(J_2(J_2+1)-J_1(J_1+1)) \tag{13}$$

Equation 13 should give frequencies that approximately equal the frequencies given by the "old" quantum mechanical equation, ν=$\frac{Jh}{4\pi^2 I}$[1]. This is true when J_2=J_1+1. Plugging J_1+1 into Equation 13 for J_2 above gives[1]:

$$\nu = 2B(J+1) \tag{14}$$

Because the lower state would be inserted into the equation above, then rotational transitions are seperated by $2B$ with $J = 0, 1, 2...$ Therefore the selection rule of the linear rigid rotor is $\Delta J = \pm 1$.

1.3.3. The Rigid Rotor for Symmetric Tops

If the molecule is not linear but has a threefold axis of symmetry or higher, it is known as a symmetric top rotor. In this type of molecule, there exists two types of simultaneous rotations. One along the angular momentum vector, $\mathbf{P}$, and one along the symmetry axis of the molecule (P_z). This is because one principle axis of inertia must lie along the symmetry axis. There are two scenarios in which this occurs. When $I_a<I_b=I_c$ it is called a prolate molecule (cigar shaped) and when $I_a=I_b<I_c$ it is called an oblate molecule (disc shaped). Although there are two different outcomes, the math is generally the same. Here we examine the prolate case and extend the answer to the oblate case afterward.

We start with Equation 9 since this is the key equation for rigid rotor systems. As we have already stated in the prolate symmetric top, $I_a<I_b=I_c$, so this will be plugged in giving[11]:

$$E_r = \frac{1}{2}\left(\frac{P_a^2}{I_a} + \frac{P_b^2 + P_c^2}{I_b}\right) \tag{15}$$

and taking into account $P^2=P_a^2+P_b^2+P_c^2$ gives the new equation[11]:

$$E_r = \frac{1}{2}\left(\frac{P_a^2}{I_a} + \frac{P^2 - P_a^2}{I_b}\right) \tag{16}$$

This last equation, when algebraically manipulated, can then give the Hamiltonian of the symmetric top[1, 2, 11]:

$$\mathbf{H_{rot}} = \frac{P^2}{2I_b} + \frac{1}{2}\left(\frac{1}{I_a} - \frac{1}{I_b}\right)P_a^2 \tag{17}$$

Going back the linear diatomic and polyatomic Hamiltonian for a rigid rotor found in Equation 10, $\mathbf{H_{rot}} = \frac{P^2}{2I_b}$, this rotation holds since in the symmetric top there is still that

rotation taking place. The difference is in each Hamiltonian's rotation about the axis of symmetry. For a prolate molecule, that is happening about P_a. Remembering that the P^2 and P_a^2 are vector quantities, it follows that these vectors should have an additive effect on one another in the rotational Hamiltonian for the symmetric top.

To find the energy values of this rotation, the eigenvalues for the operator P_a are $\hbar K$ where $\hbar = \frac{h}{2\pi}$ and K is a new quantum number.[2] It follows then, that if the operator P_a is squared, the eigenvalues of such an operator would be squared as well giving $\hbar^2 K^2$. Utilizing this and Equation 12, then carrying out an operation of Equation 17 should give the energy states[2]:

$$E_{JK} = hBJ(J+1) + \frac{1}{2}\frac{h^2}{4\pi^2}\left(\frac{1}{I_a} - \frac{1}{I_b}\right)K^2 \tag{18}$$

$$E_{JK} = hBJ(J+1) + \frac{h^2}{8\pi^2}\left(\frac{1}{I_a} - \frac{1}{I_b}\right)K^2 \tag{19}$$

It is now necessary to define the other two rotational constants, A and C. A is $\frac{h}{8\pi^2 I_a}$ and C is $\frac{h}{8\pi^2 I_c}$. From this we obtain the final energetic state[2]:

$$E_{JK} = h(BJ(J+1) + (A-B)K^2) \tag{20}$$

for a prolate symmetric top. If this were an oblate case, then the only difference would be the constant A replaced with C giving[1]:

$$E_{JK} = h(BJ(J+1) + (C-B)K^2) \tag{21}$$

From this, we can start to determine selection rules for this type of rotor. To do this, we need to understand the energy states of K. Since P_a^2 is an element of P^2, it follows that K should go as J. In fact, the possible states of K are[1]:

$$K = +J, J-1, J-2, ..., -J \tag{22}$$

Because of this J dependency, there are $2J+1$ levels of K possible. Since, however, K appears as a square term in Equations 20 and 21, all positive K levels doubly degenerate with negative K levels. This gives a total of $J+1$ K levels [1, 2].

In a symmetric top molecule, the dipole will lie along the axis of symmetry [1, 2]. The transition matrix elements of a dipole moment aligned along the symmetry axis will only be nonzero when $J \rightarrow J$, $J \rightarrow J \pm 1$ and $K \rightarrow K$ according to reference [2]. This gives the selection rules:

$$\Delta J = 0, \pm 1; \ \Delta K = 0 \tag{23}$$

Using Equations 20 and 21 and solving for a transition with the equation $\nu = \frac{E_{J'K'} - E_{JK}}{h}$ now we can plug in ΔK=0. With this, the energy seperations for a true symmetric rigid rotor become those found for the linear rigid rotor, $2B(J+1)$.

1.3.4. The Rigid Rotor for Asymmetric Tops

Last of all, if the molecule has lower than a threefold axis of symmetry, it is referred to as asymmetric. The moments of inertia for a molecule in this case are related by[12]:

$$I_a \neq I_b \neq I_c \tag{24}$$

Under these conditions, the axes of the molecule are arranged such that $I_a < I_b < I_c$, thereby putting the most mass on the a axis of the molecule. However, as $I_b \rightarrow I_a$ or $I_b \rightarrow I_c$, a symmetric top molecular description is approached. Because the moments of inertia are directly related to the rotational constants, A, B, and C, a formalism for the degree of asymmetry can be obtained by the expression[2]:

$$\kappa = \frac{2B - A - C}{A - C} \tag{25}$$

known as Ray's asymmetry parameter. This is understood as a measure of asymmetry for a molecule. As $C \rightarrow B$, then $\kappa \rightarrow$ -1 and approaches the prolate symmetric top. As $A \rightarrow B$,

then $\kappa \to +1$ and approaches the oblate symmetric top model. These two scenarios explain the possible K levels of an asymmetric top. In the symmetric top, positive K levels were doubly degenerate with their negative counterparts due to a squared energy term, giving $J{+}1$ K states. However, in the asymmetric case, this degeneracy is removed and the $2J{+}1$ number of possibilities arises again. This is because the K level designated, be it K_{-1} or K_1, represent levels in the prolate or oblate limit. In reality however, the level lies somewhere in between but cannot be determined and K becomes a "bad" quantum number and is given the title pseudo-quantum number or "label" instead.

Because of Equation 24, there is no simplification of a rotational Hamiltonian. Therefore, the Hamiltonian for takes on the general form[2]:

$$\mathbf{H_{rot}} = AP_a^2 + BP_b^2 + CP_c^2 \tag{26}$$

where A, B, and C are the rotational constants defined above and P_a, P_b, and P_c are the angular momentum operators. If combined with Equation 25 and using $P^2 = P_a^2 + P_b^2 + P_c^2$, then it has been shown by Ray [13] that the Hamiltonian becomes[2]:

$$\begin{aligned} \mathbf{H_{rot}} &= \frac{1}{2}(A+C)P^2 + \frac{1}{2}(A-C)\mathbf{H}(\kappa) \\ \text{where } \mathbf{H}(\kappa) &= P_a^2 + \kappa P_b^2 - P_c^2 \end{aligned} \tag{27}$$

This gives rotational energy states of [2]:

$$E = \frac{1}{2}(A+C)J(J+1) + \frac{1}{2}(A-C)E_{J_{K_{-1}K_1}}(\kappa) \tag{28}$$

where $E_{J_{K_{-1}K_1}}(\kappa)$ is defined by an explicit equation for each state and is available in tables.[1, 2, 12]

The general selection rule for an asymmetric top is that $\Delta J{=}\ 0,\ \pm 1$. However, the selection rules for the K states for this type of rotor depend on the type of transition taking place. Since the dipole moment for an asymmetric top may lie along the a, b, or c axis, then

there are 3 types of transitions labelled a-type, b-type, and c-type. These selection rules are simply a symmetry operation and may be viewed as simply a change in parity (going from an even to odd or vice versa) amongst the correct states. In the $J_{K_{-1}K_1}$ notation, an a-type has a change in parity of only the K_1 label, a b-type has a change in parity in K_{-1} and K_1, and a c-type has a change in parity of the K_{-1} label only.

In a laboratory setting, the difficulty of an asymmetric top problem is approached through expression of the parameterized Hamiltonian as a matrix followed by a matrix diagonalization routine.[14] Once diagonalized, the diagonal components are the eigenvalues (i.e. the rotational energy levels). The parameters in the Hamiltonian matrix (for example, A, B, and C) are iteratively least squares fit to assigned, measured transitions until it reaches a minimum root mean squared value.

1.3.5. Centrifugal Distortion

Although to this point we have treated the molecular systems as rigid, they simply are not. As the molecule rotates, it has some freedom to move around depending on the strength of the bonds. When it is rotating, a centrifugal force acts to push the atoms away from each other.[11] This is similar to putting two masses on the end of a bungee chord and setting the system to rotate. While the system is rotating, the masses will pull away from each other depending on the strength of the chord itself. This is an elongation of the bond between the two masses which, in turn, increases the moment of inertia, I.

Increasing this moment of inertia will, in effect, lower the rotational constant. In fitting spectra, this force must be accounted for and is labelled with the constant, D or Greek symbol Δ. Different dependencies on J (and K) give the centrifugal distortion constant different subscripts of J (and K-or both). Typically, the centrifugal distortion constant is on the order of kHz and the resolution of the spectrometer is able to discern such a value.

Since this term is dependent on the rotational energy state, it goes as a function of the angular momentum, J, into the energy equation for a linear system as[11]:

$$F(J) = BJ(J+1) - D_J J^2 (J+1)^2 \tag{29}$$

and into the rotational Hamiltonian as[1, 15]:

$$\mathbf{H_{rot}} + \mathbf{H_{cd}} = B\mathbf{J}^2 - D_J\mathbf{J}^4 \tag{30}$$

where it is shown the dependency of the rotational constant B and the centrifugal distortion constant on the angular momentum vector, **J**.

In the symmetric case, centrifugal distortion also has a K level dependency. The Hamiltonian for such a system is similar to that of the linear case above, but now with extra K dependent terms (prolate case)[2]:

$$\mathbf{H_{rot}} + \mathbf{H_{cd}} = B\mathbf{J}^2 + (A-B)\mathbf{K}^2 - D_J\mathbf{J}^4 - D_{JK}\mathbf{J}^2\mathbf{K}^2 + D_K\mathbf{K}^4 \tag{31}$$

where D_J, D_{JK}, D_K are all first-order centrifugal distortion terms. There exists higher order distortion terms. This Hamiltonian will give the rotational energy states (again, for the prolate case)[2]:

$$E_{JK} = h(BJ(J+1) + (A-B)K^2 - D_J J^2(J+1)^2 - D_{JK}J(J+1)K^2 + D_K K^4) \tag{32}$$

which, in turn, give transition frequencies of the form[2]:

$$\nu = 2B(J+1) - 4D_J(J+1)^3 - 2D_{JK}(J+1)K^2 \tag{33}$$

Asymmetric tops pose an involved mathematical problem when trying to construct the correct Hamiltonian.[2] To ease the mathematical rigor of this construction, Watson was able to construct a Hamiltonian known as a Watson-A reduced Hamiltonian for highly asymmetric tops and a Watson-S reduced for slightly asymmetric tops.[16, 17] This Hamiltonian allows for easier determination of high order centrifugal distortion constants. At the time it was a powerful tool to be able to choose the correct reduced Hamiltonian and more easily construct the Hamiltonian. Now it is routine for a computer to handle this calculation with such speed

that the choice of reduced Hamiltonian is almost irrelevant. The parameters in this reduced Hamiltonian roughly relate to those stated earlier for the symmetric top by the following table[2]:

TABLE 1.1. Symmetrical Top to Watson-A Centrifugal Distortion Relationships.

Parameter
$D_J \approx \Delta_J$
$D_{JK} \approx \Delta_{JK}$
$d_J \approx \delta_J$

These distortion constants will be integrated and shown in the total Hamiltonian in the next section.

1.3.6. Kraitchman Substitution

Bond length/angle determination is a large part of structural determination in microwave spectroscopy. In a molecule where multiple isotopologues have been measured, a set of rotational constants exist for each isotope. It has been shown by Kraitchman[18] that in these instances (under an assumed Born-Oppenheimer approximation) it is possible to determine the coordinate position of the isotopically substituted atom. This method is known as the Kraitchman Substitution analysis.

The Kraitchman Substitution works off of the idea that a mass substitution does not change any parameter in the measured rotational constant except for the mass in the moment of inertia. Since the moment of inertia tensor is found by the coordinates of each atom, the coordinate locations can then be determined to the uncertainty of the experiment. Basically, two equations are now equal to one another. The Kraitchman Substitution analysis does utilize a square term so negative valued coordinates will not be rendered, but usually be properly understood through decent theoretical work.

Once the coordinates of one atom are known if the process is repeated with other atoms in the molecule successively attached to one another, then bond lengths and angles can be known to a high degree of uncertainty through the use of simple trigonometry.

1.3.7. Nuclear Electric Quadrupole Coupling

One coupling that gives rise to splittings in the molecular rotation spectra is due to nuclear electric quadrupole coupling. If one or more of the atoms in a closed shell molecule (no unpaired electrons) has a nuclear spin quantum value, I, of ≥ 1, then the nuclear spin vector, $\mathbf{I}$, will couple with the angular momentum vector $\mathbf{J}$ in the following way[2]:

$$\mathbf{F} = \mathbf{J} + \mathbf{I}, \mathbf{J} + \mathbf{I} - 1, \mathbf{J} + \mathbf{I} - 2, ... \mid \mathbf{J} - \mathbf{I} \mid \tag{34}$$

where the quantum number $\mathbf{F}$ goes as a Clebsch-Gordon series. The vectors couple in such a way to make the new quantum number, F, the vector which represents the total angular momentum. This is shown in the figure where an actual rotation of the molecule is represented by the dashed lined circle. Because of the dependence of F on I and J, as J gets large the splittings become increasingly more difficult to resolve because of the large number of F states possible. This makes the lower microwave ranges, such as 8-18 GHz utilized in this work, advantageous for accurately determining nuclear quadrupole coupling constants because there are fewer splittings in the spectra.

The quadrupolar Hamiltonian used in such a coupling is[2]:

$$\mathbf{H_{quad}} = \frac{eQq_J}{2J(2J-1)I(2I-1)} \left[3(\mathbf{I} \cdot \mathbf{J})^2 + \frac{3}{2}\mathbf{I} \cdot \mathbf{J} - \mathbf{I}^2\mathbf{J}^2 \right] \tag{35}$$

where e is the charge of an electron, Q is the quadrupolar moment, and q_J is the electric field gradient. The total angular momentum is defined as the vector sum of the rotational angular momentum and the nuclear spin vector, or $\mathbf{F} = \mathbf{J} + \mathbf{I}$. This gives:

$$\mathbf{F}^2 = (\mathbf{J} + \mathbf{I})^2 \quad = \quad \mathbf{J}^2 + 2\mathbf{I} \cdot \mathbf{J} + \mathbf{I}^2$$

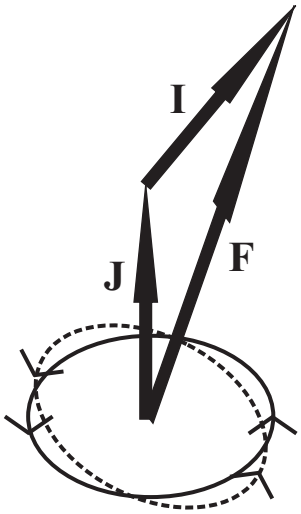

FIGURE 1.2. Vectors **J** and **I** coupling together to give vector **F**. The solid circle represents the motion of the molecule without the coupling while the dashed circle represents the nuclear spin coupled molecular motion.

$$\text{giving } \mathbf{I}\cdot\mathbf{J} = \frac{1}{2}\left(\mathbf{F}^2-\mathbf{J}^2-\mathbf{I}^2\right) \tag{36}$$

Matrix elements of the operators $\mathbf{I}\cdot\mathbf{J}$, $(\mathbf{I}\cdot\mathbf{J})^2$ and $\mathbf{I}^2\mathbf{J}^2$ are [2]:

$$\begin{aligned}
\langle F,J,I \mid \mathbf{I}\cdot\mathbf{J} \mid F,J,I\rangle &= \frac{1}{2}\,C \\
\langle F,J,I \mid (\mathbf{I}\cdot\mathbf{J})^2 \mid F,J,I\rangle &= \frac{1}{4}\,C^2 \\
\langle F,J,I \mid \mathbf{I}^2\mathbf{J}^2 \mid F,J,I\rangle &= J(J+1)I(I+1) \\
\text{where } C &= F(F+1)-J(J+1)-I(I+1)
\end{aligned} \tag{37}$$

The resultant energy levels are defined by[2]:

$$E_Q = \frac{eQq_J}{2J(2J-1)I(2I-1)}\left[\frac{3}{4}\,C(C+1)-J(J+1)I(I+1)\right] \tag{38}$$

The adjustable parameter used in the Hamiltonian that describes the coupling of **I** with **J** is referred to as the nuclear quadrupole coupling tensor eQq or, more commonly, χ. It is a tensor because the electric field gradient is a tensor and the charge of an electron and

the quadrupolar moment are scalar quantities. Each component of the nuclear quadrupole coupling tensor can be determined by Fourier transform microwave (FTMW) spectroscopy. In the pricipal axes configuration, the on-diagonal terms, χ_{aa}, χ_{bb}, and χ_{cc} are Laplacian and add together to give a value of zero.[2]

It is also useful to understand what the nuclear quadrupolar coupling tensor represents from an electronic point of view. As mentioned, χ is directly related to the electric field gradient, q. The electric field gradient tensor provides insight into the electronic environment around the nucleus in question. If the electric field gradient were entirely spherical, such as a chloride ion, then q=0 so eQq=0. If, however, there is some deviation from this spherical regime, such change would manifest itself through a larger magnitude of the eQq. The orbitals participating in such deviations are usually p-orbitals due to their non-spherical shape and proximity to the nucleus.

A common Hamiltonian used for analyzing spectral data containing a nuclear spin takes on the form:

$$\mathbf{H_{tot}} = \mathbf{H_{rot}} + \mathbf{H_{cd}} + \mathbf{H_{quad}} \tag{39}$$

where $\mathbf{H_{rot}}$, $\mathbf{H_{cd}}$, and $\mathbf{H_{quad}}$ are the rotational, centrifugal distortion, and quadrupole coupling Hamiltonians, respectively. In some cases, $\mathbf{H_{quad}}$ can contribute a large amount to the total Hamiltonian. An illustration of this is in perfluoroiodoethane[19] (as will be discussed later), where dipole forbidden transitions that arise are a consequence of matrix elements components having near degenerate values for off-diagonal components of different energy states. The large off-diagonal component of χ facilitates a mixing of states which can form a pathway that breaks down dipole allowed selection rules and arises in forbidden transitions.

1.3.8. Magnetic Hyperfine Effects and Constants

Just because a molecule may not undergo nuclear electric quadrupole coupling, does not mean that energy levels in the rotational regime are not split. Any spin in a molecule can couple with the end-over-end rotation of a molecule giving rise to a split in energy levels.

This spin can arise from a number of places, but this work will deal with spin from any unpaired electrons present in the molecule or nuclear spins with $I \geq \frac{1}{2}$. When either or both of these conditions are met, the molecule may undergo magnetic hyperfine splitting.

1.3.8.1. Magnetic Spin-Rotation Coupling. When dealing with nuclear magnetic coupling, the vectors **I** and **J** couple in the same way as described with nuclear electric quadrupole coupling, but the mathematics and information contained in these values are a little different. The Hamiltonian used for magnetic coupling is[2]:

$$\mathbf{H}_{mag} = -\mu \cdot \mathrm{H} \tag{40}$$

where μ is the nuclear spin magnetic moment and H is the field generated by the molecular rotation. Because the magnetic Hamiltonian has a dependency on the molecular rotation, conceptually it is easy to understand without having to dive into rigorous mathematics that since the moment of inertia is a tensor, this value too will be seperated into tensor components. Which is the case. The Hamiltonian operator using vectors for the magnetic Hamiltonian operator then can be described with **I** and **J** as[2]:

$$\mathbf{H}_{mag} = C_{J,i}\mathbf{I} \cdot \mathbf{J} \text{ where} \tag{41}$$

$$C_{J,i} = \frac{1}{J(J+1)} \sum_{g=x,y,z} C_{gg}(J,i|J_g^2|J,i) \text{ and} \tag{42}$$

$$C_{gg} = -g_I \beta_I h_{gg} \tag{43}$$

where g_I and β_I are the dimensionless gyromagnetic ratio (g factor) for a particular nucleus and the nuclear magneton, respectively and C_{gg} values are the diagonal elements of the nuclear magnetic coupling tensor (also called the magnetic spin-rotation coupling constants). Equation 36 from the description of nuclear electric quadrupole coupling showed that $\mathbf{I} \cdot \mathbf{J} = \frac{1}{2}\left(\mathbf{F}^2 - \mathbf{J}^2 - \mathbf{I}^2\right)$ giving the energies of the nuclear magnetic coupling as being[2]:

$$E_M = \frac{C_{J,i}}{2}[F(F+1) - I(I+1) - J(J+1)]. \tag{44}$$

It should be noted, however, that when a molecule experiences both nuclear electric quadrupole and nuclear magnetic coupling, there are not extra quantum numbers because the molecular and nuclear spin coupling is the same, giving the same F value. The only way it exhibits itself in these situations is through the need of the magnetic spin-rotation coupling constants. Furthur evaluation of what information can be derived from these values is covered in the later chapters.

1.3.8.2. Coupling with an Unpaired Electron. The second place magnetic hyperfine interactions occur are with molecules with electronic angular momentum. These are molecules with one or more unpaired electrons. Hyperfine effects in these cases depend on four coupling constants, a, b, c, and d are described by[1, 20]:

$$a = \frac{2\mu_0\mu_I}{I}\left(\frac{1}{r^3}\right)_{av} \tag{45}$$

$$b = \frac{2\mu_0\mu_I}{I}\left[\frac{8\pi}{3}\psi^2(0) - \frac{3\cos^2\theta - 1}{2r^3}\right]_{av} \tag{46}$$

$$c = \frac{3\mu_0\mu_I}{I}\left(\frac{3\cos^2\theta - 1}{r^3}\right)_{av} \tag{47}$$

$$d = \frac{3\mu_0\mu_I}{I}\left(\frac{\sin^2\theta}{r^3}\right)_{av} \tag{48}$$

where μ_0 and μ_I are the Bohr magneton and nuclear magnetic moment, respectively, I is the value of the nuclear spin, r is the distance between the electron and the nucleus, θ is angle between r and the molecular axis, and $\psi^2(0)$ is the probability of finding the electron at the nucleus. The values a involves an average of the electron or electrons providing orbital angular momentum while c and d are averaged over the electrons providing spin angular momentum. Usually these coincide so that one can just evaluate these terms with respect to the "unpaired" electrons. Because of the specificity of the electrons involved in these averages, the magnetic coupling constants are more explicit than the electric quadrupole

coupling constants in these molecules because those values are averaged over all electrons in the molecule.

Because of the dependency of b on $\psi^2(0)$, this provides a probe into the amount of s-orbital character involved in the unpaired electron. If the amount of s-orbital character is appreciable, $b \gg a$, and can be expected to dominate. When other orbitals are involved, however, a combination of a, c, and d must be looked at to get the proper contributions to the hyperfine structure.

1.3.9. Born-Oppenheimer Breakdown Effects

Many of the constants such as A, B, and C, described in this chapter and following chapters have been become known as the band constants and are isotopically dependent. These values are derived from a Morse potential energy well.[1] When determining and equilibrium bond length for diatomic molecules, constants are obtained from measurements of transitions in varying vibrational states and extrapolated to the bottom of the well to obtain an equilibrium structure, r_e. For example B_e would be the equilibrium rotational constant.

Under the Born-Oppenheimer approximation, this extrapolation should give the same r_e for all isotopologues measured. To the resolution of experiments in microwave spectroscopy, however, this is not always the case and the Born-Oppenheimer approximation breaks down. When this happens, an alternative description of the constants are used.

A similar type of potential, introduced by Dunham[21] can be used to find molecular constants near the potential minimum. These constants, labelled Y_{kl}, can be determined using the relationship[1]:

$$E_{v,J} = \sum_{kl} Y_{kl} \left(v + \frac{1}{2} \right)^k [J(J+1)]^l \tag{49}$$

where Y_{kl} are the Dunham parameters, v and J are the vibrational and rotational quantum numbers, respectively. The parameters Y_{kl} have been related to the more familiar band

constants in Table 1.2. Mass-independent variables can usually then be backed out of the equation by the relationship:

$$Y_{kl} = U_{kl}\mu^{-(k+2l)/2} \tag{50}$$

where U_{kl} are the mass independent Dunham parameters and μ is the reduced mass of the molecule. Watson has then shown that when this relation does not hold, U_{kl} must be adjusted to include Born-Oppenheimer breakdown (BOB) terms. The equation takes on the form[22, 23]:

$$Y_{kl} = U_{kl}\left(1 + \frac{m_e}{M_A}\Delta_{kl}^{A} + \frac{m_e}{M_B}\Delta_{kl}^{B}\right)\mu^{-(k+2l)/2} \tag{51}$$

where m_e is the electron rest mass, M_A and M_B denote the atomic masses of each atom (where m_e, M_A and M_B should all be in the same units), and Δ_{kl}^{A} and Δ_{kl}^{B} are the fitted BOB parameters for each atom. Since these parameters have an inverse dependence on the mass of the atom involved, lighter atoms, such as hydrogen, will exhibit BOB at much less resolution than heavier atoms.

TABLE 1.2. Relating the Y_{kl} Dunham Parameters to the Band Constants

$Y_{10} \approx \omega_e$	$Y_{11} \approx -\alpha_e$
$Y_{01} \approx B_e$	$Y_{12} \approx -\beta_e$
$Y_{02} \approx -D_e$	$Y_{30} \approx \omega_e y_e$
$Y_{03} \approx H_e$	$Y_{21} \approx \gamma_e$
$Y_{20} \approx -\omega_e x_e$	$Y_{40} \approx \omega_e z_e$

1.4. Instrumental Theory and Background

Based on the ideas of Flygare and others, the theory behind the fast passage spectroscopy microwave technique can be broken down into three distinct subsections. These are, (i)

polarization pulse described by the Bloch equations, (ii) molecular excitation and relaxation, and (iii) digitization of signal and Fourier transform analysis.

1.4.1. Polarization Pulse and Bloch Equations

Early microwave spectroscopy techniques involved evacuating a sample cell made out of a waveguide. The sample would be introduced into a cell where the amount of original electromagnetic throughput had already been measured. As the frequency was adjusted, the molecules would create a loss in transmittance if they interacted with the light. This technique is useful for determining spectra at room temperature and for molecules with dipoles ≤ 1 debye (D) (as this technique transition matrix is a function of only the dipole moment). The technique, however, is limited by the pathlength of the cell, which affects sensitivity, and the collisions of the molecules (collisional broadening) which affects the resolution of the experiment. Intensities of spectra would be largely distributed, populating a large number of states due to the higher temperatures of the experiment (usually at room temperature). This would make lower quantum vibrational-rotational state transitions have smaller intensities compared to their lower temperature experimental counterparts.

In order to account for these problems, tests were performed in a waveguide cell by Flygare and coworkers to look at what is referred to as a "fast passage" technique.[8] This event involved both a transient absorption and transient emission measurement of a transition. This could more easily be referred to as a sweep through the transition and measuring its relaxation. In this event, a microwave pulse was used to polarize the molecule in a short amount of time relative to the relaxation time. In the experiment a 10 μs pulse length was used. Normal relaxation times of a molecule are approximately 100 μs. Excitation and relaxation are discussed in furthur detail in the following subsection.

The pulse used to perform the fast passage event is called a polarization pulse. According to Ref.[8] and Ref.[9], this pulse is governed by a set of equations known as the Bloch equations. This set of equations contains within it molecular relaxation terms as well. For now though, we focus only on the polarization terms. Nuclear magnetic resonance (NMR) has the same type of theoretical equations governing the pulse and molecular relaxation.

Since microwave spectroscopy is essentially an electric analog of the NMR technique, it is no surprise the same type of theory governs this microwave technique. For fast passage spectroscopy these equations are[8]:

$$\begin{aligned} \frac{dP_r}{dt} \; + \; \Delta\nu P_i \; + \; \frac{P_r}{T_2} \;\; &= \;\; 0 \\ \frac{dP_i}{dt} \; - \; \Delta\nu P_r \; + \; \kappa^2\mathcal{E}\left(\frac{\hbar\Delta N}{4}\right) \; + \; \frac{P_r}{T_2} \;\; &= \;\; 0 \\ \frac{d}{dt}\left(\frac{\hbar\Delta N}{4}\right) \; - \; \mathcal{E}P_i \; + \; \frac{\hbar}{4}\,\frac{(\Delta N - \Delta N_0)}{T_1} \;\; &= \;\; 0 \end{aligned} \tag{52}$$

$$\begin{aligned} \alpha\frac{dP_r}{d(\Delta\nu)} \; + \; \Delta\nu P_i \;\; &= \;\; 0 \\ \alpha\frac{dP_i}{d(\Delta\nu)} \; - \; \Delta\nu P_r \; + \; \left(\frac{\hbar\kappa^2\mathcal{E}}{4}\right)\Delta N \;\; &= \;\; 0 \\ \alpha\frac{d}{d(\Delta\nu)}\left(\frac{\hbar\Delta N}{4}\right) \; - \; \mathcal{E}P_i \;\; &= \;\; 0 \end{aligned} \tag{53}$$

where P_r and P_i are the real and imaginary polarization terms; ΔN_0 and ΔN are the population difference between the two states initially and at a given time, respectively; $\Delta\nu$ is the difference between a transition frequency and the microwave frequency (or frequency range); $\mathcal{E}$ is a general function of z and t in the solving of the time dependent energy; T_1 is the relaxation time for the population difference and T_2 is the relaxation time for the polarization; κ is a term related to the transition dipole moment matrix element; and α is an arbitrary term representing the sweep speed, $\frac{d\Delta\nu}{dt}$.

The two sets of equations are actually equal to each other with two caveats. First, the chain rule has been utilized with the arbitrary α term. The second, however, is a less obvious, yet highly useful principle, to set the sweep duration time $\ll T_1$,T_2. If the time duration of the pulse is short compared to the relaxation times, then those values in Equations 52 are essentially zero due to their large denominators. These terms are also called collisional dampening terms (needed for waveguide experiments especially). When obeyed, these are

the equations needed to create the fast passage event and sweep through transitions so that there is no interference of the pulse with the signal itself.

From the Bloch equations it is evident that there are two factors that control the pulse power, or throughput of the polarization: the amount of time spent on the polarization (the chirp duration) represented by $\frac{d}{dt}$ in the equations, and the range of frequencies in a polarization represented by the $\Delta\nu$ term. This is essentially shown by the sweep speed, α. Because power is a direct function of time, one can understand the power of a pulse as being inversely related to the sweep speed. If the time of the pulse generated is lengthened, then the polarizing pulse has greater power and a smaller sweep speed. If the window of frequencies are shortened, the pulse again has more power and a smaller sweep speed. This is a useful experimental control that will be talked about in the next chapter.

1.4.2. Excitation and Relaxation

Following the Bloch equations above, a molecule can have a polarizing microwave pulse swept through it for a given amount of time and across a range of frequencies (known as the fast passage event). Molecular species with a dipole may interact with the polarizing pulse resulting in a macroscopic polarization. This is shown in the figure below. As the electric field is taken away, the molecules relax back to random orientations. This relaxation is detected as a time diminishing oscillating electric field. This signal is referred to as a free induction decay (FID).

When a molecule with a dipole in space meets an oscillating electric field, the molecule will attempt to align its dipole along with the field so long as the electric field is of a frequency of one of the molecule's rotational transitions. The creation of such an oscillating field is known as the *excitation*. In order to excite a molecule using the excitation pulse, three components must be present, (i) sufficient pulse power, (ii) molecular dipole moment, and (iii) excitation frequency must match molecular transition frequency.

As mentioned earlier, the appearance of a transition lies solely in the transition matrix not being zero. But, Of course, sensitivity also plays a role in actually observing molecular signals. The amount of molecules that can be polarized has some dependence upon the

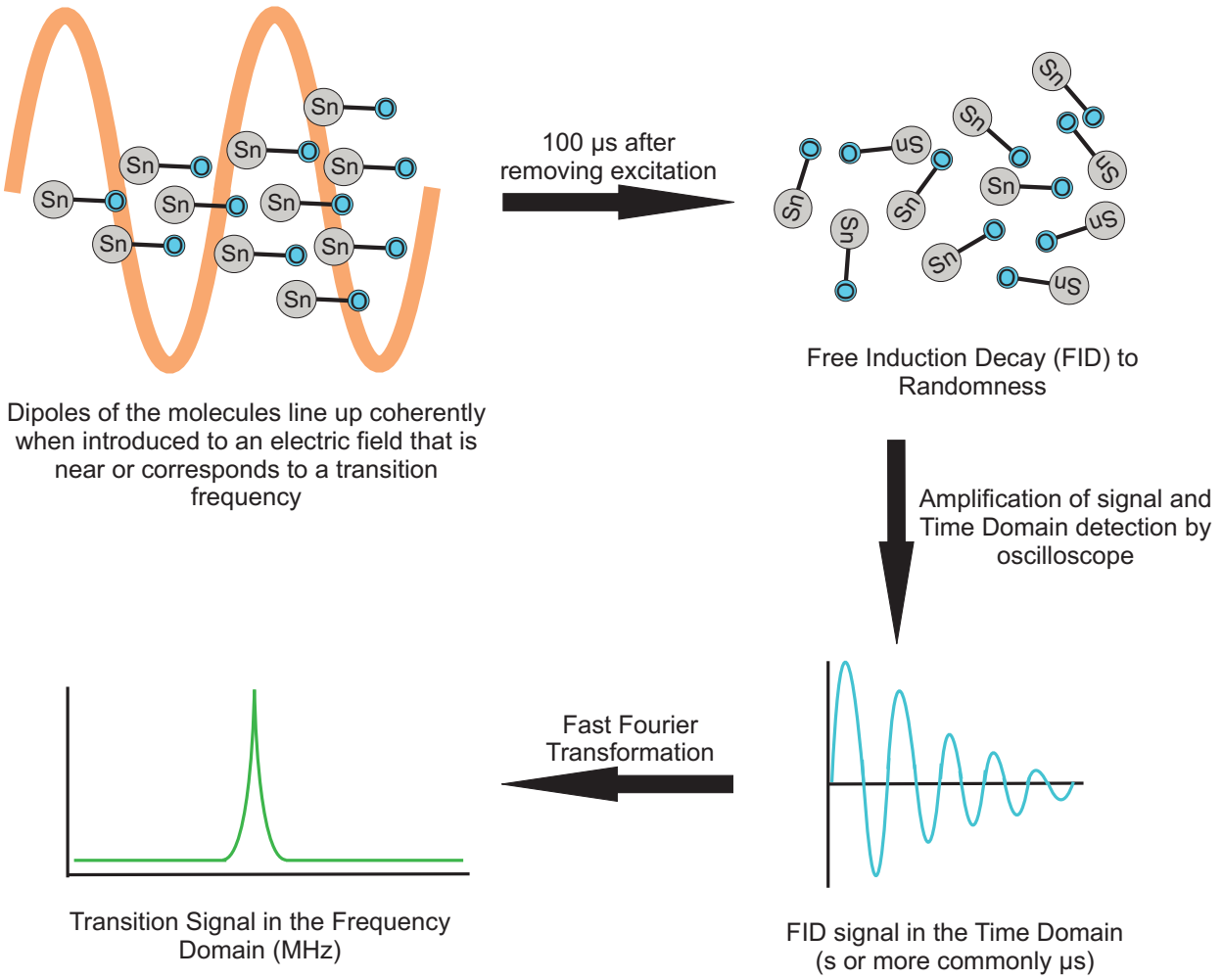

FIGURE 1.3. Excitation then relaxation of molecules during and after polarization. Dipoles line up giving the molecules the same orientation while rotating in space. After removal of the light, the molecules decohere producing a free induction decay (FID) in the time domain. The FID is fast Fourier transformed and a frequency domain signal is produced.[24]

dipole moment operator. If the dipole moment operator is small compared to the power of the polarization, then only a few molecules will be polarized. If there is only enough power produced by the excitation to line up a few molecules, then there will not be sufficient signal to overcome the background signal and the transition would not be observed.

The signal produced by the molecules is referred to as the *relaxation*. Shown in the figure above as the "FID signal in the time domain", the actual relaxation is a free induction decay of the sample of molecules lining up in uniformity to the oscillating field and then

slowly moving back to random orientations. This relaxation occurs on the order of ≈100 μs for rotational transitions which gives rise to kHz resolution capabilities in signal. The larger the amplitude of the free induction decay, the more intense a transition or transitions in the frequency domain.

The excitation/relaxation of molecules in this way is called a resonance technique. In description of a resonance technique, a simple tuning fork analogy can be used. If one were to strike a tuning fork and then place it near another tuning fork of the same frequency, the new tuning fork would come into resonance with the original fork. If one were to then take the original tuning fork away and now measure the new fork as it is restored to equilibrium in the time domain, they would observe a free induction decay. Fourier transform this FID and the frequencies of the two tuning forks would be rediscovered.

1.4.3. Digitization of Signal and Fourier Transform Analysis

In highly resolved spectroscopies, signal manipulation/digitization is always a concern. In order to have highly resolved transitions without too much signal loss, it is crucial to manipulate the signal to a form where it can be interpreted by the hardware and software available to the spectroscopist. The ability to capture signal in the time domain and Fourier transform it back to the frequency domain increased resolution immensely and was only dependent on the length of the FID. Not only that, but now the background could be lessened by turning off the excitation completely and only detecting the signal of the molecules in "silence."

1.4.3.1. Fourier transformation. In simplest terms, a Fourier transform from the time domain to the frequency domain is a mathematical process of the form[25]:

$$F(\omega) = \int_{-\infty}^{\infty} f(t) e^{-j\nu t} dt \tag{54}$$

where ν is the frequency, t is time, and j is $2\pi i$. Where, in our experiment, the function of time is a complex oscillating function that can contain within it many frequencies.

Strictly speaking, the Fourier transform in the expression above is over the entire time domain. In reality, however, it is impractical and unnecessary to process such a large amount of data; the FIDs for a rotational transition last on the order of 100 μs. To adjust for the amount of data being processed, computers/oscilloscopes use a time gating system with what is called a fast Fourier transformation (FFT) algorithm comprised of many smaller order summations.[25] The resolution of a fast Fourier transformed FID is a function of the length of the FID itself. The longer the FID, the better the resolution (but the slower the process due to increased number of operations). In NMR, FIDs are on the order of milliseconds to seconds and linewidths are very small (<Hz resolution). In rotational spectroscopy, however, typical FIDs are on the order of μs making the resolution a bit worse than that of NMR, but still highly resolved (kHz resolution) when compared to those of infrared (cm^{-1} resolution) or UV-Visible (nm resolution) methodologies.

The FFT used in our experiment is a Cooley-Tuckey algorithm [26] originally used in a pulsed microwave technique by Ekkers and Flygare.[27] In reference [27], a mathematical formalism is used to describe resolution ($\Delta\nu$) and bandwidth (F) in the frequency domain of the Cooley-Tuckey FFT. These are given by:

$$\Delta\nu = (n \cdot \Delta t)^{-1} \tag{55}$$

$$F = (2\Delta t)^{-1} \tag{56}$$

where n is the number of points in the time domain and Δt is the time between each point (their resolution). This formalism will be utilized in chapter 2 for determining base peak resolution and bandwidth of the spectrometer.

Doing a fast Fourier transform has many advantages. Although relaxation times are on the order of 100 μs, typically the signal is only averaged with a 20 μs FID collected and gated. This is because the oscilloscope slows down considerably when trying to take in as much data as is needed for 100 μs and, therefore, becomes a bottleneck for experimental techniques. One idea would be to give increased resolution by adding zeros to the end

of the FID. This artificial data manipulation has not been performed here. In this work, the linewidths are ≈80 kHz full width half maximum (FWHM).This is sufficient to achieve accurate and precise rotational parameter assignment with reasonable uncertainties (as good as 6 kHz) in measurement assignment.

CHAPTER 2

EXPERIMENT AND INSTRUMENTATION

2.1. The Chirped Pulse Fourier Transform Microwave Spectrometer

As mentioned in the Introduction chapter, knowledge of fast passage microwave spectroscopy has been available for quite sometime.[8] This idea was realized, however, with advances in technology and the work of Pate and co-workers on the chirped pulse Fourier transform microwave (CP-FTMW) spectrometer.[5, 6, 7] Where "chirped pulse" has become a modern synonym for fast passage. This spectrometer utilizes a fast microwave pulse, i.e. a "chirped-pulse" made with a fast (4.2 GS/s) arbitrary waveform generator (AWG). The signal is multiplied up, mixed, and powered heavily with a 1 kW traveling wavetube amplifier (TWTA). This amount of power allows for a spectral range of 7.5-18.5 GHz to be probed. Because the range of the spectrometer is 11 GHz, the signal can only be manipulated and digitized with a suitable, broadband, (12 GHz) oscilloscope.

2.2. A Search Accelerated, Correct Intensity Fourier Transform Microwave Spectrometer with Laser Ablation Source

Inspired by the CP-FTMW spectrometer[5, 6, 7] and earlier fast passage experiments by Flygare and co-workers[9, 8], the search accelerated, correct intensity Fourier transform microwave (SACI-FTMW) spectrometer was created at the University of North Texas (UNT).[28] Although the first design came with a laser ablation source(commented on later), a new edition of the technique has most recently been utilized on gases and volatile liquids and renamed to a CP-FTMW spectrometer to coincide with convention. The circuit diagram for this spectrometer is detailed below in Figure 2.1.

2.2.1. Overview of the SACI-FTMW

Following the schematic given in Figure 2.1, the original SACI-FTMW experiment involves a monochromatic microwave pulse of frequency, ν, being split by a power divider and mixed with a linear frequency sweep produced by an AWG. The value of the frequency, ν is between 8 and 18 GHz. The linear frequency sweep range that we use varies from molecule to molecule, depending on the dipole moment, but always starts at 250 MHz and goes as high as 2000 MHz producing $\nu \pm 2000$ MHz with a $\nu \pm 250$ MHz "dead zone". The mixed microwaves are then amplified by a 5W solid state amplifier which provides the power needed to polarize a sample of gas. The powered microwaves are then broadcast through an antenna horn rated between 8-18 GHz. They then interact with gas molecules that have been pulsed from a solenoid valve. The signal from the interaction is received with a second antenna horn rated between 8-18 GHz, amplified with a low noise amplifier, and mixed back down with the original center frequency. The signal is then digitized by a fast scope capable of digitizing data at 40 gigasamples per second (40 GS/s) with a 12 GHz bandwidth. This process is repeated for at least 10,000 acquisitions at either a 2 or 4 Hz speed. This whole process can take from 45 minutes to 2.5 hours of acquisition time. The collected spectrum is a 250-2000 MHz region containing the upper and lower sidebands of the original scan folded on top of one another. A second experiment then has to be carried out 1 MHz above the original center frequency, $\nu+$ 1 MHz, to distinguish the two sidebands.

Although inspired by the CP-FTMW spectrometer mentioned earlier, the SACI-FTMW spectrometer with laser ablation source slightly differs from that instrument in a few distinct ways. The most notable of these being the 5W power amplifier and the elimination of multiplier components. These differences have the effect of lowering the cost of the spectrometer while maintaining the power of a broadband technique. This is achieved through accelerating search times while still giving the flexibility to digitize smaller ranges of spectra. The changes in design from the original chirped-pulse experiment[7] also focus the spectrometer's use toward more purely rotational studies[19, 29, 30, 31, 32, 33, 34, 35, 36, 37, 38], but also have been used on vibrational-rotational studies[39].

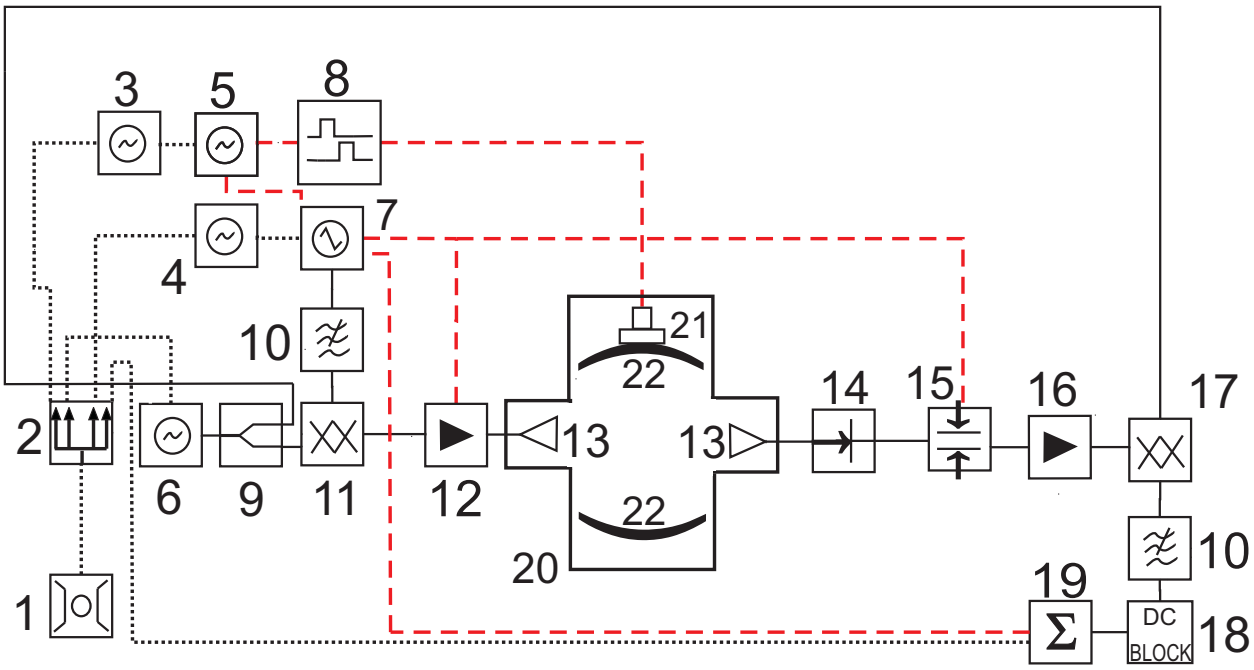

FIGURE 2.1. The original SACI-FTMW spectrometer. Solid lines are microwave frequencies for use in experiment. Dotted lines are reference frequencies. Red dashed lines are timing control connections. Components are 1. Stanford Research Systems 10 MHz Rb Standard Model FS725, 2. 10 MHz Distribution Amplifier, Wenzel Associates 600-15888, 3. Nexyn Corporation 640 MHz Phase Locked Oscillator, NXPLOS-0064-02381, 4. Nexyn Corporation 3.96 GHz Phase Locked Oscillator NXPLOS-0396-02381, 5. Tektronix AWG2041 Arbitrary Waveform Generator, 6. Microwave Synthesizer, HP 8341A, 7. Tektronix AWG 710B 4.2 GS/s Arbitrary Waveform Generator, 8. Stanford Research Systems DG535 Pulse Generator, 9. Power Divider, Narda 4456.2, 10. Low Pass Filter, Minicircuits VLF-1800+, 11. Mixer, Miteq DB0418LW1, 12. 5W Power Amplifier, Microwave PowerL0818-37, 13. Horn Antennae, Amplifier Research AR4004, 14. Power Limiter, Advanced Control Components ACLM-4539-C36-1K, 15. SPDT Switch, SMT SFD0526, 16. Low Noise Amplifier, AML Communications AML818L4501, 17. Mixer, Miteq DM0520LW1, 18. DC-250 MHz Block, 19. Oscilloscope, Tektronix TDS6124C 40GS/s 12GHz, 20. Vacuum Chamber, 21. Series 9 Solenoid Valve, Parker-Hannifin, 22.Fabry-Perót Cavity.

2.3. Achieving Broadband

There are many obstacles to obtaining fast passage broadband spectroscopy in the microwave region. These include, but are not limited to, digitization of signal, producing enough power to polarize the molecules over large regions, and being able to produce fast polarizing pulses to be able to undergo the fast passage event. Overcoming these obstacles is currently due to both technological and design barriers.

2.3.1. Bloch Equations and the Linear Frequency Sweep

From earlier discussions in chapter 1 on the Bloch equations (Equations 52 and 53) and relaxation times, FIDs are on the order of ≈100 μs. Due to the FID length, 10 μs should be an upper limit polarizing pulse duration as it is still an order of magnitude shorter than the FID. Normal practice in the experimental technique is a pulse duration of ≈4-5 μs. As a chirp duration approaches the upper limit, the only other way to provide power to the pulse is to adjust the chirp frequency range. When needed, this parameter is adjusted to observe spectra with weaker dipole moments. These are programmable parameters in the arbitrary waveform generator.

2.3.1.1. Arbitrary waveform generator. The chirp, as mentioned before, must be made very quickly ($\leq$ 10 μs) in comparison to the relaxation times. In order to achieve this, an instrument must be employed that can create a large range of microwave frequencies on a short timescale. This instrument is an arbitrary waveform generator (AWG) with a large sampling rate. In the SACI-FTMW experiment, this sampling rate is 4.2 GS/s on the Tektronix® AWG710B, allowing for a microwave pulse of DC-2100 MHz. 2100 MHz is the Nyquist frequency [40] limit and is the upper limit due to aliasing[25], which is discussed later in the Digitization of Signal subsection.

In the original fast passage experiments, Flygare et al. were able to achieve 50 MHz bandwidth in a waveguide cell through the manipulation of sinusoidal microwaves in the 10 μs timeframe.[8] The ability to create fast sweeps of larger ranges were not available at that time because of microwave pulse sampling limitations. The linear frequency sweep that is produced by the AWG in the SACI-FTMW and CP-FTMW experiments, though, have

faster sampling rates (4.2 GS/s) capable of producing larger frequency ranges on the same timescale, ≤ 10 μs, allowing large search regions (up to 2100 MHz chirps).

A linear frequency sweep, or chirp, is one that progresses from a starting frequency to a stopping frequency in one smooth transition. The equation for such a sweep goes as[41]:

$$V(t) = A \sin\left[2\pi\nu_1 t + 2\pi\nu_2 \int_0^t \frac{t}{T}\, dt + \phi_0\right] \tag{57}$$

where t is the time, A is the amplitude, just assigned as one (1) or zero (0) for on and off, respectively. The start and stop frequencies in the sweep are ν_1 and ν_2, respectively; ϕ_0 is initial phase of the sweep (= 0 for one sinusoidal pulse), and T is the sweep time, also referred to as chirp duration. This equation must be programmed into the AWG along with marker logic to begin and end each pulse. It is within this program regime where pulse power adjustments can be made to help intensify the spectra during a scan. These pulses are then mixed with a center frequency and proceed toward the rest of the experiment.

2.3.2. Amplification

Amplification of microwaves for polarization and for signal acquisition are both fundamental needs of fast passage techniques.[7, 28] Without these technologies being readily available, the experiment is extremely difficult to perform on a level high enough to be transferrable to unknown molecular spectra. They provide both the power to line up electric dipoles over a large range of frequencies and the signal to noise ratio amplification to detect these transitions.

2.3.2.1. 5 Watt power amplifier. According to the equation sets 52 and 53, a broadband or large range of frequencies needs to be able to polarize many transitions on a fast timescale. This is only possible through some form of a high power amplifier. In the CP-FTMW experiment, a 1 kW TWTA amplifier is used to polarize a frequency span of 11 GHz. This size amplifier, however, is very expensive (>\$100,000). In order to lower the cost of the SACI-FTMW, a 5W solid state amplifier is used instead ($\sim$ \$10,000). As mentioned in the *Bloch Equations and Linear Frequency Sweep* section, a large amount of power is needed

to sweep the entire region. To overcome this, the experiment is performed in smaller chirp ranges which lessen the need for such power costs. This keeps the broadband idea intact, but still does not eliminate the need for a search. It is for this reason the technique was given the "Search Accelerated" portion of its name.

Because the amount of power is large coming out of the power amplifier, there must be a way to switch the microwaves on and off. The 5W power amplifier by Microwave Power™ has this switch built in and controlled through transistor-transistor logic (TTL). If this were not the case, a second switch would need to be placed in between the power amplifier and the broadcast antennae horn in order to protect the low noise amplifier in the circuit.

2.3.2.2. Low Noise Amplifier. The low noise amplifier is a device which takes an input signal and amplifies the signal with little noise introduction. This, in turn, minimizes signal to noise ratio loss. A large gain value and a low noise value give the component this ability. Without this amplification stage, no signal would be strong enough to detect. The amplifier in our SACI-FTMW has changed from an AML Communications™ amplifier (45 dB Gain, 2.5 dB Noise Figure) in the original experimental setup to a more recent Miteq™ (45 dB Gain, 1.4 dB Noise Figure) low noise amplifier to help increase the sensitivity of the instrument.

2.3.3. Antennae Horn

One inherent problem with using the cavity experiment to achieve broadband is that it is a *cavity* and must be tuned to a resonant frequency. This tuning of the spectrometer acts as a band pass for the microwaves allowing only a narrowband of frequencies through. This problem is overcome by eliminating the mirrors that create the cavity and replacing them with microwave horn antennae. These antennae are essentially waveguide adapters with a gain horn attached to them. This allows for 1 pulse to be broadcast and received per averaging cycle lowering the Q factor, a measurement of the microwave spectrometer's sensitivity, from 10,000 to 1. This sensitivity, however, can be displaced by powering the excitation pulse enough to ensure proper molecular polarization and performing multiple acquisitions.

Another aspect of the cavity experiment is that some frequencies tune differently than others. That is to say that the tuned frequencies are not given the same amount of power in each search because of differences in each tuning event. This diminishes the reliability of the intensities of the spectra in a cavity experiment and can complicate assignment. In a chirped pulse type experiment, however, the horns have a similar power distribution throughout the range that they are rated for allowing for equal powering across a range of frequencies. This gives the "correct intensity" aspect of the spectrometer as shown in the figure below[39].

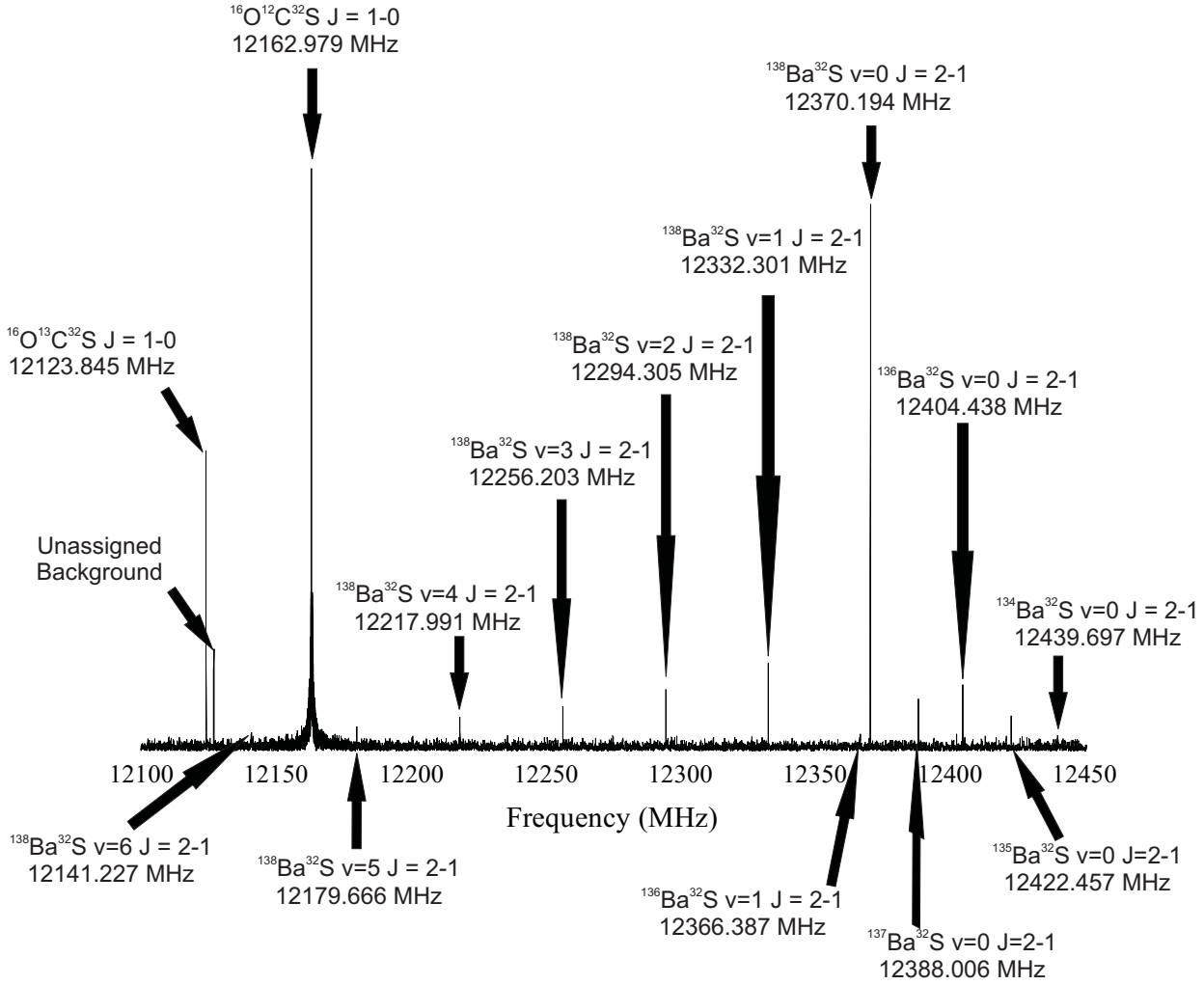

FIGURE 2.2. A sample spectrum of the diatomic molecule barium sulfide showing correct relative intensities.

2.3.4. Digitization of Signal

Another major factor in achieving broadband is the digitization of signal. The digitization component of the instrument requires two parameters to be met in order to fast Fourier transform (FFT) adequately. The component must first be able to record many points at small time intervals (typically picosecond time scale). The signal referred to here is the FID, usually acquired on a 20 μs time frame. In order to account for at least 20 μs on a picosecond time frame, hundreds of thousands of points are required to be taken. Usually 800,000 points are acquired for a single FID.

As discussed in Equations 55 and 56 of chapter 1, in order to utilize a fast Fourier transformation with high resolution, a large sampling rate is needed to digitize signal in the microwave region properly. In the SACI-FTMW spectrometer, a Tektronix® TDS6124C with a 40 GS/s sampling rate is utilized. This permits a bandwidth of up to 20 GHz to be studied according to the Nyquist requirement[40], but the specifications on the oscilloscope report a conservative 12 GHz bandwidth. The Nyquist requirement is the need for the sampling frequency to be twice that of the frequency being detected. This requirement eliminates aliasing. *Aliasing* is when signals become unable to be determined due to sampling problems[25]. This translates to "ghost signals" (extraneous peaks) or poor frequency measurements in the spectra.

The second requirement for digitization of signal is that the signal must average for many cycles. This can be achieved in two ways, on the oscilloscope or on a second external averaging station (for instance a computer). Although the signal from some spectra come in a single shot, the weaker transitions take more averages to acquire. Since the technique is broadband, all spectra must run for the same number of acquisitions, which implies a large number of cycles. Typically spectra are averaged directly on the oscilloscope for at least 10,000 averaging cycles.

2.3.5. Phase Stability and Timing

As shown in all diagrams of spectrometers in this chapter, all timing mechanisms are clocked to a 10 MHz Rb standard in some way. This standard is needed to induce complete

phase stability and timing. Along with timing mechanisms, the AWG 710B, the oscilloscope, and all the phase locked oscillators are linked to the standard frequency.

In order for accurate measurement of frequencies, the pulse generated by both AWGs must be phase locked. This is achieved through a clocking device called a Phased Locked Oscillator (PLO). A PLO is a device which is designed to take in a reference standard frequency (10 MHz), and convert it to a second locked frequency. The AWG 710B is phase locked to a 3.96 GHz PLO which allows the AWG to create a steady linear frequency sweep up to approximately 2 GHz while the AWG 2041 is clocked to 640 MHz PLO. The external clocks allow for the points in the programming to be the same each time a cycle is ran. This similarity is needed such that signals stay consistently in the same phase and do not average each other away.

The AWG 2041 is the main clocking device of the entire experiment. Simple jitter tests show that there is less than 10 ns of jitter in marker pulses created by the clocked AWG 2041. Since this device controls both the firing of the AWG 710B and the firing of the molecules from the pulsed nozzle, no more than 20 ns difference lies within the pulses of these events. Any other timing miscues would be caused by the internal timings of those devices. 20 ns maximum time difference is sufficient phase stability for 2-4 GHz bandwidth experiments.

2.4. Molecular Sampling

Because microwave spectroscopy is a gas phase technique, many different sampling techniques have been implemented. This is not always trivial considering that frequently molecules, especially larger molecules, tend to have low vapor pressures or are solids at room temperatures. It is prudent to note all sampling techniques are pulsed into the chamber by a Parker-Hannifin^{TM} Series 9 solenoid valve (shown in Figure 2.1) controlled by an Iota One^{TM} transistor-transistor logic (TTL) control box.

2.4.1. Gas Mixture Sampling

The first technique is used on samples that already exist in the gas phase. Preparation of the sample typically involves making a 3% (by pressure) gas mixture of the sample gas

in an inert backing gas (usually argon), 4-5 atm total pressure. The sample is then directly attached to the solenoid valve via a line from the mixture. This sampling technique has been implemented in molecules such as perfluoroiodoethane[19] and bromodifluoroacetonitrile[38].

2.4.2. Volatile Liquid Sampling

The second type of sampling technique is utilized for the study of volatile liquid compounds. This method involves introducing a U-shaped teflon tube to the sampling line before the solenoid valve. Approximately 1-2 mL of sample is introduced to the line via a pipette. The sample, residing at the bottom of the tube, is then bubbled through with a carrier gas (usually argon) at pressures of 1-3 atm through the pulsing of the solenoid valve. The lower pressures warm up the expansion slightly (discussed in the *Supersonic Expansion* section). Sometimes, the sample is too volatile and will evaporate before 10,000 cycles can be reached. In those cases, the tube is put on ice to slow the evaporation enough to run the experiment fully.

2.4.3. Solid Sampling and the Laser Ablation Source

Although not focused on in this work, the original SACI-FTMW experiment featured a laser ablation source. This allowed for sampling of metal containing species including, but not limited to, diatomic and transient species.[28, 42, 43, 44]

The nozzle design first introduced by Walker et al.[4] is based upon the design of Smalley and co-workers.[45] The nozzle involves a slightly machined Parker-Hannafin^{TM} Series 9 solenoid valve to screw into a specialized valve fitting. This fitting, as shown in Figure 2.3, contains a 0.635 cm bored hole that runs perpendicular to the valve orientation but slightly askew to the spine of the valve. An inlet hole for a focused Nd:YAG 1064 nm laser that ends at the metal rod cavity is located perpendicular to the metal rod housing. Along the spine of the fitting, a 0.4366 cm hole has been bored for the flow of the pulsed gas from the solenoid valve.

The metal rod must be rotated in order to provide a fresh surface to ablate with each successive pulse. This rotation is provided by a motor that holds the rod and repeatedly

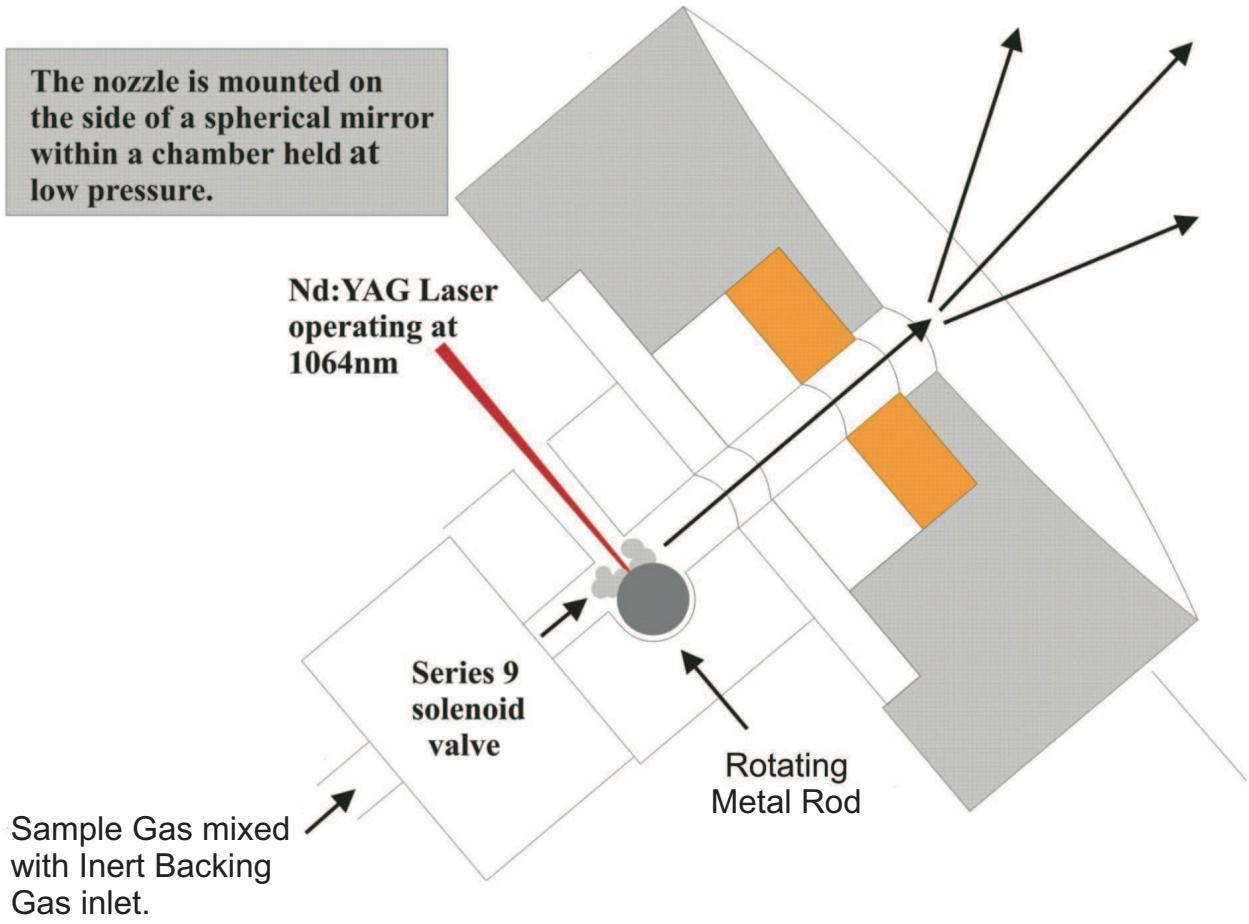

FIGURE 2.3. The Walker-Gerry Ablation Nozzle Design.

rotates the rod to an upper limit and then returns back down to a lower limit. As the rod is rotated, the experiment is timed as to hit the metal rod with the laser, ablating the surface right as the sample gas flows over the rod creating both stable and transient types of metal containing compounds in the gas phase.

2.5. Supersonic Expansion

The solenoid valve is simply a spring loaded valve which contains a magnetic component called a "slug" which houses a spring and a conical plastic sealing mechanism called a

"poppit". The slug is held into place by a spring in between the slug and the valve head. On the valve head, there is a 0.762 mm diameter circular orifice. A firing of the valve occurs when the poppit is pulled away from the orifice and the seal is broken and restored. The interior of the valve is shown in Figure 2.4.

The experiment happens in a vacuum chamber held at 10^{-5} torr. This allows a situation where there are high pressure molecules on one side of the orifice and a low pressure region on the other side. Once the valve is open, the molecules rush to the region of low pressure. If the pressure of the gas behind the orifice is large enough (typically $\geq$ 1 atm), the mean distance between molecules is smaller than the diameter of the orifice. When the valve opens, a "molecular beam" is created with all the molecules having very similar speeds. Since all molecules are traveling with the similar kinetic energy, few (if any) molecules are colliding with one another. This is referred to as a "collision free expansion" or "molecular flow"[11]. This is shown in Figure 2.4. These molecules, however, are moving at such high velocities that typically they are supersonic with respect to molecules , so the term "supersonic expansion" is used.

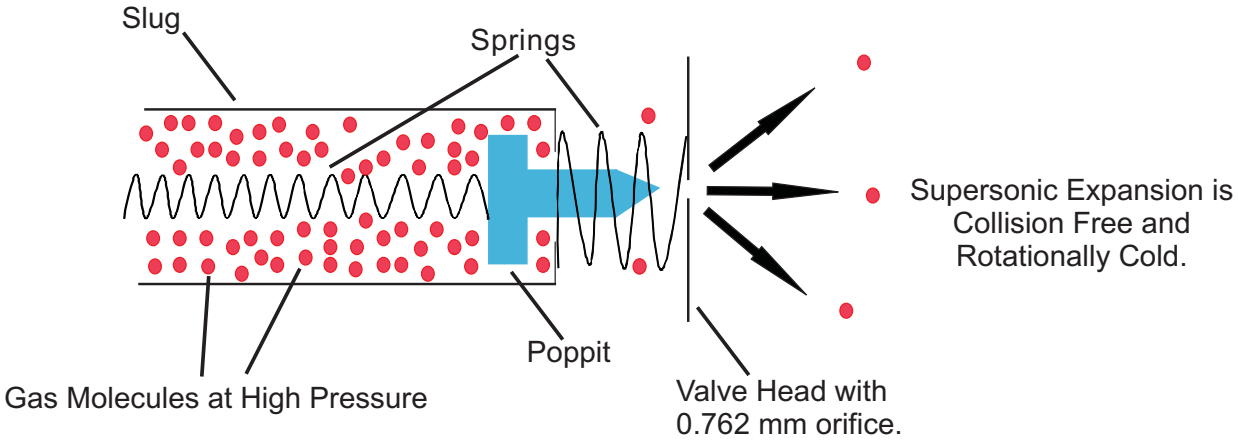

FIGURE 2.4. The interior of the solenoid valve. A firing of the valve allows for a rush of molecules at high pressure to escape supersonically. The supersonic expansion is collision free and rotationally cold. See text for details.

The purpose of the supersonic expansion is to utilize the Maxwell Distribution of Speeds, defined mathematically as[11]:

$$f(v) = 4\pi \left(\frac{M}{2\pi RT} \right)^{\frac{3}{2}} v^2 e^{\frac{-Mv^2}{2RT}} \tag{58}$$

where M is the molecular weight of the gas, T is the temperature, R is the gas constant, and v is the velocity of the gas. The distribution's girth is dependent on temperature and molecular mass. Low temperatures and high molecular masses give rise to narrower speed distributions while high temperatures and low molecular masses produce broader speed distributions.

As stated earlier, all of the molecules in a pulse of the valve are all traveling at very similar speeds. This gives a very narrow distribution of speeds and, therefore, a cold translational temperature. Since rotational and translational energy is quite efficient, rotational energies used in the Boltzmann distribution of states is only slightly higher in temperature.[3, 11] *Physical Chemistry* by Atkins reports these values as 1 K and 10 K, respectively[11], while experiments carried out on the Balle-Flygare cavity experiment report these temperatures as 0.3 K and ranging from 1-4 K, respectively[3]. These low rotational temperatures force the molecule to populate lower J quantum states which facilitate observation of transitions having these J values.

Since gas mixtures are typically $\leq 3\%$, the carrier gas is responsible for most of the molecular mass of the sample in question. Therefore choice of a proper carrier gas is key in the expansion. The equation above implies that larger molecular masses invoke a colder expansion, and that is the case as determined by some experiments performed and presented on barium sulfide, BaS.[39] The average speeds of some carrier gases in the jet for a microwave experiment have been studied by Flygare.[46]

Lastly, it should be noted that although this technique gives translational and rotationally cold distributions of molecules, the vibrational temperature exchange is not as efficient. Atkins reports this value as being on the order of 100 K.[11] This has been observed in our work with BaS where up to the $\nu = 6$, $J = 2 \leftarrow 1$ transition for the main isotopologue was observed.[39]

2.6. Improvements on the Original Design

Since the original spectrometer design, many improvements have been made on the SACI-FTMW setup. The original design included a mix down stage from the original center frequency which required a second experiment performed 1 MHz above the original center frequency to distinguish the sidebands. This section refers to our efforts to overcome this problem and to increase the sensitivity of the instrument.

2.6.1. Phase Locked Oscillator Mix Down

In the original SACI-FTMW design, the center frequency was divided such that one portion was used for excitation of the molecules while the other was mixed down with signal and used for digitization. Although this setup is reliable when performing the broadband experiment, it is not practical and it unneccessarily wastes sample in our laboratory. This is due to the fact that a second experiment must be ran slightly off value from the center frequency say, 1 MHz, to determine at what frequency the transition takes place. This is because the experiment becomes a mixture of a $\nu \pm$ (250-2000) MHz spectra. The positive side designating the upper sideband and the negative side designating the lower sideband. The spectra, when mixed back down with the center frequency, are laid atop one another in the digitization of the signal. The second experiment determines the sideband in which the transition appears. This technique is useful for phase stability in the experiment and would be more useful if the oscilloscope could only digitize up to 2 GHz of spectrum.

Since the oscilloscope used in the experiment can digitize up to 12 GHz of frequency (possibly more), then it becomes useful to mix down with a Phased Locked Oscillator (PLO). This technique was utilized in the CP-FTMW spectrometer.[7] A PLO will give off a single phase locked frequency when attached to a standard. If the $\nu \pm$ 250-2000 MHz (where ν lies between 8-18 GHz)is mixed with a PLO with a frequency above the range of the spectrometer say, at 19 GHz, then the signal gets adjusted to 19000 $\pm$ ($\nu \pm$ 250-2000) and only that sideband able to be digitized on a 40 GS/s oscilloscope is collected (i.e. the lower sideband). Signal measured at 8 GHz is seen as 11 GHz on the scope, 10 GHz is measured as 9 GHz, and so on. Therefore, the data must be corrected for this in order to measure

the transition at its appropriate frequency. A picture of the experimental setup is given in Figure 2.5 at the end of the chapter.

Employment of the PLO mix down allows for the frequency sweep produced by the AWG to now range from direct current (DC), or ≈0, to 2000 MHz (instead of starting at 250 MHz). This is because originally the 250 MHz DC Block would block any spectra appearing between DC-250 MHz when mixed down with the center frequency so any spectra excited in this region would not make it through to digitization, creating the "dead" zone. The dead zones would require seperate searches to cover the region of spectra previously not obtained. This would waste sample and time. The addition of the PLO stage standardized these searches by only requiring one to tune to a center frequency without the worry of extra experiments or missing regions of spectra.

2.6.2. Direct Digitization

When there is no mix-down stage and the amplified signal is connected directly into the oscilloscope, this is called direct digitization. This technique greatly enhances signal strength because there is no power loss due to mixing of the signal with some other source (i.e. microwave synthesizer or phase locked oscillator). In Figure 2.5, this would be done by simply eliminating components 16-19 and connecting component 15 directly to component 20.

Using this technique has the advantages of sensitivity, but greatly limits the frequency range of the spectrometer. The company's specifications, as mentioned earlier, report a ceiling frequency range of 12 GHz for a FFT. However, in house tests have shown that if the dipole is sufficiently large or the spectra is strong, measurements of up to 17 GHz or more have been achieved by the direct digitization technique but there is a large power dropoff in these regions. This, however, has not been confirmed to be linked to the direct digitization itself but rather a oscilloscope digitization problem. The scope's bandwidth, according to Tektronix® is noted by a loss of 3 dB of signal input versus scope output and exponentially drops off from there. This means that at frequencies 12 GHz some signals just may not be strong enough to overcome the scope's dropoff. This technique was first

utilized on bromofluoroacetonitrile[35], a larger molecule with a dense spectra. Even with the bandwidth limitations of the scope, the molecule was measured in the 8-14 GHz region.

2.6.3. Current Spectrometer and Automation

The improvements on the original design mentioned to this point have culminated in a new design of a chirped-pulse fast passage technique that involves either a PLO mix down stage or a directly digitized experiment. Recently, larger molecules have been the focus of many experiments. Since these spectra are typically more dense, direct digitization is not such the handicap that it is with the more sparsely populated spectra (such as linear or diatomic molecules). When the higher frequencies are needed, a PLO mix down is employed to get the spectra that lies above the bandwidth of the oscilloscope.

Along with the direct digitization improvements, an easier way of obtaining and handling of spectra has been discovered through automation of the technique. This automation employs the use of the National Instruments^{TM} software LabView^{TM}.The arbitrary waveform generator, oscilloscope, microwave synthesizer, and pulse delay generator are all connected to a personal computer (PC) via multiple General Purpose Interface Bus (GPIB) IEEE-488 cables. The PC carries the LabView^{TM} software which tells the setup how many acquisitions are desired, how many frequency ranges, the size of each range, the desired FID size, and the location to save the data. Multiple runs at each frequency range can then be collected, compiled, and analyzed on another computer while another run can be made. This setup is completely standalone and has "set it and forget it" capabilities without wasting sample. It has been furthur described in the literature.[47]

Alongside the electronics of the current spectrometer, three types of sampling methods have been utilized through the pulsed nozzle: gas, volatile liquid sampling, and a laser ablation source. All three will be covered in later parts of this work. This allows the spectrometer to have a wide range of uses for quickly obtaining spectral data. This technique is standalone or works well as a quick way to search for transitions, get a fit of parameters and then continue to search for less intense lines with other techniques. Finally, the technique

allows the flexibility to study many types of systems from very complicated to prototypical without the complication of large search times for molecules.

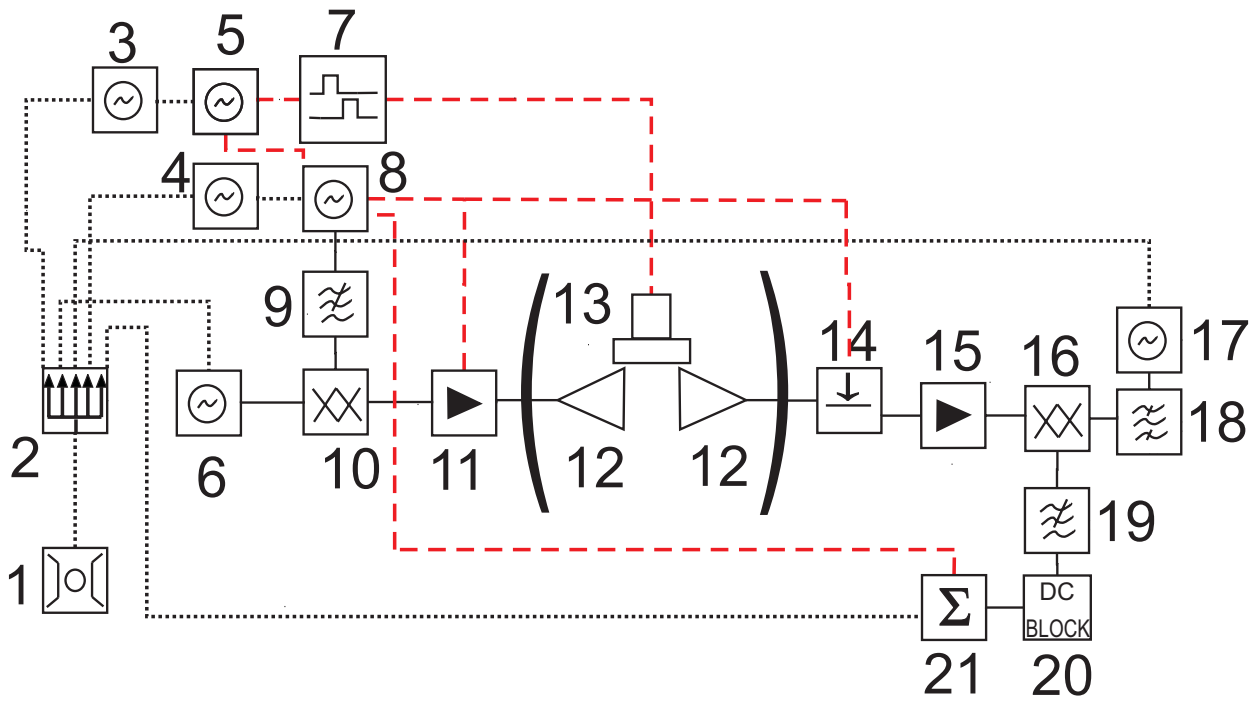

FIGURE 2.5. The chirped pulse Fourier Transform spectrometer using a Phased Locked Oscillator Mix Down. Solid lines are microwave frequencies for use in experiment. Dotted lines are reference frequencies. Red dashed lines are timing control connections. Components are 1. Stanford Research Systems 10 MHz Rb Standard Model FS725, 2. 10 MHz Distribution Amplifier, Wenzel Associates 600-15888, 3. Nexyn Corporation 640 MHz Phase Locked Oscillator, NXPLOS-0064-02381, 4. Nexyn Corporation 3.96 GHz Phase Locked Oscillator NXPLOS-0396-02381, 5. Tektronix AWG2041 Arbitrary Waveform Generator, 6. Microwave Synthesizer, HP 8341A, 7. Berkeley Nucleonics Corporation Pulse Generator, 8. Tektronix AWG 710B 4.2 GS/s Arbitrary Waveform Generator, 9. Low Pass Filter, Minicircuits VLF-1800+, 11. Mixer, Miteq DB0418LW1, 11. 5W Power Amplifier, Microwave PowerL0818-37, 12. Horn Antennae, Amplifier Research AR 4004, 13. Series 9 Solenoid Valve, Parker-Hannifin, 14. SPST Switch 0.5-18.0 GHz, Advanced Technical Materials AMT31517D, 15. Low Noise Amplifier, Miteq AMF-6F-0800-1800-14-10P, 16. Mixer, Miteq DM0520LW1, 17. Phase Locked Oscillator Nexyn 18.99 GHz, NXPLOS-TX-1899-02405, 18. 18.99 GHz Bandpass Filter 19. 12 GHz Lowpass Filter, 20. DC-250 MHz Block, 21. Oscilloscope, Tektronix TDS6124C 40GS/s 12GHz.

CHAPTER 3

CHIRPED PULSE FOURIER TRANSFORM MICROWAVE SPECTROSCOPY OF PERFLUOROIODOETHANE

3.1. Introduction[1]

Fluorinated molecules such as perfluoroiodoethane have been shown to undergo telomerization to fluorinated polymers.[48] Radical reactions of this type are understood to initiate by an iodine atom leaving and the reaction proceeding through a series of radical reaction steps.

Only two other perfluorinated alkyl iodides, namely perfluoroiodomethane[49] and *trans*-perfluoroiodopropane[31] have previously been studied by microwave spectroscopy. So far, this family of molecules has been shown to have slightly larger values for the Iodine nuclear electric quadrupole coupling tensor χ_{zz} components than their alkyl iodide analogues.[31]

The structure of perfluoroiodoethane, as well as barriers to internal rotation, have previously been studied by electron diffraction[50], Raman/infrared[51], and far-infrared[52] experiments. Electron diffraction experiments conclude a C–C–I bond angle of of 113.4° and, notably, show the structure as having a F–C–C–I dihedral angle of 171.9°.[50] The Raman/infrared and far-infrared experiments performed report different barriers to internal rotation about the C–C bond as being 2480 cm^{-1}[51] and 1917 $\pm$ 48 cm^{-1}[52]. In this work we report structural details for perfluoroiodoethane obtained through microwave spectroscopic measurements and quantum chemical calculations.[19]

3.2. Experiment

An approximately 3% solution of perfluoroiodoethane gas (Aldrich®, 98%) in argon was

[1]Chapter reproduced in full from Ref. [19] from Elsevier©

prepared; backing pressures of 4 - 5 bar were used. This gas mix was then used in a search accelerated, correct intensity Fourier transform microwave (SACI-FTMW) spectrometer. This instrument was described in detail in chapter 2. Briefly, the instrument mixes a microwave pulse of frequency ν with a fast 4 μs linear frequency sweep of DC-1 GHz generating a ν $\pm$ 1 GHz broadband pulse. The pulse is then amplified (5 W) using a solid state amplifier and broadcast onto the gas sample through a horn antenna. The sample of gas was pulsed through a Parker-Hannifin^{TM} solenoid valve with a 0.762 mm orifice into a vacuum chamber held at 10^{-5} bar. After a delay of 1 μs, a second antenna horn receives any free induction decay (FID). The signal is then passed through an amplification stage and then proceeds to be directly digitized on a 12 GHz, 40 GS/s oscilloscope (Tektronix^{TM} TDS6124 Digital Oscilloscope). A sample portion of this spectra is shown in Figure 3.1.

The experimental sequence described above takes place at a rate of 4 Hz and FIDs were averaged for approximately 30,000 acquisitions. Signal averaged regions of 2 GHz were obtained in 2-3 hours. Linewidths for these experiments are approximately 80 kHz and a 15 kHz uncertainty was attributed to frequency measurements. In those cases where transitions were blended, a 50 kHz uncertainty was assigned.

3.3. Quantum Chemical Calculations

Quantum chemical calculations were performed primarily to aid in spectral assignment. An m06-2X density functional method[53, 54] with a 6-311G** basis set[55, 56] obtained from the EMSL basis set library[57, 58] was utilized with the GAMESS software suite.[59] We also performed a simple calculation for an assumed *anti* conformation utilizing typical bond lengths and bond angles found in the literature[60]. This calculation was made using the PMIFST program from the Programs for ROtational SPectroscopy (PROSPE) website.[61]

3.4. Results and Analysis

The quantum chemical calculated parameters are tabulated in Table 3.1. A picture of this calculated structure can be found in Figure 3.2. The A, B, and C rotational constants

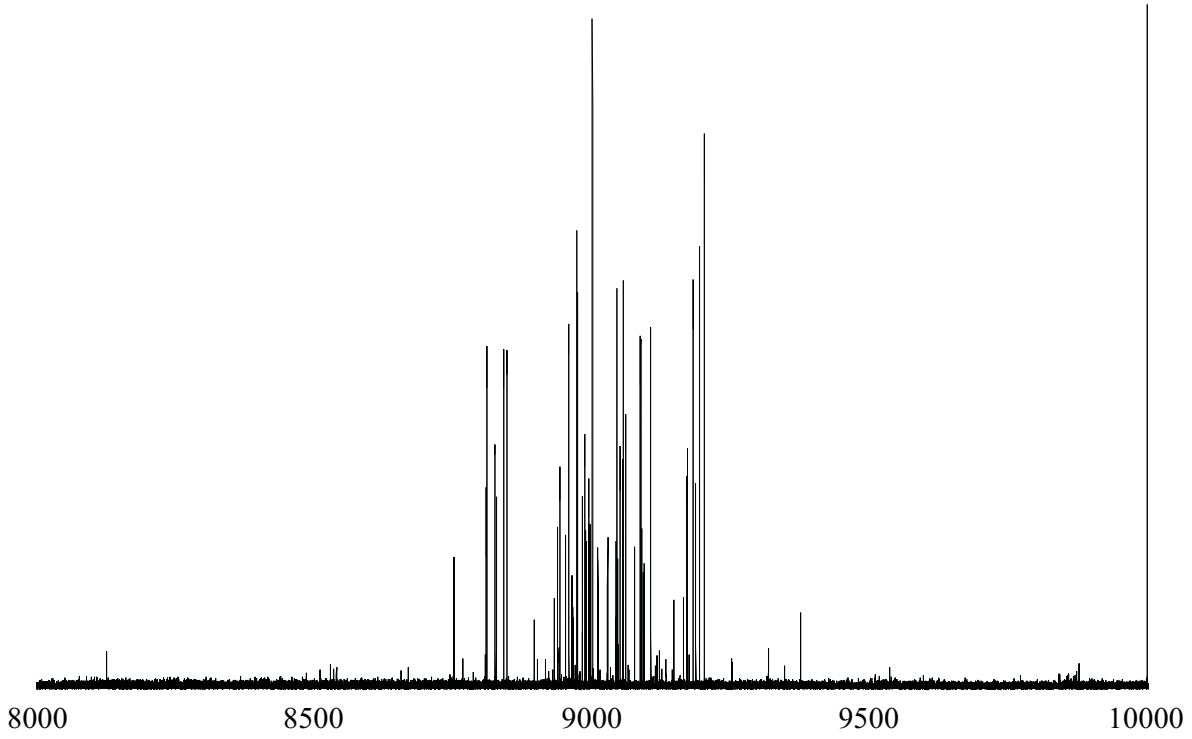

FIGURE 3.1. Sample spectrum of perfluoroiodoethane centered at 9000 MHz after 30,000 averaging cycles.

from our calculations are compared to the electron diffraction work[50] in Table 3.2. Iodine-127 has a large quadrupole moment (Q = -696(12) mb; $I = \frac{5}{2}$)[62] and an initial guess of the ^{127}I nuclear electric quadrupole coupling tensor was made using previous work on perfluoroiodopropane.[31] The quadrupole coupling tensor was then employed alongside the rotational constants from the quantum chemical calculation in Pickett's SPCAT program [63] in order to begin quantum number assignment.

Amongst 247 assigned transitions, only one conformer of perfluoroiodoethane was observed. No *c*-type spectra were observed amongst *a*- and *b*-type, R- and Q-branch spectra. Two forbidden $\Delta J = 2$ transitions were also observed. Less abundant ^{13}C spectra were not observed in the spectrum.

The AABS package[64] from the PROSPE website was utilized in the analysis.[61] Quantum number assignments were achieved through matching predicted spectral patterns with

TABLE 3.1. Calculated Structural Parameters for Perfluoroiodoethane.[a]

Bond	Length	Angle	Measurement
r(C(1) - F(1))	1.326 Å	∠(F(1),C(1),C(2))	110.8°
r(C(1) - F(2))	1.326 Å	∠(F(2),C(1),C(2))	110.3°
r(C(1) - F(3))	1.330 Å	∠(F(3),C(1),C(2))	108.8°
r(C(1) - C(2))	1.540 Å	∠(F(4),C(2),C(1))	107.8°
r(C(2) - F(4))	1.335 Å	∠(F(5),C(2),C(1))	108.0°
r(C(2) - F(5))	1.336 Å	∠(I,C(2),C(1))	112.6°
r(C(2) - I)	2.155 Å	∠(I,C(2),F(4))	109.9°
		∠(I,C(2),F(5))	109.9°
		Dihedral ∠(I,C(2),C(1),F(3))	178.5°

[a] See text for details of the calculation.

their observed counterparts. This task was further facilitated due to the "correct intensity" feature of the SACI-FTMW spectrometer; see Figure 3.3. Figure 3.3 also shows why a 50 kHz uncertainty was assigned to blended transitions, as the figure indicates a pair of transitions in the predicted spectra that are very close in energy to one another. These transitions are only seen as a single broad line in the observed spectra, slightly increasing the line width. A total of 247 observed transitions have been assigned and tabulated this way. All transitions together with assignments may be found in the supplementary data.

TABLE 3.2. Predicted and Literature Rotational Constants for Perfluoroiodoethane.

Parameter	Simple Calculation[a]	m06-2X/6-311G**	Electron Diffraction[b][50]
A / MHz	2155.0	2194.3	2177.9
B / MHz	811.1	777.2	785.1
C / MHz	746.1	719.6	721.6

[a] Obtained using typical structural values from Ref. [60].

[b] Rotational constants derived from Cartesian coordinate structure given in Ref.[50].

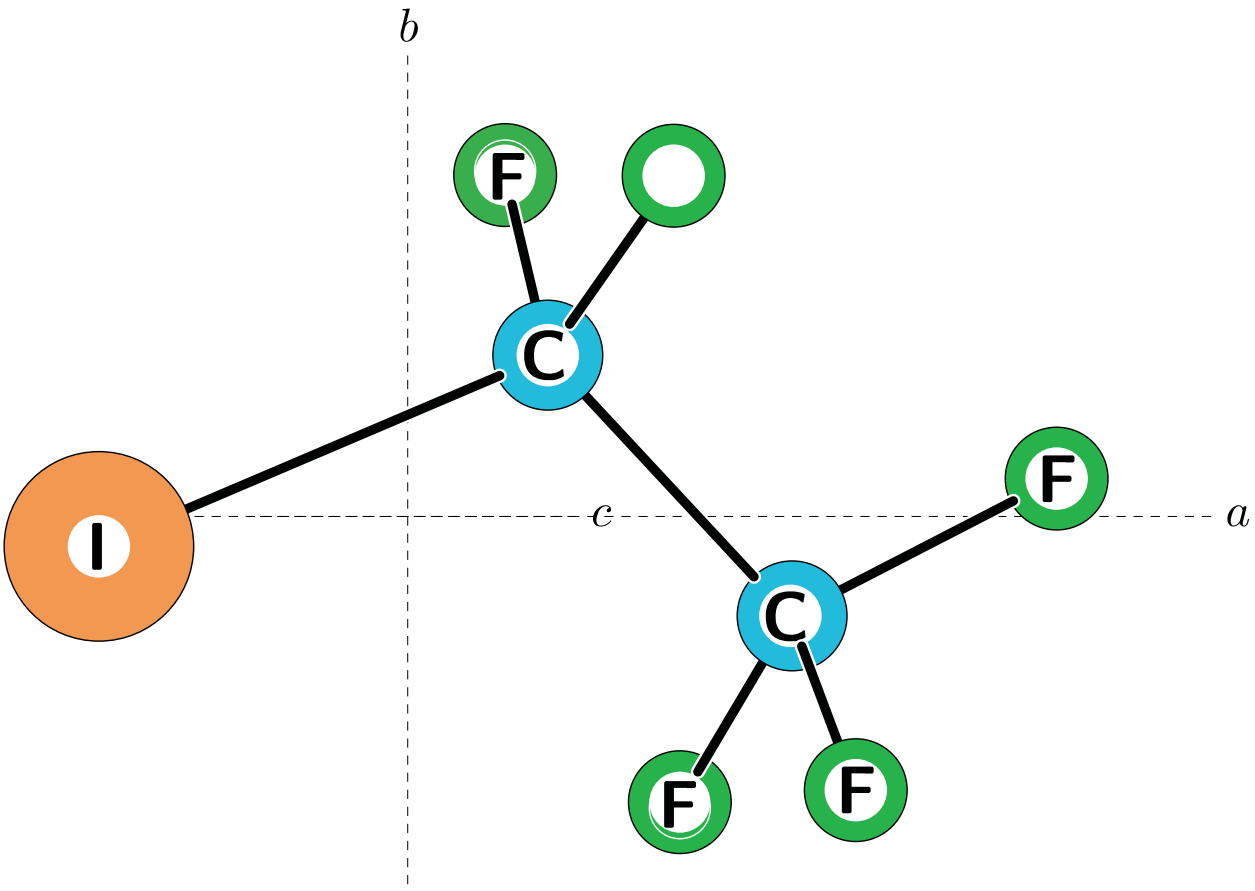

FIGURE 3.2. Calculated structure of perfluoroiodoethane in the *ab* plane.

Following assignment, rotational constants A, B, and C; centrifugal distortion constants, Δ_J, Δ_{JK}, and δ_J; ^{127}I nuclear electric quadrupole tensor values, χ_{aa}, χ_{bb}, χ_{cc}, and $\mid \chi_{ab} \mid$; and ^{127}I nuclear spin-rotation constants, M_{aa}, M_{bb}, and M_{cc} in the Flygare notation[65] were determined using Pickett's SPFIT program[63] with a Watson-A reduced Hamiltonian [16, 17] in the I^r representation. The experimental spectral constants have been tabulated in Table 3.3. Only the χ_{ab} off-diagonal component of the ^{127}I-nuclear electric quadrupole coupling tensor was required in order to achieve a satisfactory fit.

As mentioned, there is a discrepancy in the literature as to the value of the barrier to internal rotation about the C–C bond, 2480 cm^{-1}[51] versus 1917 ± 48 cm^{-1}[52]. Both values, however, are generally too high to observe effects due to internal rotation and, indeed, no evidence of internal rotation was observed in the spectrum.

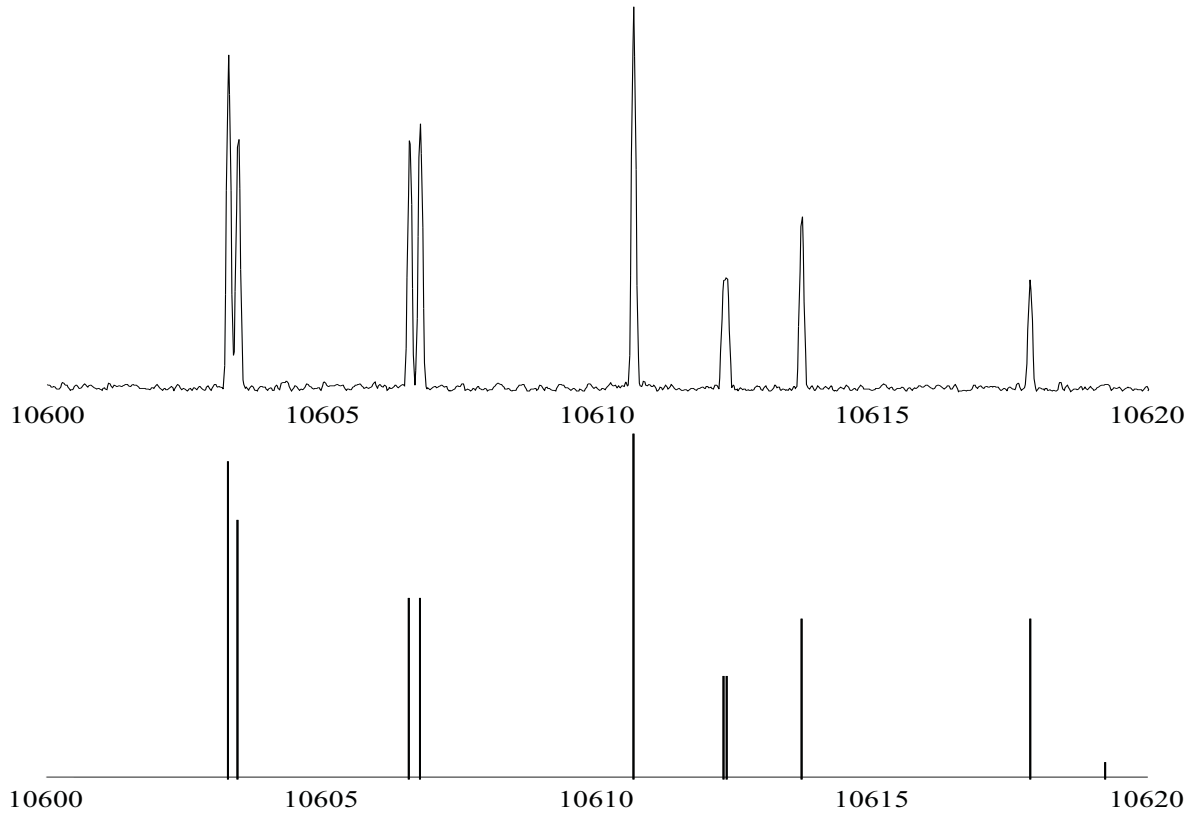

FIGURE 3.3. Comparison of perfluoroiodoethane spectra (top) with the predicted spectra (bottom) between 10600 and 10620 MHz.

3.5. Discussion

3.5.1. Structure

The bond angles and bond lengths of the quantum chemical calculated structure are detailed in Table 3.1. The values of the C–F bond lengths in the table are consistent with those of trifluoromethane (1.332 ± .008 Å) and trifluorochloromethane (1.328 ± .02 Å) found in the literature.[60] The calculated C–I bond length of 2.155 Å is in accordance with the cited C–I bond length of perfluoroiodoethane from the electron diffraction work (2.139 ± .017 Å).[50] The calculated C–C single bond length of 1.540 Å is also in accordance with typical C–C single bond literature values[60] and also the electron diffraction work (1.554 ± .012 Å).[50] As for the bond angles from the calculation, all of the angles lie within 4° of the standard tetrahedral bond angle of 109.5°.

TABLE 3.3. Spectroscopic Parameters for Perfluoroiodoethane.

Parameter	Experiment
A / MHz	2178.39031(38)[a]
B / MHz	782.01491(18)
C / MHz	722.30778(14)
Δ_J / kHz	0.05148(98)
Δ_{JK} / kHz	0.0566(36)
δ_J / kHz	0.00591(64)
χ_{aa} / MHz	-1739.8608(95)
χ_{bb} / MHz	663.0608(145)
χ_{cc} / MHz	1076.8007(110)
$\mid \chi_{ab} \mid$ / MHz	1052.618(21)
M_{aa} / kHz	2.47(50)
M_{bb} / kHz	2.86(26)
M_{cc} / kHz	2.65(25)
η_a^b	0.2378
N[c]	247
RMS[d]	0.39320

[a] Numbers in parentheses give standard errors

(1σ, 67% confidence level) in units of the least significant figure.

[b] The asymmetry of the χ tensor in the principal inertial axes system, $\eta_a = (\chi_{bb} - \chi_{cc})/\chi_{aa}$.

[c] Number of observed transitions used in the fit.

[d] Root mean square deviation of the fit, $\sqrt{\left(\sum \left[((\text{obs} - \text{calc})\,/\text{error})^2\right]\,/\text{Nlines}\right)}$

The angle of interest, however, is the dihedral ∠IC(2)C(1)F(3). The quantum chemical calculations show perfluoroiodoethane to be in an essentially *anti* conformation with a I–C–C–F dihedral angle of 178.5° (see Table 3.1). This, however, is almost certainly a convergence limit issue and, if the criteria for convergence was increased, would probably

converge to 180°. However, electron diffraction work previously carried out showed a significantly different perfluoroiodoethane dihedral angle of 171.9°.[50] This number was obtained using the Cartesian structure given in the article.

From experimental data, the combination of no observed *c*-type transitions and only needing the χ_{ab} off-diagonal component of the ^{127}I nuclear electric quadrupole tensor point to an *anti* conformation, i.e. a ≈180° ICCF dihedral angle. The values of the second moments[2] are reported in Table 3.4. A small P_{cc} value of 89.287603(103) amuÅ^2 is obtained in contrast to the values of P_{aa} and P_{bb} of 556.960945(103) amuÅ^2 and 142.707553(103) amuÅ^2, respectively. The relatively small P_{cc} value is also consistent with an *anti* conformation with just four out of plane fluorine atoms.

TABLE 3.4. Second Moments from Experiment.

Parameter	Measurement[a]
P_{aa} / amuÅ^2	556.960945(103)
P_{bb} / amuÅ^2	142.707553(103)
P_{cc} / amuÅ^2	89.287603(103)

[a] Numbers in parentheses give standard errors (1σ, 67% confidence level) in units of the least significant figure.

3.5.2. Iodine Nuclear Electric Quadrupole Coupling

Nuclear electric quadrupole splitting arising from the coupling of the nuclear spin of ^{127}I with the rotation of the molecule was observed. All three diagonal components, χ_{aa}, χ_{bb}, and χ_{cc} were determined along with one off-diagonal component, χ_{ab}. These values are reported in Table 3.3. The sign of χ_{ab} cannot be determined, therefore only the magnitude of this parameter is reported. For comparison with similar molecules, the nuclear electric quadrupole coupling tensor has been diagonalized into the *xyz* space-fixed axis system using the QDIAG utility program from the PROSPE website.[61] These values are reported in Table 3.5.

Table 3.5 also reports the χ_{xx}, χ_{yy}, and χ_{zz} values for perfluoroiodoethane are compared to two previous studies performed on the the non-fluorinated analogue, iodoethane.[66, 67] The value of χ_{zz} for perfluoroiodoethane is reported as -2135.746(41) MHz as compared to -1814.56(59) MHz[67] and -1815.693(210) MHz[66] for iodoethane. The increase in the magnitude of χ_{zz} of approximately 17% from the previous studies of iodoethane to the perfluorinated derivative is consistant with a decrease in the ionicity of the C–I bond in iodoethane. A similar observation has been discussed before in ref.[31] in regards to the comparison of χ_{zz} for *trans*-1-iodoperfluoropropane with 1-iodopropane.

TABLE 3.5. The Iodine Nuclear Electric Quadrupole Coupling Tensor Rotated into the Principal Axis System for Perfluoroiodoethane compared to Previous Iodoethane Work.

Parameter	CF_3CF_2I	CH_3CH_2I[67]	CH_3CH_2I[66]
χ_{zz} / MHz	-2135.746(41)[a]	-1814.56(59)	-1815.693(210)
χ_{xx} / MHz	1058.945(48)	900.79(59)	902.046(138)
χ_{yy} / MHz	1076.801(1)	913.762(24)	913.648(73)
η[b]	0.00836(3)	0.00715(32)	0.00639[c]
θ^d_{za}	20.611(1)°	20.607(14)°	20.637°

[a] Numbers in parentheses give standard errors (1σ, 67% confidence level) in units of the least significant figure.

[b] The asymmetry of the χ tensor in the space-fixed axes system, $\eta = (\chi_{xx} - \chi_{yy})/\chi_{zz}$.

[c] Error not reported.

[d] The angle between the z and a axis. θ_{zb} is the +90° complement of θ_{za}

Also reported in Table 3.5 is η, the cylindrical asymmetry of the χ tensor in the space-fixed axis system.[2] The value reported in Table 3.5 for η shows only a slight increase in asymmetry of the tensor when compared to the previous iodoethane studies.[66, 67] All values reported are very close to zero, indicating near cylindrical symmetry of the electric field gradient about the C–I bond. The experimental data collected indicates that the main difference in

χ between these two molecules lies in the difference between the group electronegativities of the alkyl and perfluoroalkyl groups.

The ^{127}I χ_{zz} value for perfluoroiodoethane is also compared to other perflourinated iodoalkyl molecules[31, 49] as well as the non-fluorinated analogues[66, 67, 68, 69] in Table 3.6. In this small sampling, the magnitude of χ_{zz} for perfluoroiodoethane is slightly less than the magnitude of the other molecules in the class. CF_3I, CF_3CF_2I, and *trans*-$CF_3CF_2CF_2I$, all share similar ionicity (or covalency) of the C–I bond even as -CF_3 or -CF_2 groups are added. This trend is not followed in the transition from iodomethane to iodoethane, but is resumed again in the iodoalkyl's when transitioning from iodoethane to *trans*-iodopropane.

TABLE 3.6. Comparison of Iodine Nuclear Electric Quadrupole Coupling Constants for a Series of simple Alkyl Iodide and Perfluoroalkyl Iodide Compounds.

Molecule	χ_{zz} / MHz	Ref.
CH_3I	-1934.080(10)	[68]
CH_3CH_2I	-1814.56(59)	[67]
	-1815.693(210)	[66]
trans-$CH_3CH_2CH_2I$	-1814.55(55)	[69]
CF_3I	-2144.7(6)	[49]
CF_3CF_2I	-2135.746(41)	This Work
trans-$CF_3CF_2CF_2I$	-2142.4509(76)	[31]

3.5.3. Forbidden Transitions

Two traditionally forbidden $\Delta J = 2$ transitions were observed for perfluoroiodoethane. These transitions are the $6_{2,4}\ \frac{15}{2} \leftarrow 4_{3,1}\ \frac{13}{2}$ and $7_{3,4}\ \frac{17}{2} \leftarrow 5_{4,1}\ \frac{15}{2}$, see Table 3.7. Given the large χ_{ab} value for perfluoroiodoethane, traditionally dipole forbidden transitions may become "quadrupole allowed" through nearly degenerate energy levels connected via χ_{ab}. The coefficient of mixing, P_{mix}, between states is given in the SPFIT/SPCAT software through

the EGY output file.[63] A $P_{\rm mix}$ of unity indicates a "pure" state while a $P_{\rm mix}$ of 0.5 means the state is completely mixed with one other energy state for a two state system. In Table 3.7, values of $P_{\rm mix}$ for the energy levels involved in the forbidden transitions are presented.

TABLE 3.7. Observed Forbidden Transitions for Perfluoroiodoethane.

$J'_{K_{-1},K_{+1}}$	F'	$P^a_{\rm mix}$	$J''_{K_{-1},K_{+1}}$	F''	$P^a_{\rm mix}$	Frequency /MHz	Obs-Calc / kHz
$6_{2,4}$	$\frac{15}{2}$	0.9721	$4_{3,1}$	$\frac{13}{2}$	0.9450	9545.16434	4.1[b]
$7_{3,4}$	$\frac{17}{2}$	0.9557	$5_{4,1}$	$\frac{15}{2}$	0.9858	9674.48249	-11.4[b]

[a] $P_{\rm mix}$ is the mixing coefficient for the rotational energy level and is obtained from the SPCAT software. See text for details.

[b] Note, 15 kHz assigned uncertainty in line centers.

In perfluoroiodoethane the off-diagonal component of the nuclear electric quadrupole coupling tensor is χ_{ab}. This means that the forbidden transition must be due to mixing of one of the energy levels with a third intermediate state linked via a *c*-type change in parity. This is more easily illustrated in Figure 3.4 for the perfluoroiodoethane $6_{2,4}\ \frac{15}{2} \leftarrow 4_{3,1}\ \frac{13}{2}$ transition.

The observed, forbidden transition in Figure 3.4 is a *b*-type transition. In order to be allowed by the χ_{ab} component, at least one of the states, either $6_{2,4}\ \frac{15}{2}$ or $4_{3,1}\ \frac{13}{2}$, must mix with a state linked by "*c*-type" parity. To locate this state, the EGY file from SPCAT was utilized. This file shows wavefunction energy levels and coefficients. Since the value of $P_{\rm mix}$ for the $4_{3,1}\ \frac{13}{2}$ showed a larger deviation from unity than the $6_{2,4}\ \frac{15}{2}$ state, then possible *c*-type parity mixtures of this energy state were looked at first. The state that fit this criteria was the $5_{2,3}\ \frac{13}{2}$ energy state. The $5_{2,3}\ \frac{13}{2}$ level is seperated in energy from the $4_{3,1}\ \frac{13}{2}$ level by approximately 500 MHz, and has the required *c*-type parity relation to the $4_{3,1}\ \frac{13}{2}$ level.

An observed *a*-type transition, $6_{2,4}\ \frac{15}{2} \leftarrow 5_{2,3}\ \frac{13}{2}$, transition was observed at 9055.416(15) MHz. The $6_{2,4}\ \frac{15}{2} \leftarrow 4_{3,1}\ \frac{13}{2}$ transition was observed at 9545.164(15) MHz giving a "closed loop" energy difference between the $4_{3,1}\ \frac{13}{2}$ and $5_{2,3}\ \frac{13}{2}$ energy states of 489.748(15) MHz

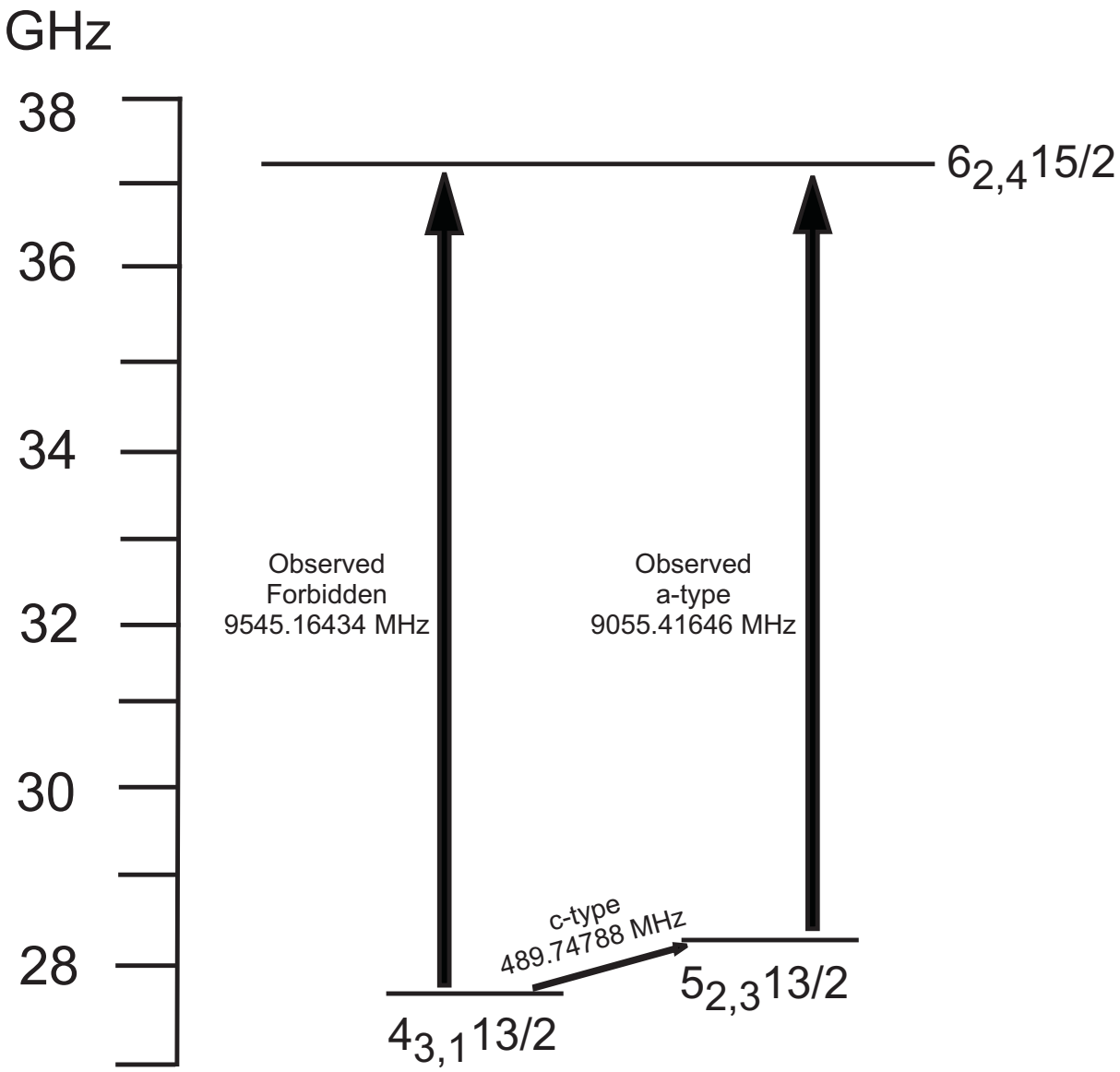

FIGURE 3.4. Forbidden Transition Pathway for the $6_{2,4}\ \frac{15}{2} \leftarrow 4_{3,1}\ \frac{13}{2}$ Transition.

in agreement with the EGY file produced from SPCAT. The observation of both dipole forbidden transitions presented in Table 3.7 may be rationalized in this way.

3.6. Conclusion

The spectrum for the main isotopologue of perfluoroiodoethane has been recorded and assigned in the 8.0 to 11.9 GHz region on a Chirped-Pulse Fourier Transform Microwave spectrometer. Rotational constants have been determined and reported. Nuclear electric

quadrupole coupling constants for the ^{127}I atom have been determined for the first time and compared to related species. Forbidden transitions of the type $\Delta J = 2$ have been observed and rationalized. The absence of *c*-type transitions and the observation of only one conformation in the spectrum is consistent with an *anti* configuration in which the ICCF dihedral angle $\approx$180°.

CHAPTER 4

ELECTRONIC AND GEOMETRIC CONSIDERATIONS OF BROMODIFLUOROACETONITRILE UTILIZING FAST PASSAGE FOURIER TRANSFORM MICROWAVE SPECTROSCOPY

4.1. Introduction[1]

Replacing hydrogen atoms with fluorine atoms in a molecule has been shown to have interesting electronic and structural effects.[19, 31, 34, 33, 35, 36, 47, 70, 71, 72, 73, 74] Typically, the electronic variance between the fluorinated species and its hydrogenated analogue has been linked to the electronegativity (electron withdrawing nature) of the fluorine atom. Changes in the electronic environment between these analogues can be monitored with the χ_{zz} component of the nuclear quadrupole coupling tensor. Changes in the magnitude of χ_{zz} give insight into the changes in the electronic environment of the quadrupolar nucleus in question. An example of this type is shown in Table 4.1 for propionyl chloride where there exists a noticeable change in the χ_{zz} value upon fluorination. When applicable, changes in the electronic environment may be studied at more than one nucleus. An example of this is the comparison of chloroacetyl chloride with chlorodifluoroacetyl chloride also located in Table 4.1. In both of these scenarios, fluorination has been shown to have an effect on the electronic environment at the nuclei in question.[47, 70]

Fluorination of a molecule also leads to interesting geometric effects. Materials such as Teflon© (polytetrafluoroethene), for example, have been shown to have a helical structure not found in hydrocarbon polymer analogues.[76] Understanding the mechanism of these structural effects has been a focus of research in the field of rotational spectroscopy.[19, 31, 70, 71]

[1]Chapter reproduced in full from Ref. [38] from Elsevier©

TABLE 4.1. Fluorination Effects on Nuclear Electric Quadrupole Coupling Constants.

^{35}Cl			
Molecule	χ_{zz} / MHz		Ref.
Propionyl Chloride	-59.49(35)[a]		[47]
Perfluoropropionyl Chloride	-65.41(15)		[47]
^{35}Cl/^{35}Cl			
Molecule	–C(=O)Cl χ_{zz} / MHz	–CX_2Cl χ_{zz} / MHz	Ref.
t-Chloroacetyl chloride	-62.4(19)	-77.9(17)	[75]
g-Chlorodifluoroacetyl chloride	-65.3(27)	-74.4(31)	[70]

[a] Numbers in parentheses give standard errors

(1σ, 67% confidence level) in units of the least significant figure.

Bromodifluoroacetonitrile is useful in this regard because, due to the presence of two quadrupolar nuclei, one can investigate both the electronic and geometric effects due to fluorination. While rotational spectroscopy has traditionally given geometric structures[1, 2], the high resolution of chirped pulse Fourier transform microwave (CP-FTMW) spectroscopy allows observation of hyperfine splitting from quadrupolar nuclei and, therefore, accurate determination of nuclear quadrupole coupling constants (NQCCs). By comparing these values across a family of increasingly flourinated species, insight into the changes in electronic structure due to fluorination may be achieved. Recent literature on the rotational spectra of bromoacetonitrile[77] and bromofluoroacetonitrile[35] together with this work allows these comparisons. In this chapter a microwave study producing some electronic and geometric structural parameters for the title molecule bromodifluoroacetonitrile, $CBrF_2CN$, is presented.

4.2. Experiment

An approximately 3% solution of bromodifluoroacetonitrile gas (Aldrich®, 98%) in argon was prepared; backing pressures of 4 - 5 bar were used. This gas mix was then used in a CP-FTMW spectrometer. This instrument has been described in detail elsewhere[28] and is

based upon the chirp pulse experiment previously introduced by Pate and coworkers.[5, 6, 7] Briefly, the instrument mixes a microwave pulse of frequency ν with a fast (5 μs) linear frequency sweep of DC-1 GHz generating a $\nu \pm 1$ GHz broadband pulse. The pulse is then amplified using a 5 Watt solid state amplifier and broadcast onto the gas sample through a horn antenna. The sample of gas was pulsed through a Parker-Hannifin^{TM} solenoid valve with a 0.762 mm orifice into a vacuum chamber held at 10^{-5} torr. The supersonic expansion forces the molecules into cold ($\approx$ 4K) rotational temperatures. The radiation is then turned off and a second antenna horn receives a free induction decay (FID) signal from the decohering molecular ensemble. The signal is then passed through an amplification stage and then proceeds to be directly digitized on a 12 GHz, 40 GS/s oscilloscope (Tektronix^{TM} TDS6124 Digital Oscilloscope). A sample portion of this spectra centered at 13 GHz is shown in the top portion of Figure 4.1.

All transitions measured in the 7.7-18 GHz range were accumulated for at least 10,000 FID averages. For ^{13}C species, 20,000 FIDs were acquired in the 8-14 GHz range. Collection of the averaged FIDs was achieved through the use of an automated experimental setup. This setup has been described previously.[47] Each experimental sequence takes place at a rate of 4 Hz. Linewidths in the experiment are approximately 80 kHz and a 25 kHz uncertainty was attributed to most frequency measurements. Blended spectra received an uncertainty of 50 kHz and, when the spectra had to be assigned by eye, a 30 kHz uncertainty was assigned.

4.3. Quantum Chemical Calculations[2]

As molecules under investigation by microwave spectroscopy become more and more complex, quantum chemical calculations become more and more integral to such investigations.

The primary purpose of the calculations made here is to predict ^{79}Br, ^{81}Br, and ^{14}N NQCCs in bromodifluoroacetonitrile of sufficient accuracy to assist with assignment of the microwave hyperfine structure. Calculation of the NQCCs requires, of course, a molecular structure on which to make the calculation. Thus, in Subsection 4.3.1, calculation is

[2]All calculations and methodologies provided by W. C. Bailey

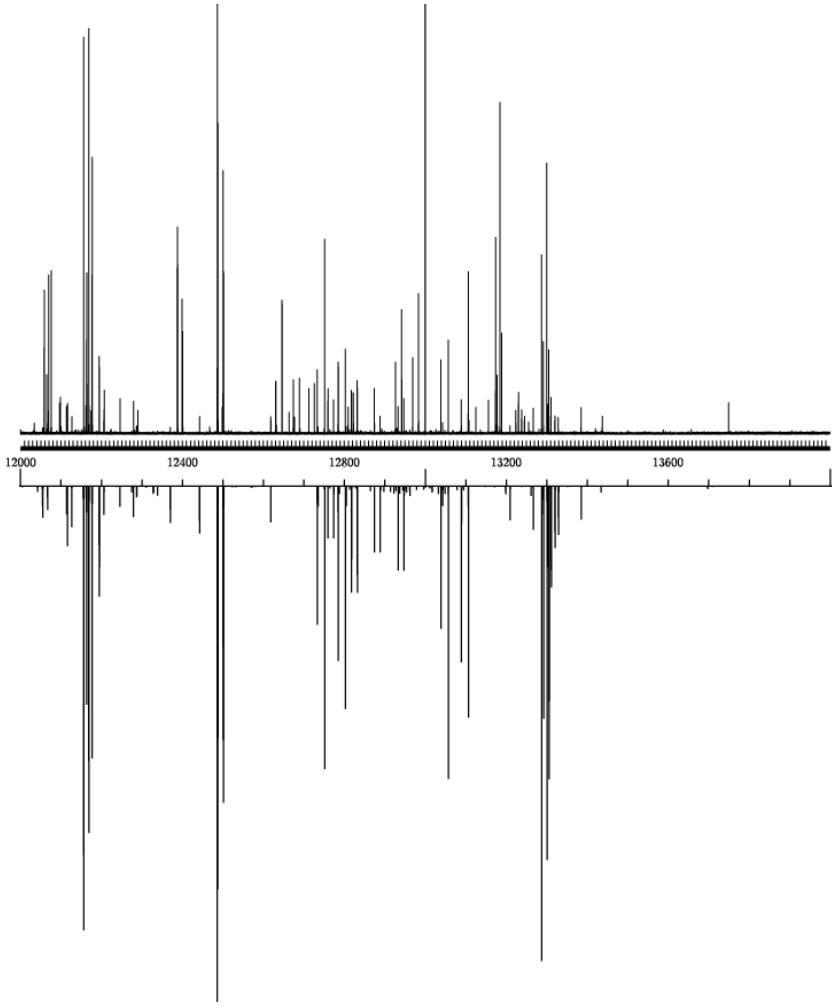

FIGURE 4.1. Top portion: sample spectrum of bromodifluoroacetonitrile centered at 13000 MHz after 20,000 averaging cycles. Bottom portion: $C^{79}BrF_2CN$ prediction.

made of an approximate equilibrium structure of bromodifluoroacetonitrile. Then, in Subsection 4.3.2, calculation is made on this structure of the bromine and nitrogen NQCCs. All calculations for this work were made with the Gaussian 03 suite of programs.[78]

4.3.1. Approximate Equilibrium Structure

An approximate equilibrium structure was derived by MP2/aug-cc-pVTZ optimization followed by empirical correction of the optimized bond lengths via the following equations[70, 79]:

$$\text{C–C } r_e^{emp}(\text{Å}) = 0.95547 \times r_{opt} + 0.06568,\ \text{RSD} = 0.0012\text{Å} \tag{59}$$

$$\text{C–F } r_e^{emp}(\text{Å}) = 0.97993 \times r_{opt} + 0.02084,\ \text{RSD} = 0.0014\text{Å} \tag{60}$$

$$\text{C–B } r_e^{emp}(\text{Å}) = 0.99078 \times r_{opt} + 0.02591,\ \text{RSD} = 0.0003\text{Å} \tag{61}$$

$$\text{C} \equiv \text{N } r_e^{emp}(\text{Å}) = 0.69449 \times r_{opt} + 0.34294,\ \text{RSD} = 0.0020\text{Å} \tag{62}$$

Here, r_{opt} is the MP2/aug-cc-pVTZ optimized bond length. RSD is the standard deviation of the residuals, which may be taken as an estimate of uncertainty in the approximate equilibrium bond lengths, ${r_e}^{emp}$.

Derivation of these linear regression equations was accomplished by MP2/aug-cc-pVTZ optimization of a number of molecules containing C–C, C–F, C–Br, and C≡N bonds for which equilibrium structures have been published and are located in Appendix B. Then, for each bond type, linear regression was made of optimized bond lengths versus equilibrium bond lengths.

Molecular structure parameters of bromodifluoroacetonitrile so derived are given in Table 4.2. The geometry is shown in Figure 4.2.

TABLE 4.2. Calculated Structural Parameters for Bromodifluoroacetonitrile.[a]

Bond	Calculated Length	Angle	Calculated Angle
r(C(1) - F(1))	1.335 Å	∠(Br,C(1),C(2))	109.99°
r(C(1) - F(2))	1.335 Å	∠(F(1),C(1),C(2))	109.87°
r(C(1) - Br)	1.924 Å	∠(F(2),C(1),C(2))	109.87°
r(C(1) - C(2))	1.469 Å	∠(N,C(2),C(1))	179.87°
r(C(2) - N)	1.156 Å	∠(Br,C(1),C(2),N)	0.00°

[a] See text for details of the calculation.

4.3.2. Nuclear Quadrupole Coupling Constants

Components of the NQCC tensor χ_{ij} are related to those of the electric field gradient tensor q_{ij} by

$$\chi_{ij}(\text{MHz}) = (eQ/h) \times q_{ij}(\text{a.u.}), \tag{63}$$

where e is the fundamental electric charge, Q is the electric quadrupole moment of the nucleus in question, and h is Planck's constant. The coefficient eQ/h is taken as a best-fit parameter determined by linear regression analysis of calculated q_{ij} on the experimental structures of a number of molecules versus experimental χ_{ij}. The premise that underlies this procedure is that errors inherent in the computational model - as well as zero-point vibrations and relativistic effects - are systematic and can be corrected, as least partially, by the best-fit coefficient eQ/h.

For bromine, the recommended model for calculation of q_{ij} is B1LYP/TZV(3df,3p). B1LYP is Becke's one-parameter method with Lee-Yang-Parr correlation as implemented by Adamo and Barone.[80, 81] TZV are Ahlrichs bases[82] augmented here with 3 sets of d and one set of f polarization functions on heavy atoms, and 3 sets of p functions on hydrogens. These polarization functions are those recommended for use with Pople 6-311G bases, and were obtained online from the EMSL[3] Basis Set Library.[57, 58] For conversion of q_{ij} to χ_{ij}, eQ/h (^{79}Br) = 77.628(43) MHz/a.u. and eQ/h (^{81}Br) = 64.853(40) MHz/a.u..[83, 79]

For nitrogen, the recommended model for calculation of q_{ij} is B3PW91/6-311+G(df,pd). B3PW91 is Becke's three-parameter method [84] with the correlation functional of Perdew and Wang [85], 6-311+G(df,pd) are Pople-type bases. With this model, eQ/h = 4.5586(40) MHz/a.u..[86, 79]

[3]Environmental Molecular Sciences Laboratory, which is a national scientific user facility sponsered by the Office of Biological and Environmental Research of the Department of Energy, and is located at Pacific Northwest National Laboratory. https://bse.pnl.gov/bse/portal.

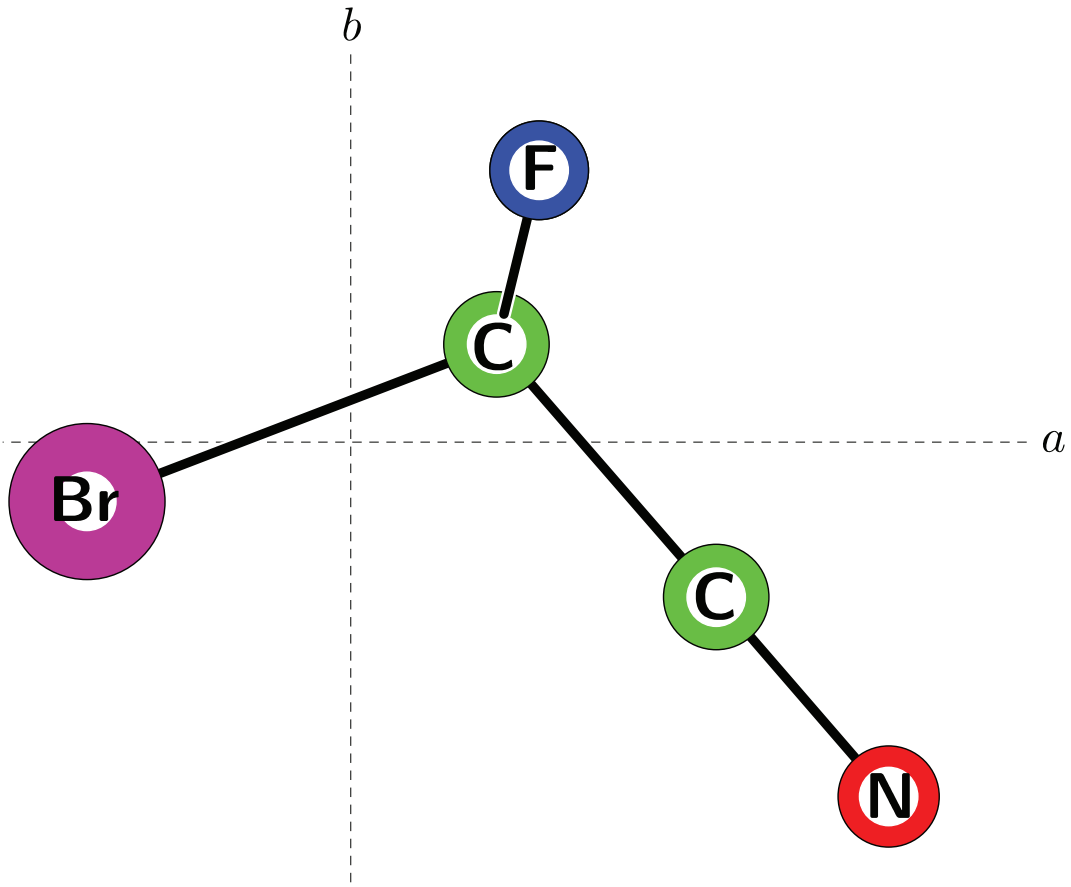

FIGURE 4.2. Calculated structure of $C^{79}BrF_2CN$ in the *ab* plane. The *c*-axis is directly perpendicular to the page. The second flourine is located directly behind the flourine shown.

^{79}Br, ^{81}Br, and ^{14}N inertial axes NQCCs calculated by these methods on the structure derived in Subsection 4.3.1 are given in Table 4.3, along with the corresponding experimental NQCCs.

4.4. Results and Analysis

The spectra are dense with 799 transitions measured for the two major isotopologues (^{79}Br/^{81}Br) and 889 total transitions. The intensity of the spectra combined with the sensitivity of the instrument provided for the observation of ^{13}C substituted species in natural abundance. Bromodifluoroacetonitrile is an asymmetric top ($\kappa \approx$ -0.72) with many spectral features aiding assignment. The spectra mainly consisted of harmonic *a*-type, *R*-branch transitions. For the parent isotopologues, however, some *b*-type, *R*-branch and *a*- and *b*-type, *Q*

TABLE 4.3. Predicted and Experimental Rotational Constants and Nuclear Electric Quadrupole Coupling Constants for the Main Isotopologues of Bromodifluoroacetonitrile.

	$C^{79}BrF_2C^{14}N$		$C^{81}BrF_2C^{14}N$	
Parameter	Predicted	Experimental	Predicted	Experimental
A / MHz	3480.53	3464.121(1)[a]	3477.40	3460.9822(4)[a]
B / MHz	1745.44	1742.5317(3)	1729.65	1726.8014(3)
C / MHz	1459.76	1456.3421(3)	1448.15	1444.7863(2)
$\chi_{aa}^{(Br)}$ / MHz	519.9	512.643(4)	436.3	430.265(4)
$\chi_{bb}^{(Br)}$ / MHz	-209.3	-204.693(6)	-176.8	-173.037(6)
$\chi_{cc}^{(Br)}$ / MHz	-310.6	-307.915(5)	-259.5	-257.228(4)
$\mid \chi_{ab}^{(Br)} \mid$ / MHz	292.7	297.0(1)	242.1	245.5(1)
$\chi_{aa}^{(N)}$ / MHz	-0.787	-0.747(4)	-0.760	-0.723(3)
$\chi_{bb}^{(N)}$ / MHz	-1.682	-1.673(6)	-1.709	-1.703(5)
$\chi_{cc}^{(N)}$ / MHz	2.469	2.420(4)	2.469	2.426(4)
$\mid \chi_{ab}^{(N)} \mid$ / MHz	3.329	3.4(1)	3.325	3.1(1)

[a] Numbers in parentheses give standard errors (1σ, 67% confidence level)
in units of the least significant figure.

branch transitions were also observed. No c-type spectra were observed for any isotopologue, consistent with the expectation of an ab plane of symmetry.

The spectra were assigned using Pickett's SPFIT/SPCAT suite of programs.[63] For this molecule a Hamiltonian of the form

$$\mathbf{H} = H_R + H_{CD} + H_{Q(Br)} + H_{Q(N)} + H_{SR(Br)} \tag{64}$$

was used, where H_R, H_{CD}, $H_{Q(Br)}$, $H_{Q(N)}$, $H_{SR(Br)}$ are the rigid rotor, centrifugal distortion, $^{79}Br/^{81}Br$ nuclear electric quadrupole coupling, ^{14}N nuclear electric quadrupole coupling, and $^{79}Br/^{81}Br$ nuclear magnetic spin-rotation contributions to the Hamiltonian used in the fit, respectively. The fit was done in the I^r representation using a Watson-S reduced

Hamiltonian.[17] The two quadrupole coupling nuclei were handled using the $\mathbf{F}_1 = \mathbf{J} + \mathbf{I_{Br}}$ and $\mathbf{F} = \mathbf{F}_1 + \mathbf{I_N}$ coupling schemes.

The quantum chemical results of Section 4.3 provided a nice starting point for assignment. Table 4.3 emphasizes this by showing the good agreement between calculated molecular rotational constants, as well as ^{79}Br and ^{14}N nuclear quadrupole coupling constants, and the final corresponding experimental constants. This good starting point, used in conjunction with the correct relative intensity feature of the chirped pulse experiment[28], greatly eased the burden of assignment. A graphical front-end program known as the AABS package[64] from the PROSPE website[61] was used to aid in quantum number assignments. This program works with the powerful SPFIT/SPCAT programs by outputting the spectral prediction of SPCAT into a graphical format which may be viewed on a personal computer in one window with the experimental spectra displayed in another window. The bottom portion of Figure 4.1 shows the prediction using the experimental constants of one isotopologue with respect to the measured spectra. This is similar to what one would see using the AABS package. A number of other programs from the PROSPE website were also used in this work.

The fitted parameters for all isotopologues are given in Table 4.4. Only χ_{ab} off-diagonal components of the nuclear electric quadrupole coupling tensors were required, consistent with the expectation of an *ab*-plane of symmetry. As already mentioned, ^{13}C substituted species were measured in natural abundance. However, for these ^{13}C species the large data sets of transitions needed to accurately determine all parameters were not available. Thus, centrifugal distortion constants, nuclear magnetic spin-rotation constants and, in some cases, off-diagonal quadrupole coupling parameters were held to their respective ^{79}Br/^{81}Br parent isotopic values. A listing of all assigned transitions, fits, and calculations are available in Appendix B.

4.5. Discussion

A Kraitchman isotopic substitution analysis[18] was performed at the bromine and carbon atoms. The results of this analysis are compared in Table 4.5 to the calculated structure of Section 3. The bromine calculated principal coordinates lie within the Costain errors[87] of

TABLE 4.4. Spectroscopic Parameters for Bromodifluoroacetonitrile.

Parameter	$C^{79}BrF_2CN$	$C^{81}BrF_2CN$	$^{13}C^{79}BrF_2CN$	$^{13}C^{81}BrF_2CN$	$C^{79}BrF_2{}^{13}CN$	$C^{81}BrF_2{}^{13}CN$
A / MHz	3464.121(1)[a]	3460.9822(4)	3459.876(6)	3456.4(3)	3453.0(3)	3450.2(1)
B / MHz	1742.5317(3)	1726.8014(3)	1740.248(2)	1724.436(2)	1727.078(5)	1711.405(2)
C / MHz	1456.3421(3)	1444.7863(2)	1453.975(1)	1442.370(6)	1443.696(6)	1432.154(1)
D_J / kHz	0.313(6)	0.311(5)	0.313[d]	0.311[d]	0.313[d]	0.311[d]
D_{JK} / kHz	-0.99(2)	-0.91(1)	-0.99[d]	-0.91[d]	-0.99[d]	-0.91[d]
D_K / kHz	1.5(3)	2.94(3)	1.5[d]	2.94[d]	1.5[d]	2.94[d]
d_1 / kHz	-0.085(2)	-0.088(3)	-0.085[d]	-0.088[d]	-0.085[d]	-0.088[d]
$\chi_{aa}^{(Br)}$ / MHz	512.643(4)	430.265(4)	513.65(8)	430.6(2)	511.(1)	426.6(1)
$\chi_{bb}^{(Br)}$ / MHz	-204.693(6)	-173.037(6)	-205.85(13)	-174.1(4)	-203.3(11)	-169.1(1)
$\chi_{cc}^{(Br)}$ / MHz	-307.915(5)	-257.228(4)	-307.8(1)	-256.5(3)	-307.7(5)	-257.5(1)
$\lvert\chi_{ab}^{(Br)}\rvert$ / MHz	297.0(1)	245.5(1)	296.(1)	246.(4)	297.0(1)[d]	251.(2)
$\chi_{aa}^{(N)}$ / MHz	-0.747(4)	-0.723(3)	-0.66(9)	-0.9(2)	-0.1(2)	-0.94(9)
$\chi_{bb}^{(N)}$ / MHz	-1.673(6)	-1.703(5)	-1.67(11)	-2.0(3)	-1.9(4)	-1.06(13)
$\chi_{cc}^{(N)}$ / MHz	2.420(4)	2.426(4)	2.33(7)	2.9(2)	2.0(3)	2.0(1)
$\lvert\chi_{ab}^{(N)}\rvert$ / MHz	3.4(1)	3.1(1)	3.(2)	3.1[d]	3.4[d]	3.1[d]
M_{aa} / kHz	1.2(6)	0.4(5)	1.2[d]	0.4[d]	1.2[d]	0.4[d]
M_{bb} / kHz	3.9(5)	4.5(4)	3.9[d]	4.5[d]	3.9[d]	4.5[d]
M_{cc} / kHz	3.3(5)	4.8(4)	3.3[d]	4.8[d]	3.3[d]	4.8[d]
N[b]	362	437	35	20	12	23
RMS[c]	0.42910	0.34911	0.64337	0.89973	0.99302	0.684037

[a] Numbers in parentheses give standard errors (1σ, 67% confidence level) in units of the least significant figure.

[b] Number of observed transitions used in the fit.

[c] Root mean square deviation of the fit, $\sqrt{\left(\sum\left[\left((\text{obs}-\text{calc})/\text{error}\right)^2\right]/\text{Nlines}\right)}$

[d] Held value to main isotopologue.

the Kraitchman coordinates, while the two carbon substituted species are in fair agreement with the calculated structure. C(1)–Br, C–C, and ∠(C(2),C(1),Br) determined from the Kraitchman values are 1.902±0.003 Å, 1.495±0.007 Å, and 110.5±0.3°, respectively. These are also compared in Table 4.5 with the calculated parameters, and are in decent agreement. Data for these calculations can be found in Appendix B.

Second moments, moments of inertia, inertial defects, and Ray's asymmetry parameters are shown in Table 4.6.[1, 2] For those isotopologues measured, the P_{cc} values are very

TABLE 4.5. Kraitchman Isotopic Substitution Coordinates for Substituted Atoms vs. Calculational Coordinates.

Bromine	Calculated	Kraitchman[a,b]
a / Å	-1.1572	1.157(1)
b / Å	-0.2600	0.261(5)
c / Å	0.0000	0.000[c]
Carbon-1		
a / Å	0.6394	0.617(2)
b / Å	0.4292	0.4243(3)
c / Å	0.0000	0.000[c]
Carbon-2		
a / Å	1.6029	1.6108(9)
b / Å	-0.6799	0.6926(96)
c / Å	0.0000	0.000[c]
Bond, Angle		
r(C(1) - Br)	1.924 Å	1.902(3) Å
r(C(1) - C(2))	1.469 Å	1.495(7) Å
∠(Br,C(1),C(2))	109.99°	110.5(3)°

[a] Kraitchman analysis does not give algebraic sign component.

[b] Numbers in parentheses give errors (Costain for coordinates[87]) in units of the least significant figure(s).

[c] No error given because calculation is for a planar atom and nonplanar calculations render an imaginary number. Imaginary numbers, in turn, are usually indicative of a value of 0 for the coordinate in question.

similar while there is more change in the P_{aa} and P_{bb} quantities. This is further evidence of the BrCCN backbone lying in the ab plane.

4.5.1. Nuclear Electric Quadrupole Coupling

All inertial axes NQCC tensors in Table 4.4 have been diagonalized into their NQCC principal axes components. The results of these diagonalizations are located in Table 4.7.

TABLE 4.6. Experimental Second Moments, Moments of Inertia, Ray's Asymmetry Parameters and Inertial Defects for six isotopologues of Bromodifluoroacetonitrile.

Parameter	$C^{79}BrF_2CN$	$C^{81}BrF_2CN$	$^{13}C^{79}BrF_2CN$	$^{13}C^{81}BrF_2CN$	$C^{79}BrF_2{}^{13}CN$	$C^{81}BrF_2{}^{13}CN$
P_{aa} / amuÅ^2	245.57781(9)[a]	248.22043(7)	245.9611(5)	248.62(1)	248.160(4)	250.851(4)
P_{bb} / amuÅ^2	101.44163(9)	101.57456(7)	101.6233(5)	101.76(1)	101.899(4)	102.029(4)
P_{cc} / amuÅ^2	44.44791(9)	44.44728(7)	44.4452(5)	44.45(1)	44.461(4)	44.449(4)
I_a / amuÅ^2	145.88954(4)	146.02185(2)	146.0685(3)	146.22(1)	146.359(4)	146.478(4)
I_b / amuÅ^2	290.02572(5)	292.66771(5)	290.4063(3)	293.0692(3)	292.6208(8)	295.3006(3)
I_c / amuÅ^2	347.01943(7)	349.79499(5)	347.5844(2)	350.381(1)	350.059(1)	352.8804(2)
Δ / amuÅ^2	-88.8958(1)	-88.89456(7)	-88.8905(5)	-88.90(1)	-88.921(5)	-88.898(4)
κ	-0.714919	-0.720250	-0.714569	-0.719899	-0.717930	-0.723246

[a] Numbers in parentheses give standard errors (1σ, 67% confidence level) in units of the least significant figure.

Since the sign of the off-diagonal component, χ_{ab}, is not determinable by experiment[88], and since calculation of the diagonal parameters was quite reliable, the calculated sign convention was used in the diagonalization. These values are positive for both the bromine and the nitrogen off-diagonals.

It is worth noting some of the large uncertainties in the NQCC values of Table 4.7. This is not due to attributed experimental uncertainties but to the size of the data set. Some isotopologues did not have enough transitions to determine all the needed parameters in the Hamiltonian. When this was the case, some values were held to the parent isotopic value. Sometimes this involved NQCC tensor elements. When there was enough data to release a parameter, the amount of data was sometimes still limited so that the fit had a large uncertainty. This, however, was not the case in the parent isotopologues so any furthur comparisons or conclusions drawn across a family or about bromodifluoroacetonitrile use only these values as a basis.

NQCCs for ^{79}Br and ^{14}N in related molecules are located in Table 4.8. It is interesting to monitor the magnitudes of χ_{zz} for bromine across the family versus that of the nitrogen

TABLE 4.7. ^{79}Br, ^{81}Br, and ^{14}N Nuclear Electric Quadrupole Coupling Tensor in the NQCC Principal Axes System and Related Properties for Bromodifluoroacetonitrile.

	$C^{79}BrF_2C^{14}N$		$C^{81}BrF_2C^{14}N$		$^{13}C^{79}BrF_2C^{14}N$	
	^{79}Br	^{14}N	^{81}Br	^{14}N	^{79}Br	^{14}N
χ_{zz} / MHz	619.65(6)[a]	-4.64(10)	517.54(6)	-4.35(10)	619.8(6)	-4.2(20)
χ_{xx} / MHz	-307.915(5)	2.22(10)	-257.228(5)	1.93(10)	-307.8(1)	1.88(197)
χ_{yy} / MHz	-311.70(6)	2.420(4)	-260.31(6)	2.426(4)	-312.0(6)	2.33(7)
η[b]	0.0061(1)	0.042(21)	0.0060(1)	0.115(23)	0.007(1)	0.10(47)
θ^c_{za}	19.814(5)°	48.9(1)°	19.570(6)°	49.5(1)°	19.72(5)°	49.7(32)°
	$^{13}C^{81}BrF_2C^{14}N$		$C^{79}BrF_2{}^{13}C^{14}N$		$C^{81}BrF_2{}^{13}C^{14}N$	
	^{81}Br	^{14}N	^{79}Br	^{14}N	^{81}Br	^{14}N
χ_{zz} / MHz	518.0(25)	-4.6(2)	618.4(9)	-4.5(3)	518.3(13)	-4.1(1)
χ_{xx} / MHz	-256.5(3)	1.7(2)	-307.7(5)	2.0(3)	-257.5(1)	2.0(1)
χ_{yy} / MHz	-261.5(25)	2.9(2)	-310.7(10)	2.5(2)	-260.8(13)	2.1(1)
η[b]	0.0097(50)	0.261(62)	0.005(2)	0.114(82)	0.006(3)	0.024(39)
θ^c_{za}	19.5(2)°	50.0(16)°	19.87(3)°	52.4(17)°	20.1(1)°	45.5(7)°

[a] Numbers in parentheses give standard errors (1σ, 67% confidence level) in units of the least significant figure.

[b] The asymmetry of the χ tensor in the space-fixed axes system, $\eta = (\chi_{xx} - \chi_{yy})/\chi_{zz}$.

[c] The angle between the z and a axis. θ_{zb} is the $+90°$ complement of θ_{za}

across the family. The magnitude of the bromine χ_{zz} drops as one fluorine is added to bromoacetonitrile, but as the second fluorine is added it increases. The nitrogen χ_{zz}, however, which is only 3 atoms down from the fluorination event, continuously increases in magnitude from bromoacetonitrile to bromodifluoroacetonitrile.

Focusing on the bromine, χ_{zz} magnitudes for the sequence are ordered $CH_2BrCN > CBrF_2CN > CHBrFCN$. The Townes-Dailey model[89] is often used to interpret the magnitudes of nuclear electric quadrupole coupling constants. One aspect of the model is to

TABLE 4.8. Comparison of ^{79}Br and ^{14}N Nuclear Electric Quadrupole Coupling Constants following Successive Fluorination of Bromoacetonitrile.

^{79}Br			
Molecule	χ_{zz} / MHz	η^a	Ref.
$CH_2{}^{79}BrC^{14}N$	635.2743(27)[b]	0.00935(1)	[77]
$CH^{79}BrFC^{14}N$	612.223(64)	-0.0624(2)	[35]
$C^{79}BrF_2C^{14}N$	619.65(6)	-0.0061(1)	This Work
^{14}N			
Molecule	χ_{zz} / MHz	η^a	Ref.
$CH_2{}^{79}BrC^{14}N$	-4.3126(22)	-0.06507(53)	[77]
$CH^{79}BrFC^{14}N$	-4.49(14)	-0.108(63)	[35][c]
$C^{79}BrF_2C^{14}N$	-4.64(10)	0.042(21)	This Work

[a] The asymmetry of the χ tensor in the principal axes system, $\eta = (\chi_{xx} - \chi_{yy})/\chi_{zz}$.

[b] Numbers in parentheses give standard errors

(1σ, 67% confidence level) in units of the least significant figure.

[c] Corrected diagonalization values from Ref. [35].

relate these magnitudes to electronegativity differences and bond ionicities. In this case, the outcome of the application of the model is surprising in that the C–Br bond ionicity does not change smoothly with increasing fluorination. To examine this matter further, a Natural Bond Order (NBO) analysis[90] was performed on all three molecules at the MP2/aug-cc-pVTZ level to determine the level of ionicity for each quadrupolar atom studied. For the bromine centers, the NBO natural charge was +0.047 for CH_2BrCN, +0.076 for $CBrF_2CN$, and +0.058 for CHBrFCN which does not follow the experimental trend. The bromine χ_{zz} values when examined closer, however, vary only by ≈2% across the family. This makes it difficult to compare the values and draw definitive conclusions from the experimental trend. Higher level theoretical studies may prove useful in understanding these bonding schemes.

Nitrogen, however, shows a different picture from the other end of the molecule. As fluorine is added across the family, the magnitude of χ_{zz} increases. However, for CHBrFCN and $CBrF_2CN$, the magnitudes of χ_{zz} are within the given uncertainties of one another, again making conclusive comparisons difficult. An NBO analysis for nitrogen, however, rendered natural charges of -0.249, -0.280, and -0.324 for $CBrF_2CN$, CHBrFCN, and CH_2BrCN, respectively, in agreement with experiment. Therefore, an explanation for the increase in magnitude due to the fluorines "pulling" more and more electron density toward their side of the molecule as they are being added is reasonable. In a sense, we pass from $\delta^+CH_2Br–CN\delta^-$ to $\delta^-CBrF_2–CN\delta^+$. This passing, in turn, increases the bond covalency of CN which causes an increase in the magnitude of χ_{zz}.

4.6. Conclusion

The microwave spectrum of bromodifluoroacetonitrile has been collected and analyzed. Rotational, centrifugal distortion, nuclear electric quadrupole coupling, and nuclear magnetic spin-rotation constants have been determined and reported. Quantum chemical calculations were made of the molecular structure, rotational constants, and nuclear quadrupole coupling constants. ^{13}C isotopologues were observed and their parameters are also reported. An analysis of the structure of the BrCCN backbone of bromodifluoroacetonitrile shows it to be planar with Kraitchman bond lengths of 1.902±0.003 Å and 1.495±0.007 Å for the C–Br and C–C bonds, respectively, with a C–C–Br bond angle of 110.5±0.3°. Inertial axes NQCC tensors have been diagonalized into their NQCC principal axes components, and compared to related molecules. Changes to the nuclear electric quadrupole coupling tensor among the family of monobrominated acetonitriles have been rationalized in terms of electronegativity changes with successive flourination, but conclusive arguments on the matter need further study.

CHAPTER 5

FAST PASSAGE SPECTRUM OF PIVALOYL CHLORIDE

5.1. Introduction[1]

Properties of simple acyl chlorides have been studied for years. From internal rotations to torsional strain, spectroscopy of all kinds has dominated the field with regards to characterizing these molecules. Of these simple acyl chlorides, acetyl, propionyl, and butyryl chloride have been observed using microwave spectroscopy[91, 92, 93, 94], but pivaloyl chloride, $(CH_3)_3CCOCl$, has not. However, far-infrared work of pivaloyl chloride did provide values on the barriers to internal rotation.[95]

This chapter presents the microwave spectrum and assignment of pivaloyl chloride, shown in Figure 5.1, to provide nuclear quadrupole coupling constants and to look for evidence of internal rotation in the molecule. Both the ^{35}Cl and ^{37}Cl isotopologues have been observed and their nuclear quadrupole coupling constants determined. Looking at previous studies of other acyl chlorides, pivaloyl chloride is similar to these molecules in functionality and reactivity, but is slightly different structurally due to the presence of a tertiary butyl group adjacent to the COCl framework instead of a methyl, primary or secondary carbon in this position. Acyl chlorides are also known as some of the most reactive carboxylic acid derivatives, which also increases the difficulty of study. Even though pivaloyl chloride is no exception, it is the least reactive of the simple acyl chlorides.[96]

Pivaloyl chloride, as calculations predict, is expected to be quite asymmetric. It has an asymmetry parameter, κ, of -0.630 calculated from *ab initio* calculations at the MP2/6-311+G(3d,3p) level.[78] One might also anticipate internal rotation in accordance with other molecules in its class.[91, 92, 93, 94, 95, 97, 98, 99] These types of qualities in a molecule

[1]Chapter reproduced in full from Ref. [29] from Elsevier©

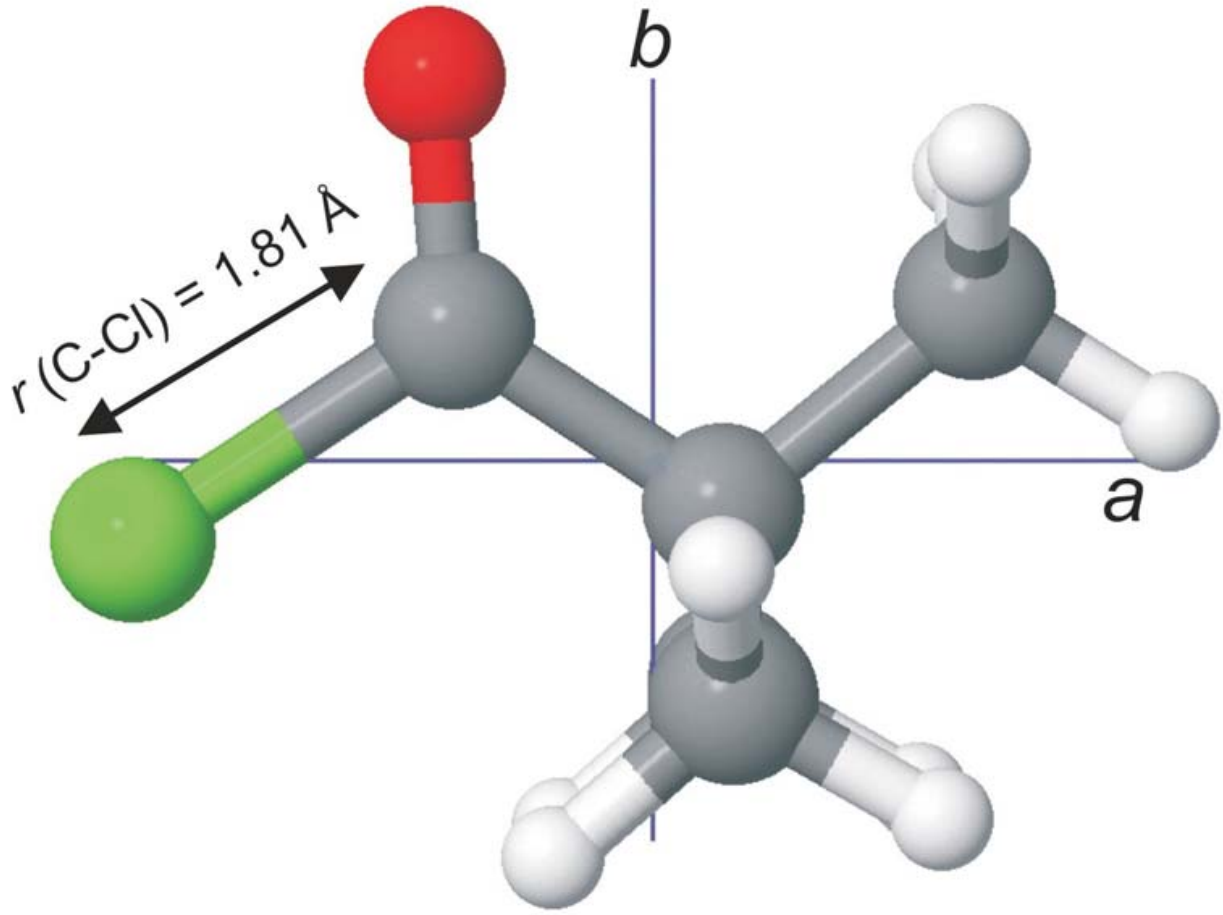

FIGURE 5.1. Structure of pivaloyl chloride as estimated from *ab initio* calculations.

can quickly begin to complicate spectra and increase the difficulty of assigning spectra. This internal rotation could arise from the tertiary butyl group's arrangement relative to the COCl framework or from the rotation of each of the individual methyl groups. If the barrier to any of these rotations is low, splitting of the spectrum will occur and, as stated before, seriously complicate the spectrum.[2] Previous high resolution studies of the ground vibrational state rotational spectrum of the closely related molecule pivalaldehyde [99], showed small ($\backsim$ 50 kHz) splittings in some of the *b*-type transitions arising from the C(=O)H group rotation, although no effects due to the methyl group motions were observed at the low effective temperature of the supersonic expansion. Since the expected barrier for rotation of the tertiary butyl group in pivaloyl chloride was determined by far-infrared measurements to

be more than double that found in pivalaldehyde (807 cm^{-1} versus 337 cm^{-1}), any internal rotation splittings in the microwave spectrum of pivaloyl chloride would be expected to be of significantly smaller magnitude than observed in pivalaldehyde[95, 99], perhaps not resolvable at all by our techniques.

Previous studies of the group of acyl chlorides gave a good starting point as to the carbon-chlorine bond distance. The generic distances for acyl chlorides are slightly less than 1.79 Å.[91, 92, 93] This varies a bit from the 1.77 Å given for a standard carbon-chlorine bond[60], although the slightly longer distance is close to the *ab initio* value (to be discussed later). The carbon-chlorine bond distance in pivaloyl chloride should be similar to the other acyl chlorides with any differences in this distance coming from the tertiary-butyl end of the molecule in question. Structurally speaking it is the prototypical tertiary butyl acyl chloride, making it an important addition to the previous studies of simple acyl chlorides.

5.2. Experimental methods

All experiments were performed on 98% Fluka® pivaloyl chloride without further purification. Since pivaloyl chloride has a vapor pressure of 36 mmHg at 20 degrees Celsius, a simple gas mixture was prepared by passing argon backing gas at a pressure of 2-3 atmospheres over and through a sample of liquid residing in the bottom of a "U" shaped tube. The resulting gas mixture is then pulsed out of a Parker-Hannifin™ Series 9 nozzle with an orifice of .030 inches and into a cavity where it undergoes supersonic expansion.

The gas expansion was then studied on three spectrometers: (a) a Search Accelerated Correct Intensity Fourier Transform Microwave (SACI-FTMW) spectrometer functional within the 8-18 GHz range, (b) a cavity based radio frequency spectrometer with the capacity to measure transitions below 4 GHz, and (c) a Balle-Flygare instrument capable of working from 4-26 GHz, although only the SACI-FTMW will be focused on in this work. They are all well described in other literature.[3, 5, 15, 28, 100, 101] Not all the measurements that were made on the molecule will be reported in this work as they pertain to other spectrometers.

5.2.1. SACI-FTMW

The SACI-FTMW instrument used in this experiment is based on two previous spec-

trometers: (a) the Chirped Pulse Fourier Transform Microwave (CP-FTMW) spectrometer introduced by Pate and co-workers and (b) the SACI-FTMW spectrometer with laser ablation source described by Grubbs et al.[5, 28] These setups involve the use of a broadband spectrometer with the capacity to scan large regions of microwave spectra at a time. The setup for this experiment is the same as the SACI-FTMW spectrometer described above except there is no coupling of the spectrometer with a laser ablation source. This spectrometer has the capability to measure transitions between 8 and 18 GHz in up to 4 GHz steps. For full details of the components used, refer to reference [28].

Briefly, large regions of spectra are excited by mixing a linear frequency sweep produced by an arbitrary waveform generator (AWG) with the fixed frequency output of a microwave synthesizer. The resulting upper and lower sidebands are amplified, then broadcast into the gas pulse. Any molecular signal is then detected with a second horn placed approximately 20 cm from the broadcast horn. The nozzle through which the sample is pulsed is placed perpendicular to the horn axis at a fixed distance approximately 7.5 to 8 cm directly above the center of the horns halfway between the antennae. After detection, the signal is amplified by a low-noise amplifier, mixed down from the original microwave input, then digitized and fast Fourier transformed on a high bandwidth oscilloscope.

As alluded to above, the microwave synthesizer may be set to any center frequency and following the AWG mixing stage, creates a sweep of microwave frequencies above and below this center frequency equal to the span of frequencies created by the AWG. In this experiment, the range was set from 250 MHz to 1250 MHz due to the 250 MHz DC Block. When mixed with the center frequency, this results in a 2500 MHz total scan with a 500 MHz "dead zone" 250 MHz above and below the center frequency.

Because the scan created by this technique produces a spectrum both above and below the center frequency with no way to distinguish on which side of the center frequency a transition lies, a way to obtain the absolute frequency of the transition must be employed. To do this, a separate scan with the microwave synthesizer set 1 MHz above the original center frequency was performed and analyzed to obtain the shift in the spectra. Each of

these spectra acquisitions involved 10,000 averaging cycles and gave linewidths of about 50 kHz (FWHM $\backsim$ 50 kHz). The resolution of this experiment is $\backsim$ 200 kHz and the uncertainty of measurements are $\backsim$ 25 kHz. The time for this averaging to take place is about 2.5 hours per experiment, but the most intense transitions can be seen in one shot. Figure 5.2 shows the results of one of these runs offset from a 10900 MHz center frequency.

5.3. Results and analyses

To guide the early interpretation of the broadband spectra, *ab initio* calculations at the MP2/6-311+G(3d,3p) level using Gaussian 03 were employed.[78] These calculations rendered a C-Cl bond distance of 1.81 Å, as shown in Figure 5.1, and provided rotational constants and chlorine nuclear quadrupole coupling constants which aided in the assignment. Values for the rotational and nuclear quadrupole coupling constants from *ab initio* calculations and experiment are located in Table 5.1.

Second moments, Kraitchman single isotopic substitution principal axis coordinates, and dipole moment calculations are located in Table 5.2.[2, 18] These calculations suggested the presence of very weak, if any, *c*-type transitions in the spectrum. The *ab initio* calculations rendered μ_a, μ_b, and μ_c dipole moments of 2.45 D, 1.68 D, and 0.00 D, respectively (Table 5.2). Since any *c*-type transitions would therefore probably be weak, *a*-type and *b*-type transitions, as expected, dominated the spectra, easing peak assignment. No *c*-type transition could be observed despite repeated averaging at several predicted frequencies. An estimate for an upper bound of μ_c is addressed later in the analysis section. A look at the planar moments and principal axis coordinates confirmed the *ab* symmetry plane that *ab initio* calculations had predicted.[2]

5.3.1. Spectral assignment of the ^{35}Cl and ^{37}Cl isotopes

The *ab initio* values of the rotational constants were used in SPCAT [63] to provide a guide for the assignment of the broadband spectra, allowing easy identification of the ^{35}Cl isotopologue spectrum. Since SPCAT reports relative intensities, when it is coupled with the SACI-FTMW data, peak assignment can be achieved both through the frequency and

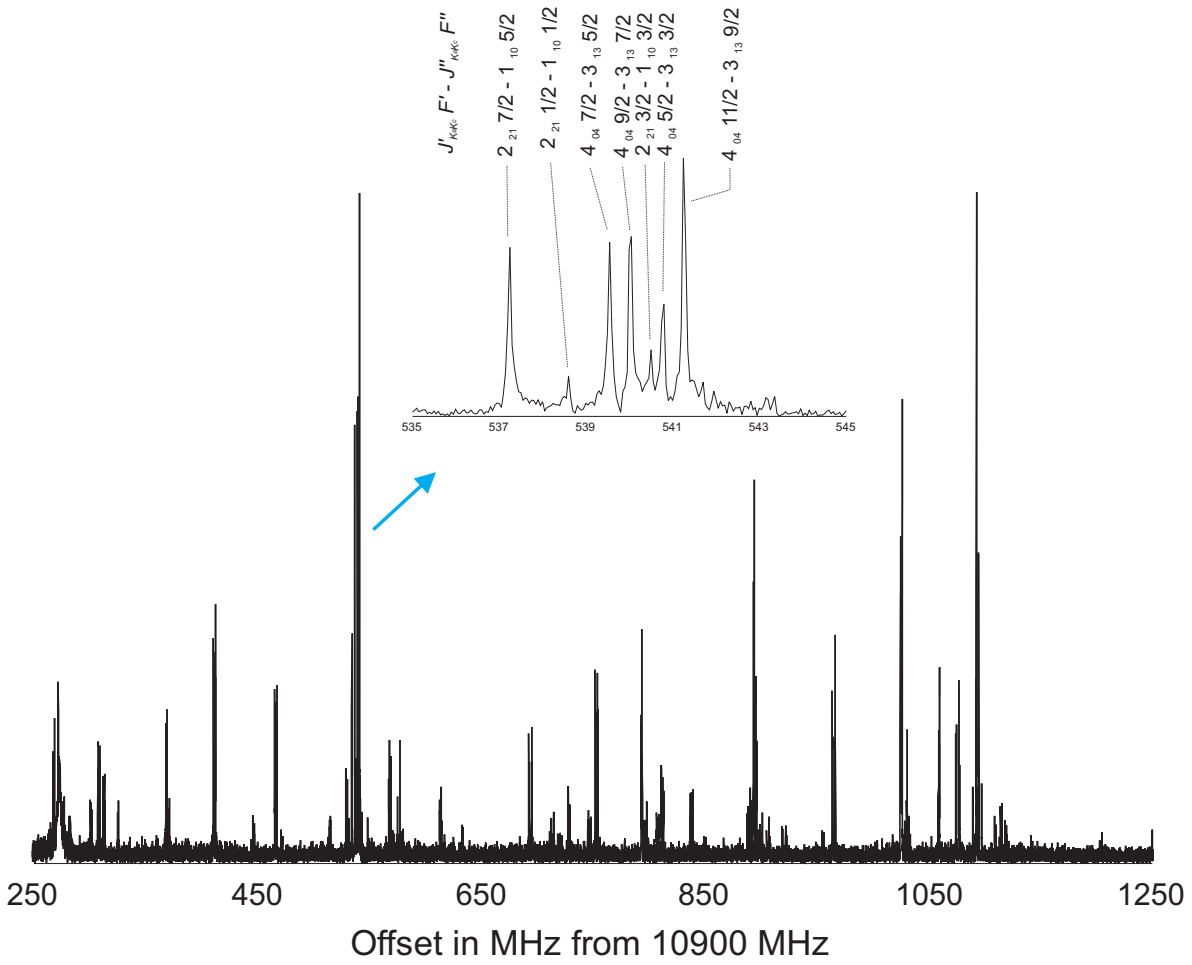

FIGURE 5.2. A 250-1250 MHz scan of pivaloyl chloride set at a center frequency of 10900 MHz. Due to mixing, this group of spectra is actually a scan of 250-1250 MHz above and 250-1250 MHz below 10900 MHz giving 2 GHz of spectra folded on top of each other. A second experiment is carried out at a center frequency 1 MHz above the first to determine what side of the center frequency the spectra lies. The inset shows an expanded region of spectra and shows several hyperfine components of the $J'_{K_aK_c} \leftarrow J''_{K_aK_c} = 2_{21} \leftarrow 1_{10}$ (540 MHz below the center frequency) and $4_{04} \leftarrow 3_{13}$ (540 MHz above the center frequency) transitions of the ^{35}Cl isotopologue of pivaloyl chloride.

relative intensity of each transition. The SACI-FTMW spectrometer is able to measure a broadband of frequencies at the same power in one data acquisitioning event eliminating

TABLE 5.1. Calculated and Experimental Rotational and Nuclear Electric Quadrupole Coupling Constants for Pivaloyl Chloride.[a]

	^{35}Cl		
	Ab Initio	^{35}Cl	^{37}Cl
A / MHz	2983.7	2977.99378(82)	2973.53738(65)
B / MHz	1722.4	1708.71195(33)	1671.393907(267)
C / MHz	1435.9	1430.038196(182)	1402.807756(136)
Δ_J / kHz		0.1536(39)	0.14132(296)
Δ_{JK} / kHz		0.7695(287)	0.8045(231)
Δ_K / kHz		−0.537(154)	−0.816(127)
δ_J / kHz		0.03284(253)	0.02792(175)
δ_K / kHz		−1.8076(257)	−1.837(36)
χ_{aa} / MHz[b]	−30.28	−33.1906(29)	−26.8353(23)
χ_{bb}-χ_{cc} / MHz[b]	−9.20	−11.78216(500)	−8.61228(400)
χ_{cc} / MHz[b]	19.74	22.48638(501)	17.72381(401)
χ_{ab} / MHz	39.38	43.590(245)	33.789(295)
N (Number of Transitions)		170	130
$\Delta\nu_{rms}$ /kHz[c]		16.4	14.5

[a] Numbers in parentheses are one standard deviation in units of the least significant figure.

[b] It should be noted that the three diagonal nuclear quadrupole coupling constants are not independent of each other; χ_{cc} is derived from the fitted quantities in SPFIT (3/2 χ_{aa} and 1/4 (χ_{bb}-χ_{cc})).

[c] All transitions fit to the required precision of 1 kHz for Balle-Flygare and 25 kHz for SACI-FTMW.

discrepancies in intensity measurements due to tuning or sampling differences sometimes present in typical cavity experiments.

Assignment and fitting of the spectrum was achieved utilizing Pickett's SPCAT and SPFIT programs with a Watson A-reduction Hamiltonian.[17, 63] The assignment technique for the quantum numbers of pivaloyl chloride was achieved by matching observed relative

TABLE 5.2. Second Moments, Principal Axis Coordinates, and Dipole Moment Components for Pivaloyl Chloride.[a]

	^{35}Cl	^{37}Cl	*Ab Initio* Calculations
P_{aa} / uÅ^{2} [b]	239.73202(8)	246.33673(6)	
P_{bb} / uÅ^{2} [b]	113.67047(8)	113.92579(6)	
P_{cc} / uÅ^{2} [b]	56.03407(8)	56.03308(6)	
$\mid a \mid$ / Å[c]	1.8318(8)		1.8304
$\mid b \mid$ / Å[c]	0.3699(41)		0.3655
$\mid c \mid$ / Å[c,d]	0.023(65)		0.00
μ_a / D			2.45
μ_b / D			1.68
μ_c / D			0.00

[a] Numbers in parentheses are one standard deviation in units of the least significant figure.

[b] Second moment value.

[c] Principal axis coordinates of the Cl atom from Kraitchman single isotopic substitution equations.

[d] Term is imaginary.

intensities to corresponding predicted transitions with similar intensities and frequencies. The most intense transitions of chlorine-35 were assigned first. Within this regime, K_a = 0 and K_a = 1 *a*-type transitions of the molecule were assigned first (due to their typical strength of signal), then the *b*-type transitions and so forth. In this work, a range of J = 1-0 to 6-5 transitions were observed, with K_a values ranging up to K_a = 3. This approach was useful considering that SPFIT and SPCAT can give relative peak-to-peak intensities and was particularly helpful in confirming the assignment of hyperfine components. This assignment technique was then employed for the chlorine-37 isotopomer once a satisfactory fit was obtained for the chlorine-35 isotopologue. The assignment of the chlorine-37 isotopologue, therefore, was relatively straightforward using rotational constants and nuclear quadrupole coupling constants obtained from *ab initio* calculations.

After the SACI-FTMW data assignment was complete, accurate knowledge of the location of the $J_{K_aK_c} = 1_{01}$ - 0_{00} and several low-lying Q-branch transitions for both isotopologues were known from the SPFIT and SPCAT programs.[63] The radio frequency experiment was employed to measure these transitions and to refine the analysis of the nuclear quadrupole coupling constants for the isotopes of chlorine. The χ_{ab} off-diagonal term in the program aided in this process by more accurately fitting the measured lines to experimental uncertainty and predicting the precise frequency of transitions to be measured by the cavity based radio frequency technique. Removal of the χ_{ab} off-diagonal term from the fitted parameters increased the rms of the chlorine-35 isotope to 30.0 kHz and the rms of the chlorine-37 isotope to 21.5 kHz. With this term, chlorine-35 and chlorine-37 have a rms value of 16.4 kHz and 14.5 kHz, respectively, as tabulated in Table 5.1.

Transitions with higher J values were difficult to assign using the SACI-FTMW spectrometer alone due to the proximity of the hyperfine components to one another and the 50 kHz linewidth and 200 kHz resolution of the SACI-FTMW experiment; this was the primary reason for our use of a Balle-Flygare spectrometer. With it, the higher resolution facilitated assignment of some of the hyperfine transitions that the SACI-FTMW spectrometer did not resolve. Because the SACI-FTMW horn antennae range is 8-18 GHz, the Balle-Flygare was also employed for measurements made between 4 and 8 GHz.

5.3.2. Analysis of the results

Due to the $I = \frac{3}{2}$ nuclear spin of both ^{35}Cl and ^{37}Cl nuclei, hyperfine structure was expected and observed for all transition types between 800 and 18800 MHz. The line listings for all the observed transitions along with their assignments is given in Table 5.3. Rotational constants for this molecule were also found by the use of quantum number assignments and successive fits using the SPFIT program. These rotational constants along with the nuclear quadrupole coupling constants are located in Table 5.1.

Pivaloyl chloride is an asymmetric molecule for which no c-type transitions were observed. This is consistent with the *ab initio* calculations for a zero μ_c dipole moment. Using simple intensity estimates of the observed lines and the *ab initio* estimates of the μ_b dipole moment

component gives an upper limit of approximately 0.05 Debye for the *c*-type transitions. This would render a ratio of μ_c/μ_b of approximately 0.03. Evidence for this *ab* symmetry plane, as discussed before, is provided by several pieces of experimental data located in Table 5.2. First of all, the second moment calculations performed on this molecule indicate an *ab* plane of symmetry by rendering almost identical P_{cc} values for both chlorine isotopes.[2] Secondly, Kraitchman single isotopic substitution calculations gave a *c*-coordinate value of almost zero for the chlorine atom, consistent with this *ab* plane.[2] The existence of an *ab* symmetry plane is also in agreement with other simple acyl chlorides acetyl and propionyl chloride.[91, 92] Lastly, the χ_{cc} ratio of chlorine-35 to chlorine-37 isotopes renders a value of 1.26871(40) consistent within error to the literature chlorine nuclear quadrupole moment ratio of 1.26889(3).[102]

As mentioned above, the barrier to internal rotation in pivaloyl choride is significantly larger than pivalaldehyde (807 cm^{-1} versus 337 cm^{-1}) as obtained from far-infrared studies.[95] The splittings observed in pivalaldehyde, as mentioned by Cox et al., were approximately 50 kHz and only observed in *b*-type transitions.[99] These measurements indicate that the splittings due to internal rotation would be small in pivaloyl chloride. This is consistent with our observations of pivaloyl chloride because resolution of internal rotational splittings were not accomplished even with the highly resolved Balle-Flygare and radio frequency experiments.

5.4. Conclusion

The pivaloyl chloride spectrum in the range of 800 to 18800 MHz has been measured and analysed. Much of the spectrum was recorded using our newly constructed SACI-FTMW spectrometer. The pivaloyl chloride spectrum, at the resolution of this work, contained no observed internal rotation indicating a higher barrier to internal rotation than in the related pivalaldehyde molecule. No *c*-type transitions were observed and experiment confirmed the existence of an *ab* symmetry plane. Experimental rotational constants and chlorine nuclear quadrupole coupling constants have been obtained for pivaloyl chloride for the first time.

CHAPTER 6

OBSERVED HYPERFINE STRUCTURE IN THE CHIRPED PULSE SPECTRA OF TIN MONOSULFIDE

6.1. Introduction[1]

Two of the major criticisms of fast passage chirped pulse microwave spectroscopy is the sensitivity and resolution of the technique in comparison to the Balle-Flygare cavity technique.[3] As this cavity technique is the "weapon of choice" in the microwave community, this concern is well warranted of any new technique and a good basis for comparison. However, broadband rotational spectroscopy has been shown in earlier chapters of this work as well as in the literature[33, 36, 37] to possess the resolution to determine nuclear hyperfine structure and the sensitivity to observe species that are <1% naturally abundant.

Three of the ten isotopes, ^{115}Sn, ^{117}Sn, and ^{119}Sn have a nuclear spin ($I = \frac{1}{2}$). Although SnS has been extensively studied by rotational spectroscopy[103, 104, 105, 106, 107], no determination of the nuclear magnetic spin-rotation hyperfine structure has previously been done. The ^{117}Sn and ^{119}Sn are important nuclear magnetic resonance (NMR) nuclei and measuring magnetic shielding parameters can give insight into the chemical shifts provided by these nuclei in the NMR technique. Because of the importance of these nuclei to the NMR technique, establishing an absolute chemical shielding scale for tin-containing molecules is important and examples are found in the literature.[108] Measurement of the nuclear magnetic spin-rotation coupling constants for these nuclei provide measurements both (a) pertaining to well defined quantum states and (b) free of lattice or solvent effects. Both of these points makes the data provided in this work tractable to the theoretical and computational chemistry communities. This work presents the first reported measurement

[1]Chapter reproduced in part from Ref. [42] from Elsevier©

of both the $J = 1 \leftarrow 0$ transitions and the nuclear magnetic spin-rotation constants provided by the ^{115}Sn, ^{117}Sn, and ^{119}Sn nuclei of tin monosulfide.

6.2. Experiment

Experiments were performed on the chirped pulse microwave Fourier transform spectrometer at the University of North Texas. The spectrometer setup is located in previous literature[28] with the direct digitization setup.[47] The key component of this instrument is the addition of a laser ablation source. This source is made possible through the customization of the head of a Parker-Hannifin^{TM}Series 9 solenoid valve similar to the Smalley nozzle[45] and modeled after that of Walker and Gerry.[4] This head allows for a metal rod to be inserted through the top of the nozzle into a motor which spins the rod providing a continuously fresh surface. The fundamental of a 1064 nm Nd:YAG, pulsed laser beam can then be focused into a hole on one side of the head with an exit hole through the front of the nozzle. For every solenoid pulse there is one nozzle pulse creating the entire laser event.

The solenoid valve is backed by a reservoir of gas that has a precursor for the desired molecule in which to study. For this study, SnS was the desired resultant molecule, so carbonyl sulfide, OCS, was chosen. 0.3% mixtures of the gas in argon at a total pressure of 5 bar. As the solenoid valve is pulsed gas rushes over the metal at the same time as the laser. In that moment, the molecules of gas and metal have enough energy to rearrange to make desired, as well as unknown molecules, to be studied by the microwave spectrometer.

Because the creation of a molecule must take place in the customized head, timings between the firing of the solenoid pulse, laser and microwaves are all extremely crucial. This is one reason to use OCS over other gases. OCS has a strong transition at 12163 MHz which is used in timings calibration. The chirped pulse spectrometer gives real time intensities so that one can first sample each nozzle pulse and adjust the solenoid valve and microwave timings so that OCS comes in very strong, then turn on the laser and adjust the laser timings until OCS is very weak in intensity. Once this is achieved, the laser ablation event is parameterized.

After the laser ablation event takes place, the molecules are pulsed into the chirped pulse,

Fourier transform microwave (CP-FTMW) spectrometer.[28, 47] Briefly, the spectrometer used microwave pulses of 2 GHz by creating 6μs chirps on an arbitrary waveform generator mixed with a center frequency generated on a microwave synthesizer, ν, giving $\nu \pm 1$ GHz chirps. The chirps are amplified (5W) on a solid state amplifier and broadcast onto a molecular beam, undergoing the supersonic expansion, by an antenna horn. Approximately 0.2 μs after excitation, a second antenna horn receives a molecular signal in the form of 40 μs free induction decays (FIDs). The FIDs are amplified and collected directly on a 12 GHz bandwidth, 40 GS/s scope where they are averaged and fast Fourier transformed for 10,000 averaging cycles. Figure 6.1 shows a sample of the collected spectrum.

6.3. Results and Analysis

Figure 6.1 shows $J = 1 \leftarrow 0$ transitions in the ground vibrational state for eight of the ten $^{x}Sn^{32}S$ isotopologues of tin monosulfide. Although the $^{112}Sn^{32}S$ is not pictured, it was observed, giving nine of ten $^{x}Sn^{32}S$ isotopologues measured in the ground vibrational state. The figure also notes the observation of transitions within multiple vibrational states as well. Indeed, up to $v = 6$ was observed for some SnS isotopologues as well as $J = 2 \leftarrow 1$ for multiple vibrational states. All measured transitions, along with their quantum number assignments and natural abundance, are located in Appendix D. Spectral linewidths were approximately 50 kHz (FWHM) and a 5 kHz uncertainty was given to line centers. Transitions were assigned using Pickett's SPFIT/SPCAT software[63] constants from the literature[107] greatly eased transition assignment.

As mentioned earlier, this work focuses on the nuclear magnetic hyperfine structure brought about by the spin-containing tin nuclei, particularly the ^{119}Sn and ^{117}Sn isotopes. Figure 6.2 shows an example of this structure in the $J = 1 \leftarrow 0$ transition splitting for $^{119}Sn^{32}S$. A fit of the rotational constants, B, and nuclear magnetic spin-rotation constants, C_I, were performed on the measured $J = 1 \leftarrow 0$ of $^{117}Sn^{32}S$ and $^{119}Sn^{32}S$ in SPFIT[63] as mentioned earlier. These values are reported in Table 6.1. The centrifugal distortion constants, D, reported in the table represent a calculation based from the mass independent terms in Table 6.3 (calculation mentioned later). The ^{115}Sn isotopologue of SnS was not

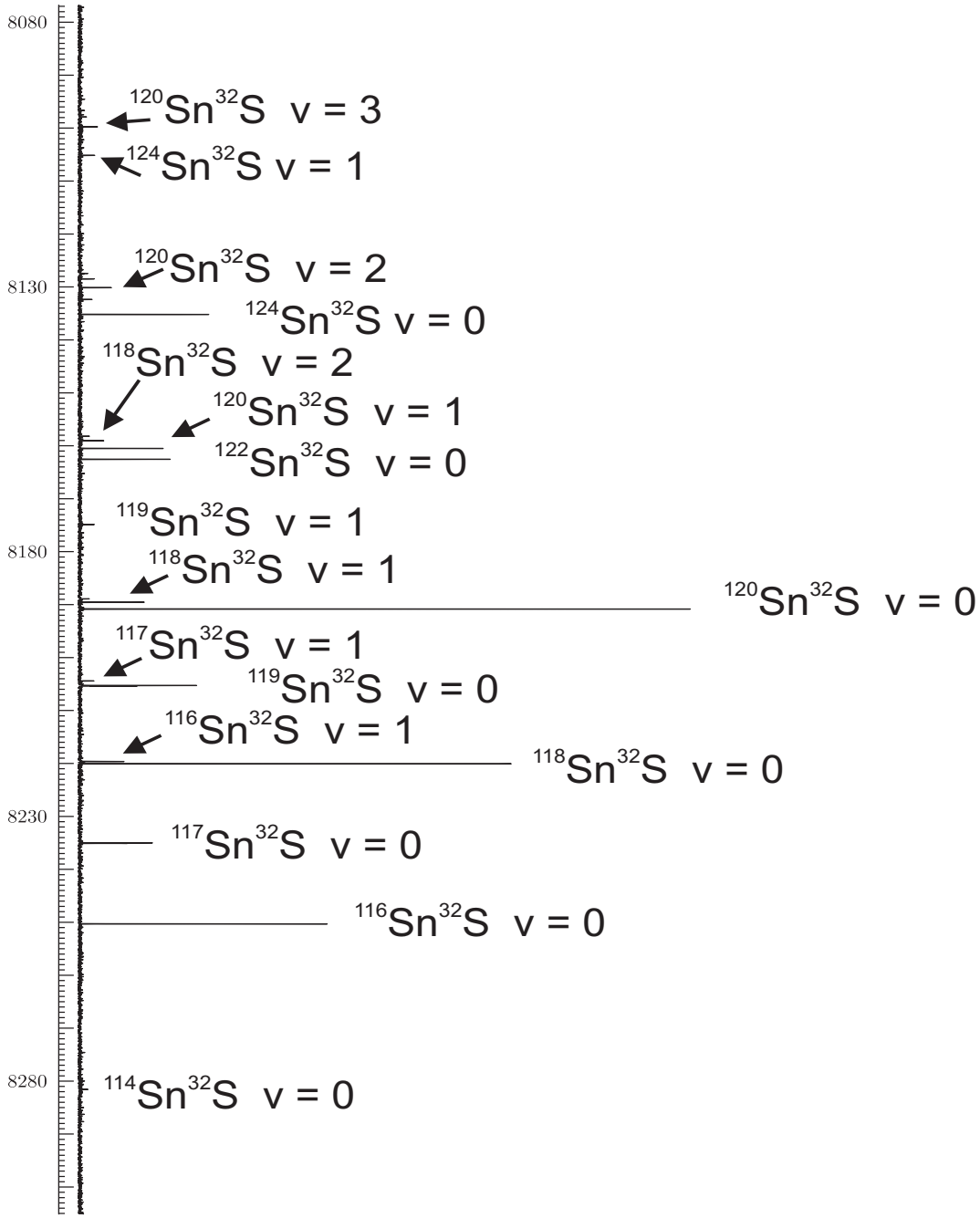

FIGURE 6.1. A 220 MHz portion of a 2 GHz spectrum recorded using our laser ablation-equipped, chirped pulse Fourier transform microwave spectrometer. The spectrum shows the $J = 1 \leftarrow 0$ transitions for SnS. Not all spectral features are labelled.

observed in this work and, therefore, not reported.

The constant C_I is proportional to the rotational constant, B, by the following equations[65, 109, 110]:

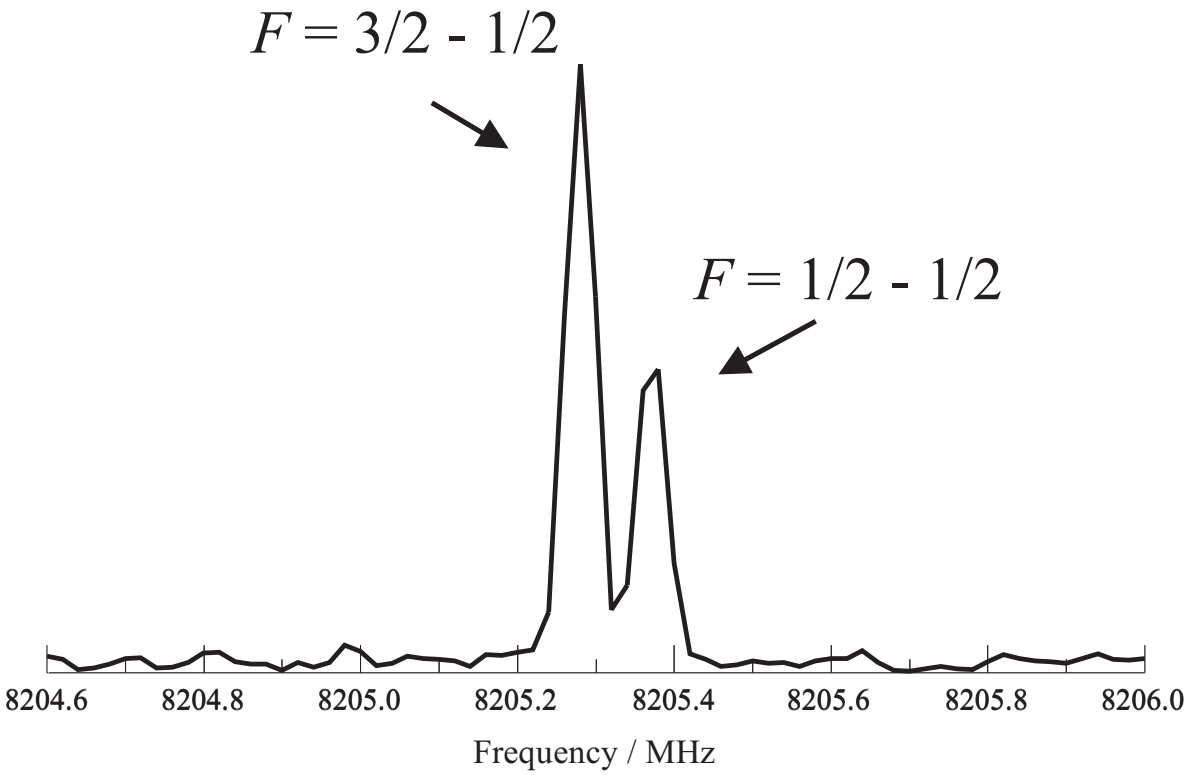

FIGURE 6.2. The $J = 1 \leftarrow 0$ transition for $^{119}Sn^{32}S$.

TABLE 6.1. Determined Spectroscopic Constants for $^{117}Sn^{32}S$ and $^{119}Sn^{32}S$.

Isotopomer	v	B / MHz	D /kHz[a]	C_I(Sn) / kHz
$^{117}Sn^{32}S$	0	4117.5196(18)[b]	1.4453(124)	-56.7(47)
$^{117}Sn^{32}S$	1	4102.2247(18)	1.4453(124)	-57.1(47)
$^{119}Sn^{32}S$	0	4102.6570(18)	1.4349(123)	-59.5(47)

[a] All D values were mass scaled from the D value for the $^{120}Sn^{32}S$ isotopomer obtained from U_{02} in Table 6.3.

[b] Numbers in parentheses represent the estimated uncertainties in units of the least significant figure. These uncertainties are estimated from the measurement uncertainties.

(65) $C_I = C_I(\text{nucl}) + C_I(\text{elec})$ where:

$$C_I(\text{nucl}) = -\frac{4\pi e\mu_N g_N B_e Z_l}{hcr_e} \quad (66)$$

$$C_I(\text{elec}) = -\frac{4\pi e\mu_N g_N B_e}{hcm_e} \times \sum_k \frac{\langle 0|L_x|k\rangle\langle k|L_x r^{-3}|0\rangle + \langle 0|L_x r^{-3}|k\rangle\langle k|L_x|0\rangle}{E_0 - E_k} \quad (67)$$

where e is the magnitude of the elementary charge, μ_N is the nuclear magneton, g_N is the nuclear g-factor, B_e is the equilibrium rotational constant, h is Planck's constant, c is the speed of light, r_e is the internuclear separation, m_e is the rest mass of the electron, and L_x represents the angular momentum operator. Z_l in a diatomic molecule represents the atomic number of the nucleus opposite of the nucleus pertaining to C_I. Taking a ratio of C_I/B for $^{117,119}Sn^{32}S$ is found to be -0.000014(2) which is very close to the value of -0.000012(2) for $^{117,119}Sn^{16}O$ [110] suggesting similar electronic structures for the two molecules, which is expected.

6.3.1. Magnetic Shielding Tensor Evaluations

Nuclear magnetic spin-rotation constants can be, and often are, related to the nuclear magnetic shielding tensor via the Ramsey-Flygare equations.[65, 109, 111, 112, 113] From the equations above it can be seen that the nuclear spin-rotation constant, C_I, has a nuclear contribution dependent only on nuclear positions and an electronic contribution that is second order dependent upon the ground and excited electronic state wavefunctions. In practice, the electronic contribution is obtained by experimentally determining C_I and the nuclear contribution then subtracting the nuclear contribution from C_I. The nuclear and electronic contributions to the can then be related to the diamagnetic, σ_d, and paramagnetic, σ_p contributions to the shielding tensor by the following equations[109, 112, 113, 114]:

$$\sigma_p = -\frac{eh}{12\pi m_e c\mu_N g_N B_e} C_I(\text{elec}) \quad (68)$$

$$\sigma_d = \sigma_d(\text{free atom}) - \frac{eh}{12\pi m_e c\mu_N g_N B_e} C_I(\text{nucl}) \quad (69)$$

using the defined values from Equations 66 and 67 and the atomic values for σ_d(free atom) can be obtained from the literature. The average magnetic shielding, σ_{avg}, may then be

calculated by summing σ_d and σ_p. This value is used in determining chemical shifts in NMR measurements.

σ_{avg} was calculated for $^{119}Sn^{32}S$ using a relativistically calculated σ_d(free atom) value of 6203 ppm.[115] A relativistically calculated free atom value was used over a non-relativistic free atom value because the relativistic value has been shown to give more reliable results for tin in SnO.[110] The calculated value for σ_{avg} was $^{119}Sn^{32}S$ 1960(70) ppm and, when compared to other Sn-chalcogenides in Table 6.2, fits the decreasing trend going down a group.

TABLE 6.2. Contributions to the ^{119}Sn Magnetic Shieldings and the Shielding Spans in the Tin Chalcogenides.

Molecule	σ_p / ppm	σ_d / ppm	σ_{av} / ppm	Ω /ppm
$Sn^{16}O$[a]	-3510(27)[b]	6244	2734	5203(40)
$Sn^{32}S$[c]	-4470(70)	6430	1960(70)	6350(100)
$Sn^{80}Se$[d]	-4912	6203	1291	7163
$Sn^{130}Te$[d]	-5263	6203	940	7604

[a] Ref.[110].

[b] Numbers in parentheses represent one standard deviation in units of the least significant figure.

[c] This work.

[d] Ref.[116].Uncertainties were not given.

Ω, the span of the shielding tensor, avoids many approximations used in calculating σ_{avg} and can be directly calculated from C_I by the following equation[117]:

$$\Omega = \left(\frac{m_p}{2m_e g_N B_e}\right) C_I \tag{70}$$

where $m_{p,e}$ is the mass of the proton and electron respectively, g_N is the nuclear g-factor and B_e is the equilibrium rotational constant. The equation mentioned above neglects the very small quadrupole term, Ω_p.[117] Using the equation, a value of 6350(100) ppm for $^{119}Sn^{32}S$

is obtained, and is also compared to other Sn-chalcogenides in Table 6.2. Again, the value calculated here fits the increasing trend passing down the chalcogen group.

6.3.2. Dunham Analysis

Next, a Dunham-type, mass independent fit[21] was performed to all transitions in Appendix D. The fitting procedure has been written in-house and does not account for nuclear hyperfine structure. In the cases where nuclear hyperfine splitting was observed, a "hypothetical line center" (HLC) was achieved by running a prediction of the transition with the experimental constants in the absence of the nuclear spin. HLCs and transitions without structure were then fit using the expression:

$$E_{v,J} = \sum_{kl} \frac{U_{kl}}{\mu^{(k+2l)/2}} \left(v + \frac{1}{2}\right)^k [J(J+1)]^l \tag{71}$$

where U_{kl} are the mass independent Dunham parameters, v and J are the vibrational and rotational quantum numbers, respectively, and μ is the reduced mass of the molecule. Atomic masses were taken from the 2003 Atomic Mass Evaluation.[118] The results of this fit are located in Table 6.3 below. These values may then be translated into the more familiar mass dependent terms, Y_{kl}, using the following equation:

$$Y_{kl} = U_{kl}\mu^{-(k+2l)/2} \tag{72}$$

The inclusion of Born-Oppenheimer breakdown (BOB) terms were not necessary to achieve a satisfactory fit. It is worth noting, however, that BOB terms are necessary when working with larger SnS data sets.[119]

6.3.3. Relative Intensities

Lastly, it is interesting to note the relative intensities of transitions in the reported spectrum as a test against the results of previous calibration materials for the laser ablation equipped experiment.[28] If one normalizes the abundances of the different isotopologues of SnS to the main isotopologue, $^{120}Sn^{32}S$, we find a ratio of abundance of 1:0.142 for

TABLE 6.3. Parameters for SnS Obtained From a Fit to Measured Transition Data.[a]

Parameter	Value
U_{01} / u MHz	103565.576(28)[b]
U_{02} / u^2 MHz	-0.911(78)
U_{11} / u$^{\frac{3}{2}}$ MHz	-1922.19(10)
U_{21} / u^2 MHz	-4.152(76)
RMS / kHz	2.65

[a] Measured data is located in Appendix D.

[b] Numbers in parentheses represent one standard deviation in units of the least significant figure.

$^{120}Sn^{32}S$:$^{122}Sn^{32}S$. If the same normalization scheme is set up to transitions assigned to each isotopologue, then for the ratio of $^{120}Sn^{32}S$:$^{122}Sn^{32}S$ sharing the same quantum numbers, a ratio of 1:0.148 is found. This qualitative agreement between abundance and transition intensity is useful when making transition quantum number assignments.

6.4. Conclusions

The rotational spectra of tin monosulfide, SnS, between 8 and 17 GHz has been measured and reported on a laser ablation equipped CP-FTMW spectrometer. The resolution of the experiment provided for the observation of nuclear hyperfine structure due to the ^{117}Sn and ^{119}Sn nuclei in SnS. Nuclear spin-rotation hyperfine constants were determined and reported for the first time. These constants have been utilized in determination of the magnetic shielding tensor value of SnS and compared to other Sn-chalcogenides. Mass independent Dunham parameters were determined and reported. BOB terms were not needed to sufficiently fit the available data within the region. Relative intensity ratios observed by the CP-FTMW are in very good agreement with those of the isotopologues in question, confirming the same observations made on calibration molecules used previously on the laser ablation equipped CP-FTMW spectrometer.

CHAPTER 7

OPEN-SHELL DIATOMICS AND LASER ABLATION PRODUCT CHEMISTRY AS STUDIED BY CHIRPED PULSE SPECTROSCOPY

7.1. Introduction

The use of a laser ablation technique in conjunction with a supersonic beam is a technique that has been used for approximately 30 years.[45] It has been used in the formation of molecules as small as diatomics[4] to as large as the buckminsterfullerene[120] as well as transient species. The use of such technology in conjunction with a Fourier transform microwave (FTMW) spectrometer has been done for at least 20 years.[121]

Coupling of such instrumentation to a chirped pulse Fourier transform microwave (CP-FTMW) spectrometer has not been accomplished, however until recently.[28] The power of such technology coupled with a chirped pulse spectrometer has been shown in previous chapters and will be investigated in the multiple studies performed here.

In this study, three molecules were looked at, barium monosulfide, BaS, lead monochloride, PbCl, and tin monochloride, SnCl.

7.2. Experiment

The molecules in this experiment were created using a metallic rod of barium, lead, or tin in a solenoid valve equipped with a customized head known as a Walker-Gerry ablation nozzle.[4] The ablation setup has been mentioned previously in the literature[28] and in chapter 2. Briefly, a rotating metal rod runs perpendicular to both a gas pulse and a fundamental laser pulse from a 1064nm Nd:YAG laser. As the laser ablates a spinning metal rod, a gas moving in a supersonic expansion simultaneously sweeps over the rod allowing for new species to form. This new species then carries into the spectrometer where its microwave spectrum may be collected and analyzed.

In general, 0.3% gas mixtures of carbonyl sulfide (OCS) or chlorine gas (Cl_2) were made in a carrier noble gas of helium (He) or argon (Ar) brought to total pressures of 4-5 bar. The experiment is carried out in a chamber held at $\approx 10^{-5}$ torr with a 4 Hz solenoid valve pulse rate. For "softer" (more malleable) metals, a laser power percentage of ≈75% is used while ≈90% laser power was used for "harder" (less malleable) metals.[1] More explicit experimental details within each study will be covered in the subsequent sections.

Each molecule is studied on a CP-FTMW described previously in the literature.[28, 47] Briefly, an arbitrary waveform generator creates $\approx 3\mu$s linear frequency sweeps of DC to 1 GHz (variations in the pulse will be explained in each section). This is then mixed additively with a center frequency ν, giving a range of frequencies of $\nu \pm 1$ GHz. This broadband pulse is amplified to 5 Watts and broadcast over an antennae horn where it comes into contact with a supersonically expanding gas to be studied. The pulse is turned off and a molecular free induction decay (FID) is collected from a second antennae horn. This FID is low-noise amplified. After amplification the FID is directly digitized and fast Fourier transformed (FFT) on a high power oscilloscope where the results may then be analyzed.

7.3. Barium Monosulfide, BaS[2]

BaS is a closed shell molecule with a $^1\Sigma$ ground state. The original driving force to studying BaS was to evaluate the need for Born-Oppenheimer breakdown (BOB) parameters[119] as well as measure any hyperfine structure due to any spin-containing isotopes of barium or sulfur. Because of these motivations, rotational transitions of BaS had already been observed at UNT by the high resolution Balle-Flygare cavity setup with laser ablation source[15], but not reported. Millimeter-wave (mm-wave) studies had already been performed on BaS with reported parameters[122], which eased the search for these transitions. A listing of these transitions can be found in Appendix E.

The major difference in the two studies was in the synthesis of BaS. The cavity utilized a laser ablation source while the mm-wave study synthesized the molecule in an oven by

[1] Nd:YAG peak laser power is 50mJ/pulse for the laser utilized in the experiments

[2] Presentation given is Ref. [39]

vaporizing metallic barium in the presence of OCS. The reaction for the oven synthesis reported in the literature is shown as being[122]:

(73) $$\mathrm{Ba} + \mathrm{OCS} \rightarrow \mathrm{BaS} + \mathrm{CO}.$$

The chemistry taking place in the ablation event, however, is not well known. In fact, this is the first experiment of this kind known to the author. There are also many parameters in this event to take into account. Since the laser and backing gas simultaneously meet at the metal, there is a large amount of energy introduced into the system. Does the constitution and/or concentration of gases used in the backing gas matter? Does the carrier gas constitution and/or pressure matter? Due to issues concerning the correct relative intensities on the cavity (tuning sweet spots), these questions cannot be easily answered using this technique. A more qualitative and quantitative measurement must be made if this was to be studied.

7.3.1. Experimental Methods

Because the transition strength in the cavity was strong (ca. 2:1 signal:noise ratio in <10 shots for the main isotopologue) and correct relative intensities were needed, the experiment was performed on the CP-FTMW with laser ablation source to observe the intensity ratios between isotopologues in the $v = 0$ vibrational state. This spectrometer is the same as the cavity as being *in situ*, but has been shown to give correct relative intensities.[28] This was achieved with the settings from the cavity experiment. These were 0.3% gas mixture of OCS in Ar at $\approx$ 4.5 bar and laser power of 75% maximum at a nozzle rate of 4 Hz for 10,000 averaging cycles centered at 12 GHz. A sample spectra for this is in Figure 7.1 (ran for 96508 averaging cycles).

For the laser ablation tests, the parameters chosen to be adjusted for the experiment were backing gas pressure, backing gas concentration, laser power, He carrier gas instead of Ar, and H_2S instead of OCS. If changing one of these parameters made a difference, it was determined that the difference would exhibit itself by alteration of the vibrational state

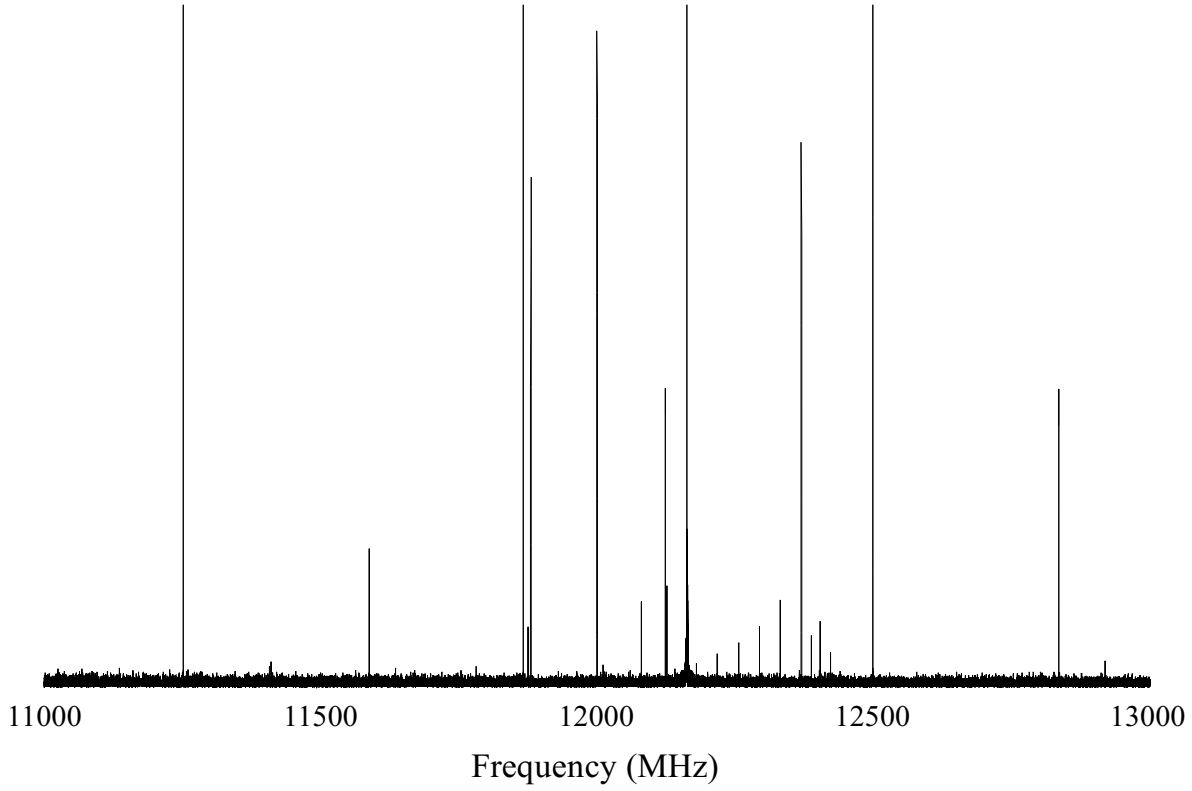

FIGURE 7.1. Spectra of BaS taken at 12 GHz center frequency with cavity parameters at 96508 averaging cycles.

intensity ratios with respect to $v = 0$. If no parameter change worked, then it could be determined that the chemistry is dominated by the supersonic expansion.

7.3.2. Results and Analysis

The $J = 2 \leftarrow 1$, $v = 0$ relative intensities were observed to be 8.94:1 for $^{138}Ba^{32}S$ to $^{136}Ba^{32}S$ while the natural isotopic ratio is 9.12:1. As this was in good agreement with one another quanitatively, it was determined that this run could be used as a control for any other experiments. A zoomed in view of the control run can be found in Figure 7.2. The v=x:$v = 0$ ratios were then determined as a basis of comparison. These ratios can be found in Table 7.1.

7.3.2.1. Laser Power. The first experiment was the adjustment of the laser power in the ablation event. This test may seem the most obvious to the reader because it is directly

TABLE 7.1. Control Vibrational State Ratios for the $J = 2 \leftarrow 1$ Rotational Transitions of BaS.

Ratio	Arbitrary Intensities	Value
$v = 1/v = 0$	2.57/15.9	0.162
$v = 2/v = 0$	1.81/15.9	0.114
$v = 3/v = 0$	1.32/15.9	0.083
$v = 4/v = 0$	1.01/15.9	0.064
$v = 5/v = 0$	0.73/15.9	0.046
$v = 6/v = 0$	0.56/15.9	0.035

associated with an adjustment with the amount of energy introduced into the event. Laser powers were adjusted between 65 and 90% maximum laser power at 5% increments except for the 70% laser power setting. The subsequent intensity ratios were recorded and are reported in Table 7.2.

When moving to 10,000 averaging cycles, only up to the $v = 2$ state was observed. Therefore, these were used for comparison against the control. It was observed from this data set that as the laser power is increased, there is a trend toward populating the higher vibrational states. The tradeoff, however, is a decrease in the overall intensities.

These results may be for two different reasons. One, a lowering of the overall intensity may be a result of the laser populating many different vibrational states at one time. This, in turn, lowers the amount of molecules in any one individual state creating a significant decrease in the intensity because now the transitions occuring are outside of the sensitivity of the instrument for the number of acquisitions in the experiment. A second argument may be that there are some molecules moving into higher vibrational states while others are destroyed/never made because of the increase in the laser power. It is unclear at this time which one of these arguments is the correct argument. Many more signal acquisitions (ca. 1 million) may give insight as to the correct argument.

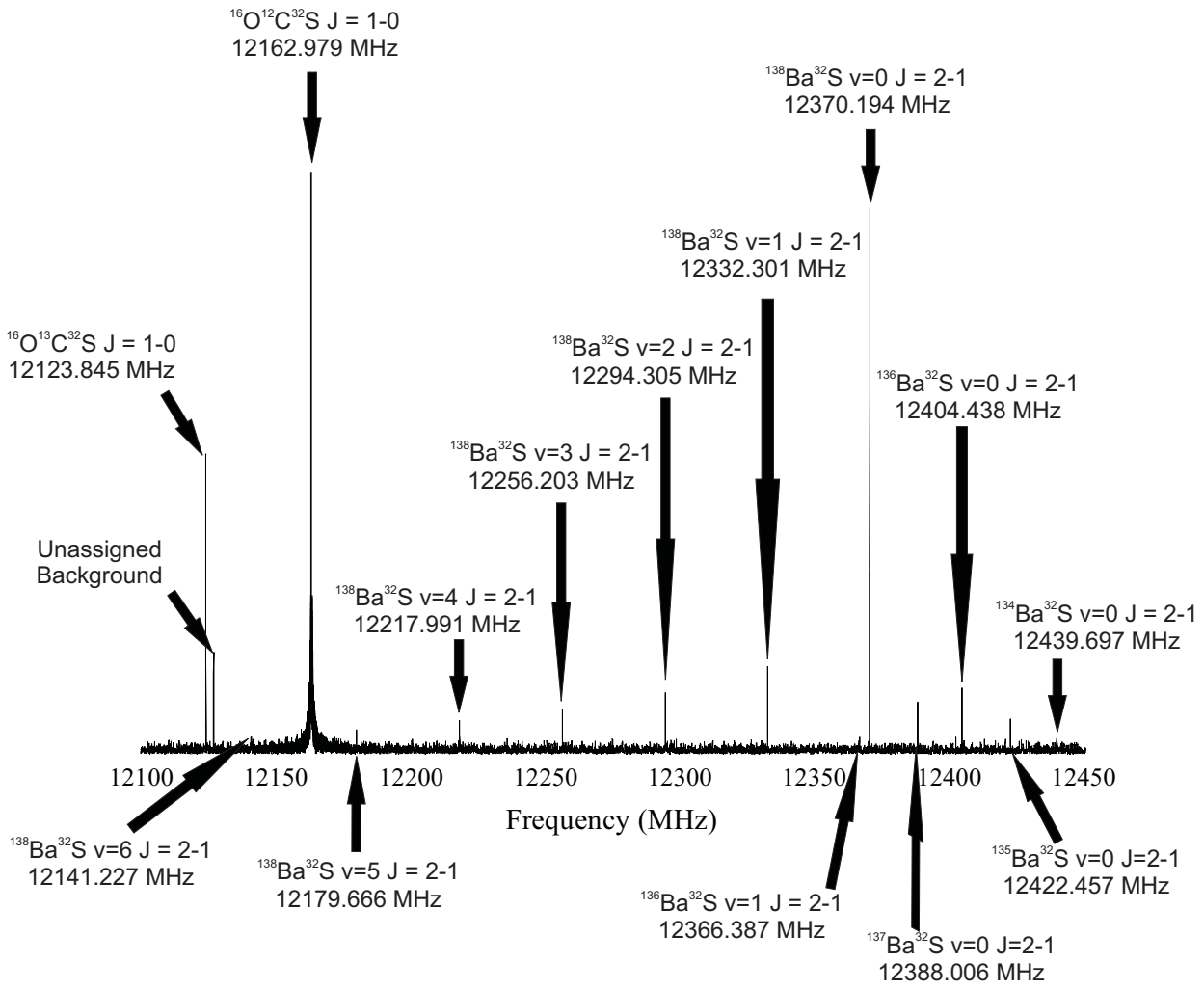

FIGURE 7.2. A Zoom-In of the Barium Sulfide Control Spectra. All Known Transitions have been Labelled.

7.3.2.2. Backing Gas Pressure. The next variable to be studied was the backing gas pressure. Because higher backing pressures increase the velocity of the gas, the mathematics of the supersonic expansion dictate that the temperature of the expansion is colder giving way to the lower vibrational states. If the chemistry of the ablation event is governed by the expansion only, then, as the pressure is lowered, higher vibrational states should be populated giving way to larger $v = 2/v = 0$ ratios. The results of the experiment are found in Table 7.3.

Table 7.3, however shows inconsistent trends that make it difficult to draw conclusions from in regards to the ablation setup. The $v = 2/v = 0$ ratios seem to rise and drop with

TABLE 7.2. Vibrational State Ratios for the $J = 2 \leftarrow 1$ Rotational Transitions of BaS Adjusting Laser Power.

Laser Power	Ratio	Arbitrary Intensities	Value	Control
65%	$v = 1/v = 0$	2.434/16.782	0.145	0.162
	$v = 2/v = 0$	1.857/16.782	0.111	0.114
75%	$v = 1/v = 0$	6.851/32.666	0.210	0.162
	$v = 2/v = 0$	5.564/32.666	0.170	0.114
80%	$v = 1/v = 0$	3.504/17.022	0.206	0.162
	$v = 2/v = 0$	2.864/17.022	0.168	0.114
85%	$v = 1/v = 0$	1.841/7.033	0.262	0.162
	$v = 2/v = 0$	1.456/7.033	0.207	0.114
90%	$v = 1/v = 0$	0.648/2.351	0.276	0.162
	$v = 2/v = 0$	0.576/2.351	0.245	0.114

respect to the control independent of a trend while the $v = 1/v = 0$ ratios do the same. The data does clearly show, however, that higher bands are intensified at lower pressures and there is a significant drop in intensity when moving from 4704 gas units to 3709 gas units. The larger intensity bands at higher pressures would be expected by the jet. The drop in intensity, however, could be evidence of a warming in the expansion or simply an experimental timings issue. Timing parameters were held generally the same across a family of experiments to minimize the amount of variables being tested. Overall, the data are inconclusive in relation to the backing gas pressures.

7.3.2.3. Concentration of OCS. The concentration of the gas mixture was tested for the ablation event. Since the ablation event consists of elemental metal being ablated in the presence of a backing gas mixture of a reagent and carrier gas, only an increase in the intensity is expected as the concentration is increased until the metal becomes a limiting

TABLE 7.3. Vibrational State Ratios for the $J = 2 \leftarrow 1$ Rotational Transitions of BaS Adjusting Backing Gas Pressure.[a]

Pressure/ Gas Units[b]	Ratio	Arbitrary Intensities	Value	Control
6718	$v = 1/v = 0$	4.330/21.721	0.199	0.162
	$v = 2/v = 0$	3.583/21.721	0.165	0.114
5720	$v = 1/v = 0$	4.157/20.620	0.202	0.162
	$v = 2/v = 0$	3.235/20.620	0.157	0.114
4704	$v = 1/v = 0$	2.375/11.642	0.204	0.162
	$v = 2/v = 0$	1.921/11.642	0.165	0.114
3709	$v = 1/v = 0$	0.861/4.60	0.187	0.162
	$v = 2/v = 0$	0.530/4.60	0.115	0.114
2692	$v = 1/v = 0$	0.702/3.36	0.209	0.162
	$v = 2/v = 0$	0.5401/3.36	0.161	0.114
1707	$v = 1/v = 0$	0.738/4.01	0.184	0.162
	$v = 2/v = 0$	0.611/4.01	0.152	0.114

[a] Backing pressure experiments performed with OCS in Ar.

[b] 1560 Gas Units = 1 atm.

reactant, then peak intensities should level. The results of these experiments are located in Table 7.4.

Although the data set is small in Table 7.4, there is a trend of increasing intensity as the concentration is increased, but to a limit. At 0.9% the signal was no longer visible at the 10,000 acquisition cutoff. The outcome of this experiment is strange in that when a common gas mixture is ran, it is usually at 3% concentration, an order of magnitude more than some of these here. The ratios, however, are consistent with the control values indicating no change in the vibrational state distributions, only peak intensities (all peaks are stronger/weaker).

Although not explicitly mentioned in the literature, rich gas mixes are a common attribute of the laser ablation technique. What exactly is occurring in the laser ablation event to need

TABLE 7.4. Vibrational State Ratios for the $J = 2 \leftarrow 1$ Rotational Transitions of BaS Adjusting OCS Concentrations.[a]

Concentration /% OCS	Ratio	Arbitrary Intensities	Value	Control
0.3%	$v = 1/v = 0$	0.729/4.58	0.164	0.162
	$v = 2/v = 0$	0.560/4.58	0.122	0.114
0.6%	$v = 1/v = 0$	0.979/6.16	0.159	0.162
	$v = 2/v = 0$	0.739/6.16	0.120	0.114
0.9%	$v = 1/v = 0$	No Signal	N/A	0.162
	$v = 2/v = 0$	No Signal	N/A	0.114

[a] OCS in an Ar carrier gas.

such low concentrations of gas is unclear. A better test for the future would be to dip below 0.3% concentrations and test these ratios.

7.3.2.4. Carrier Gas Experiments. The next set of experiments performed were the carrier gas experiments. In this set of tests, all variables remained constant as a mixture of OCS was created in Ar and He carrier gas. According to the supersonic expansion, the mass the gas is inversely proportional to the average temperature. If this mass is lowered in the ablation event, this should rise the temperature of the jet. If the event is dominated by the expansion then this should populated higher vibrational states. A table of the results in OCS is located in Table 7.5.

Evaluating Table 7.5, there is not a large change in the distribution of the first and second vibrational states relative to the ground when using He instead of Ar. In fact, the He run matched better with the control for these set of data than the Ar run did. One considerable difference is again the intensity. This difference, however, may be attributed to the timing differences between using a He carrier gas and an Ar carrier gas. Also, the expansion may be considerably warmer rotationally because rotational temperature energy exchange is more efficient than the vibrational temperature exchange in the jet.[3] The higher rotational levels may be getting populated in the He expansion. The distribution of higher

TABLE 7.5. Vibrational State Ratios for the $J = 2 \leftarrow 1$ Rotational Transitions of BaS Adjusting Carrier Gas Constitutions.[a]

Carrier Gas	Ratio	Arbitrary Intensities	Value	Control
Argon	$v = 1/v = 0$	3.085/14.518	0.212	0.162
	$v = 2/v = 0$	2.131/14.518	0.147	0.114
Helium	$v = 1/v = 0$	0.935/6.267	0.149	0.162
	$v = 2/v = 0$	0.742/6.267	0.118	0.114

[a] OCS in carrier gas mixtures.

vibrational states ($v \geq 3$) relative to the ground. It is in these states that the best answer may lie in determining the vibrational state distribution in the ablation setup. This would require more acquisitions (again ca. 1 million acquisitions) to give substantial signal-to-noise ratios for the higher vibrational states to accurately determine the ratios to the ground vibrational state.

7.3.2.5. Backing Gas Constitution. Until now, all experiments and conclusions drawn have been on the vibrational state distributions of BaS have been with carried out with OCS in the backing gas mixture. Since the reaction should only need a source of sulfur to carry out the synthesis of BaS in the laser ablation, H_2S was used as a last test to try and understand the chemistry in the ablation nozzle. H_2S was ran in both Ar and He carrier gases to see any relationships to the OCS experiments. The results of these experiments is in Table 7.6

Experiments of H_2S ran with in He did not give conclusive results because of signal, but the Ar run provided for a very interesting result when compared to the control. The $v = 1/v = 0$ ratio for H_2S in Ar was significantly larger than the control experiment while the $v = 2/v = 0$ ratio was slightly lower. The vibrational state population in these experiments lean toward $v = 1$ state more heavily than in previous experiments. So much so that it may be adjusting the distributions of the $v = 0$ and $v = 2$ states. Many more experiments would need to be ran on H_2S and other sulfur-containing gases to confirm whether or not this is

TABLE 7.6. Vibrational State Ratios for the $J = 2 \leftarrow 1$ Rotational Transitions of BaS using H_2S instead of OCS in the Gas Mixture.[a]

Carrier Gas	Ratio	Arbitrary Intensities	Value	Control
Argon	$v = 1/v = 0$	0.788/3.805	0.207	0.162
	$v = 2/v = 0$	0.397/3.805	0.104	0.114
Helium	$v = 1/v = 0$	No Signal/0.771	N/A	0.162
	$v = 2/v = 0$	No Signal/0.771	N/A	0.114

[a] H_2S tested in both Ar and He.

actually the case or an experimental anomaly (and the process). If this is the case, however, it would mean that there is more going on with the chemistry of the BaS synthesis than just the need of a source of sulfur.

7.3.2.6. Rotational Constants and Other Notes. Lastly, it is important to note that rovibrational constants were obtained for the data set using the higher resolution cavity measurements and are reported for $^{138}Ba^{32}S$ in Table 7.7. They are compared against the previous work of Winnewisser[122] and are in good agreement. The most noteable contribution was the inclusion of BOB parameters for the isotopologue. The fit was achieved through an in house Dunham analysis.[21] This analysis does not take into account hyperfine structure, but the reported isotopologue has $I = 0$ for ^{138}Ba and ^{32}S so this is not needed. Hyperfine structure was observed for $^{135}Ba^{32}S$ and $^{137}Ba^{32}S$ isotopologues, for which one vibrational state of $^{135}Ba^{32}S$ has been assigned while the others have yet to be assigned (see Appendix E).

7.3.3. Conclusions

The microwave spectrum for BaS has been reported from 6-19 GHz using cavity and CP-FTMW spectrometers. Vibrational state population analysis have been performed using the relative intensity feature of the CP-FTMW experiment in an attempt to understand the laser ablation event. Preliminary studies indicate that the laser power, carrier gas, and backing gas constitutions all seem to affect the final vibrational state populations in comparison to

TABLE 7.7. Rovibrational Constants for $^{138}Ba^{32}S$ compared to Literature.

Parameter	This Work	Literature[122]
Y_{01} / MHz	3097.28318(674)[a]	3097.28216(26)
Y_{02} / kHz	-0.918966(198)	-0.918568(63)
Y_{03} / mHz	-0.033(32)	Not Reported
Y_{11} / MHz	-9.44831(323)	-9.44620(33)
Y_{21} / kHz	-12.240(113)	-13.323(66)
Y_{31} / kHz	-0.1314(105)	Not Reported
Y_{12} / Hz	-1.017(234)	-1.554(73)
Y_{22} / Hz	-0.1956(873)	Not Reported
Δ_{01}^{Ba} / Unitless	-3.257(559)	Not Reported
Δ_{01}^{S} / Unitless	-5.1045(780)	Not Reported

[a] Uncertainties in parenthesis are given to the least significant figure.

a control, but more studies are needed to be certain that these are not results indicative of a small data set. Rovibrational constants have been determined, reported, and compared to the main isotopologue $^{138}Ba^{32}S$. Hyperfine splitting was observed for the less abundant $^{135}Ba^{32}S$ and $^{137}Ba^{32}S$ isotopologues.

7.4. Tin Monochloride, SnCl[3]

Tin monochloride, SnCl, is an open-shell diatomic molecule with a $^2\Pi_r$ ground state. Traditionally, molecules such as SnCl have been problematic studying experimentally because of the complexity of the problem. Heavy metal containing molecules can be computationally complex and also have relativistic complications when trying to predict spectra even at high levels of theory. Even if the structure of this type of molecule can be determined well (including low resolution rotational constants), because of the many spins involved (in this case due to an unpaired electron and a quadrupolar nuclei), the spectra is difficult to assign and often difficult to locate experimentally using the Balle-Flygare cavity technique.

[3]Section taken in part from presentation given in Ref. [43]

For these reasons, CP-FTMW spectroscopy was chosen to study this molecule. It allows for broad regions of spectra to be scanned which allows for fast search times. A previous rotational band study of $^{120}Sn^{35}Cl$ in the ultraviolet (UV) region gave rotational constants[123] which were used as a starting region for the search.

7.4.1. Experimental Methods

Two spectrometers were used in this study. The automated CP-FTMW with laser ablation source detailed in the literature[47, 28] and the Balle-Flygare type cavity spectrometer with laser ablation source also detailed in the literature[15]. The CP-FTMW spectrometer was used as a searching tool while the cavity was used in resolving dense spectra. CP-FTMW 40 μs FID averages were taken for 50,000 acquisitions and used 500 MHz "chirps" to give 1 GHz ranges of spectra with 3.5 μs chirp durations were used. Gas mixtures of Cl_2 and other parameters were the same as described earlier in the chapter. A portion of this spectrum can be found in Figure 7.3.

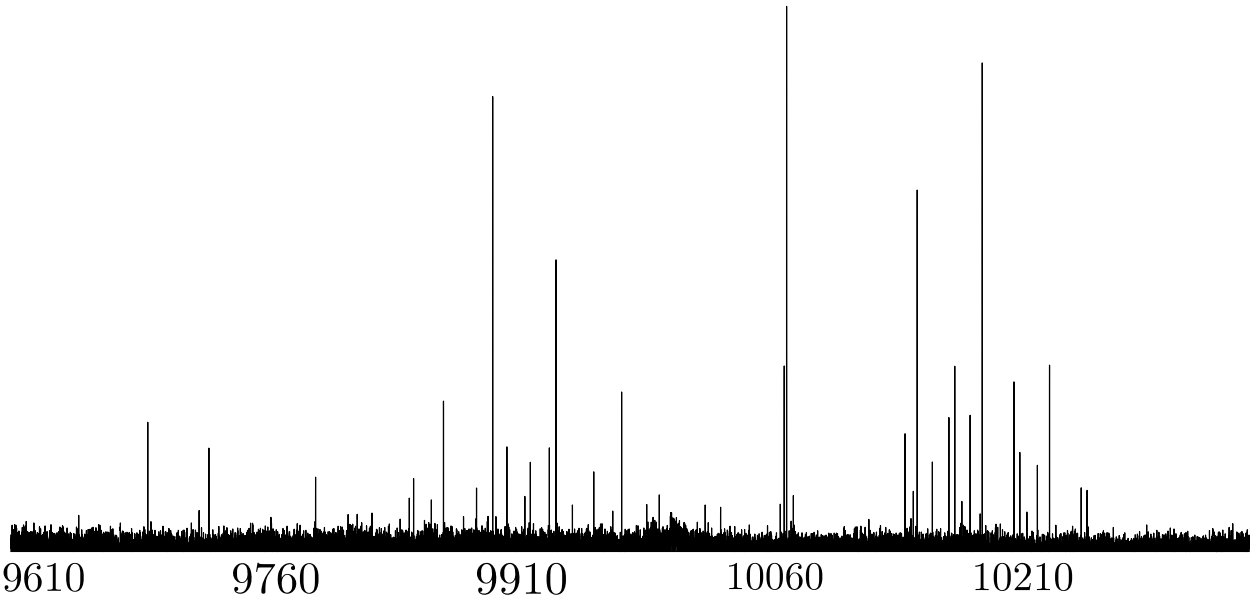

FIGURE 7.3. A Portion of SnCl Spectra Obtained at 10 GHz showing $J' - J'' = 1.5 \leftarrow 0.5$.

7.4.2. Results and Conclusions

Spectral runs of SnCl were collected at 10 and 16.5 GHz. A listing of all measured transitions can be found in Appendix E. Spectral fits of the data were attempted, but due to the complexity of the experiment (multiple spins, ground state configuration, multiple isotopologues), no successful fit was obtained even with literature data available. More information was needed. In order to aid in this assignment, cavity measurements were used.

Cavity measurements in the region allowed for a higher resolution look into the transitions already measured by the CP-FTMW. This is shown in Figure 7.4. In frequency regions above 15 GHz, the bandwidth of the scope provides problems for sensitivity when directly digitizing. For the measurements made in this region, the cavity experiment was used some as a searching tool to determine if some less intense transitions may have been missed. Figure 7.5 shows a comparison of transition measurements around 16900 MHz between the cavity and broadband techniques.

As mentioned earlier, many attempts at an assignment were made, but not successful and are still in progress. Magnetic and nuclear quadrupole hyperfine structure complicated the spectra. Whenever a fit did seem to present itself, incorrect prediction of transitions or illogical magnitudes and values of constants would arise when compared to similar molecules and their trends.

7.5. Lead Monochloride, PbCl[4]

Lead monochloride, PbCl, is also an open-shell diatomic with a $^2\Pi_r$ ground state. PbCl is interesting for a few reasons. The first is the same as that for SnCl. There are many electrons in systems such as PbCl and SnCl complicating electronic calculations. This, coupled with the fact that there is a heavy metal in the molecule requires many approximations to be made in these types of molecules when doing computations. Are these approximations good? There needs to be some experimental data available to help out with these problems.

A second, more notable reason to study PbCl is to help in the quest for seeking an electron's dipole moment. Under the standard model of particle physics, electrons are spherical

[4]Section taken in part from presentation given in Ref. [44]

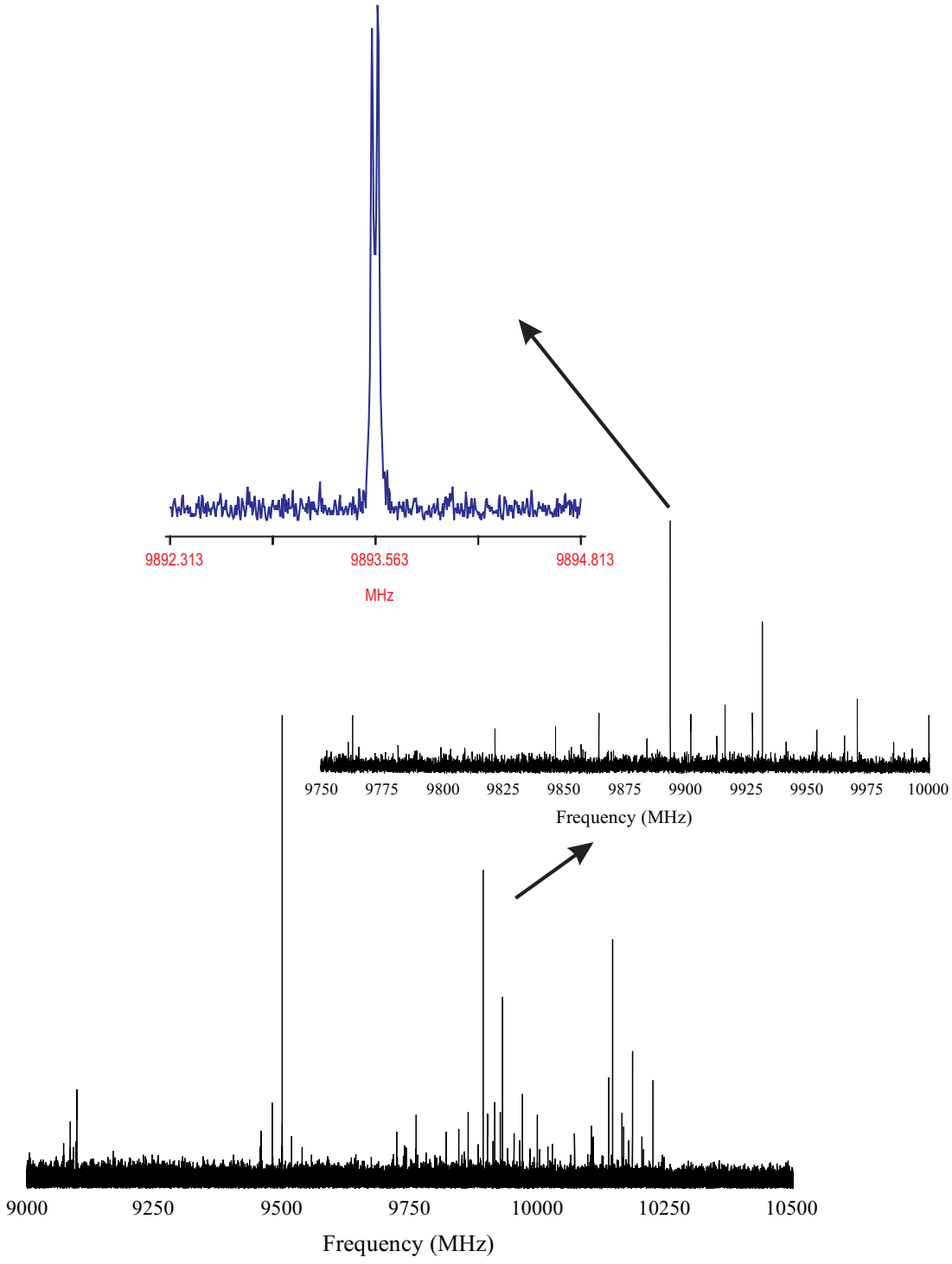

FIGURE 7.4. A Cavity Zoom In of a $J = 1.5 \leftarrow 0.5$ SnCl transition measured on the cavity at 9893.5609 MHz.

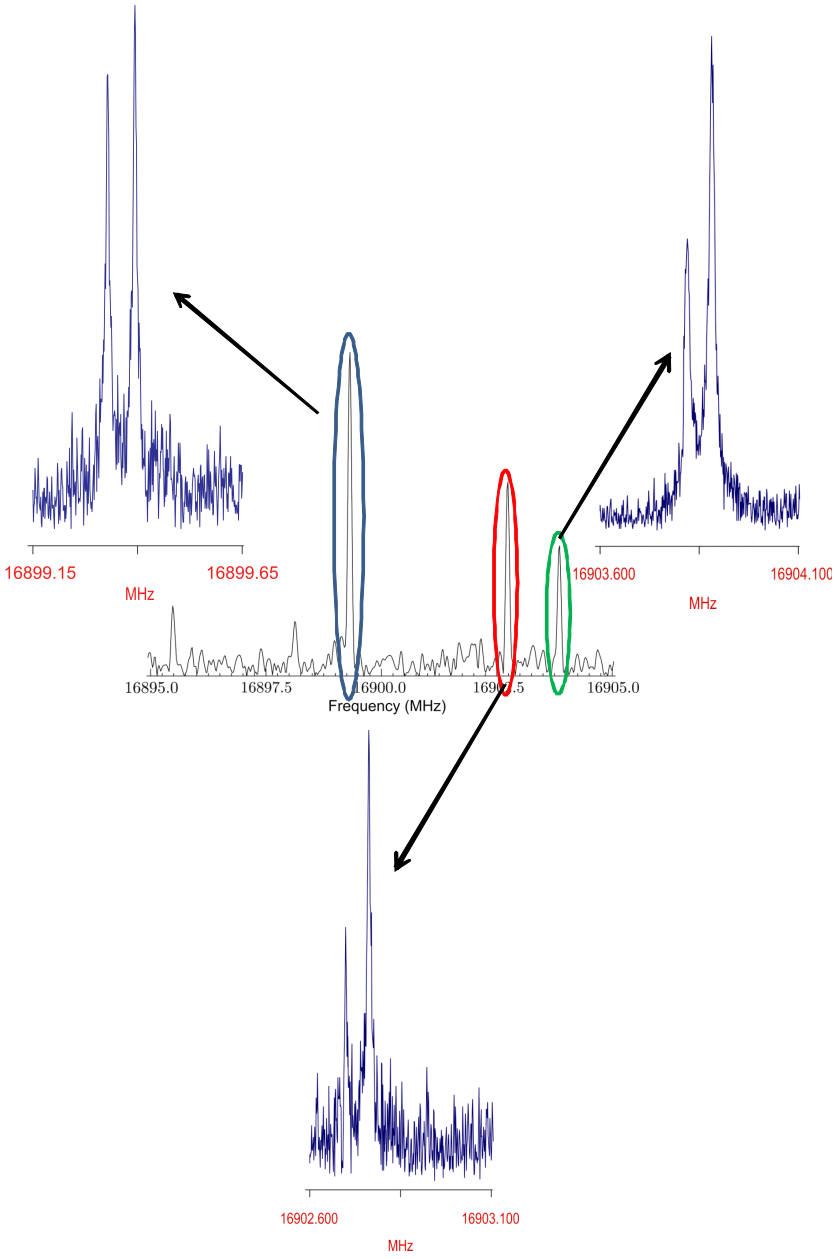

FIGURE 7.5. Three SnCl $J = 2.5 \leftarrow 1.5$ transitions measured around 16900 MHz.

point charges. If a dipole moment for the electron can be measured, it could change the standard model. It has been suggested that lead halides could be used in researching this matter.

7.5.1. Experimental Methods

The techniques utilized in this study were mentioned at the beginning of the chapter with no notable modifications. The only difference here was that the cavity technique had been utilized first to find transitions. Once transitions were found, the CP-FTMW with laser ablation source correct intensity feature was utilized to aid in assignment. Figure 7.6 shows a comparison of all techniques utilized.

7.5.2. Results and Analysis

A previous study of PbCl in the infrared for $^{208}Pb^{35}Cl$[124] gave a good starting place for both searching for transitions and assigning them. To assign them, a fit of the previous data set provided for a nice place to start when trying to understand the physics of the problem. In the study, Fink and coworkers studied the $X_2\ ^2\Pi_{\frac{3}{2}} \rightarrow X_1\ ^2\Pi_{\frac{3}{2}}$ transitions of PbF and PbCl. The assigned quantum numbers in the paper were set up in Pickett's SPFIT/SPCAT software[63] with the help of the documentation provided by the program. Proper assignment of the quantum numbers reproduced the fit in the literature.

When trying to understand the assignment, it is important to understand the parity of a transition. The constant p that determines this was reported as -0.020367 cm^{-1}. In the rotational transitions measured at UNT, there was approximately 600 MHz between two sets of transitions measured for PbCl, this was recognized as the e and f parity[125] transitions. With this knowledge in hand, it could be understood that furthur splitting would be due to magnetic and nuclear hyperfine structure.

Using the Fink data and the transitions measured at UNT, a tentative assignment has been made for the $^{208}Pb^{35}Cl$, but not the other transitions. With both sets of data, the hyperfine parameters d, $a-(b+c)/2$, and eQq_{eff} have been determined and are reported in Table 7.8 against the previously reported Fink literature values[124]. A sample input file with measured transitions and their quantum numbers can be found in Appendix E.

In order to understand the parameters given in Table 7.8, PbCl was compared against other tetral monochlorides for which the hyperfine parameters are known. This data is given

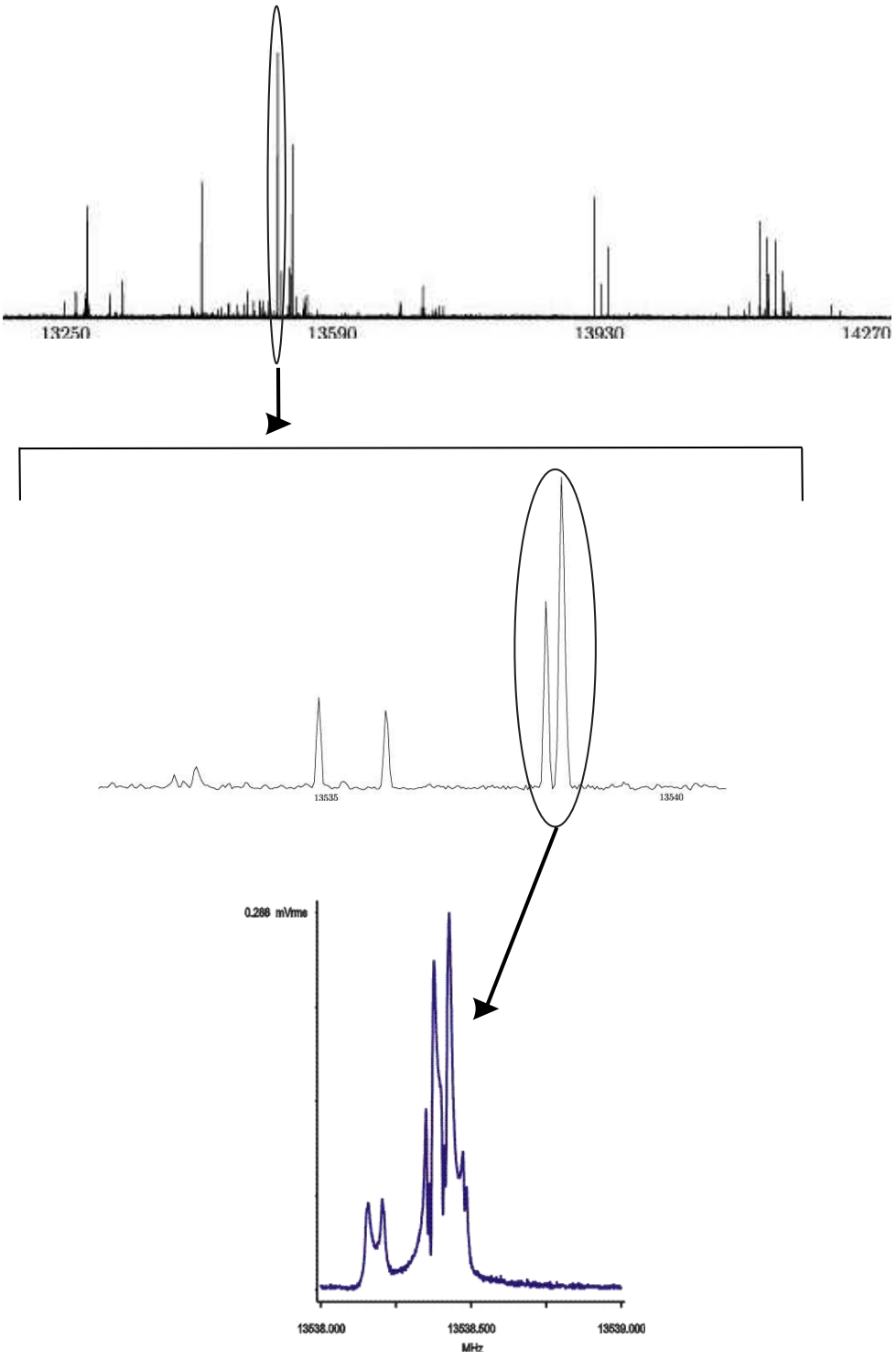

FIGURE 7.6. PbCl Transition Shown from the CP-FTMW to the Cavity Experiment. Resolution from the Cavity shows many Transitions not resolved by the CP-FTMW.

TABLE 7.8. Spectroscopic Parameters for $^{208}Pb^{35}Cl$ Compared Against Literature.

Parameter	This Work with Lit.	Literature Only[124]
B / MHz	2801.8554(48)[a]	2801.89(6)
D / kHz	1.076(47)	1.01(9)
A / MHz	248333381(13)	248333535(3)
A_D / MHz	72.1111(15)	71.896(6)
p / MHz	-610.944(36)	-610.59(2)
p_D / kHz	-1.694(98)	-0.22(6)
$\mid d \mid$ / MHz	40.832(36)	Not Reported
$a-(b+c)/2$ / MHz	30.170(43)	Not Reported
eQq_{eff} / MHz	-24.94(15)	Not Reported
Microwave RMS / kHz	4.97	N/A

[a] Uncertainties in parenthesis are given to the least significant figure.

in Table 7.9. When making these comparisons, PbCl fits nicely into the trends moving down the group.

TABLE 7.9. Hyperfine Parameters for $^{208}Pb^{35}Cl$ Compared Against Literature.

Parameter	CCl[126]	SiCl[127]	PbCl
$\mid d \mid$ / MHz	82.212	46.40(94)[a]	40.8326(55)
$a-(b+c)/2$ / MHz	93.96	49.84(73)	30.170(13)
$eQq_{1/eff}$ / MHz	-34.26	-23.13	-24.943(29)

[a] Uncertainties in parenthesis are given to the least significant figure.

In the literature studies of CCl and SiCl, where a, b, c, and d were determined, it was found that $b \sim -c/3$. The Fermi contact term, typically labelled b_F, is equal to $b+(c/3)$. This term is proportional to $\psi^2(0)$, or the amount of s orbital character.[1] If this term is ~ 0, then the unpaired electron in the molecule has little, if any s-orbital character, which

is expected from a valence electron standpoint in these molecules. As furthur evidence, an MP2/LANL2DZ calculation for PbCl gives b_F =0.002 MHz.

Due to the trend that these molecules have essentially zero for the Fermi contact term, most of the change in $a-(b+c)/2$ is probably due to the a term. d is also decreasing across the table, which means that these values need to be understood. The equations for a and d are[1, 20]:

$$a = \frac{2\mu_0\mu_I}{I}\left(\frac{1}{r^3}\right)_{av} \quad (74)$$

$$d = \frac{3\mu_0\mu_I}{I}\left(\frac{\sin^2\theta}{r^3}\right)_{av}. \quad (75)$$

The dependence over $\left(\frac{1}{r^3}\right)_{av}$ is similar to that of a quadrupole coupling constant, indicating increasing ionicity, which is expected and also reflected in the $eQq_{1/eff}$ values.

7.5.3. Conclusions

Transitions for the open-shell diatomic PbCl have been observed. Used in conjunction with other literature measurements, a tentative assignment of the $^{208}Pb^{35}Cl$ isotopologue has been reported. Hyperfine parameters have been determined and reported. The hyperfine parameters have been compared against the literature values of other tetral chlorides. The resulting hyperfine values have been interpreted as moving from a covalent CCl to a more ionic PbCl system.

7.6. Overall Conclusions

The molecules of BaS, SnCl, and PbCl have all been measured spectroscopically on a CP-FTMW spectrometer. Through the relative intensity features, the spectrometer has demonstrated the ability to measure *in situ* chemistry of the ablation nozzle and ease assignment of spectra. Measurements of SnCl have shown the ability of the spectrometer to look at molecules utilizing the laser ablation source without utilizing the cavity experiment first, demonstrating its capacity as a stand-alone technique. Rotational constants and interpretations thereof have been provided when possible.

CHAPTER 8

CONCLUSIONS AND FUTURE WORK

Fast passage Fourier transform microwave spectroscopy has been utilized to create a search accelerated broadband technique. This technique has been shown to provide correct intensity spectra at up to 4000 times the speed of that of the typical cavity technique at a fraction of the cost of other broadband rotational techniques. This correct intensity feature in conjunction with theory has been shown to be useful in assigning otherwise difficult spectra in a fraction of the time. The spectra characterized in this work has shown to be of sufficient resolution to observe small energetic splittings such as magnetic and electronic hyperfine structures. The spectra presented in this work also provided insight into the sensitivity of the technique by providing examples of spectra containing weak isotopologues (<1%) in natural abundance as well as some examples of multiple types of dipole transitions.

The technique also was shown to include a way to sample molecules of gas, liquids, and laser ablation-created species into a supersonic expansion. Using the spectrometer, these molecules could then be studied *in situ* to provide information about geometric and electronic structure through the determination of rotational, nuclear electric hyperfine, and magnetic hyperfine constants. The technique has also been used as a probe to understanding chemistry happening in a laser ablation event by testing parameters of the event and comparing the vibrational state distribution through a control.

The existing technology utilized in this experiment could be furthur utilized for some future endeavors. For instance, the arbitrary waveform generator used to create the chirp can make a second sinusoidal pulse at a specific frequency of a known transition to perform double resonance experiments. These types of experiments are useful in mapping out transition pathways and can be utilized in transition assignment. This would greatly aid in the under-

standing of the mechanism by which dipole forbidden transitions occur.

Multiple free induction decay (FID) collection and furthur laser ablation work is also a goal of the experiment. Multiple FID collection is possible because the valve pulses at most at a rate of 4 Hz. The FID of a rotational transition is on the order of 100-150 μs, which means multiple excitations and relaxations can occur in this span as long as molecules have not been evacuated below detection limits. This would give quicker detection with less sample usage. With the laser ablation work, actinides and lanthanide containing diatomics could be quickly found and studied giving some insight into f-electron chemistry .

Understanding the nature of the chemical bond is at the heart of all molecular spectroscopy. Details such as nuclear electric quadrupole coupling constants have been provided in this work. They have, in turn, been categorized with other similar molecules (in the same relative axes systems) to provide insight into electronic environments for the nuclei in question. It has been shown in many of these experiments that perfluorination of a molecule can significantly change the electronic environment of a molecule due to the electron withdrawing capacity of the fluorine atom. These effects have been observed through these types of comparisons amongst families of similar molecules. This high level of insight into a molecule is hard to find in any other technique.

In conclusion, this work provides detailed spectroscopic studies on molecules either purchased or created. The data was collected on a novel, broadband microwave spectrometer and analyses of these spectra has provided insight into the nature of a variety of chemical bonds.

APPENDIX A

PERFLUOROIODOETHANE DATA

Output from SPFIT/SPCAT and edited with PIFORM.[63, 61] Quantum numbers in table are given as $J'_{K_{-1},K_{+1}}$, $F'+\frac{1}{2} \leftarrow J''_{K_{-1},K_{+1}}$, $F''+\frac{1}{2}$. Transition frequencies and assignments for the observed anti conformer of perfluoroiodoethane. Below that is the fitted parameters.

TABLE A.1. Perfluoroiodoethane Transitions Measured in MHz

									obs	o-c	error	blends	
												o-c	wt
1:	3	2	2	6	2	1	1	5	8654.7702	0.0056	0.015		
2:	3	2	2	4	2	1	1	3	8742.8655	0.0015	0.015		
3:	3	2	2	5	2	1	1	4	8784.6886	-0.0095	0.015		
4:	3	2	1	6	2	1	2	5	8806.8651	0.0127	0.015		
5:	3	2	1	5	2	1	2	4	9026.7758	0.0015	0.015		
6:	3	3	1	2	2	2	0	2	11571.1887	-0.0222	0.015		
7:	3	3	1	6	2	2	0	5	11620.6733	0.0023	0.015		
8:	3	3	0	5	2	2	1	4	11651.8139	0.0040	0.050	0.0001	0.50
9:	3	3	1	5	2	2	0	4	11651.8139	-0.0038	0.050	0.0001	0.50
10:	4	2	3	7	3	1	2	6	10088.9581	0.0050	0.015		
11:	5	1	5	4	4	0	4	3	8477.9247	0.0025	0.015		
12:	5	1	5	5	4	0	4	4	8484.1035	-0.0005	0.050	-0.0005	0.50
13:	5	1	5	5	4	0	4	4	8484.1035	-0.0005	0.050	-0.0005	0.50
14:	5	1	5	6	4	0	4	5	8508.7080	0.0006	0.015		
15:	5	1	5	8	4	0	4	7	8527.4988	0.0019	0.015		
16:	5	1	5	7	4	0	4	6	8533.2012	-0.0019	0.015		
17:	5	2	4	8	4	1	3	7	11486.5081	-0.0015	0.015		
18:	5	2	4	5	4	1	3	4	11501.1388	-0.0142	0.015		
19:	5	2	4	6	4	1	3	5	11525.2678	-0.0061	0.015		
20:	6	1	6	8	5	1	5	8	8538.7164	0.0057	0.015		
21:	6	0	6	8	5	0	5	8	8668.3379	-0.0040	0.015		
22:	6	1	6	7	5	1	5	7	8766.4335	-0.0059	0.015		
23:	6	1	6	5	5	1	5	4	8808.1228	-0.0014	0.015		
24:	6	1	6	6	5	1	5	5	8810.0791	-0.0017	0.015		
25:	6	1	6	7	5	1	5	6	8824.7661	-0.0013	0.015		

26:	6	1	6	4	5	1	5	3	8826.5446	-0.0017	0.015
27:	6	1	6	8	5	1	5	7	8839.5999	-0.0009	0.015
28:	6	1	6	9	5	1	5	8	8846.3033	-0.0001	0.015
29:	6	2	5	8	5	2	4	8	8848.3974	-0.0096	0.015
30:	6	5	2	7	5	5	1	6	8895.5350	-0.0028	0.015
31:	6	0	6	7	5	0	5	7	8901.4193	-0.0078	0.015
32:	6	2	4	8	5	2	3	8	8921.3480	-0.0010	0.015
33:	6	2	5	7	5	2	4	7	8928.7044	-0.0076	0.015
34:	6	5	1	8	5	5	0	7	8931.3633	-0.0031	0.015
35:	6	0	6	5	5	0	5	4	8937.2118	-0.0027	0.015
36:	6	4	3	7	5	4	2	6	8939.4239	-0.0132	0.015
37:	6	4	2	7	5	4	1	6	8939.4762	-0.0012	0.015
38:	6	0	6	6	5	0	5	5	8941.8564	-0.0025	0.015
39:	6	0	6	4	5	0	5	3	8951.7293	-0.0008	0.015
40:	6	0	6	7	5	0	5	6	8957.9821	-0.0024	0.015
41:	6	4	3	8	5	4	2	7	8962.6964	-0.0010	0.015
42:	6	4	2	8	5	4	1	7	8962.8004	-0.0067	0.015
43:	6	4	3	6	5	4	2	5	8964.8999	0.0008	0.015
44:	6	4	2	6	5	4	1	5	8965.1689	-0.0002	0.015
45:	6	1	5	8	5	1	4	8	8969.0414	-0.0031	0.015
46:	6	0	6	9	5	0	5	8	8972.3726	-0.0003	0.015
47:	6	0	6	8	5	0	5	7	8972.8416	-0.0011	0.015
48:	6	3	4	7	5	3	3	7	8975.5854	0.0031	0.015
49:	6	3	3	7	5	3	2	7	8977.8341	0.0024	0.015
50:	6	2	5	6	5	2	4	5	8981.6821	0.0017	0.015
51:	6	5	2	6	5	5	1	5	8982.0759	0.0043	0.015
52:	6	2	5	8	5	2	4	7	8986.8584	-0.0025	0.015
53:	6	3	3	8	5	3	2	8	8987.4349	0.0122	0.015
54:	6	2	5	5	5	2	4	4	8987.5986	0.0002	0.015
55:	6	3	3	7	5	3	2	6	8989.4075	-0.0015	0.015
56:	6	2	5	7	5	2	4	6	8993.0340	-0.0015	0.015
57:	6	3	4	8	5	3	3	7	8993.5867	-0.0004	0.015
58:	6	3	3	8	5	3	2	7	8995.6816	-0.0004	0.015

59:	6	1	6	5	5	1	5	5	8995.8306	-0.0065	0.015		
60:	6	2	4	7	5	2	3	7	9000.3486	-0.0096	0.015		
61:	6	3	4	6	5	3	3	5	9008.7967	-0.0004	0.015		
62:	6	3	3	6	5	3	2	5	9010.1010	-0.0011	0.015		
63:	6	3	4	6	5	3	3	6	9012.6875	0.0000	0.015		
64:	6	3	3	6	5	3	2	6	9014.2715	0.0086	0.015		
65:	6	2	5	4	5	2	4	3	9027.4942	0.0012	0.015		
66:	6	1	6	4	5	1	5	4	9031.8998	0.0033	0.015		
67:	6	4	2	4	5	4	1	4	9036.2483	0.0205	0.050	0.0078	0.50
68:	6	4	3	4	5	4	2	4	9036.2483	-0.0049	0.050	0.0078	0.50
69:	6	4	3	5	5	4	2	4	9042.4909	0.0006	0.015		
70:	6	4	2	5	5	4	1	4	9042.6492	0.0023	0.015		
71:	6	3	4	5	5	3	3	4	9042.9376	-0.0009	0.015		
72:	6	2	5	9	5	2	4	8	9044.4539	0.0016	0.015		
73:	6	3	3	5	5	3	2	4	9045.2458	0.0011	0.015		
74:	6	0	6	6	5	0	5	6	9047.0227	-0.0004	0.015		
75:	6	2	4	6	5	2	3	5	9049.7135	0.0025	0.015		
76:	6	2	5	6	5	2	4	6	9053.6686	-0.0061	0.015		
77:	6	2	4	5	5	2	3	4	9054.0724	0.0024	0.015		
78:	6	2	4	8	5	2	3	7	9055.4165	0.0001	0.015		
79:	6	2	4	7	5	2	3	6	9059.5374	-0.0009	0.015		
80:	6	3	4	5	5	3	3	5	9063.8301	-0.0012	0.015		
81:	6	3	3	5	5	3	2	5	9065.9759	0.0060	0.015		
82:	6	4	3	9	5	4	2	8	9075.2787	-0.0004	0.015		
83:	6	4	2	9	5	4	1	8	9075.5919	-0.0020	0.015		
84:	6	3	4	9	5	3	3	8	9085.7577	0.0018	0.015		
85:	6	3	3	9	5	3	2	8	9087.4886	0.0020	0.015		
86:	6	2	4	4	5	2	3	3	9089.5545	0.0029	0.015		
87:	6	3	4	4	5	3	3	3	9091.6389	-0.0015	0.015		
88:	6	3	3	4	5	3	2	3	9093.4510	0.0003	0.015		
89:	6	2	4	9	5	2	3	8	9105.4891	0.0026	0.015		
90:	6	2	5	5	5	2	4	5	9113.4191	-0.0008	0.015		
91:	6	2	4	6	5	2	3	6	9116.6487	-0.0041	0.015		

92:	6	5	1	5	5	5	0	4	9120.5676	-0.0042	0.015		
93:	6	0	6	5	5	0	5	5	9124.5537	-0.0029	0.015		
94:	6	1	5	7	5	1	4	7	9132.9996	0.0042	0.015		
95:	6	2	5	4	5	2	4	4	9143.9212	-0.0062	0.015		
96:	6	5	2	9	5	5	1	8	9146.8818	0.0020	0.050	0.0005	0.50
97:	6	5	1	9	5	5	0	8	9146.8818	-0.0011	0.050	0.0005	0.50
98:	6	0	6	4	5	0	5	4	9157.6365	-0.0072	0.015		
99:	6	4	3	4	5	4	2	3	9163.7585	0.0075	0.050	-0.0016	0.50
100:	6	4	2	4	5	4	1	3	9163.7585	-0.0108	0.050	-0.0016	0.50
101:	6	1	5	5	5	1	4	4	9170.2398	0.0004	0.015		
102:	6	1	5	6	5	1	4	5	9170.8794	0.0001	0.015		
103:	6	2	4	5	5	2	3	5	9174.1114	0.0005	0.015		
104:	6	1	5	7	5	1	4	6	9181.9189	0.0007	0.015		
105:	6	1	5	4	5	1	4	3	9186.4753	0.0025	0.015		
106:	6	1	5	8	5	1	4	7	9192.8891	0.0015	0.015		
107:	6	2	4	4	5	2	3	4	9201.6221	-0.0007	0.015		
108:	6	1	5	9	5	1	4	8	9201.6226	0.0026	0.015		
109:	6	1	5	6	5	1	4	6	9251.2277	0.0044	0.015		
110:	6	5	1	4	5	5	0	3	9252.5935	0.0015	0.015		
111:	6	1	5	5	5	1	4	5	9316.7659	-0.0003	0.015		
112:	6	1	5	4	5	1	4	4	9346.0284	-0.0046	0.015		
113:	6	2	4	8	4	3	1	7	9545.1643	0.0041	0.015		
114:	6	1	6	5	5	0	5	4	9840.4623	0.0322	0.015		
115:	6	1	6	6	5	0	5	5	9842.0186	0.0029	0.015		
116:	6	4	2	5	6	3	3	4	9855.8760	0.0046	0.015		
117:	6	1	6	7	5	0	5	6	9856.8227	0.0054	0.015		
118:	6	1	6	4	5	0	5	3	9858.3023	0.0138	0.015		
119:	6	4	2	9	6	3	3	9	9866.7245	-0.0182	0.015		
120:	6	1	6	8	5	0	5	7	9873.4192	-0.0021	0.015		
121:	6	1	6	9	5	0	5	8	9876.5101	-0.0032	0.015		
122:	7	0	7	6	6	1	6	5	9510.0989	-0.0014	0.015		
123:	7	0	7	7	6	1	6	6	9516.3672	0.0089	0.015		
124:	7	0	7	8	6	1	6	7	9529.0904	-0.0020	0.015		

125:	7	0	7	10	6	1	6	9	9535.2000	-0.0090	0.015		
126:	7	0	7	9	6	1	6	8	9538.0981	-0.0064	0.015		
127:	7	3	4	9	5	4	1	8	9674.4835	-0.0114	0.015		
128:	7	4	4	10	7	3	5	10	9899.7087	0.0096	0.015		
129:	7	1	7	8	6	1	6	8	10221.2004	-0.0055	0.015		
130:	7	1	7	6	6	1	6	5	10281.1641	-0.0022	0.015		
131:	7	1	7	7	6	1	6	6	10283.3332	-0.0017	0.015		
132:	7	1	7	5	6	1	6	4	10293.9129	-0.0015	0.015		
133:	7	1	7	8	6	1	6	7	10294.3660	-0.0013	0.015		
134:	7	1	7	9	6	1	6	8	10305.4936	-0.0015	0.015		
135:	7	1	7	10	6	1	6	9	10308.8690	-0.0001	0.015		
136:	7	2	6	9	6	2	5	9	10313.8773	0.0077	0.015		
137:	7	0	7	8	6	0	6	8	10356.5131	0.0035	0.015		
138:	7	1	7	7	6	1	6	7	10373.6973	-0.0002	0.015		
139:	7	6	1	8	6	6	0	7	10411.9989	-0.0056	0.015		
140:	7	0	7	6	6	0	6	5	10413.3162	0.0004	0.015		
141:	7	0	7	7	6	0	6	6	10416.5147	-0.0002	0.015		
142:	7	0	7	5	6	0	6	4	10424.3550	0.0003	0.015		
143:	7	0	7	8	6	0	6	7	10427.9253	0.0001	0.015		
144:	7	0	7	9	6	0	6	8	10438.6831	0.0000	0.015		
145:	7	0	7	10	6	0	6	9	10439.3506	0.0011	0.015		
146:	7	5	2	8	6	5	1	7	10452.5717	-0.0038	0.015		
147:	7	6	1	9	6	6	0	8	10453.1745	-0.0001	0.015		
148:	7	1	7	6	6	1	6	6	10466.9073	-0.0154	0.015		
149:	7	6	1	7	6	6	0	6	10477.0884	-0.0069	0.015		
150:	7	5	2	9	6	5	1	8	10479.7301	0.0008	0.015		
151:	7	1	6	9	6	1	5	9	10483.7813	0.0041	0.015		
152:	7	4	4	8	6	4	3	7	10488.7019	0.0257	0.015		
153:	7	4	4	8	6	4	3	8	10492.3749	0.0068	0.015		
154:	7	2	6	7	6	2	5	6	10497.8468	-0.0012	0.015		
155:	7	5	3	7	6	5	2	6	10500.8675	-0.0070	0.050	-0.0017	0.50
156:	7	5	2	7	6	5	1	6	10500.8675	0.0035	0.050	-0.0017	0.50
157:	7	2	6	8	6	2	5	7	10501.4682	-0.0012	0.015		

158:	7	4	4	9	6	4	3	8	10503.7093	-0.0007	0.050	0.0008	0.50	
159:	7	4	3	9	6	4	2	8	10503.7093	0.0024	0.050	0.0008	0.50	
160:	7	2	6	6	6	2	5	5	10504.0272	-0.0004	0.015			
161:	7	0	7	7	6	0	6	7	10505.5688	0.0152	0.015			
162:	7	2	6	9	6	2	5	8	10509.9143	-0.0005	0.015			
163:	7	3	5	8	6	3	4	7	10517.6620	0.0015	0.015			
164:	7	4	3	7	6	4	2	6	10520.6712	-0.0036	0.015			
165:	7	4	4	7	6	4	3	6	10520.8208	-0.0084	0.015			
166:	7	3	4	8	6	3	3	7	10522.4621	0.0013	0.015			
167:	7	2	6	5	6	2	5	4	10525.4015	-0.0008	0.015			
168:	7	3	5	7	6	3	4	6	10528.1117	-0.0033	0.015			
169:	7	3	4	7	6	3	3	6	10533.6668	-0.0015	0.015			
170:	7	2	6	10	6	2	5	9	10534.3169	0.0000	0.015			
171:	7	4	3	6	6	4	2	6	10543.4465	0.0086	0.015			
172:	7	2	5	8	6	2	4	8	10548.2321	-0.0055	0.015			
173:	7	3	5	7	6	3	4	7	10553.5053	0.0022	0.015			
174:	7	3	4	7	6	3	3	7	10558.5377	0.0155	0.015			
175:	7	3	5	9	6	3	4	8	10561.2185	0.0038	0.015			
176:	7	4	3	6	6	4	2	5	10564.8129	0.0025	0.015			
177:	7	4	4	6	6	4	3	5	10564.8608	-0.0022	0.015			
178:	7	3	4	9	6	3	3	8	10565.7122	0.0045	0.015			
179:	7	3	5	6	6	3	4	5	10575.2119	-0.0021	0.015			
180:	7	3	5	10	6	3	4	9	10576.7834	0.0018	0.015			
181:	7	3	4	6	6	3	3	5	10579.5277	-0.0041	0.015			
182:	7	4	3	9	6	4	2	9	10579.7214	-0.0073	0.015			
183:	7	4	4	9	6	4	3	9	10579.9771	0.0041	0.015			
184:	7	3	4	10	6	3	3	9	10581.2764	0.0023	0.015			
185:	7	5	2	6	6	5	1	5	10584.6628	-0.0072	0.050	-0.0039	0.50	
186:	7	5	3	6	6	5	2	5	10584.6628	-0.0004	0.050	-0.0039	0.50	
187:	7	0	7	6	6	0	6	6	10596.0145	0.0010	0.015			
188:	7	6	1	6	6	6	0	5	10597.0260	-0.0059	0.015			
189:	7	2	5	7	6	2	4	6	10599.1439	0.0013	0.015			
190:	7	2	5	8	6	2	4	7	10603.2981	0.0023	0.015			

191:	7	2	5	6	6	2	4	5	10603.4709	0.0015	0.015
192:	7	4	3	10	6	4	2	9	10606.5871	0.0038	0.015
193:	7	4	4	10	6	4	3	9	10606.7789	0.0026	0.015
194:	7	2	5	9	6	2	4	8	10610.6571	0.0022	0.015
195:	7	4	4	5	6	4	3	4	10612.2979	0.0050	0.015
196:	7	4	3	5	6	4	2	4	10612.3542	-0.0028	0.015
197:	7	3	5	5	6	3	4	4	10613.7128	-0.0034	0.015
198:	7	3	4	5	6	3	3	4	10617.8607	-0.0024	0.015
199:	7	2	5	5	6	2	4	4	10621.8141	0.0018	0.015
200:	7	5	3	10	6	5	2	9	10624.6964	0.0059	0.015
201:	7	3	5	6	6	3	4	6	10630.2533	0.0049	0.015
202:	7	2	5	10	6	2	4	9	10630.8846	0.0036	0.015
203:	7	3	4	6	6	3	3	6	10635.3974	-0.0022	0.015
204:	7	2	6	6	6	2	5	6	10635.7705	0.0032	0.015
205:	7	6	1	10	6	6	0	9	10642.8643	0.0041	0.015
206:	7	0	7	5	6	0	6	5	10644.7844	0.0004	0.015
207:	7	1	6	8	6	1	5	8	10648.0536	0.0030	0.015
208:	7	2	5	7	6	2	4	7	10656.2558	-0.0011	0.015
209:	7	5	2	5	6	5	1	4	10662.0289	-0.0010	0.015
210:	7	2	6	5	6	2	5	5	10681.7370	0.0055	0.015
211:	7	1	6	6	6	1	5	5	10697.8948	0.0023	0.015
212:	7	1	6	7	6	1	5	6	10699.6447	0.0027	0.015
213:	7	1	6	8	6	1	5	7	10707.9447	0.0019	0.015
214:	7	1	6	5	6	1	5	4	10710.2460	0.0025	0.015
215:	7	1	6	9	6	1	5	8	10716.3555	0.0030	0.015
216:	7	1	6	10	6	1	5	9	10721.6467	0.0042	0.015
217:	7	6	1	5	6	6	0	4	10725.8147	-0.0037	0.015
218:	7	2	5	6	6	2	4	6	10727.8632	-0.0061	0.015
219:	7	1	6	7	6	1	5	7	10768.9482	0.0012	0.015
220:	7	2	5	5	6	2	4	5	10769.3810	0.0158	0.015
221:	7	1	6	6	6	1	5	6	10843.7860	0.0065	0.015
222:	7	1	6	5	6	1	5	5	10886.0328	-0.0043	0.015
223:	7	1	7	7	6	0	6	6	11183.4899	-0.0017	0.015

224:	7	1	7	6	6	0	6	5	11184.3816	-0.0002	0.015
225:	7	1	7	8	6	0	6	7	11193.1966	-0.0036	0.015
226:	7	1	7	5	6	0	6	4	11200.4573	-0.0155	0.015
227:	7	1	7	9	6	0	6	8	11206.0658	-0.0080	0.015
228:	7	1	7	10	6	0	6	9	11213.0072	-0.0024	0.015
229:	8	0	8	7	7	1	7	6	11106.3474	-0.0047	0.015
230:	8	0	8	8	7	1	7	7	11112.7244	0.0114	0.015
231:	8	0	8	9	7	1	7	8	11122.9340	0.0021	0.015
232:	8	0	8	11	7	1	7	10	11124.2925	0.0034	0.015
233:	8	0	8	10	7	1	7	9	11129.0686	0.0011	0.015
234:	8	1	8	8	7	1	7	7	11751.2725	-0.0044	0.015
235:	8	1	8	6	7	1	7	5	11758.6589	0.0006	0.015
236:	8	1	8	9	7	1	7	8	11759.8949	-0.0044	0.015
237:	8	1	8	10	7	1	7	9	11768.4786	-0.0008	0.015
238:	8	1	8	11	7	1	7	10	11770.3698	-0.0018	0.015
239:	8	0	8	7	7	0	7	6	11877.4140	-0.0042	0.015
240:	8	0	8	8	7	0	7	7	11879.6926	0.0029	0.015
241:	8	0	8	6	7	0	7	5	11886.3344	0.0098	0.015
242:	8	0	8	9	7	0	7	8	11888.2025	-0.0042	0.015
243:	8	0	8	10	7	0	7	9	11896.4584	0.0002	0.015
244:	8	0	8	11	7	0	7	10	11897.9611	0.0118	0.015
245:	9	1	8	10	8	2	7	9	10487.7473	-0.0157	0.015
246:	11	0	11	13	10	2	8	12	8987.2986	0.0004	0.015
247:	13	3	11	16	12	4	8	15	9671.8363	-0.0012	0.015

PARAMETERS IN FIT:

10000	A	/	/MHz	2178.39031(96)	1
20000	B	/	/MHz	782.01491(46)	2
30000	C	/	/MHz	722.30778(37)	3
200	Delta J	/	/kHz	0.0514(24)	4
1100	Delta JK		/kHz	0.0566(91)	5

```
       40100     deltaJ /  /kHz            0.0059(15)                          6
   110010000      CHIaa /  /MHz         -1739.860(23)                          7
  -110020000      CHIbb /  /MHz          1739.860(23)           = -1.00000 *  7
   110030000      CHIcc /  /MHz          1076.800(28)                          8
  -110020000      CHIbb /  /MHz         -1076.800(28)           = -1.00000 *  8
   110610000      CHIab /  /MHz         -1052.618(53)                          9
    10010000       M.aa /  /MHz            0.0024(12)                        10
    10020000       M.bb /  /MHz            0.00286(65)                       11
    10030000       M.cc /  /MHz            0.00265(62)                       12

MICROWAVE AVG =       -0.000004 MHz, IR AVG =        0.00000
MICROWAVE RMS =        0.005925 MHz, IR RMS =        0.00000
END OF ITERATION  1 OLD, NEW RMS ERROR=        0.39320         0.39320

 distinct frequency lines in fit:   239
      distinct parameters of fit:    12

for standard errors previous errors are multiplied by:   0.403459

PARAMETERS IN FIT WITH STANDARD ERRORS ON THOSE THAT ARE FITTED:

       10000         A  /  /MHz         2178.39031(38)                       1
       20000         B  /  /MHz          782.01491(18)                       2
       30000         C  /  /MHz          722.30778(14)                       3
         200     Delta J/  /kHz            0.05148(98)                       4
        1100     Delta JK  /kHz            0.0566(36)                        5
       40100     deltaJ /  /kHz            0.00591(64)                       6
   110010000      CHIaa /  /MHz         -1739.8608(95)                       7
  -110020000      CHIbb /  /MHz          1739.8608(95)           = -1.00000 *  7
   110030000      CHIcc /  /MHz          1076.800(11)                         8
  -110020000      CHIbb /  /MHz         -1076.800(11)           = -1.00000 *  8
   110610000      CHIab /  /MHz         -1052.618(21)                        9
    10010000       M.aa /  /MHz            0.00247(50)                       10
```

```
     10020000       M.bb /  /MHz            0.00286(26)                        11
     10030000       M.cc /  /MHz            0.00265(25)                        12

 CORRELATION COEFFICIENTS, C.ij:

           A  /     B  /     C  /     -Delta J -Delta J -deltaJ  CHIaa /  CHIcc /

A  /        1.0000
B  /        0.3290   1.0000
C  /       -0.2071  -0.1156   1.0000
-Delta J/  -0.0146  -0.6809  -0.5566   1.0000
-Delta JK  -0.4068  -0.4333  -0.2724   0.3982   1.0000
-deltaJ /  -0.3041  -0.7835   0.6043   0.2474   0.1145   1.0000
CHIaa /    -0.1568  -0.0373   0.0331   0.0100   0.0214   0.0470   1.0000
CHIcc /     0.0970   0.0000  -0.0246   0.0000   0.0120  -0.0551  -0.5098   1.0000
CHIab /     0.0921  -0.0936  -0.0669   0.1329   0.0726   0.0440   0.0424   0.0001
M.aa /     -0.3010   0.1009   0.1659  -0.1562  -0.1277   0.0157   0.1151  -0.0889
M.bb /      0.0665   0.2578  -0.0787  -0.0842  -0.0585  -0.2632  -0.0685  -0.0006
M.cc /      0.0462  -0.0112   0.2530  -0.1158  -0.0334   0.2129  -0.1046   0.0801

           CHIab /  M.aa /   M.bb /   M.cc /

CHIab /     1.0000
M.aa /     -0.2422   1.0000
M.bb /     -0.0188   0.1036   1.0000
M.cc /      0.0216  -0.0769  -0.4632   1.0000

 Mean value of |C.ij|, i.ne.j =   0.1629
 Mean value of  C.ij,  i.ne.j =  -0.0496


 Worst fitting lines (obs-calc/error):
```

```
  114:    2.1       152:    1.7         6:   -1.5       119:   -1.2
  220:    1.1       245:   -1.0       226:   -1.0       174:    1.0
  148:   -1.0       161:    1.0        18:   -0.9       118:    0.9
   36:   -0.9         4:    0.8        53:    0.8       244:    0.8
  127:   -0.8       230:    0.8       241:    0.7        60:   -0.6
  128:    0.6        29:   -0.6         3:   -0.6       125:   -0.6
  123:    0.6        64:    0.6       171:    0.6       165:   -0.6
  227:   -0.5        31:   -0.5       136:    0.5        33:   -0.5
  182:   -0.5        98:   -0.5       149:   -0.5       153:    0.5
   42:   -0.4       221:    0.4        59:   -0.4       126:   -0.4
   95:   -0.4       218:   -0.4        19:   -0.4        76:   -0.4
   81:    0.4        22:   -0.4       188:   -0.4       200:    0.4
   20:    0.4       139:   -0.4

                                      ------------------------------------
_________________________________________/ SPFIT output reformatted with PIFORM
```

APPENDIX B

BROMODIFLUOROACETONITRILE DATA

Quantum chemical calculations comparisons to literature.[1]

TABLE B.1. C–C Bond Lengths (Å). $r_e^{emp} = 0.95547 \times r_{opt} + 0.06568$, where r_{opt} = MP2/aug-cc-pVTZ optimization.

Molecule	$\frac{r_e}{r_m^p}$	r_{opt}	r_e^{emp}	$\mid r_e - r_e^{emp} \mid$	Ref.
NC–CP	1.3759	1.3718	1.3764	0.0005	[128]
HCC–CN	1.3764	1.3722	1.3768	0.0004	[129]
NC–CN	1.3839	1.3778	1.3821	0.0018	[130]
CH_2=CH(CN)	1.429	1.4290	1.4310	0.002	[131]
CH_2=C$(CN)_2$	1.437	1.4338	1.4357	0.001	[132]
CH_3CN	1.457	1.4570	1.4578	0.001	[133]
HCC–CH_3	1.458	1.4584	1.4592	0.001	[134]
$CH_2(CN)_2$	1.464	1.4628	1.4634	0.001	[132]
CH_2=CH(–CH_3)	1.4957	1.4952	1.4943	0.0014	[135]
CH_3–CH_2Cl	1.5096	1.5112	1.5096	0.0000	[135]
CH_3–CH_2–CH_3	1.5209	1.5236	1.5214	0.0006	[135]
CH_3CH_3	1.522	1.5238	1.5216	0.000_4	[136]
			AVG[a]	0.0009	
			RMS[b]	0.0011	

[a] AVG is average absolute difference.

[b] RMS is root mean square difference.

[1] All caculations and literature comparisons were performed and provided by W. C. Bailey.

TABLE B.2. C–F Bond Lengths (Å). $r_e^{emp} = 0.97993 \times r_{opt} + 0.02084$, where r_{opt} = MP2/aug-cc-pVTZ optimization.

Molecule	r_e	r_{opt}	r_e^{emp}	$\mid r_e - r_e^{emp} \mid$	Ref.
FCO^+	1.2014	1.2054	1.2021	0.0007	[137]
FCN	1.26405	1.2683	1.2637	0.0003	[138]
HCCF	1.2765	1.2804	1.2755	0.0010	[139]
FCH	1.305	1.3095	1.3041	0.001	[140]
$O{=}CF_2$	1.311	1.3161	1.3105	0.000_5	[141]
O=CFCl	1.3232	1.3304	1.3245	0.0013	[142]
CHF_3	1.3284	1.3363	1.3303	0.0019	[143]
c-CHF=CHCl	1.331	1.3350	1.3290	0.002	[144]
CH_2F_2	1.3508	1.3591	1.3527	0.0019	[145]
CH_3F	1.382	1.3879	1.3809	0.001	[146]
			AVG[a]	0.0012	
			RMS[b]	0.0013	

[a] AVG is average absolute difference.

[b] RMS is root mean square difference.

TABLE B.3. C–Br Bond Lengths (Å). $r_e^{emp} = 0.99078 \times r_{opt} + 0.02591$, where r_{opt} = MP2/aug-cc-pVTZ optimization.

Molecule	$\frac{r_e}{r_m^\rho}$	r_{opt}	r_e^{emp}	$\mid r_e - r_e^{emp} \mid$	Ref.
BrCN	1.7875	1.7778	1.7873	0.0002	[147]
FCN	1.7908	1.7815	1.7910	0.0002	[148]
HCCF	1.8835	1.8750	1.8836	0.0001	[149]
FCH	1.9235	1.9155	1.9238	0.0003	[150]
O=CF_2	1.9340	1.9255	1.9336	0.0003	[151]
			AVG[a]	0.0002	
			RMS[b]	0.0002	

[a] AVG is average absolute difference.

[b] RMS is root mean square difference.

TABLE B.4. C≡N Bond Lengths (Å). $r_e^{emp} = 0.69449 \times r_{opt} + 0.34294$, where r_{opt} = MP2/aug-cc-pVTZ optimization.

Molecule	$\frac{r_e}{r_m^p}$	r_{opt}	r_e^{emp}	$\mid r_e - r_e^{emp} \mid$	Ref.
HCN	1.15324	1.1670	1.1534	0.0002	[152]
$CH_2(CN)_2$	1.155	1.1697	1.1553	0.000	[153]
CH_3CN	1.156	1.1698	1.1553	0.001	[133]
FCN	1.15680	1.1714	1.1564	0.0004	[138]
H_2C=CHCN	1.157	1.1731	1.1577	0.001	[131]
NCCN	1.1578	1.1755	1.1593	0.0015	[130]
H_2C=$C(CN)_2$	1.158	1.1726	1.1573	0.001	[153]
CNCN	1.1581	1.1740	1.1582	0.0001	[130]
ClCN	1.1589	1.1752	1.1591	0.0002	[154]
SiH_3CN	1.159	1.1743	1.1585	0.000_5	[155]
BrCN	1.15951	1.1756	1.1594	0.0001	[147]
HCCCN	1.1605	1.1771	1.1604	0.0001	[129]
NCCP	1.16406	1.1816	1.1636	0.0005	[128]
			AVG[a]	0.0005	
			RMS[b]	0.0006	

[a] AVG is average absolute difference.

[b] RMS is root mean square difference.

All data and calculation outputs for bromodifluoroacetonitrile. Quantum numbers in table are given as $J'_{K_{-1},K_{+1}}$, $F_1'+\frac{1}{2}$, $F'+\frac{1}{2} \leftarrow J''_{K_{-1},K_{+1}}$, $F_1''+\frac{1}{2}$, $F''+\frac{1}{2}$. Frequency measurements in table are given in MHz.

TABLE B.5. $C^{79}BrF_2CN$ Transitions Measured in MHz

											obs	o-c	error	blends o-c	blends wt	Notes
1:	2	1	2	3	3	1	0	1	2	2	7788.3966	0.0079	0.025			
2:	2	1	2	3	4	1	0	1	2	3	7788.8429	-0.0012	0.025			
3:	2	1	2	3	2	1	0	1	2	1	7789.1068	-0.0132	0.025			
4:	2	1	2	4	4	1	0	1	3	3	7836.7402	0.0083	0.025			
5:	2	1	2	4	5	1	0	1	3	4	7837.2715	0.0078	0.025			
6:	2	1	2	1	2	1	0	1	1	2	7889.3684	-0.0061	0.025			
7:	2	1	2	2	3	1	0	1	1	2	7965.7307	-0.0136	0.025			
8:	3	0	3	5	6	2	1	2	4	5	7978.8713	0.0039	0.025			
9:	3	0	3	5	5	2	1	2	4	4	7979.0841	-0.0067	0.025			
10:	4	1	3	6	7	3	2	2	5	6	8502.4770	0.0103	0.025			
11:	4	1	3	6	6	3	2	2	5	5	8502.8448	0.0087	0.025			
12:	3	1	3	2	1	2	1	2	2	1	9061.3496	0.0181	0.025			
13:	3	1	3	3	3	2	1	2	3	4	9115.2092	-0.0043	0.025			
14:	3	1	3	3	3	2	1	2	3	3	9115.4618	-0.0059	0.025			
15:	3	1	3	3	4	2	1	2	3	4	9115.6519	0.0027	0.025			
16:	3	1	3	3	4	2	1	2	3	3	9115.8965	-0.0069	0.025			
17:	3	1	3	3	2	2	1	2	3	3	9116.0885	-0.0047	0.025			
18:	3	1	3	5	5	2	1	2	4	5	9133.0139	-0.0020	0.025			
19:	3	1	3	5	5	2	1	2	4	4	9133.6917	0.0043	0.025			
20:	3	1	3	5	6	2	1	2	4	5	9133.8416	0.0010	0.025			
21:	3	1	3	5	4	2	1	2	4	4	9134.7011	0.0028	0.025			
22:	3	1	3	2	2	2	1	2	1	1	9136.7717	-0.0043	0.025			
23:	3	1	3	2	3	2	1	2	1	2	9137.2918	-0.0007	0.025			
24:	3	1	3	2	1	2	1	2	1	1	9137.7146	0.0023	0.025			

25:	3	1	3	4	4	2	1	2	3	4	9165.2933	-0.0040	0.025
26:	3	1	3	4	4	2	1	2	3	3	9165.5520	0.0005	0.025
27:	3	1	3	4	5	2	1	2	3	4	9165.9019	0.0152	0.025
28:	3	1	3	4	3	2	1	2	3	3	9166.3235	0.0034	0.025
29:	3	1	3	3	3	2	1	2	2	2	9169.0783	-0.0069	0.025
30:	3	1	3	3	4	2	1	2	2	3	9169.5113	-0.0009	0.025
31:	3	1	3	3	2	2	1	2	2	1	9169.6993	0.0047	0.025
32:	3	1	3	4	5	2	1	2	4	5	9244.1588	0.0018	0.025
33:	3	1	3	4	4	2	1	2	4	4	9244.2300	-0.0089	0.025
34:	3	1	3	4	5	2	1	2	4	4	9244.8439	0.0155	0.025
35:	3	0	3	2	3	2	0	2	2	3	9362.5787	-0.0027	0.025
36:	3	0	3	2	1	2	0	2	2	2	9362.7633	-0.0091	0.025
37:	3	0	3	2	1	2	0	2	2	1	9362.8145	-0.0026	0.025
38:	3	0	3	3	3	2	0	2	3	2	9403.4167	0.0182	0.025
39:	3	0	3	3	3	2	0	2	3	3	9403.6071	-0.0026	0.025
40:	3	0	3	3	4	2	0	2	3	4	9403.6909	-0.0098	0.025
41:	3	0	3	3	4	2	0	2	3	3	9403.8408	-0.0071	0.025
42:	3	0	3	3	2	2	0	2	3	3	9403.9569	0.0058	0.025
43:	3	0	3	5	5	2	0	2	4	5	9461.4831	0.0075	0.025
44:	3	0	3	5	5	2	0	2	4	4	9461.7572	0.0021	0.025
45:	3	0	3	5	6	2	0	2	4	5	9461.9312	0.0078	0.025
46:	3	0	3	5	4	2	0	2	4	4	9462.2846	-0.0200	0.025
47:	3	0	3	4	4	2	0	2	3	4	9462.7861	-0.0049	0.025
48:	3	0	3	4	4	2	0	2	3	3	9462.9389	0.0007	0.025
49:	3	0	3	4	5	2	0	2	3	4	9463.1149	-0.0141	0.025
50:	3	0	3	4	3	2	0	2	3	3	9463.3789	0.0010	0.025
51:	8	1	7	9	8	8	0	8	9	8	9463.8976	0.0172	0.025
52:	8	1	7	9	10	8	0	8	9	10	9463.9876	-0.0129	0.025
53:	3	2	2	2	3	2	2	1	1	2	9469.0640	-0.0005	0.025
54:	3	0	3	3	3	2	0	2	2	2	9492.7094	-0.0051	0.025
55:	3	0	3	3	4	2	0	2	2	3	9492.9795	0.0019	0.025
56:	3	0	3	3	2	2	0	2	2	1	9493.1116	0.0110	0.025
57:	3	0	3	2	2	2	0	2	1	1	9493.4324	-0.0031	0.025

58:	3	0	3	2	3	2	0	2	1	2	9493.7060	0.0010	0.025
59:	3	0	3	2	1	2	0	2	1	1	9493.9143	-0.0066	0.025
60:	3	2	2	5	5	2	2	1	4	4	9560.2987	0.0027	0.025
61:	3	2	2	4	4	2	2	1	4	4	9562.0295	-0.0006	0.025
62:	3	2	2	4	5	2	2	1	4	5	9562.2345	-0.0066	0.025
63:	3	0	3	4	5	2	0	2	4	5	9592.7917	-0.0020	0.025
64:	3	2	1	2	1	2	2	0	1	1	9598.2005	0.0080	0.025
65:	3	2	2	3	4	2	2	1	2	3	9598.3910	-0.0023	0.025
66:	3	2	2	2	3	2	2	1	2	3	9600.9967	0.0156	0.025
67:	3	2	1	4	3	2	2	0	4	4	9688.4028	-0.0073	0.025
68:	3	2	1	4	5	2	2	0	4	4	9688.5485	0.0064	0.025
69:	3	2	1	4	4	2	2	0	4	4	9688.7122	0.0207	0.025
70:	3	2	1	4	4	2	2	0	4	3	9689.0855	0.0152	0.025
71:	3	2	1	5	5	2	2	0	4	4	9689.1971	-0.0239	0.025
72:	3	2	1	3	4	2	2	0	2	3	9726.1816	0.0038	0.025
73:	3	2	1	2	3	2	2	0	2	3	9730.6750	-0.0050	0.025
74:	3	2	1	4	5	2	2	0	3	4	9816.4489	-0.0201	0.025
75:	3	2	1	3	3	2	2	0	3	2	9816.6282	-0.0055	0.025
76:	3	2	1	5	4	2	2	0	3	3	9816.7827	-0.0018	0.025
77:	3	1	2	2	3	2	1	1	3	4	9902.3325	0.0023	0.025
78:	3	1	2	2	1	2	1	1	2	1	9938.0149	-0.0062	0.025
79:	3	1	2	2	1	2	1	1	2	2	9938.1032	0.0201	0.025
80:	3	1	2	2	3	2	1	1	2	3	9938.2834	-0.0037	0.025
81:	3	1	2	2	2	2	1	1	2	2	9938.6314	0.0123	0.025
82:	3	1	2	3	4	2	1	1	3	4	9984.6988	-0.0147	0.025
83:	3	1	2	2	1	2	1	1	1	1	9988.2473	0.0017	0.025
84:	3	1	2	2	3	2	1	1	1	2	9988.4821	0.0011	0.025
85:	3	1	2	2	2	2	1	1	1	1	9988.7873	0.0057	0.025
86:	3	1	2	5	4	2	1	1	4	4	9990.7171	0.0067	0.025
87:	3	1	2	5	5	2	1	1	4	4	9991.2280	-0.0188	0.025
88:	3	1	2	5	6	2	1	1	4	5	9991.2930	0.0000	0.025
89:	3	1	2	3	2	2	1	1	2	1	10020.5489	-0.0006	0.025
90:	3	1	2	3	4	2	1	1	2	3	10020.6762	0.0057	0.025

91:	3	1	2	3	3	2	1	1	2	2	10020.9281	0.0039	0.025
92:	3	1	2	4	3	2	1	1	3	3	10023.2614	0.0136	0.025
93:	3	1	2	4	5	2	1	1	3	4	10023.5013	0.0038	0.025
94:	3	1	2	4	4	2	1	1	3	3	10023.5829	-0.0199	0.025
95:	3	1	2	4	4	2	1	1	4	4	10075.8223	0.0118	0.025
96:	3	1	2	4	5	2	1	1	4	5	10076.0072	-0.0111	0.025
97:	3	1	2	4	3	2	1	1	4	3	10076.0793	-0.0051	0.025
98:	3	1	3	2	2	2	0	2	2	2	10527.4377	-0.0156	0.025
99:	3	1	3	2	3	2	0	2	2	3	10527.9986	0.0005	0.025
100:	3	1	3	3	3	2	0	2	3	4	10546.8797	0.0046	0.025
101:	3	1	3	3	3	2	0	2	3	3	10547.0171	-0.0052	0.025
102:	3	1	3	3	4	2	0	2	3	4	10547.3112	0.0004	0.025
103:	3	1	3	3	2	2	0	2	3	2	10547.4413	0.0048	0.025
104:	3	1	3	3	2	2	0	2	3	3	10547.6555	0.0076	0.025
105:	3	1	3	4	4	2	0	2	3	4	10596.9618	0.0029	0.025
106:	3	1	3	4	4	2	0	2	3	3	10597.1144	0.0083	0.025
107:	3	1	3	4	5	2	0	2	3	4	10597.5461	-0.0021	0.025
108:	3	1	3	4	3	2	0	2	3	2	10597.6576	-0.0056	0.025
109:	3	1	3	4	3	2	0	2	3	3	10597.8794	0.0048	0.025
110:	3	1	3	5	5	2	0	2	4	5	10616.0658	-0.0062	0.025
111:	3	1	3	5	5	2	0	2	4	4	10616.3556	0.0040	0.025
112:	3	1	3	5	6	2	0	2	4	5	10616.9001	0.0035	0.025
113:	3	1	3	5	4	2	0	2	4	3	10616.9917	-0.0085	0.025
114:	3	1	3	5	4	2	0	2	4	4	10617.3392	-0.0232	0.025
115:	3	1	3	3	3	2	0	2	2	2	10636.1274	0.0003	0.025
116:	3	1	3	3	4	2	0	2	2	3	10636.5929	0.0053	0.025
117:	3	1	3	3	2	2	0	2	2	1	10636.8068	0.0095	0.025
118:	3	1	3	2	2	2	0	2	1	1	10658.6005	-0.0011	0.025
119:	3	1	3	2	3	2	0	2	1	2	10659.1226	0.0010	0.025
120:	3	1	3	2	1	2	0	2	1	1	10659.5401	0.0023	0.025
121:	3	1	3	4	4	2	0	2	4	4	10726.9039	0.0008	0.025
122:	3	1	3	4	5	2	0	2	4	5	10727.2129	0.0000	0.025
123:	4	0	4	4	5	3	1	3	4	5	11307.8869	0.0130	0.025

124:	4	0	4	6	7	3	1	3	5	6	11331.2055	-0.0091	0.025
125:	4	0	4	6	6	3	1	3	5	5	11331.4022	-0.0004	0.025
126:	4	0	4	3	2	3	1	3	2	1	11334.7976	-0.0016	0.025
127:	4	0	4	3	4	3	1	3	2	3	11334.9834	-0.0101	0.025
128:	4	0	4	5	6	3	1	3	4	5	11353.2138	0.0137	0.025
129:	4	0	4	4	3	3	1	3	3	2	11358.0550	-0.0079	0.025
130:	4	0	4	4	5	3	1	3	3	4	11358.1338	0.0224	0.025
131:	4	0	4	5	6	3	1	3	5	6	11463.5183	0.0018	0.025
132:	2	2	1	3	3	1	1	0	3	3	11743.4754	-0.0002	0.025
133:	2	2	1	3	4	1	1	0	3	4	11743.9387	-0.0031	0.025
134:	2	2	1	3	2	1	1	0	3	2	11744.1438	0.0013	0.025
135:	2	2	1	2	3	1	1	0	1	2	11772.5487	-0.0062	0.025
136:	2	2	1	3	2	1	1	0	2	1	11820.7753	0.0035	0.025
137:	2	2	1	3	4	1	1	0	2	3	11821.2174	0.0008	0.025
138:	2	2	1	3	2	1	1	0	2	2	11821.7014	-0.0006	0.025
139:	2	2	1	3	3	1	1	0	2	2	11821.8093	-0.0015	0.025
140:	2	2	1	2	3	1	1	0	3	4	11833.2432	-0.0094	0.025
141:	2	2	1	4	3	1	1	0	3	3	11870.0063	0.0000	0.025
142:	2	2	1	4	4	1	1	0	3	3	11870.2772	-0.0030	0.025
143:	2	2	1	4	5	1	1	0	3	4	11870.6067	-0.0040	0.025
144:	2	2	1	4	3	1	1	0	3	2	11870.7762	-0.0057	0.025
145:	2	2	1	1	2	1	1	0	1	2	11904.4703	-0.0010	0.025
146:	2	2	1	2	2	1	1	0	2	1	11910.1023	0.0051	0.025
147:	2	2	1	2	3	1	1	0	2	3	11910.5174	-0.0099	0.025
148:	2	2	1	2	2	1	1	0	2	2	11911.0333	0.0057	0.025
149:	4	1	4	3	3	3	1	3	3	3	12054.5164	-0.0029	0.025
150:	4	1	4	3	4	3	1	3	3	4	12054.8417	-0.0046	0.025
151:	4	1	4	3	2	3	1	3	3	2	12054.9807	-0.0033	0.025
152:	2	2	0	3	2	1	1	1	3	2	12066.5559	0.0050	0.025
153:	2	2	0	3	4	1	1	1	3	4	12066.7613	0.0050	0.025
154:	2	2	0	3	3	1	1	1	3	3	12067.2370	0.0018	0.025
155:	2	2	0	2	3	1	1	1	1	2	12113.5488	-0.0005	0.025
156:	2	2	0	3	2	1	1	1	2	2	12115.6551	-0.0018	0.025

157:	2	2	0	3	3	1	1	1	2	2	12115.8161	0.0014	0.025
158:	2	2	0	3	4	1	1	1	2	3	12116.0005	0.0035	0.025
159:	2	2	0	3	2	1	1	1	2	1	12116.1861	0.0019	0.025
160:	4	1	4	4	5	3	1	3	4	5	12126.6371	-0.0034	0.025
161:	4	1	4	6	6	3	1	3	5	6	12155.1768	-0.0110	0.025
162:	4	1	4	6	7	3	1	3	5	6	12156.1104	-0.0095	0.025
163:	4	1	4	6	5	3	1	3	5	5	12157.1079	-0.0081	0.025
164:	4	1	4	3	3	3	1	3	2	3	12162.6676	-0.0056	0.025
165:	4	1	4	3	3	3	1	3	2	2	12163.1920	-0.0010	0.025
166:	4	1	4	3	4	3	1	3	2	3	12163.4309	-0.0049	0.025
167:	4	1	4	5	5	3	1	3	4	5	12168.1339	-0.0072	0.025
168:	4	1	4	5	5	3	1	3	4	4	12168.7299	-0.0005	0.025
169:	4	1	4	5	6	3	1	3	4	5	12168.9166	0.0021	0.025
170:	4	1	4	5	4	3	1	3	4	4	12169.6837	0.0005	0.025
171:	4	1	4	4	4	3	1	3	3	4	12176.1849	-0.0059	0.025
172:	4	1	4	4	4	3	1	3	3	3	12176.6268	0.0002	0.025
173:	4	1	4	4	5	3	1	3	3	4	12176.8835	0.0054	0.025
174:	4	1	4	4	3	3	1	3	3	3	12177.5210	0.0008	0.025
175:	2	2	0	4	3	1	1	1	3	2	12194.1495	0.0029	0.025
176:	2	2	0	4	5	1	1	1	3	4	12194.3927	0.0022	0.025
177:	2	2	0	4	3	1	1	1	3	3	12194.6769	0.0036	0.025
178:	2	2	0	4	4	1	1	1	3	3	12195.0552	0.0032	0.025
179:	2	2	0	2	2	1	1	1	2	2	12205.8839	0.0018	0.025
180:	2	2	0	2	3	1	1	1	2	3	12206.1819	-0.0020	0.025
181:	2	2	0	2	1	1	1	1	2	1	12206.4226	-0.0038	0.025
182:	2	2	0	1	2	1	1	1	1	2	12245.9204	-0.0003	0.025
183:	5	1	4	4	5	4	2	3	3	4	12274.4902	-0.0024	0.025
184:	5	1	4	4	4	4	2	3	3	3	12274.8372	-0.0127	0.025
185:	4	1	4	5	6	3	1	3	5	6	12279.2185	-0.0123	0.025
186:	5	1	4	7	8	4	2	3	6	7	12286.7253	-0.0140	0.025
187:	5	1	4	7	7	4	2	3	6	6	12287.1500	0.0060	0.025
188:	5	1	4	5	6	4	2	3	4	5	12327.9171	-0.0122	0.025
189:	5	1	4	5	5	4	2	3	4	4	12328.2605	0.0082	0.025

```
190:  5  1  4  6  5    4  2  3  5  4       12338.2667   0.0118  0.025
191:  2  2  0  1  2    1  1  1  2  3       12338.5495  -0.0057  0.025
192:  5  1  4  6  6    4  2  3  5  5       12338.6707   0.0010  0.025
193:  4  0  4  3  3    3  0  3  3  4       12369.5089   0.0116  0.025
194:  4  0  4  3  3    3  0  3  3  3       12369.7288  -0.0066  0.025
195:  4  0  4  3  4    3  0  3  3  4       12370.0092  -0.0048  0.025
196:  4  0  4  3  2    3  0  3  3  2       12370.1286  -0.0042  0.025
197:  4  0  4  4  4    3  0  3  4  5       12441.8192  -0.0011  0.025
198:  4  0  4  4  4    3  0  3  4  4       12442.1537  -0.0046  0.025
199:  4  0  4  4  5    3  0  3  4  5       12442.2743  -0.0187  0.025
200:  4  0  4  4  3    3  0  3  4  3       12442.3414   0.0085  0.025
201:  4  0  4  4  5    3  0  3  4  4       12442.6528   0.0217  0.025
202:  4  0  4  6  6    3  0  3  5  6       12485.5455  -0.0059  0.025
203:  4  0  4  6  6    3  0  3  5  5       12486.0029   0.0036  0.025
204:  4  0  4  6  7    3  0  3  5  6       12486.1974   0.0095  0.025
205:  4  0  4  6  5    3  0  3  5  5       12486.7555   0.0023  0.025
206:  4  0  4  5  5    3  0  3  4  5       12487.0795  -0.0032  0.025
207:  4  0  4  5  5    3  0  3  4  4       12487.4227   0.0020  0.025
208:  4  0  4  5  6    3  0  3  4  5       12487.6268   0.0076  0.025
209:  4  0  4  5  4    3  0  3  4  4       12488.0830   0.0020  0.025
210:  4  0  4  3  3    3  0  3  2  3       12499.8908  -0.0027  0.025
211:  4  0  4  3  3    3  0  3  2  2       12500.1635   0.0005  0.025
212:  4  0  4  3  4    3  0  3  2  3       12500.4134   0.0030  0.025
213:  4  0  4  3  2    3  0  3  2  2       12500.9007  -0.0008  0.025
214:  4  0  4  4  4    3  0  3  3  4       12501.2544   0.0058  0.025
215:  4  0  4  4  4    3  0  3  3  3       12501.4883   0.0015  0.025
216:  4  0  4  4  5    3  0  3  3  4       12501.7118  -0.0095  0.025
217:  4  0  4  4  3    3  0  3  3  2       12501.7496  -0.0101  0.025
218:  4  0  4  4  3    3  0  3  3  3       12502.1126   0.0117  0.025
219:  4  0  4  5  6    3  0  3  5  6       12618.4868  -0.0028  0.025
220:  4  2  3  3  3    3  2  2  2  2       12732.8463   0.0402  0.050  -0.0011 0.50
221:  4  2  3  3  4    3  2  2  2  3       12732.8463  -0.0424  0.050  -0.0011 0.50
222:  4  2  3  3  2    3  2  2  2  2       12732.9672   0.0324  0.030
```

223:	4	2	3	3	3	3	2	2	3	3	12735.4273	0.0266	0.050
224:	4	2	3	6	6	3	2	2	5	5	12751.3898	0.0019	0.025
225:	4	2	3	6	5	3	2	2	5	4	12751.5177	-0.0132	0.025
226:	4	3	2	3	2	3	3	1	2	2	12759.1586	0.0043	0.025
227:	4	3	2	3	4	3	3	1	2	3	12759.3887	-0.0163	0.025
228:	4	3	2	3	2	3	3	1	2	1	12759.5181	0.0057	0.025
229:	4	3	1	3	2	3	3	0	2	2	12773.2729	-0.0012	0.025
230:	4	3	1	3	2	3	3	0	2	1	12773.6303	-0.0080	0.025
231:	4	3	2	5	5	3	3	1	5	5	12773.7595	-0.0001	0.025
232:	4	3	2	5	6	3	3	1	5	6	12773.9364	-0.0100	0.025
233:	4	3	2	5	4	3	3	1	5	4	12774.0023	0.0140	0.025
234:	4	2	3	4	4	3	2	2	4	3	12783.8265	-0.0008	0.025
235:	4	2	3	4	5	3	2	2	4	5	12783.9158	-0.0035	0.025
236:	4	2	3	4	5	3	2	2	3	4	12785.1075	-0.0176	0.025
237:	4	3	1	5	5	3	3	0	5	5	12787.7486	-0.0041	0.025
238:	4	3	1	5	6	3	3	0	5	6	12787.9057	-0.0193	0.025
239:	4	3	1	5	4	3	3	0	5	4	12787.9834	0.0198	0.025
240:	4	2	3	5	5	3	2	2	4	4	12802.5860	0.0002	0.025
241:	4	2	3	5	6	3	2	2	4	5	12802.7022	0.0086	0.025
242:	4	2	3	5	5	3	2	2	5	5	12804.3180	-0.0018	0.025
243:	4	2	3	5	6	3	2	2	5	6	12804.4393	0.0062	0.025
244:	4	3	2	6	6	3	3	1	5	5	12817.6722	0.0046	0.025
245:	4	3	2	6	7	3	3	1	5	6	12817.8218	-0.0036	0.025
246:	4	3	1	6	6	3	3	0	5	5	12831.8659	0.0030	0.025
247:	4	3	1	6	7	3	3	0	5	6	12831.9942	-0.0116	0.025
248:	4	3	2	4	4	3	3	1	3	4	12874.5012	-0.0154	0.025
249:	4	3	1	4	4	3	3	0	3	3	12888.5414	0.0063	0.025
250:	4	3	2	3	3	3	3	1	3	3	12922.1259	0.0072	0.025
251:	4	3	2	5	5	3	3	1	4	4	12933.0058	-0.0080	0.025
252:	4	3	2	5	6	3	3	1	4	5	12933.0913	-0.0175	0.025
253:	4	3	1	3	4	3	3	0	3	4	12936.2692	-0.0017	0.025
254:	4	3	1	5	5	3	3	0	4	4	12947.0868	0.0218	0.025
255:	4	3	2	4	4	3	3	1	4	4	12947.4951	-0.0039	0.025

256:	4	3	1	4	4	3	3	0	4	4	12961.7330	0.0002	0.025
257:	4	3	1	4	5	3	3	0	4	5	12961.8173	-0.0153	0.025
258:	4	2	2	3	2	3	2	1	2	2	13038.3038	0.0053	0.025
259:	4	2	2	3	4	3	2	1	2	3	13038.5478	0.0011	0.025
260:	4	2	2	3	3	3	2	1	2	2	13038.6359	-0.0084	0.025
261:	4	2	2	3	3	3	2	1	2	3	13038.7847	-0.0044	0.025
262:	4	2	2	3	4	3	2	1	3	4	13043.0357	-0.0131	0.025
263:	4	2	2	3	3	3	2	1	4	3	13043.3163	-0.0026	0.025
264:	4	2	2	6	5	3	2	1	5	5	13056.5849	0.0148	0.025
265:	4	2	2	6	5	3	2	1	5	4	13056.8043	-0.0192	0.025
266:	4	2	2	6	6	3	2	1	5	5	13056.9048	-0.0039	0.025
267:	4	2	2	6	5	3	2	1	4	4	13057.1091	0.0094	0.050
268:	4	2	2	4	4	3	2	1	5	4	13088.8721	0.0184	0.025
269:	4	2	2	4	5	3	2	1	3	4	13089.1788	-0.0028	0.025
270:	4	2	2	4	4	3	2	1	4	3	13089.4116	0.0004	0.025
271:	4	2	2	5	6	3	2	1	5	6	13106.0352	-0.0051	0.025
272:	4	2	2	5	4	3	2	1	4	4	13106.2746	-0.0083	0.025
273:	4	2	2	5	4	3	2	1	3	3	13106.3293	0.0142	0.025
274:	4	2	2	5	5	3	2	1	4	5	13106.7029	0.0015	0.025
275:	4	2	2	5	5	3	2	1	3	4	13106.8095	0.0037	0.025
276:	4	1	3	3	4	3	1	2	3	4	13209.5258	-0.0043	0.025
277:	4	1	3	3	3	3	1	2	3	3	13209.6239	-0.0055	0.025
278:	4	1	4	4	4	3	0	3	4	4	13260.7064	-0.0042	0.025
279:	4	1	4	4	5	3	0	3	4	5	13261.0636	0.0038	0.025
280:	4	1	3	4	5	3	1	2	4	5	13266.6721	-0.0064	0.025
281:	4	1	3	6	5	3	1	2	5	5	13287.0211	-0.0063	0.025
282:	4	1	3	6	6	3	1	2	5	6	13287.9055	-0.0038	0.025
283:	4	1	3	3	2	3	1	2	2	2	13291.4829	0.0037	0.025
284:	4	1	3	3	4	3	1	2	2	3	13291.9200	0.0065	0.025
285:	4	1	3	3	3	3	1	2	2	3	13292.2297	-0.0027	0.025
286:	4	1	3	5	4	3	1	2	4	4	13300.1467	0.0128	0.025
287:	4	1	3	5	6	3	1	2	4	5	13300.4832	0.0098	0.025
288:	4	1	3	5	5	3	1	2	4	5	13300.7712	0.0110	0.025

289:	4	1	4	5	5	3	0	3	4	4	13302.9018	0.0034	0.025
290:	4	1	4	5	6	3	0	3	4	5	13303.3533	0.0196	0.050
291:	4	1	3	4	3	3	1	2	3	3	13305.1640	-0.0015	0.025
292:	4	1	3	4	5	3	1	2	3	4	13305.4502	-0.0123	0.025
293:	4	1	3	4	4	3	1	2	3	3	13305.5267	0.0206	0.025
294:	4	1	3	4	4	3	1	2	3	4	13305.7311	0.0054	0.025
295:	4	1	4	6	6	3	0	3	5	5	13310.6150	0.0060	0.025
296:	4	1	4	6	7	3	0	3	5	6	13311.1143	0.0211	0.050
297:	4	1	4	4	4	3	0	3	3	3	13320.0408	0.0017	0.025
298:	4	1	4	4	5	3	0	3	3	4	13320.4877	-0.0003	0.025
299:	4	1	4	4	3	3	0	3	3	2	13320.5905	-0.0007	0.025
300:	4	1	4	3	3	3	0	3	2	2	13328.3562	-0.0030	0.025
301:	4	1	4	3	4	3	0	3	2	3	13328.8479	-0.0046	0.025
302:	4	1	4	3	2	3	0	3	2	1	13328.9655	0.0013	0.025
303:	4	1	3	5	5	3	1	2	5	5	13385.0477	-0.0008	0.025
304:	4	1	3	5	4	3	1	2	5	4	13385.2585	0.0245	0.025
305:	4	1	4	5	5	3	0	3	5	5	13433.8807	0.0021	0.025
306:	4	1	4	5	6	3	0	3	5	6	13434.2201	0.0160	0.025
307:	5	0	5	5	6	4	1	4	4	5	14625.8032	0.0052	0.025
308:	3	2	2	4	4	2	1	1	3	3	14725.4152	0.0055	0.025
309:	3	2	2	4	5	2	1	1	3	4	14725.5891	0.0102	0.025
310:	3	2	2	3	4	2	1	1	2	3	14760.3185	-0.0114	0.025
311:	3	2	2	5	5	2	1	1	4	4	14775.8834	0.0002	0.025
312:	3	2	2	5	6	2	1	1	4	5	14776.3655	0.0054	0.025
313:	3	2	2	5	4	2	1	1	4	3	14776.4986	-0.0061	0.025
314:	3	2	2	2	3	2	1	1	1	2	14813.1187	0.0073	0.025
315:	5	1	5	7	8	4	1	4	6	7	15152.7952	-0.0070	0.025
316:	5	1	5	4	4	4	1	4	3	3	15158.6995	0.0027	0.025
317:	5	1	5	4	5	4	1	4	3	4	15158.8445	-0.0026	0.025
318:	5	1	5	6	6	4	1	4	5	5	15159.3082	0.0083	0.025
319:	5	1	5	6	7	4	1	4	5	6	15159.4330	0.0029	0.025
320:	5	1	5	5	5	4	1	4	4	4	15165.6845	0.0052	0.025
321:	5	1	5	5	6	4	1	4	4	5	15165.8429	0.0000	0.025

322:	5	0	5	5	6	4	0	4	5	6	15399.2341	-0.0043	0.025
323:	5	0	5	7	7	4	0	4	6	6	15434.3815	0.0053	0.025
324:	5	0	5	7	8	4	0	4	6	7	15434.5681	0.0087	0.025
325:	5	0	5	6	6	4	0	4	5	5	15435.9983	0.0045	0.025
326:	5	0	5	6	7	4	0	4	5	6	15436.1947	0.0080	0.025
327:	5	0	5	4	4	4	0	4	3	3	15442.5610	-0.0012	0.025
328:	5	0	5	4	5	4	0	4	3	4	15442.7779	-0.0005	0.025
329:	5	0	5	5	5	4	0	4	4	4	15444.3555	0.0040	0.025
330:	5	0	5	5	6	4	0	4	4	5	15444.5724	0.0078	0.025
331:	3	2	1	4	5	2	1	2	3	4	15724.8811	0.0043	0.025
332:	3	2	1	5	6	2	1	2	4	5	15803.5883	0.0002	0.025
333:	3	2	1	5	5	2	1	2	4	4	15804.4957	-0.0015	0.025
334:	5	2	4	4	5	4	2	3	3	4	15906.1748	-0.0045	0.025
335:	5	2	4	7	8	4	2	3	6	7	15910.6369	-0.0050	0.025
336:	5	2	4	5	6	4	2	3	4	5	15932.7526	0.0000	0.025
337:	5	2	4	6	7	4	2	3	5	6	15936.1608	0.0037	0.025
338:	5	1	5	6	6	4	0	4	5	5	15974.7797	0.0023	0.025
339:	5	1	5	6	7	4	0	4	5	6	15975.1317	-0.0127	0.025
340:	5	1	5	7	7	4	0	4	6	6	15977.3277	0.0039	0.025
341:	5	1	5	7	8	4	0	4	6	7	15977.7131	0.0056	0.025
342:	5	3	3	5	6	4	3	2	4	5	16101.7639	-0.0004	0.025
343:	5	3	2	7	8	4	3	1	6	7	16111.4713	0.0095	0.025
344:	5	3	3	6	7	4	3	2	5	6	16120.6995	-0.0241	0.025
345:	5	4	2	6	6	4	4	1	5	5	16134.1465	0.0128	0.025
346:	5	3	2	5	6	4	3	1	4	5	16149.1266	0.0152	0.025
347:	5	3	2	6	7	4	3	1	5	6	16168.9394	0.0139	0.025
348:	5	3	2	6	6	4	3	1	5	6	16169.0330	0.0002	0.025
349:	5	2	3	4	5	4	2	2	3	4	16462.4077	-0.0142	0.025
350:	5	2	3	7	8	4	2	2	6	7	16466.6017	0.0135	0.025
351:	5	2	3	5	6	4	2	2	4	5	16487.1454	-0.0050	0.025
352:	5	2	3	6	7	4	2	2	5	6	16490.3651	-0.0062	0.025
353:	5	1	4	7	8	4	1	3	6	7	16535.7685	-0.0125	0.025
354:	5	1	4	4	5	4	1	3	3	4	16540.0870	-0.0113	0.025

```
 355:  5  1  4  6  7    4  1  3  5  6        16542.6228  -0.0019  0.025
 356:  5  1  4  5  5    4  1  3  4  4        16547.1944  -0.0248  0.025
 357:  5  1  4  5  4    4  1  3  4  3        16547.2758  -0.0008  0.025
-------------------------------------------------------------------------------

PARAMETERS IN FIT:

       10000         A  /  /MHz         3464.121(5)                          1
       20000         B  /  /MHz         1742.5317(9)                         2
       30000         C  /  /MHz         1456.3421(9)                         3
         200        DJ  /  /kHz            0.31(1)                           4
        1100       DJK  /  /kHz           -0.99(6)                           5
        2000        DK  /  /kHz            1.(1)                             6
       40100        d1  /  /kHz           -0.085(5)                          7
   110010000      CHIaa /  /MHz          512.64(1)                          8
  -110020000      CHIbb /  /MHz         -512.64(1)             = -1.00000 *  8
   110030000      CHIcc /  /MHz         -307.91(1)                          9
  -110020000      CHIbb /  /MHz          307.91(1)             = -1.00000 *  9
   110610000      CHIab /  /MHz         -297.0(3)                          10
   220010000      CHIaa /  /MHz           -0.74(1)                         11
  -220020000      CHIbb /  /MHz            0.74(1)             = -1.00000 * 11
   220030000      CHIcc /  /MHz            2.42(1)                         12
  -220020000      CHIbb /  /MHz           -2.42(1)             = -1.00000 * 12
   220610000      CHIab /  /MHz           -3.4(3)                          13
    10010000        Maa /  /MHz            0.001(1)                        14
    10020000        Mbb /  /MHz            0.003(1)                        15
    10030000        Mcc /  /MHz            0.003(1)                        16

 MICROWAVE AVG =        0.000179 MHz, IR AVG =        0.00000
 MICROWAVE RMS =        0.008956 MHz, IR RMS =        0.00000
 END OF ITERATION  1 OLD, NEW RMS ERROR=        0.34842         0.34842

  distinct frequency lines in fit:   356
```

```
      distinct parameters of fit:    16

 for standard errors previous errors are multiplied by:   0.356524

 PARAMETERS IN FIT WITH STANDARD ERRORS ON THOSE THAT ARE FITTED:

       10000         A  /  /MHz         3464.121(1)                          1
       20000         B  /  /MHz         1742.5317(3)                         2
       30000         C  /  /MHz         1456.3421(3)                         3
         200        DJ  /  /kHz            0.313(6)                          4
        1100       DJK  /  /kHz           -0.99(2)                           5
        2000        DK  /  /kHz            1.5(3)                            6
       40100        d1  /  /kHz           -0.085(2)                          7
   110010000      CHIaa /  /MHz          512.643(4)                         8
  -110020000      CHIbb /  /MHz         -512.643(4)           = -1.00000 *  8
   110030000      CHIcc /  /MHz         -307.915(5)                        9
  -110020000      CHIbb /  /MHz          307.915(5)           = -1.00000 *  9
   110610000      CHIab /  /MHz         -297.0(1)                         10
   220010000      CHIaa /  /MHz           -0.747(4)                       11
  -220020000      CHIbb /  /MHz            0.747(4)           = -1.00000 * 11
   220030000      CHIcc /  /MHz            2.420(4)                       12
  -220020000      CHIbb /  /MHz           -2.420(4)           = -1.00000 * 12
   220610000      CHIab /  /MHz           -3.4(1)                         13
    10010000        Maa /  /MHz            0.0012(6)                      14
    10020000        Mbb /  /MHz            0.0038(5)                      15
    10030000        Mcc /  /MHz            0.0033(5)                      16

 CORRELATION COEFFICIENTS, C.ij:

           A  /     B  /     C  /     -DJ  /   -DJK  /  -DK  /   d1  /    CHIaa /

A  /        1.0000
B  /        0.3902   1.0000
```

```
C  /       -0.4435  -0.0404   1.0000
-DJ  /      0.0975  -0.6005  -0.6816   1.0000
-DJK  /    -0.1919  -0.0883   0.0144  -0.1728   1.0000
-DK  /     -0.9705  -0.3423   0.4113  -0.0783   0.0782   1.0000
d1  /      -0.4184  -0.6564   0.6601  -0.0223  -0.0435   0.3765   1.0000
CHIaa /    -0.0077   0.0629   0.0310  -0.0606  -0.0154   0.0142  -0.0213   1.0000
CHIcc /     0.0028  -0.0061  -0.0304   0.0217   0.0120  -0.0141  -0.0658  -0.4600
CHIab /     0.1715   0.1248   0.1487  -0.1695  -0.0310  -0.1719   0.0662  -0.0155
CHIaa /    -0.0106  -0.0479   0.0349   0.0105  -0.0540   0.0135   0.0612  -0.0229
CHIcc /     0.0080  -0.0365   0.0339   0.0070   0.0250  -0.0064   0.0763  -0.0310
CHIab /     0.0009  -0.0405  -0.0058   0.0332  -0.0087  -0.0011   0.0293  -0.0485
Maa /       0.0190   0.1328  -0.0012  -0.1084   0.1821  -0.0166  -0.1090   0.0031
Mbb /       0.0003   0.1809  -0.0496  -0.0591   0.0554   0.0054  -0.1756  -0.0500
Mcc /      -0.0571  -0.0689   0.2992  -0.1012  -0.0557   0.0555   0.2523  -0.0992

           CHIcc /  CHIab /  CHIaa /  CHIcc /  CHIab /  Maa /    Mbb /    Mcc /

CHIcc /     1.0000
CHIab /    -0.1396   1.0000
CHIaa /     0.0010  -0.0239   1.0000
CHIcc /     0.0241   0.0039  -0.3066   1.0000
CHIab /     0.0089  -0.0461   0.0058   0.0920   1.0000
Maa /       0.0661  -0.0486   0.0439   0.0128   0.0114   1.0000
Mbb /      -0.0439   0.0078  -0.0259  -0.0060   0.0192   0.0476   1.0000
Mcc /       0.1335  -0.1133   0.0064   0.0482   0.0124  -0.1461  -0.4214   1.0000

 Mean value of |C.ij|, i.ne.j =   0.1096
 Mean value of  C.ij,  i.ne.j =  -0.0305


 Worst fitting lines (obs-calc/error):

   222:    1.1        356:   -1.0        304:    1.0        344:   -1.0
```

```
 71:   -1.0       114:   -0.9       130:    0.9       254:    0.9
201:    0.9        69:    0.8       293:    0.8        74:   -0.8
 79:    0.8        46:   -0.8        94:   -0.8       239:    0.8
238:   -0.8       265:   -0.8        87:   -0.8       199:   -0.7
268:    0.7        38:    0.7        12:    0.7       236:   -0.7
252:   -0.7        51:    0.7       227:   -0.7       306:    0.6
 66:    0.6        98:   -0.6        34:    0.6       248:   -0.6
257:   -0.6        27:    0.6       346:    0.6        70:    0.6
264:    0.6        82:   -0.6       273:    0.6       349:   -0.6
 49:   -0.6       233:    0.6       186:   -0.6       347:    0.6
128:    0.5         7:   -0.5        92:    0.5       350:    0.5
223:    0.5       225:   -0.5

                                      ------------------------------------
-----------------------------------------/ SPFIT output reformatted with PIFORM
```

TABLE B.6. $C^{81}BrF_2CN$ Transitions Measured in MHz

												obs	o-c	error	blends o-c	blends wt	Notes
1:	2	1	2	3	3	1	0	1	2	2		7757.0161	0.0022	0.025			
2:	2	1	2	3	4	1	0	1	2	3		7757.4477	-0.0037	0.025			
3:	2	1	2	4	4	1	0	1	3	3		7798.3324	0.0109	0.025			
4:	2	1	2	4	5	1	0	1	3	4		7798.8540	-0.0010	0.025			
5:	2	1	2	4	3	1	0	1	3	2		7798.9863	-0.0041	0.025			
6:	3	0	3	4	3	2	1	2	3	2		7933.3606	-0.0106	0.025			
7:	4	1	3	3	4	3	2	2	2	3		8320.3556	-0.0055	0.025			
8:	4	1	3	3	3	3	2	2	2	2		8320.6928	0.0000	0.025			
9:	4	1	3	6	7	3	2	2	5	6		8349.8150	-0.0068	0.025			
10:	4	1	3	6	6	3	2	2	5	5		8350.2105	0.0067	0.025			
11:	4	1	3	4	5	3	2	2	3	4		8403.0886	-0.0037	0.025			
12:	4	1	3	5	4	3	2	2	4	3		8430.6158	-0.0227	0.025			
13:	4	1	3	5	6	3	2	2	4	5		8430.7048	-0.0012	0.025			
14:	4	1	3	5	5	3	2	2	4	4		8431.0124	0.0054	0.025			
15:	3	1	3	2	3	2	1	2	3	4		8954.9888	0.0017	0.025			
16:	3	1	3	2	2	2	1	2	2	2		8999.6411	-0.0025	0.025			
17:	3	1	3	2	3	2	1	2	2	3		9000.1579	-0.0029	0.025			
18:	3	1	3	2	1	2	1	2	2	1		9000.5777	0.0033	0.025			
19:	3	1	3	3	3	2	1	2	3	2		9045.3533	0.0004	0.025			
20:	3	1	3	3	3	2	1	2	3	4		9045.4648	-0.0039	0.025			
21:	3	1	3	3	3	2	1	2	3	3		9045.7242	0.0002	0.025			
22:	3	1	3	3	4	2	1	2	3	4		9045.9191	0.0125	0.025			
23:	3	1	3	3	4	2	1	2	3	3		9046.1700	0.0082	0.025			
24:	3	1	3	3	2	2	1	2	3	3		9046.3480	-0.0049	0.025			
25:	3	1	3	5	5	2	1	2	4	5		9060.3108	0.0046	0.025			
26:	3	1	3	5	5	2	1	2	4	4		9060.9754	-0.0035	0.025			
27:	3	1	3	5	6	2	1	2	4	5		9061.1280	-0.0028	0.025			

28:	3	1	3	5	4	2	1	2	4	4		9061.9777	-0.0119	0.025
29:	3	1	3	2	2	2	1	2	1	1		9063.5232	-0.0032	0.025
30:	3	1	3	2	3	2	1	2	1	2		9064.0463	-0.0005	0.025
31:	3	1	3	2	1	2	1	2	1	1		9064.4741	0.0032	0.025
32:	4	3	1	6	6	4	2	2	6	6		9069.5546	0.0064	0.025
33:	4	3	1	6	7	4	2	2	6	7		9069.6672	0.0050	0.025
34:	3	1	3	4	4	2	1	2	3	4		9087.4665	0.0018	0.025
35:	3	1	3	4	4	2	1	2	3	3		9087.7210	0.0010	0.025
36:	3	1	3	4	5	2	1	2	3	4		9088.0665	0.0160	0.025
37:	3	1	3	4	3	2	1	2	3	3		9088.4872	0.0028	0.025
38:	3	1	3	3	3	2	1	2	2	2		9090.6523	0.0026	0.025
39:	3	1	3	3	4	2	1	2	2	3		9091.0807	0.0004	0.025
40:	3	1	3	3	2	2	1	2	2	1		9091.2679	0.0026	0.025
41:	4	3	1	3	4	4	2	2	3	4		9097.1372	0.0030	0.025
42:	3	3	0	4	5	3	2	1	3	4		9152.0503	-0.0117	0.025
43:	3	1	3	4	3	2	1	2	4	3		9153.2288	0.0055	0.025
44:	3	3	0	3	4	3	2	1	3	4		9213.7659	0.0032	0.025
45:	3	0	3	2	2	2	0	2	3	3		9226.8080	-0.0059	0.025
46:	3	0	3	2	3	2	0	2	3	4		9226.9477	-0.0007	0.025
47:	3	0	3	2	1	2	0	2	3	2		9227.0934	-0.0121	0.025
48:	3	0	3	2	2	2	0	2	2	2		9301.9525	-0.0081	0.025
49:	3	0	3	2	3	2	0	2	2	3		9302.2426	-0.0069	0.025
50:	3	0	3	2	1	2	0	2	2	1		9302.4998	0.0188	0.025
51:	3	3	1	4	4	3	2	2	4	4		9304.6712	0.0079	0.025
52:	3	0	3	3	3	2	0	2	3	3		9336.1980	0.0108	0.025
53:	3	3	1	3	4	3	2	2	3	4		9366.9593	-0.0083	0.025
54:	3	3	1	3	3	3	2	2	3	3		9367.1206	-0.0177	0.025
55:	3	0	3	5	5	2	0	2	4	5		9384.9196	0.0031	0.025
56:	3	0	3	5	5	2	0	2	4	4		9385.1920	0.0006	0.025
57:	3	0	3	5	4	2	0	2	4	3		9385.3626	-0.0127	0.025
58:	3	0	3	5	4	2	0	2	4	4		9385.7307	-0.0007	0.025
59:	3	0	3	4	4	2	0	2	3	4		9385.9986	0.0141	0.025
60:	3	0	3	4	4	2	0	2	3	3		9386.1218	0.0017	0.025

61:	3	0	3	4	5	2	0	2	3	4	9386.2957	-0.0153	0.025
62:	3	0	3	4	3	2	0	2	3	2	9386.3581	0.0078	0.025
63:	3	0	3	4	3	2	0	2	3	3	9386.5481	0.0032	0.025
64:	3	2	2	2	3	2	2	1	1	2	9407.6449	0.0022	0.025
65:	3	0	3	3	3	2	0	2	2	2	9411.3343	0.0005	0.025
66:	3	0	3	3	4	2	0	2	2	3	9411.5878	0.0004	0.025
67:	3	0	3	3	2	2	0	2	2	1	9411.7095	0.0052	0.025
68:	3	0	3	2	3	2	0	2	1	2	9411.9799	0.0028	0.025
69:	3	0	3	2	1	2	0	2	1	1	9412.1951	0.0016	0.025
70:	4	3	2	5	6	4	2	3	5	6	9424.6874	-0.0173	0.025
71:	4	3	2	5	5	4	2	3	5	5	9424.9289	-0.0015	0.025
72:	3	3	1	5	6	3	2	2	5	6	9439.4114	-0.0119	0.025
73:	3	3	1	5	5	3	2	2	5	5	9439.7213	-0.0012	0.025
74:	4	3	2	4	5	4	2	3	4	5	9452.7133	-0.0072	0.025
75:	4	3	2	4	4	4	2	3	4	4	9452.9059	-0.0077	0.025
76:	3	2	2	5	5	2	2	1	4	4	9484.2012	0.0022	0.025
77:	3	2	2	5	6	2	2	1	4	5	9484.4073	0.0091	0.025
78:	3	2	2	4	4	2	2	1	4	4	9485.4211	0.0003	0.025
79:	3	2	2	4	5	2	2	1	4	5	9485.6327	0.0087	0.025
80:	3	0	3	4	4	2	0	2	4	3	9494.5949	0.0114	0.025
81:	3	0	3	4	5	2	0	2	4	5	9494.9927	0.0013	0.025
82:	3	0	3	4	5	2	0	2	4	4	9495.2880	0.0218	0.025
83:	3	0	3	4	3	2	0	2	4	4	9495.3664	0.0018	0.025
84:	3	3	1	2	3	3	2	2	2	3	9501.4287	0.0010	0.025
85:	3	3	1	2	2	3	2	2	2	2	9501.6090	-0.0188	0.025
86:	4	3	2	6	5	4	2	3	6	5	9505.8590	-0.0177	0.025
87:	4	3	2	6	7	4	2	3	6	7	9505.9376	0.0121	0.025
88:	4	3	2	6	6	4	2	3	6	6	9506.1910	0.0020	0.025
89:	3	2	2	3	4	2	2	1	2	3	9516.0167	0.0021	0.025
90:	3	2	2	2	3	2	2	1	2	3	9517.8431	0.0023	0.025
91:	3	2	1	2	1	2	2	0	1	1	9532.2969	-0.0020	0.025
92:	3	2	1	2	3	2	2	0	1	2	9532.4159	0.0005	0.025
93:	3	2	1	2	2	2	2	0	1	1	9532.5789	0.0193	0.025

94:	4	3	2	3	4	4	2	3	3	4	9534.3651	-0.0056	0.025
95:	3	2	1	4	3	2	2	0	4	4	9607.9217	-0.0067	0.025
96:	3	2	1	4	5	2	2	0	4	4	9608.0272	-0.0026	0.025
97:	3	2	1	4	4	2	2	0	4	4	9608.1951	0.0019	0.025
98:	3	2	1	4	5	2	2	0	4	5	9608.3118	-0.0026	0.025
99:	3	2	1	4	4	2	2	0	4	5	9608.4897	0.0117	0.025
100:	3	2	1	4	4	2	2	0	4	3	9608.5747	0.0133	0.025
101:	3	2	1	5	5	2	2	0	4	4	9608.7479	-0.0030	0.025
102:	3	2	1	5	5	2	2	0	4	5	9609.0357	0.0000	0.025
103:	5	3	3	5	5	5	2	4	5	5	9615.7750	-0.0002	0.025
104:	3	2	1	3	4	2	2	0	2	3	9639.6284	-0.0003	0.025
105:	3	2	1	3	3	2	2	0	2	2	9639.8448	0.0057	0.025
106:	3	2	1	2	3	2	2	0	2	3	9643.0025	-0.0050	0.025
107:	3	2	1	2	2	2	2	0	2	2	9643.1557	-0.0032	0.025
108:	5	3	3	7	6	5	2	4	7	6	9655.1008	-0.0219	0.025
109:	5	3	3	7	8	5	2	4	7	8	9655.1831	0.0174	0.025
110:	5	3	3	7	7	5	2	4	7	7	9655.4437	0.0022	0.025
111:	5	3	3	4	5	5	2	4	4	5	9670.9227	-0.0055	0.025
112:	5	3	3	4	4	5	2	4	4	4	9671.1759	0.0004	0.025
113:	3	2	1	4	5	2	2	0	3	4	9715.5892	0.0014	0.025
114:	3	2	1	5	4	2	2	0	3	3	9715.9540	0.0053	0.025
115:	3	2	1	5	4	2	2	0	3	4	9716.0418	-0.0146	0.025
116:	3	1	2	2	3	2	1	1	3	4	9830.6282	-0.0107	0.025
117:	3	1	2	2	1	2	1	1	2	1	9860.8301	-0.0152	0.025
118:	3	1	2	2	1	2	1	1	2	2	9860.9105	0.0129	0.025
119:	3	1	2	2	3	2	1	1	2	3	9861.1059	-0.0022	0.025
120:	3	1	2	2	2	2	1	1	2	2	9861.4503	0.0145	0.025
121:	6	3	4	6	7	6	2	5	6	7	9879.3174	0.0101	0.025
122:	6	3	4	6	6	6	2	5	6	6	9879.5952	0.0130	0.025
123:	3	1	2	3	4	2	1	1	3	4	9900.2186	-0.0123	0.025
124:	3	1	2	3	3	2	1	1	3	3	9900.2865	0.0055	0.025
125:	3	1	2	3	3	2	1	1	3	2	9900.5336	0.0041	0.025
126:	3	1	2	2	1	2	1	1	1	1	9903.4253	-0.0084	0.025

127:	3	1	2	2	3	2	1	1	1	2	9903.6697	0.0000	0.025
128:	3	1	2	2	2	2	1	1	1	2	9903.9749	0.0061	0.025
129:	3	1	2	5	4	2	1	1	4	4	9905.3548	0.0099	0.025
130:	3	1	2	5	5	2	1	1	4	4	9905.8723	-0.0186	0.025
131:	3	1	2	5	6	2	1	1	4	5	9905.9379	0.0059	0.025
132:	3	1	2	5	5	2	1	1	4	5	9906.3692	-0.0074	0.025
133:	6	3	4	8	8	6	2	5	8	8	9910.3156	0.0022	0.025
134:	3	1	2	3	2	2	1	1	2	1	9930.5716	-0.0088	0.025
135:	3	1	2	3	4	2	1	1	2	3	9930.7047	0.0046	0.025
136:	3	1	2	3	3	2	1	1	2	2	9930.9609	0.0050	0.025
137:	3	1	2	4	3	2	1	1	3	3	9932.6830	0.0099	0.025
138:	3	1	2	4	5	2	1	1	3	4	9932.9374	0.0032	0.025
139:	3	1	2	4	4	2	1	1	3	3	9933.0480	0.0019	0.025
140:	3	1	2	4	4	2	1	1	3	4	9933.2326	0.0092	0.025
141:	3	1	2	3	3	2	1	1	4	4	9944.1995	-0.0095	0.025
142:	3	1	2	4	4	2	1	1	4	4	9976.9750	0.0008	0.025
143:	3	1	2	4	5	2	1	1	4	5	9977.1560	-0.0147	0.025
144:	3	1	2	4	4	2	1	1	4	5	9977.4722	0.0123	0.030
145:	3	1	2	4	4	2	1	1	4	3	9977.6193	0.0119	0.025
146:	7	2	6	7	8	7	0	7	7	8	9977.8402	0.0077	0.025
147:	3	1	3	2	2	2	0	2	2	2	10482.6612	-0.0059	0.025
148:	3	1	3	2	3	2	0	2	2	3	10483.2099	-0.0007	0.025
149:	3	1	3	2	1	2	0	2	2	1	10483.6479	0.0023	0.025
150:	3	1	3	3	3	2	0	2	3	3	10498.5195	-0.0070	0.025
151:	3	1	3	3	4	2	0	2	3	4	10498.8242	-0.0047	0.025
152:	3	1	3	3	2	2	0	2	3	2	10498.9561	-0.0049	0.025
153:	3	1	3	4	4	2	0	2	3	4	10540.3975	0.0104	0.025
154:	3	1	3	4	4	2	0	2	3	3	10540.5233	0.0007	0.025
155:	3	1	3	4	5	2	0	2	3	4	10540.9715	-0.0013	0.025
156:	3	1	3	4	3	2	0	2	3	2	10541.0907	-0.0016	0.025
157:	3	1	3	4	3	2	0	2	3	3	10541.2842	-0.0028	0.025
158:	3	1	3	5	5	2	0	2	4	5	10556.7084	-0.0121	0.025
159:	3	1	3	5	5	2	0	2	4	4	10556.9945	-0.0009	0.025

160:	3	1	3	5	6	2	0	2	4	5	10557.5416	-0.0036	0.025
161:	3	1	3	5	4	2	0	2	4	3	10557.6529	0.0029	0.025
162:	3	1	3	5	4	2	0	2	4	4	10557.9945	-0.0116	0.025
163:	3	1	3	3	3	2	0	2	2	2	10573.6760	0.0027	0.025
164:	3	1	3	3	4	2	0	2	2	3	10574.1310	0.0009	0.025
165:	3	1	3	3	2	2	0	2	2	1	10574.3454	0.0089	0.025
166:	3	1	3	2	2	2	0	2	1	1	10592.4120	-0.0017	0.025
167:	3	1	3	2	3	2	0	2	1	2	10592.9450	0.0068	0.025
168:	3	1	3	2	1	2	0	2	1	1	10593.3357	-0.0223	0.025
169:	3	1	3	4	4	2	0	2	4	4	10649.3384	-0.0038	0.025
170:	3	1	3	4	5	2	0	2	4	5	10649.6535	0.0004	0.025
171:	3	1	3	4	3	2	0	2	4	3	10649.7315	-0.0190	0.025
172:	4	0	4	4	5	3	1	3	4	5	11195.7916	0.0158	0.025
173:	4	0	4	4	4	3	1	3	4	4	11195.8931	-0.0029	0.025
174:	4	0	4	6	7	3	1	3	5	6	11215.1973	-0.0193	0.025
175:	4	0	4	6	6	3	1	3	5	5	11215.4085	-0.0054	0.025
176:	4	0	4	3	3	3	1	3	2	3	11217.9309	0.0072	0.025
177:	4	0	4	3	2	3	1	3	2	1	11218.2326	-0.0029	0.025
178:	4	0	4	3	4	3	1	3	2	3	11218.4423	0.0067	0.025
179:	4	0	4	5	6	3	1	3	4	5	11233.9076	0.0150	0.025
180:	4	0	4	5	4	3	1	3	4	4	11234.5891	-0.0105	0.025
181:	4	0	4	4	4	3	1	3	3	4	11237.4515	-0.0027	0.025
182:	4	0	4	4	3	3	1	3	3	2	11237.8521	-0.0156	0.025
183:	4	0	4	4	5	3	1	3	3	4	11237.9415	0.0219	0.025
184:	2	2	1	3	3	1	1	0	3	3	11739.0921	0.0039	0.025
185:	2	2	1	3	4	1	1	0	3	4	11739.5493	-0.0007	0.025
186:	2	2	1	3	2	1	1	0	3	2	11739.7467	-0.0021	0.025
187:	2	2	1	2	3	1	1	0	1	2	11763.9546	-0.0006	0.025
188:	2	2	1	3	2	1	1	0	2	1	11803.5695	0.0024	0.025
189:	2	2	1	3	4	1	1	0	2	3	11804.0099	0.0029	0.025
190:	2	2	1	3	3	1	1	0	2	2	11804.5993	0.0047	0.025
191:	2	2	1	4	3	1	1	0	3	3	11845.4913	0.0114	0.025
192:	2	2	1	4	4	1	1	0	3	3	11845.7429	-0.0008	0.025

193:	2	2	1	4	5	1	1	0	3	4	11846.0815	0.0055	0.025
194:	2	2	1	4	3	1	1	0	3	2	11846.2494	0.0024	0.025
195:	2	2	1	1	2	1	1	0	1	2	11874.1545	0.0012	0.025
196:	2	2	1	2	1	1	1	0	2	1	11878.8758	-0.0105	0.025
197:	2	2	1	2	3	1	1	0	2	3	11879.2834	0.0001	0.025
198:	2	2	1	2	2	1	1	0	2	2	11879.7871	0.0042	0.025
199:	4	1	4	3	3	3	1	3	3	3	11973.4643	0.0099	0.025
200:	4	1	4	3	4	3	1	3	3	4	11973.7950	0.0137	0.025
201:	4	1	4	3	2	3	1	3	3	2	11973.9191	0.0007	0.025
202:	2	2	1	1	2	1	1	0	2	3	11989.4763	-0.0049	0.025
203:	4	1	4	4	4	3	1	3	4	4	12033.6943	0.0028	0.025
204:	4	1	4	4	5	3	1	3	4	5	12033.7899	-0.0031	0.025
205:	2	2	0	3	2	1	1	1	3	2	12056.1992	0.0024	0.025
206:	2	2	0	3	4	1	1	1	3	4	12056.4074	0.0052	0.025
207:	2	2	0	3	3	1	1	1	3	3	12056.8898	0.0085	0.025
208:	4	1	4	6	6	3	1	3	5	6	12057.5588	-0.0038	0.025
209:	4	1	4	6	7	3	1	3	5	6	12058.4847	-0.0091	0.025
210:	4	1	4	6	5	3	1	3	5	5	12059.4973	0.0076	0.025
211:	4	1	4	3	3	3	1	3	2	3	12063.9385	0.0026	0.025
212:	4	1	4	3	3	3	1	3	2	2	12064.4743	0.0138	0.025
213:	4	1	4	3	4	3	1	3	2	3	12064.6913	-0.0093	0.025
214:	4	1	4	3	2	3	1	3	2	2	12065.5569	0.0034	0.025
215:	4	1	4	5	5	3	1	3	4	5	12068.5002	0.0030	0.025
216:	4	1	4	5	5	3	1	3	4	4	12069.0793	-0.0036	0.025
217:	4	1	4	5	6	3	1	3	4	5	12069.2664	-0.0008	0.025
218:	4	1	4	5	4	3	1	3	4	4	12070.0369	0.0048	0.025
219:	4	1	4	4	4	3	1	3	3	4	12075.2555	0.0058	0.025
220:	4	1	4	4	4	3	1	3	3	3	12075.6910	0.0034	0.025
221:	4	1	4	4	5	3	1	3	3	4	12075.9410	0.0040	0.025
222:	4	1	4	4	3	3	1	3	3	3	12076.5784	-0.0031	0.025
223:	5	1	4	4	5	4	2	3	3	4	12089.3719	0.0039	0.025
224:	5	1	4	4	4	4	2	3	3	3	12089.7225	-0.0132	0.025
225:	2	2	0	2	3	1	1	1	1	2	12096.0772	-0.0016	0.025

226:	2	2	0	3	2	1	1	1	2	2	12098.0790	0.0024	0.025
227:	2	2	0	3	3	1	1	1	2	2	12098.2353	0.0044	0.025
228:	2	2	0	3	4	1	1	1	2	3	12098.4362	0.0027	0.025
229:	2	2	0	3	2	1	1	1	2	1	12098.6333	-0.0029	0.025
230:	5	1	4	7	6	4	2	3	6	5	12099.5190	-0.0088	0.025
231:	5	1	4	7	8	4	2	3	6	7	12099.5898	-0.0062	0.025
232:	5	1	4	7	7	4	2	3	6	6	12100.0167	0.0043	0.025
233:	5	1	4	5	6	4	2	3	4	5	12134.3349	0.0042	0.025
234:	5	1	4	5	5	4	2	3	4	4	12134.6755	0.0110	0.025
235:	5	1	4	6	5	4	2	3	5	4	12143.1379	-0.0167	0.025
236:	5	1	4	6	7	4	2	3	5	6	12143.2279	0.0030	0.025
237:	5	1	4	6	6	4	2	3	5	5	12143.5766	-0.0062	0.025
238:	4	1	4	5	6	3	1	3	5	6	12161.3685	-0.0065	0.025
239:	4	1	4	5	5	3	1	3	5	5	12161.4413	0.0115	0.030
240:	2	2	0	4	3	1	1	1	3	2	12163.4293	-0.0037	0.025
241:	2	2	0	4	5	1	1	1	3	4	12163.6791	0.0037	0.025
242:	2	2	0	4	4	1	1	1	3	4	12163.9664	0.0063	0.025
243:	2	2	0	4	4	1	1	1	3	3	12164.3429	0.0115	0.025
244:	2	2	0	2	2	1	1	1	2	2	12174.0662	0.0027	0.025
245:	2	2	0	2	3	1	1	1	2	3	12174.3787	-0.0016	0.025
246:	2	2	0	2	2	1	1	1	2	1	12174.6267	0.0035	0.025
247:	2	2	0	1	2	1	1	1	1	2	12206.6716	0.0005	0.025
248:	2	2	0	1	2	1	1	1	2	3	12284.9613	-0.0111	0.025
249:	4	0	4	3	3	3	0	3	3	3	12289.7805	-0.0010	0.025
250:	4	0	4	3	4	3	0	3	3	4	12290.0574	-0.0013	0.025
251:	4	0	4	3	2	3	0	3	3	2	12290.1756	-0.0013	0.025
252:	4	0	4	3	2	3	0	3	3	3	12290.5111	-0.0020	0.025
253:	4	0	4	4	4	3	0	3	4	4	12350.2938	-0.0048	0.025
254:	4	0	4	4	3	3	0	3	4	3	12350.4919	0.0133	0.025
255:	4	0	4	6	6	3	0	3	5	6	12386.7767	-0.0011	0.025
256:	4	0	4	6	6	3	0	3	5	5	12387.2173	-0.0008	0.025
257:	4	0	4	6	7	3	0	3	5	6	12387.4084	0.0031	0.025
258:	4	0	4	5	5	3	0	3	4	4	12388.3542	-0.0013	0.025

259:	4	0	4	5	6	3	0	3	4	5	12388.5583	0.0039	0.025
260:	4	0	4	5	4	3	0	3	4	4	12389.0077	0.0054	0.025
261:	4	0	4	3	3	3	0	3	2	3	12398.8842	-0.0006	0.025
262:	4	0	4	3	3	3	0	3	2	2	12399.1514	-0.0033	0.025
263:	4	0	4	3	4	3	0	3	2	3	12399.3962	-0.0004	0.025
264:	4	0	4	3	2	3	0	3	2	2	12399.8848	-0.0016	0.025
265:	4	0	4	4	4	3	0	3	3	4	12399.9975	0.0006	0.025
266:	4	0	4	4	4	3	0	3	3	3	12400.2311	-0.0004	0.025
267:	4	0	4	4	5	3	0	3	3	4	12400.4464	-0.0159	0.025
268:	4	0	4	4	3	3	0	3	3	3	12400.8346	-0.0017	0.025
269:	4	0	4	5	5	3	0	3	5	5	12498.1168	0.0129	0.030
270:	4	0	4	5	6	3	0	3	5	6	12498.1797	-0.0093	0.025
271:	4	2	3	6	6	3	2	2	5	5	12646.0387	-0.0018	0.025
272:	4	2	3	6	7	3	2	2	5	6	12646.1689	0.0114	0.025
273:	4	3	2	3	2	3	3	1	2	2	12663.2911	-0.0101	0.025
274:	4	3	2	3	4	3	3	1	2	3	12663.5287	-0.0180	0.025
275:	4	3	2	3	2	3	3	1	2	1	12663.6542	0.0031	0.025
276:	4	2	3	4	4	3	2	2	4	4	12673.3992	0.0157	0.025
277:	4	2	3	4	5	3	2	2	3	4	12674.3152	-0.0167	0.025
278:	4	3	2	5	5	3	3	1	5	5	12675.4732	0.0059	0.025
279:	4	3	2	5	6	3	3	1	5	6	12675.6305	-0.0170	0.025
280:	4	3	1	3	2	3	3	0	2	2	12676.6533	-0.0040	0.025
281:	4	3	1	3	4	3	3	0	2	3	12676.9017	-0.0121	0.025
282:	4	3	1	3	2	3	3	0	2	1	12676.9989	-0.0141	0.025
283:	4	3	1	5	5	3	3	0	5	5	12688.7390	0.0089	0.025
284:	4	2	3	5	5	3	2	2	4	4	12689.0415	0.0038	0.025
285:	4	2	3	5	6	3	2	2	4	5	12689.1540	0.0134	0.025
286:	4	2	3	5	5	3	2	2	5	5	12690.2568	-0.0026	0.025
287:	4	2	3	5	6	3	2	2	5	6	12690.3755	0.0093	0.025
288:	4	3	2	6	6	3	3	1	5	5	12712.5110	0.0040	0.025
289:	4	3	2	6	7	3	3	1	5	6	12712.6462	-0.0133	0.025
290:	4	3	1	6	5	3	3	0	5	5	12725.7156	0.0035	0.025
291:	4	3	1	6	6	3	3	0	5	5	12725.9194	0.0050	0.025

292:	4	3	1	6	7	3	3	0	5	6	12726.0358	-0.0160	0.025
293:	4	3	2	4	3	3	3	1	3	3	12759.8816	-0.0121	0.025
294:	4	3	1	4	3	3	3	0	3	3	12773.2730	0.0141	0.025
295:	4	3	1	4	4	3	3	0	3	3	12773.4036	-0.0149	0.025
296:	4	3	2	3	4	3	3	1	3	4	12799.8387	0.0056	0.025
297:	4	3	2	5	5	3	3	1	4	4	12809.3192	0.0144	0.025
298:	4	3	2	5	6	3	3	1	4	5	12809.3857	-0.0094	0.025
299:	4	3	1	3	4	3	3	0	3	4	12813.1849	0.0047	0.025
300:	4	3	2	4	4	3	3	1	4	4	12821.6334	-0.0004	0.025
301:	4	3	2	4	5	3	3	1	4	5	12821.7226	-0.0207	0.025
302:	4	3	1	4	4	3	3	0	4	4	12835.0630	-0.0017	0.025
303:	6	4	2	7	7	6	3	3	7	7	12840.0737	0.0107	0.025
304:	6	4	2	6	7	6	3	3	6	7	12852.3376	0.0037	0.025
305:	6	4	2	8	9	6	3	3	8	9	12892.9742	0.0071	0.025
306:	6	4	2	5	6	6	3	3	5	6	12905.6247	0.0014	0.025
307:	4	2	2	3	2	3	2	1	2	2	12926.1853	0.0028	0.025
308:	4	2	2	3	4	3	2	1	2	3	12926.4250	-0.0049	0.025
309:	4	2	2	3	3	3	2	1	2	2	12926.5224	-0.0030	0.025
310:	4	2	2	3	3	3	2	1	2	3	12926.6630	-0.0072	0.025
311:	4	2	2	3	2	3	2	1	3	2	12929.7156	-0.0090	0.030
312:	4	2	2	3	3	3	2	1	4	4	12929.8559	-0.0176	0.025
313:	4	2	2	6	5	3	2	1	5	5	12941.4703	0.0144	0.025
314:	4	2	2	6	6	3	2	1	5	5	12941.7784	-0.0149	0.025
315:	4	2	2	6	5	3	2	1	4	4	12942.0170	0.0034	0.025
316:	5	4	1	6	7	5	3	2	6	7	12951.4111	-0.0005	0.025
317:	5	4	1	6	6	5	3	2	6	6	12951.4751	-0.0149	0.025
318:	4	2	2	4	5	3	2	1	4	4	12968.7301	-0.0044	0.025
319:	4	2	2	4	5	3	2	1	3	4	12968.9182	0.0081	0.025
320:	4	2	2	4	4	3	2	1	4	3	12969.1963	-0.0067	0.025
321:	4	2	2	5	5	3	2	1	5	5	12982.9911	0.0073	0.025
322:	4	2	2	5	5	3	2	1	5	4	12983.2389	0.0026	0.025
323:	4	2	2	5	4	3	2	1	4	3	12983.5156	-0.0176	0.025
324:	4	2	2	5	5	3	2	1	3	4	12983.7235	0.0064	0.025

325:	5	4	2	6	6	5	3	3	6	6	13011.5324	-0.0111	0.025
326:	6	4	3	7	8	6	3	4	7	8	13013.4403	-0.0118	0.025
327:	6	4	3	7	7	6	3	4	7	7	13013.5651	0.0193	0.025
328:	5	4	1	7	8	5	3	2	7	8	13026.6797	0.0007	0.025
329:	4	4	0	4	4	4	3	1	4	4	13026.8698	0.0177	0.025
330:	6	4	3	8	9	6	3	4	8	9	13066.7034	-0.0184	0.025
331:	5	4	2	7	8	5	3	3	7	8	13086.4651	-0.0099	0.025
332:	4	1	3	3	4	3	1	2	3	4	13107.9991	-0.0031	0.025
333:	4	1	3	3	3	3	1	2	3	3	13108.0994	-0.0016	0.025
334:	4	1	3	3	3	3	1	2	3	2	13108.4325	0.0081	0.025
335:	4	4	1	6	6	4	3	2	6	6	13115.8319	0.0061	0.025
336:	4	1	4	3	4	3	0	3	3	4	13136.3217	-0.0021	0.025
337:	4	1	4	3	2	3	0	3	3	2	13136.5469	-0.0037	0.025
338:	4	4	1	3	3	4	3	2	3	3	13154.6038	0.0153	0.025
339:	4	1	3	4	4	3	1	2	4	4	13156.2001	0.0102	0.025
340:	4	1	3	6	5	3	1	2	5	5	13173.2987	0.0091	0.025
341:	4	1	3	6	7	3	1	2	5	6	13173.7733	-0.0322	0.025
342:	4	1	3	6	6	3	1	2	5	6	13174.1931	0.0009	0.025
343:	4	1	3	3	2	3	1	2	2	2	13177.1576	0.0019	0.025
344:	4	1	3	3	4	3	1	2	2	3	13177.5890	-0.0052	0.025
345:	4	1	3	3	3	3	1	2	2	3	13177.9219	0.0015	0.025
346:	4	1	3	5	4	3	1	2	4	4	13184.3281	0.0080	0.025
347:	4	1	3	5	6	3	1	2	4	5	13184.6923	0.0155	0.025
348:	4	1	3	5	5	3	1	2	4	5	13184.9639	-0.0145	0.025
349:	4	1	4	4	4	3	0	3	4	4	13188.0860	-0.0081	0.025
350:	4	1	4	4	5	3	0	3	4	5	13188.4513	-0.0034	0.025
351:	4	1	3	4	3	3	1	2	3	3	13188.6156	0.0162	0.025
352:	4	1	3	4	5	3	1	2	3	4	13188.9047	-0.0025	0.025
353:	4	1	3	4	4	3	1	2	3	4	13189.1859	0.0037	0.025
354:	4	1	4	5	5	3	0	3	4	4	13223.4802	-0.0053	0.025
355:	4	1	4	5	6	3	0	3	4	5	13223.9376	0.0087	0.025
356:	4	1	4	6	6	3	0	3	5	5	13230.1877	-0.0037	0.025
357:	4	1	4	6	7	3	0	3	5	6	13230.7030	0.0205	0.025

358:	4	1	4	4	4	3	0	3	3	3	13238.0233	-0.0037	0.025
359:	4	1	4	4	5	3	0	3	3	4	13238.4770	-0.0026	0.025
360:	4	1	4	4	3	3	0	3	3	2	13238.5886	0.0038	0.025
361:	4	1	4	3	3	3	0	3	2	3	13244.8885	-0.0085	0.025
362:	4	1	4	3	3	3	0	3	2	2	13245.1665	-0.0004	0.025
363:	4	1	4	3	4	3	0	3	2	3	13245.6583	-0.0033	0.025
364:	4	1	4	3	2	3	0	3	2	1	13245.7736	-0.0001	0.025
365:	4	1	4	3	2	3	0	3	2	2	13246.2517	-0.0084	0.025
366:	4	1	3	5	5	3	1	2	5	5	13255.7724	-0.0002	0.025
367:	4	1	3	5	6	3	1	2	5	6	13255.9007	-0.0148	0.025
368:	4	1	4	5	6	3	0	3	5	6	13333.5615	-0.0020	0.025
369:	5	0	5	7	8	4	1	4	6	7	14471.5163	0.0132	0.025
370:	5	0	5	7	7	4	1	4	6	6	14471.6277	0.0039	0.025
371:	5	0	5	5	6	4	1	4	4	5	14485.1472	0.0099	0.025
372:	3	2	2	4	4	2	1	1	3	3	14686.7171	-0.0113	0.025
373:	3	2	2	4	5	2	1	1	3	4	14686.9234	0.0185	0.025
374:	3	2	2	3	4	2	1	1	2	3	14716.5142	-0.0008	0.025
375:	3	2	2	5	5	2	1	1	4	4	14729.4397	0.0049	0.025
376:	3	2	2	5	5	2	1	1	4	5	14729.9217	0.0013	0.025
377:	3	2	2	5	4	2	1	1	4	3	14730.0539	-0.0084	0.025
378:	3	2	2	2	3	2	1	1	1	2	14760.9030	0.0001	0.025
379:	5	1	5	7	7	4	1	4	6	6	15031.3003	0.0140	0.025
380:	5	1	5	7	8	4	1	4	6	7	15031.3618	-0.0120	0.025
381:	5	1	5	4	4	4	1	4	3	3	15036.3395	0.0007	0.025
382:	5	1	5	4	5	4	1	4	3	4	15036.4791	-0.0081	0.025
383:	5	1	5	6	6	4	1	4	5	5	15036.8183	0.0009	0.025
384:	5	1	5	6	7	4	1	4	5	6	15036.9447	-0.0031	0.025
385:	5	1	5	5	5	4	1	4	4	5	15041.4783	0.0071	0.025
386:	5	1	5	5	5	4	1	4	4	4	15042.1590	0.0006	0.025
387:	5	1	5	5	6	4	1	4	4	5	15042.3199	-0.0007	0.025
388:	5	0	5	7	7	4	0	4	6	6	15314.5982	0.0011	0.025
389:	5	0	5	7	8	4	0	4	6	7	15314.7833	0.0029	0.025
390:	5	0	5	6	6	4	0	4	5	5	15315.9041	-0.0013	0.025

391:	5	0	5	6	7	4	0	4	5	6	15316.1038	0.0043	0.025
392:	5	0	5	4	4	4	0	4	3	3	15321.5169	-0.0007	0.025
393:	5	0	5	4	5	4	0	4	3	4	15321.7294	-0.0022	0.025
394:	5	0	5	5	5	4	0	4	4	4	15322.9417	-0.0005	0.025
395:	5	0	5	5	6	4	0	4	4	5	15323.1593	0.0047	0.025
396:	5	2	4	4	5	4	2	3	3	4	15774.7463	-0.0040	0.025
397:	5	2	4	7	7	4	2	3	6	6	15778.3341	0.0042	0.025
398:	5	2	4	7	8	4	2	3	6	7	15778.4236	0.0042	0.025
399:	5	2	4	5	5	4	2	3	5	5	15781.2493	0.0233	0.025
400:	5	2	4	5	5	4	2	3	4	4	15796.8748	-0.0053	0.025
401:	5	2	4	5	6	4	2	3	4	5	15796.9616	-0.0029	0.025
402:	5	2	4	6	6	4	2	3	5	5	15799.7740	-0.0108	0.025
403:	5	2	4	6	7	4	2	3	5	6	15799.8658	-0.0025	0.025
404:	5	4	2	4	5	4	4	1	3	4	15864.2892	0.0032	0.025
405:	5	4	1	4	5	4	4	0	3	4	15865.3300	-0.0019	0.025
406:	5	1	5	6	6	4	0	4	5	5	15871.9414	-0.0058	0.025
407:	5	1	5	7	7	4	0	4	6	6	15874.2577	-0.0019	0.025
408:	5	1	5	7	8	4	0	4	6	7	15874.6396	-0.0114	0.025
409:	5	1	5	5	5	4	0	4	4	4	15879.9338	-0.0200	0.025
410:	5	4	2	7	7	4	4	1	6	6	15898.3689	0.0054	0.025
411:	5	4	2	7	8	4	4	1	6	7	15898.5098	0.0019	0.025
412:	5	4	1	7	7	4	4	0	6	6	15899.4141	0.0038	0.025
413:	5	3	3	4	5	4	3	2	3	4	15911.3152	0.0073	0.025
414:	5	3	3	7	8	4	3	2	6	7	15927.6600	0.0003	0.025
415:	5	3	2	4	5	4	3	1	3	4	15957.1996	0.0012	0.025
416:	5	3	3	5	4	4	3	2	4	3	15959.8136	0.0065	0.025
417:	5	3	2	7	6	4	3	1	6	5	15972.9824	0.0001	0.025
418:	5	3	3	6	6	4	3	2	5	5	15975.6844	-0.0069	0.025
419:	5	2	3	4	5	4	2	2	3	4	16314.7707	0.0041	0.025
420:	5	2	3	7	8	4	2	2	6	7	16318.2040	0.0032	0.025
421:	5	2	3	5	6	4	2	2	4	5	16335.5103	-0.0021	0.025
422:	5	2	3	5	5	4	2	2	4	4	16335.6027	-0.0066	0.025
423:	5	2	3	6	7	4	2	2	5	6	16338.2681	0.0074	0.025

```
 424:  5  2  3  6  6    4  2  2  5  5        16338.3501  -0.0030  0.025
 425:  5  1  4  7  8    4  1  3  6  7        16395.9190  -0.0126  0.025
 426:  5  1  4  6  6    4  1  3  5  5        16401.5977  -0.0157  0.025
 427:  5  1  4  6  7    4  1  3  5  6        16401.6760   0.0165  0.025
 428:  5  1  4  5  6    4  1  3  4  5        16405.5897   0.0194  0.025
 429:  5  1  4  5  5    4  1  3  4  5        16405.8207   0.0052  0.025
 430:  6  1  6  8  8    5  1  5  7  7        17982.0355  -0.0113  0.025
 431:  6  1  6  8  9    5  1  5  7  8        17982.1255   0.0021  0.025
 432:  6  1  6  7  7    5  1  5  6  6        17985.4444   0.0185  0.025
 433:  6  1  6  7  8    5  1  5  6  7        17985.5245  -0.0062  0.025
 434:  6  1  6  5  5    5  1  5  4  4        17986.0450   0.0103  0.025
 435:  6  1  6  5  6    5  1  5  4  5        17986.1387  -0.0012  0.025
 436:  6  1  6  6  6    5  1  5  5  5        17989.4701   0.0075  0.025
 437:  6  1  6  6  7    5  1  5  5  6        17989.5779  -0.0041  0.025
-------------------------------------------------------------------------------

PARAMETERS IN FIT:

       10000         A  /  /MHz         3460.982(1)                          1
       20000         B  /  /MHz         1726.801(1)                          2
       30000         C  /  /MHz         1444.7863(7)                         3
         200        DJ  /  /kHz            0.31(1)                           4
        1100       DJK  /  /kHz           -0.91(4)                           5
        2000        DK  /  /kHz            2.94(8)                           6
       40100        d1  /  /kHz           -0.08(1)                           7
   110010000      CHIaa /  /MHz          430.26(1)                          8
  -110020000      CHIbb /  /MHz         -430.26(1)             = -1.00000 *  8
   110030000      CHIcc /  /MHz         -257.22(1)                          9
  -110020000      CHIbb /  /MHz          257.22(1)             = -1.00000 *  9
   110610000      CHIab /  /MHz         -245.5(4)                         10
   220010000      CHIaa /  /MHz           -0.72(1)                        11
  -220020000      CHIbb /  /MHz            0.72(1)             = -1.00000 * 11
   220030000      CHIcc /  /MHz            2.42(1)                         12
```

```
  -220020000      CHIbb /  /MHz          -2.42(1)             = -1.00000 * 12
   220610000      CHIab /  /MHz          -3.1(4)                           13
    10010000        Maa /  /MHz           0.0004(1)                        14
    10020000        Mbb /  /MHz           0.004(1)                         15
    10030000        Mcc /  /MHz           0.004(1)                         16

MICROWAVE AVG =       -0.000014 MHz, IR AVG =        0.00000
MICROWAVE RMS =        0.008749 MHz, IR RMS =        0.00000
END OF ITERATION  1 OLD, NEW RMS ERROR=        0.34911         0.34911

 distinct frequency lines in fit:   437
      distinct parameters of fit:    16

for standard errors previous errors are multiplied by:   0.355682

PARAMETERS IN FIT WITH STANDARD ERRORS ON THOSE THAT ARE FITTED:

       10000         A  /  /MHz         3460.9822(4)                      1
       20000         B  /  /MHz         1726.8014(3)                      2
       30000         C  /  /MHz         1444.7863(2)                      3
         200        DJ  /  /kHz            0.311(5)                       4
        1100       DJK  /  /kHz           -0.91(1)                        5
        2000        DK  /  /kHz            2.94(3)                        6
       40100        d1  /  /kHz           -0.088(3)                       7
   110010000      CHIaa /  /MHz          430.265(4)                       8
  -110020000      CHIbb /  /MHz         -430.265(4)           = -1.00000 *  8
   110030000      CHIcc /  /MHz         -257.228(4)                      9
  -110020000      CHIbb /  /MHz          257.228(4)           = -1.00000 *  9
   110610000      CHIab /  /MHz         -245.5(1)                        10
   220010000      CHIaa /  /MHz           -0.723(3)                      11
  -220020000      CHIbb /  /MHz            0.723(3)           = -1.00000 * 11
   220030000      CHIcc /  /MHz            2.426(4)                       12
  -220020000      CHIbb /  /MHz           -2.426(4)           = -1.00000 * 12
```

220610000	CHIab /	/MHz	-3.1(1)	13
10010000	Maa /	/MHz	0.0004(5)	14
10020000	Mbb /	/MHz	0.0045(4)	15
10030000	Mcc /	/MHz	0.0048(4)	16

CORRELATION COEFFICIENTS, C.ij:

	A /	B /	C /	-DJ /	-DJK /	-DK /	d1 /	CHIaa /
A /	1.0000							
B /	0.3750	1.0000						
C /	-0.2549	-0.3047	1.0000					
-DJ /	-0.1039	-0.7259	-0.3201	1.0000				
-DJK /	-0.2153	0.1129	-0.0906	-0.2494	1.0000			
-DK /	-0.5728	-0.1464	0.3734	-0.0097	-0.5311	1.0000		
d1 /	-0.2862	-0.8296	0.6173	0.4476	-0.2330	0.2823	1.0000	
CHIaa /	-0.0206	0.0446	0.0106	-0.0533	0.0978	-0.0447	-0.0270	1.0000
CHIcc /	-0.0016	-0.0157	-0.0521	0.0423	-0.0256	0.0041	-0.0221	-0.4006
CHIab /	-0.0028	-0.0120	0.2116	-0.0958	-0.0429	0.0774	0.1146	0.0037
CHIaa /	0.0233	-0.0558	0.0169	0.0440	-0.1337	0.1031	0.0513	-0.0097
CHIcc /	0.0115	0.0067	0.0059	-0.0077	0.0468	-0.0519	-0.0187	-0.0041
CHIab /	-0.0336	-0.0429	0.0223	0.0261	-0.0245	0.0444	0.0357	-0.0543
Maa /	0.1630	0.1347	-0.0269	-0.0856	0.0292	-0.1164	-0.0856	0.0703
Mbb /	0.0995	0.2443	-0.0747	-0.1409	0.0486	-0.0475	-0.1369	-0.0251
Mcc /	-0.0500	-0.0762	0.2881	-0.0776	-0.0219	0.0854	0.1029	-0.1569

	CHIcc /	CHIab /	CHIaa /	CHIcc /	CHIab /	Maa /	Mbb /	Mcc /
CHIcc /	1.0000							
CHIab /	-0.1637	1.0000						
CHIaa /	-0.0034	0.0275	1.0000					
CHIcc /	-0.0328	-0.0048	-0.3263	1.0000				
CHIab /	-0.0302	0.0192	0.0922	-0.0300	1.0000			

```
Maa /       0.0295  -0.0945   0.0640   0.0072   0.0375   1.0000
Mbb /      -0.0956  -0.0493   0.0342   0.0013   0.0253   0.2003   1.0000
Mcc /       0.2463  -0.1160  -0.0498   0.0486   0.0064  -0.0857  -0.4475   1.0000

 Mean value of |C.ij|, i.ne.j =   0.1178
 Mean value of  C.ij,  i.ne.j =  -0.0285


 Worst fitting lines (obs-calc/error):

   341:   -1.3        399:    0.9         12:   -0.9        168:   -0.9
   183:    0.9        108:   -0.9         82:    0.9        301:   -0.8
   357:    0.8        409:   -0.8        428:    0.8        327:    0.8
   174:   -0.8         93:    0.8        171:   -0.8         50:    0.8
    85:   -0.8        130:   -0.7        373:    0.7        432:    0.7
   330:   -0.7        274:   -0.7         54:   -0.7        329:    0.7
    86:   -0.7        323:   -0.7        312:   -0.7        109:    0.7
    70:   -0.7        279:   -0.7        277:   -0.7        235:   -0.7
   427:    0.7        351:    0.6        292:   -0.6         36:    0.6
   267:   -0.6        172:    0.6        426:   -0.6        276:    0.6
   182:   -0.6        347:    0.6        338:    0.6         61:   -0.6
   117:   -0.6        179:    0.6        314:   -0.6        295:   -0.6
   317:   -0.6        367:   -0.6

                                          ------------------------------------
------------------------------------------/ SPFIT output reformatted with PIFORM
```

TABLE B.7. $^{13}C^{79}BrF_2CN$ Transitions Measured in MHz

```
-------------------------------------------------------------------------------------=========
                                              obs         o-c     error     blends     Notes
```

													o-c	wt
1:	3	1	3	5	5	2	1	2	4	4		9119.5513	-0.0183	0.025
2:	3	1	3	5	6	2	1	2	4	5		9119.7064	-0.0073	0.025
3:	3	1	3	2	3	2	1	2	1	2		9123.1362	0.0015	0.025
4:	3	1	3	4	4	2	1	2	3	3		9151.4899	-0.0023	0.025
5:	3	1	3	4	5	2	1	2	3	4		9151.8566	0.0440	0.025
6:	3	1	3	3	3	2	1	2	2	2		9154.9933	-0.0148	0.025
7:	3	1	3	3	4	2	1	2	2	3		9155.4158	-0.0019	0.025
8:	3	0	3	5	5	2	0	2	4	4		9447.6083	0.0008	0.025
9:	3	0	3	5	6	2	0	2	4	5		9447.7708	0.0004	0.025
10:	3	0	3	4	4	2	0	2	3	3		9448.7654	-0.0040	0.025
11:	3	0	3	4	5	2	0	2	3	4		9448.9290	-0.0204	0.025
12:	3	0	3	3	3	2	0	2	2	2		9478.6084	-0.0089	0.025
13:	3	2	2	4	5	2	2	1	3	4		9675.1412	-0.0044	0.025
14:	3	2	1	5	6	2	2	0	4	5		9675.4481	0.0089	0.030
15:	3	1	2	2	3	2	1	1	1	2		9974.6048	-0.0048	0.025
16:	3	1	2	3	4	2	1	1	2	3		10006.8678	0.0045	0.025
17:	3	1	2	4	5	2	1	1	3	4		10009.6542	-0.0032	0.025
18:	3	1	3	5	6	2	0	2	4	5		10600.8091	-0.0271	0.025
19:	4	1	4	6	7	3	1	3	5	6		12137.2397	-0.0168	0.025
20:	4	1	4	5	6	3	1	3	4	5		12150.0619	-0.0047	0.025
21:	4	1	4	4	5	3	1	3	3	4		12158.0368	0.0033	0.025
22:	2	2	0	4	5	1	1	1	3	4		12179.4621	0.0072	0.025
23:	4	0	4	6	6	3	0	3	5	5		12466.9835	0.0113	0.025
24:	4	0	4	6	7	3	0	3	5	6		12467.1769	0.0210	0.025
25:	4	0	4	5	5	3	0	3	4	4		12468.3577	-0.0088	0.025
26:	4	0	4	5	4	3	0	3	4	3		12468.5662	-0.0132	0.025
27:	4	0	4	3	3	3	0	3	2	2		12481.1650	-0.0077	0.025
28:	4	0	4	3	4	3	0	3	2	3		12481.4358	0.0253	0.025
29:	4	0	4	4	4	3	0	3	3	3		12482.4993	0.0323	0.025
30:	4	0	4	4	5	3	0	3	3	4		12482.6962	0.0044	0.025
31:	4	2	3	6	6	3	2	2	5	5		12732.7458	0.0262	0.025

```
 32:  4  2  3  4  4    3  2  2  3  3        12766.4516   0.0111  0.025
 33:  4  2  3  5  6    3  2  2  4  5        12784.0839  -0.0250  0.025
 34:  4  1  3  6  7    3  1  2  5  6        13268.9310  -0.0253  0.025
 35:  4  1  3  5  6    3  1  2  4  5        13281.9175   0.0082  0.025
-------------------------------------------------------------------------------

PARAMETERS IN FIT:

       10000         A  /  /MHz         3459.876(8)                          1
       20000         B  /  /MHz         1740.248(2)                          2
       30000         C  /  /MHz         1453.975(1)                          3
         200        DJ  /  /kHz          [ 0.313634722]                      4
        1100       DJK  /  /kHz          [-0.991728812]                      5
        2000        DK  /  /kHz          [ 1.512226264]                      6
       40100        d1  /  /kHz          [-0.084950527]                      7
   110010000      CHIaa /  /MHz          513.6(1)                            8
  -110020000      CHIbb /  /MHz         -513.6(1)              = -1.00000 *  8
   110030000      CHIcc /  /MHz         -308.0(1)                            9
  -110020000      CHIbb /  /MHz          308.0(1)              = -1.00000 *  9
   110610000      CHIab /  /MHz         -296.(2)                            10
   220010000      CHIaa /  /MHz           -0.6(1)                           11
  -220020000      CHIbb /  /MHz            0.6(1)              = -1.00000 * 11
   220030000      CHIcc /  /MHz            2.3(1)                           12
  -220020000      CHIbb /  /MHz           -2.3(1)              = -1.00000 * 12
   220610000      CHIab /  /MHz           -3.(2)                           13
    10010000        Maa /  /MHz          [ 0.001208931214]                   14
    10020000        Mbb /  /MHz          [ 0.003856086172]                   15
    10030000        Mcc /  /MHz          [ 0.003317184194]                   16

 MICROWAVE AVG =       -0.000251 MHz, IR AVG =        0.00000
 MICROWAVE RMS =        0.016106 MHz, IR RMS =        0.00000
 END OF ITERATION  1 OLD, NEW RMS ERROR=        0.64337         0.64337
```

```
 distinct frequency lines in fit:    35
      distinct parameters of fit:     9

for standard errors previous errors are multiplied by:   0.746463

PARAMETERS IN FIT WITH STANDARD ERRORS ON THOSE THAT ARE FITTED:

       10000         A  /  /MHz         3459.876(6)                          1
       20000         B  /  /MHz         1740.248(2)                          2
       30000         C  /  /MHz         1453.975(1)                          3
         200        DJ  /  /kHz          [ 0.313634722]                      4
        1100       DJK  /  /kHz          [-0.991728812]                      5
        2000        DK  /  /kHz          [ 1.512226264]                      6
       40100        d1  /  /kHz          [-0.084950527]                      7
   110010000      CHIaa /  /MHz          513.65(8)                           8
  -110020000      CHIbb /  /MHz         -513.65(8)             = -1.00000 *  8
   110030000      CHIcc /  /MHz         -308.0(1)                            9
  -110020000      CHIbb /  /MHz          308.0(1)              = -1.00000 *  9
   110610000      CHIab /  /MHz         -296.(1)                            10
   220010000      CHIaa /  /MHz           -0.66(9)                          11
  -220020000      CHIbb /  /MHz            0.66(9)            = -1.00000 * 11
   220030000      CHIcc /  /MHz            2.33(7)                          12
  -220020000      CHIbb /  /MHz           -2.33(7)            = -1.00000 * 12
   220610000      CHIab /  /MHz           -3.(2)                           13
    10010000        Maa /  /MHz          [ 0.001208931214]                   14
    10020000        Mbb /  /MHz          [ 0.003856086172]                   15
    10030000        Mcc /  /MHz          [ 0.003317184194]                   16

 CORRELATION COEFFICIENTS, C.ij:

          A  /     B  /     C  /     CHIaa /  CHIcc /  CHIab /  CHIaa /  CHIcc /

A  /        1.0000
```

```
B  /        0.0047   1.0000
C  /       -0.0500  -0.7164   1.0000
CHIaa /    -0.1574  -0.2393   0.0007   1.0000
CHIcc /     0.2066   0.1607  -0.0047  -0.4003   1.0000
CHIab /     0.0538   0.4000  -0.1056  -0.3780   0.3610   0.0000
CHIaa /    -0.1149   0.2023  -0.2788   0.1016  -0.0565  -0.2478   0.0000
CHIcc /     0.0719   0.2707  -0.1491   0.0616  -0.1400  -0.0064   0.2026   0.0000
CHIab /    -0.0936  -0.0860   0.0250   0.0010  -0.1736  -0.0814  -0.0046  -0.0413

           CHIab /

CHIab /     0.0000

 Mean value of |C.ij|, i.ne.j =   0.1569
 Mean value of  C.ij,  i.ne.j =  -0.0389


 Worst fitting lines (obs-calc/error):

     5:    1.8         29:    1.3         18:   -1.1         31:    1.0
    28:    1.0         34:   -1.0         33:   -1.0         24:    0.8
    11:   -0.8          1:   -0.7         19:   -0.7          6:   -0.6
    26:   -0.5         23:    0.5         32:    0.4         12:   -0.4
    25:   -0.4         35:    0.3         27:   -0.3         14:    0.3
     2:   -0.3         22:    0.3         15:   -0.2         20:   -0.2
    16:    0.2         30:    0.2         13:   -0.2         10:   -0.2
    21:    0.1         17:   -0.1          4:   -0.1          7:   -0.1
     3:    0.1          8:    0.0          9:    0.0

                                          ------------------------------------
-----------------------------------------/ SPFIT output reformatted with PIFORM



-------------------------------------------------------------------------------=========
```

TABLE B.8. $C^{79}BrF_2{}^{13}CN$ Transitions Measured in MHz

											obs	o-c	error	blends o-c	blends wt	Notes
1:	3	1	3	5	5	2	1	2	4	4	9054.0359	-0.0260	0.025			
2:	3	1	3	5	6	2	1	2	4	5	9054.2025	0.0416	0.025			
3:	3	1	3	3	4	2	1	2	2	3	9089.7630	-0.0230	0.025			
4:	3	0	3	5	5	2	0	2	4	4	9380.1049	-0.0060	0.025			
5:	3	0	3	5	6	2	0	2	4	5	9380.2749	0.0192	0.025			
6:	3	0	3	3	3	2	0	2	2	2	9411.1087	0.0392	0.025			
7:	3	1	2	2	3	2	1	1	1	2	9900.4246	-0.0135	0.025			
8:	3	1	2	4	5	2	1	1	3	4	9935.4281	0.0074	0.025			
9:	3	1	2	4	4	2	1	1	3	3	9935.5479	-0.0288	0.025			
10:	4	0	4	6	6	3	0	3	5	5	12379.5253	-0.0312	0.025			
11:	4	0	4	6	7	3	0	3	5	6	12379.7322	0.0046	0.025			
12:	4	1	3	6	5	3	1	2	5	4	13171.2022	0.0190	0.025			

PARAMETERS IN FIT:

10000	A	/	/MHz	3453.0(2)		1
20000	B	/	/MHz	1727.078(3)		2
30000	C	/	/MHz	1443.696(4)		3
200	DJ	/	/kHz	[0.298865846]		4
1100	DJK	/	/kHz	[-0.98019978]		5
2000	DK	/	/kHz	[1.769141994]		6
40100	d1	/	/kHz	[-0.086059907]		7
110010000	CHIaa	/	/MHz	511.5(6)		8
-110020000	CHIbb	/	/MHz	-511.5(6)	= -1.00000 *	8
110030000	CHIcc	/	/MHz	-307.7(3)		9

```
  -110020000      CHIbb /  /MHz          307.7(3)              = -1.00000 *  9
   110610000      CHIab /  /MHz        [-296.831552385999]                   10
   220010000      CHIaa /  /MHz           -0.1(1)                            11
  -220020000      CHIbb /  /MHz            0.1(1)              = -1.00000 * 11
   220030000      CHIcc /  /MHz            2.0(2)                            12
  -220020000      CHIbb /  /MHz           -2.0(2)              = -1.00000 * 12
   220610000      CHIab /  /MHz          [-3.521379935]                      13
    10010000        Maa /  /MHz          [ 0.001208931214]                   14
    10020000        Mbb /  /MHz          [ 0.003856086172]                   15
    10030000        Mcc /  /MHz          [ 0.003317184194]                   16

MICROWAVE AVG =        0.000210 MHz, IR AVG =        0.00000
MICROWAVE RMS =        0.024694 MHz, IR RMS =        0.00000
END OF ITERATION  1 OLD, NEW RMS ERROR=        0.98774         0.98774

 distinct frequency lines in fit:    12
      distinct parameters of fit:     7

for standard errors previous errors are multiplied by:   1.530200

PARAMETERS IN FIT WITH STANDARD ERRORS ON THOSE THAT ARE FITTED:

       10000         A  /  /MHz         3453.0(3)                           1
       20000         B  /  /MHz         1727.078(5)                         2
       30000         C  /  /MHz         1443.696(6)                         3
         200        DJ  /  /kHz          [ 0.298865846]                     4
        1100       DJK  /  /kHz          [-0.98019978]                      5
        2000        DK  /  /kHz          [ 1.769141994]                     6
       40100        d1  /  /kHz          [-0.086059907]                     7
   110010000      CHIaa /  /MHz          511.(1)                            8
  -110020000      CHIbb /  /MHz         -511.(1)              = -1.00000 *  8
   110030000      CHIcc /  /MHz         -307.7(5)                           9
  -110020000      CHIbb /  /MHz          307.7(5)             = -1.00000 *  9
```

```
    110610000      CHIab /  /MHz        [-296.831552385999]                  10
    220010000      CHIaa /  /MHz           -0.1(2)                           11
   -220020000      CHIbb /  /MHz            0.1(2)              = -1.00000 * 11
    220030000      CHIcc /  /MHz            2.0(3)                           12
   -220020000      CHIbb /  /MHz           -2.0(3)              = -1.00000 * 12
    220610000      CHIab /  /MHz          [-3.521379935]                     13
     10010000        Maa /  /MHz          [ 0.001208931214]                  14
     10020000        Mbb /  /MHz          [ 0.003856086172]                  15
     10030000        Mcc /  /MHz          [ 0.003317184194]                  16

 CORRELATION COEFFICIENTS, C.ij:

           A  /     B  /     C  /     CHIaa /  CHIcc /  CHIaa /  CHIcc /

A  /        1.0000
B  /        0.3082   1.0000
C  /       -0.8124  -0.6181   1.0000
CHIaa /    -0.5294  -0.5109   0.5166   0.0000
CHIcc /    -0.5067  -0.4064   0.4188   0.6115   0.0000
CHIaa /     0.1588   0.1646  -0.2484  -0.4269  -0.0377   0.0000
CHIcc /    -0.1096  -0.2849   0.2144   0.4100   0.4710  -0.2970   0.0000

 Mean value of |C.ij|, i.ne.j =   0.3839
 Mean value of  C.ij,  i.ne.j =  -0.0721


 Worst fitting lines (obs-calc/error):

     2:    1.7          6:    1.6         10:   -1.2          9:   -1.2
     1:   -1.0          3:   -0.9          5:    0.8         12:    0.8
     7:   -0.5          8:    0.3          4:   -0.2         11:    0.2
                                          ---obs---------o-c-----error-----blends     Notes
_____________________________________/ SPFIT output reformatted with oPIFORM c  wt
```

TABLE B.9. $^{13}C^{81}BrF_2CN$ Transitions Measured in MHz

1:	3	1	3	2	3	2	1	2	1	2	9049.6259	0.0427	0.025
2:	3	1	3	4	5	2	1	2	3	4	9073.6222	-0.0213	0.025
3:	3	1	3	3	4	2	1	2	2	3	9076.6119	-0.0100	0.025
4:	3	0	3	5	5	2	0	2	4	4	9370.6796	0.0144	0.025
5:	3	0	3	5	6	2	0	2	4	5	9370.8500	-0.0119	0.025
6:	3	0	3	4	5	2	0	2	3	4	9371.7527	-0.0211	0.025
7:	3	0	3	3	4	2	0	2	2	3	9397.1115	0.0307	0.025
8:	3	0	3	2	3	2	0	2	1	2	9397.5058	-0.0222	0.025
9:	3	1	2	5	5	2	1	1	4	4	9891.5460	-0.0179	0.025
10:	3	1	2	5	6	2	1	1	4	5	9891.5778	-0.0464	0.025
11:	3	1	2	3	4	2	1	1	2	3	9916.4616	0.0061	0.025
12:	3	1	2	4	5	2	1	1	3	4	9918.6373	0.0011	0.025
13:	3	1	2	4	4	2	1	1	3	3	9918.7500	-0.0010	0.025
14:	4	0	4	6	6	3	0	3	5	5	12367.7362	0.0293	0.025
15:	4	0	4	6	7	3	0	3	5	6	12367.9196	-0.0077	0.025
16:	4	0	4	4	4	3	0	3	3	3	12380.6447	-0.0267	0.025
17:	4	1	3	6	7	3	1	2	5	6	13154.6843	0.0123	0.030
18:	4	1	3	5	6	3	1	2	4	5	13165.5513	0.0206	0.025
19:	4	1	3	4	5	3	1	2	3	4	13169.7895	-0.0055	0.025
20:	4	1	3	4	4	3	1	2	3	3	13169.8675	0.0278	0.025

PARAMETERS IN FIT:

10000	A	/	/MHz	3456.4(2)	1
20000	B	/	/MHz	1724.436(2)	2
30000	C	/	/MHz	1442.370(5)	3
200	DJ	/	/kHz	[0.311773389]	4

```
        1100       DJK  /  /kHz          [-0.913210067]                      5
        2000        DK  /  /kHz          [ 2.948099055]                      6
       40100        d1  /  /kHz          [-0.088466204]                      7
   110010000      CHIaa /  /MHz          430.6(2)                            8
  -110020000      CHIbb /  /MHz         -430.6(2)              = -1.00000 *  8
   110030000      CHIcc /  /MHz         -256.5(2)                           9
  -110020000      CHIbb /  /MHz          256.5(2)              = -1.00000 *  9
   110610000      CHIab /  /MHz         -246.(3)                           10
   220010000      CHIaa /  /MHz           -0.9(1)                          11
  -220020000      CHIbb /  /MHz            0.9(1)              = -1.00000 * 11
   220030000      CHIcc /  /MHz            2.9(2)                          12
  -220020000      CHIbb /  /MHz           -2.9(2)              = -1.00000 * 12
   220610000      CHIab /  /MHz          [-3.126505099]                     13
    10010000        Maa /  /MHz          [ 0.000413943179]                  14
    10020000        Mbb /  /MHz          [ 0.004557606488]                  15
    10030000        Mcc /  /MHz          [ 0.004803663089]                  16

MICROWAVE AVG =       -0.000334 MHz, IR AVG =        0.00000
MICROWAVE RMS =        0.022548 MHz, IR RMS =        0.00000
END OF ITERATION  1 OLD, NEW RMS ERROR=        0.89982         0.89973

 distinct frequency lines in fit:    20
      distinct parameters of fit:     8

for standard errors previous errors are multiplied by:   1.161546

PARAMETERS IN FIT WITH STANDARD ERRORS ON THOSE THAT ARE FITTED:

       10000         A  /  /MHz         3456.4(3)                          1
       20000         B  /  /MHz         1724.436(2)                        2
       30000         C  /  /MHz         1442.370(6)                        3
         200        DJ  /  /kHz          [ 0.311773389]                     4
        1100       DJK  /  /kHz          [-0.913210067]                     5
```

```
      2000        DK  /  /kHz          [ 2.948099055]                      6
     40100        d1  /  /kHz          [-0.088466204]                      7
 110010000      CHIaa /  /MHz          430.6(2)                            8
-110020000      CHIbb /  /MHz         -430.6(2)              = -1.00000 *  8
 110030000      CHIcc /  /MHz         -256.5(3)                           9
-110020000      CHIbb /  /MHz          256.5(3)              = -1.00000 *  9
 110610000      CHIab /  /MHz         -246.(4)                           10
 220010000      CHIaa /  /MHz           -0.9(2)                          11
-220020000      CHIbb /  /MHz            0.9(2)              = -1.00000 * 11
 220030000      CHIcc /  /MHz            2.9(2)                          12
-220020000      CHIbb /  /MHz           -2.9(2)              = -1.00000 * 12
 220610000      CHIab /  /MHz          [-3.126505099]                     13
  10010000        Maa /  /MHz          [ 0.000413943179]                  14
  10020000        Mbb /  /MHz          [ 0.004557606488]                  15
  10030000        Mcc /  /MHz          [ 0.004803663089]                  16

 Worst fitting lines (obs-calc/error):

   10:   -1.9          1:    1.7          7:    1.2         14:    1.2
   20:    1.1         16:   -1.1          8:   -0.9          2:   -0.9
    6:   -0.8         18:    0.8          9:   -0.7          4:    0.6
    5:   -0.5         17:    0.4          3:   -0.4         15:   -0.3
   11:    0.2         19:   -0.2         12:    0.0         13:    0.0

-------------------------------------------------------------------------------------------=========
                                                obs         o-c     error     blends     Notes
                                                                                o-c      wt
-------------------------------------------------------------------------------------------=========
  1:  3  1  3  2  3    2  1  2  1  2          9049.6259   0.0423  0.025
  2:  3  1  3  4  5    2  1  2  3  4          9073.6222  -0.0216  0.025
  3:  3  1  3  3  4    2  1  2  2  3          9076.6119  -0.0103  0.025
  4:  3  0  3  5  5    2  0  2  4  4          9370.6796   0.0140  0.025
  5:  3  0  3  5  6    2  0  2  4  5          9370.8500  -0.0120  0.025
```

```
  6:  3  0  3  4  5    2  0  2  3  4        9371.7527  -0.0212  0.025
  7:  3  0  3  3  4    2  0  2  2  3        9397.1115   0.0308  0.025
  8:  3  0  3  2  3    2  0  2  1  2        9397.5058  -0.0220  0.025
  9:  3  1  2  5  5    2  1  1  4  4        9891.5460  -0.0185  0.025
 10:  3  1  2  5  6    2  1  1  4  5        9891.5778  -0.0465  0.025
 11:  3  1  2  3  4    2  1  1  2  3        9916.4616   0.0061  0.025
 12:  3  1  2  4  5    2  1  1  3  4        9918.6373   0.0010  0.025
 13:  3  1  2  4  4    2  1  1  3  3        9918.7500  -0.0015  0.025
 14:  4  0  4  6  6    3  0  3  5  5       12367.7362   0.0289  0.025
 15:  4  0  4  6  7    3  0  3  5  6       12367.9196  -0.0078  0.025
 16:  4  0  4  4  4    3  0  3  3  3       12380.6447  -0.0275  0.025
 17:  4  1  3  6  7    3  1  2  5  6       13154.6843   0.0123  0.030
 18:  4  1  3  5  6    3  1  2  4  5       13165.5513   0.0205  0.025
 19:  4  1  3  4  5    3  1  2  3  4       13169.7895  -0.0055  0.025
 20:  4  1  3  4  4    3  1  2  3  3       13169.8675   0.0275  0.025
```

PARAMETERS IN FIT:

```
       10000         A  /  /MHz        3456.4(2)                          1
       20000         B  /  /MHz        1724.436(2)                        2
       30000         C  /  /MHz        1442.370(5)                        3
         200        DJ  /  /kHz         [ 0.311773389]                    4
        1100       DJK  /  /kHz         [-0.913210067]                    5
        2000        DK  /  /kHz         [ 2.948099055]                    6
       40100        d1  /  /kHz         [-0.088466204]                    7
   110010000      CHIaa /  /MHz         430.6(2)                          8
  -110020000      CHIbb /  /MHz        -430.6(2)              = -1.00000 *  8
   110030000      CHIcc /  /MHz        -256.5(2)                         9
  -110020000      CHIbb /  /MHz         256.5(2)              = -1.00000 *  9
   110610000      CHIab /  /MHz        -246.(3)                          10
   220010000      CHIaa /  /MHz          -0.9(1)                         11
  -220020000      CHIbb /  /MHz           0.9(1)              = -1.00000 * 11
```

```
   220030000      CHIcc /  /MHz           2.9(2)                          12
  -220020000      CHIbb /  /MHz          -2.9(2)              = -1.00000 * 12
   220610000      CHIab /  /MHz         [-3.126505099]                    13
    10010000        Maa /  /MHz         [ 0.000413943179]                 14
    10020000        Mbb /  /MHz         [ 0.004557606488]                 15
    10030000        Mcc /  /MHz         [ 0.004803663089]                 16

MICROWAVE AVG =       -0.000557 MHz, IR AVG =        0.00000
MICROWAVE RMS =        0.022545 MHz, IR RMS =        0.00000
END OF ITERATION  2 OLD, NEW RMS ERROR=        0.89973         0.89973

 distinct frequency lines in fit:    20
      distinct parameters of fit:     8

for standard errors previous errors are multiplied by:   1.161546

PARAMETERS IN FIT WITH STANDARD ERRORS ON THOSE THAT ARE FITTED:

       10000         A  /  /MHz        3456.4(3)                         1
       20000         B  /  /MHz        1724.436(2)                       2
       30000         C  /  /MHz        1442.370(6)                       3
         200        DJ  /  /kHz         [ 0.311773389]                   4
        1100       DJK  /  /kHz         [-0.913210067]                   5
        2000        DK  /  /kHz         [ 2.948099055]                   6
       40100        d1  /  /kHz         [-0.088466204]                   7
   110010000      CHIaa /  /MHz         430.6(2)                         8
  -110020000      CHIbb /  /MHz        -430.6(2)              = -1.00000 *  8
   110030000      CHIcc /  /MHz        -256.5(3)                         9
  -110020000      CHIbb /  /MHz         256.5(3)              = -1.00000 *  9
   110610000      CHIab /  /MHz        -246.(4)                         10
   220010000      CHIaa /  /MHz          -0.9(2)                        11
  -220020000      CHIbb /  /MHz           0.9(2)              = -1.00000 * 11
   220030000      CHIcc /  /MHz           2.9(2)                         12
```

```
   -220020000      CHIbb /  /MHz          -2.9(2)              = -1.00000 * 12
    220610000      CHIab /  /MHz         [-3.126505099]                     13
     10010000        Maa /  /MHz         [ 0.000413943179]                  14
     10020000        Mbb /  /MHz         [ 0.004557606488]                  15
     10030000        Mcc /  /MHz         [ 0.004803663089]                  16

 CORRELATION COEFFICIENTS, C.ij:

           A  /     B  /     C  /     CHIaa /  CHIcc /  CHIab /  CHIaa /  CHIcc /

A  /        1.0000
B  /        0.0243   1.0000
C  /       -0.9174  -0.2634   1.0000
CHIaa /     0.1565  -0.2063  -0.1892   1.0000
CHIcc /    -0.4120   0.0112   0.4434  -0.5539   0.0000
CHIab /    -0.4509   0.3279   0.4241  -0.1514   0.2061   0.0000
CHIaa /    -0.4427  -0.1735   0.4764   0.0776   0.1234   0.1887   0.0000
CHIcc /     0.5334   0.1382  -0.4971  -0.1019   0.0471  -0.0726  -0.5826   0.0000

 Mean value of |C.ij|, i.ne.j =   0.2926
 Mean value of  C.ij,  i.ne.j =  -0.0656


 Worst fitting lines (obs-calc/error):

    10:   -1.9          1:    1.7          7:    1.2         14:    1.2
    20:    1.1         16:   -1.1          8:   -0.9          2:   -0.9
     6:   -0.8         18:    0.8          9:   -0.7          4:    0.6
     5:   -0.5          3:   -0.4         17:    0.4         15:   -0.3
    11:    0.2         19:   -0.2         13:   -0.1         12:    0.0
                                          ------------------------------------
_________________________________________/ SPFIT output reformatted with PIFORM
```

TABLE B.10. $C^{81}BrF_2{}^{13}CN$ Transitions Measured in MHz

											obs	o-c	error	blends o-c	blends wt	Notes
1:	3	1	3	5	5	2	1	2	4	4	8981.4927	0.0003	0.025			
2:	3	1	3	5	6	2	1	2	4	5	8981.6529	0.0084	0.025			
3:	3	1	3	2	3	2	1	2	1	2	8984.7042	-0.0092	0.025			
4:	3	1	3	4	5	2	1	2	3	4	9008.3930	0.0105	0.025			
5:	3	1	3	3	4	2	1	2	2	3	9011.5252	0.0230	0.030			
6:	3	0	3	5	5	2	0	2	4	4	9303.6873	-0.0112	0.025			
7:	3	0	3	5	6	2	0	2	4	5	9303.8527	0.0154	0.025			
8:	3	0	3	4	5	2	0	2	3	4	9304.8975	-0.0211	0.025			
9:	3	0	3	3	4	2	0	2	2	3	9329.9058	-0.0107	0.025			
10:	3	0	3	2	3	2	0	2	1	2	9330.2073	0.0093	0.025			
11:	3	2	2	5	6	2	2	1	4	5	9400.5821	-0.0145	0.025			
12:	3	2	1	5	6	2	2	0	4	5	9522.4914	0.0103	0.025			
13:	3	1	2	2	3	2	1	1	1	2	9815.9473	0.0154	0.025			
14:	3	1	2	5	5	2	1	1	4	4	9818.2296	0.0082	0.025			
15:	3	1	2	3	4	2	1	1	2	3	9842.7182	-0.0109	0.030			
16:	3	1	2	4	3	2	1	1	3	2	9845.1248	-0.0055	0.025			
17:	3	1	2	4	4	2	1	1	3	3	9845.1594	-0.0153	0.025			
18:	4	1	4	6	7	3	1	3	5	6	11953.0604	-0.0184	0.025			
19:	4	0	4	6	6	3	0	3	5	5	12280.8979	-0.0247	0.025			
20:	4	0	4	6	7	3	0	3	5	6	12281.0840	0.0110	0.025			
21:	4	0	4	5	5	3	0	3	4	4	12282.2190	0.0255	0.025			
22:	4	0	4	5	6	3	0	3	4	5	12282.3658	0.0021	0.025			
23:	4	1	3	5	6	3	1	2	4	5	13068.6421	0.0053	0.025			

PARAMETERS IN FIT:

10000	A	/	/MHz	3450.2(1)		1
20000	B	/	/MHz	1711.405(3)		2
30000	C	/	/MHz	1432.154(2)		3
200	DJ	/	/kHz	[0.311773389]		4
1100	DJK	/	/kHz	[-0.913210067]		5
2000	DK	/	/kHz	[2.948099055]		6
40100	d1	/	/kHz	[-0.088466204]		7
110010000	CHIaa	/	/MHz	426.6(1)		8
-110020000	CHIbb	/	/MHz	-426.6(1)	= -1.00000 *	8
110030000	CHIcc	/	/MHz	-257.5(2)		9
-110020000	CHIbb	/	/MHz	257.5(2)	= -1.00000 *	9
110610000	CHIab	/	/MHz	-251.(2)		10
220010000	CHIaa	/	/MHz	-0.9(1)		11
-220020000	CHIbb	/	/MHz	0.9(1)	= -1.00000 *	11
220030000	CHIcc	/	/MHz	2.0(2)		12
-220020000	CHIbb	/	/MHz	-2.0(2)	= -1.00000 *	12
220610000	CHIab	/	/MHz	[-3.126505099]		13
10010000	Maa	/	/MHz	[0.000413943179]		14
10020000	Mbb	/	/MHz	[0.004557606488]		15
10030000	Mcc	/	/MHz	[0.004803663089]		16

MICROWAVE AVG = 0.000149 MHz, IR AVG = 0.00000

MICROWAVE RMS = 0.014120 MHz, IR RMS = 0.00000

END OF ITERATION 1 OLD, NEW RMS ERROR= 0.55241 0.55241

distinct frequency lines in fit: 23

distinct parameters of fit: 8

for standard errors previous errors are multiplied by: 0.684037

PARAMETERS IN FIT WITH STANDARD ERRORS ON THOSE THAT ARE FITTED:

10000	A	/	/MHz	3450.2(1)		1
20000	B	/	/MHz	1711.405(2)		2
30000	C	/	/MHz	1432.154(1)		3
200	DJ	/	/kHz	[0.311773389]		4
1100	DJK	/	/kHz	[-0.913210067]		5
2000	DK	/	/kHz	[2.948099055]		6
40100	d1	/	/kHz	[-0.088466204]		7
110010000	CHIaa	/	/MHz	426.6(1)		8
-110020000	CHIbb	/	/MHz	-426.6(1)	= -1.00000 *	8
110030000	CHIcc	/	/MHz	-257.5(1)		9
-110020000	CHIbb	/	/MHz	257.5(1)	= -1.00000 *	9
110610000	CHIab	/	/MHz	-251.(2)		10
220010000	CHIaa	/	/MHz	-0.94(9)		11
-220020000	CHIbb	/	/MHz	0.94(9)	= -1.00000 *	11
220030000	CHIcc	/	/MHz	2.0(1)		12
-220020000	CHIbb	/	/MHz	-2.0(1)	= -1.00000 *	12
220610000	CHIab	/	/MHz	[-3.126505099]		13
10010000	Maa	/	/MHz	[0.000413943179]		14
10020000	Mbb	/	/MHz	[0.004557606488]		15
10030000	Mcc	/	/MHz	[0.004803663089]		16

CORRELATION COEFFICIENTS, C.ij:

	A /	B /	C /	CHIaa /	CHIcc /	CHIab /	CHIaa /	CHIcc /
A /	1.0000							
B /	0.0823	1.0000						
C /	-0.7686	-0.4870	1.0000					
CHIaa /	-0.3624	-0.0732	0.3327	1.0000				
CHIcc /	0.1482	0.1404	-0.1318	-0.4634	0.0000			
CHIab /	-0.1564	0.5502	-0.0002	0.0002	0.2134	0.0000		
CHIaa /	-0.2747	0.0755	0.2614	0.0154	-0.0110	0.0476	0.0000	

```
CHIcc /     0.3859   0.1892  -0.3907  -0.2823   0.3876   0.1019  -0.4283   0.0000

 Mean value of |C.ij|, i.ne.j =   0.2415
 Mean value of  C.ij,  i.ne.j =  -0.0321



 Worst fitting lines (obs-calc/error):

    21:    1.0         19:   -1.0          8:   -0.8          5:    0.8
    18:   -0.7          7:    0.6         13:    0.6         17:   -0.6
    11:   -0.6          6:   -0.4         20:    0.4          9:   -0.4
     4:    0.4         12:    0.4         10:    0.4          3:   -0.4
    15:   -0.4          2:    0.3         14:    0.3         16:   -0.2
    23:    0.2         22:    0.1          1:    0.0

                                          ------------------------------------
-----------------------------------------/ SPFIT output reformatted with PIFORM
```

TABLE B.11. Bromodifluoroacetonitrile Calculated Structure and Nuclear Electric Quadrupole Coupling Tensors

```
N-14 in Br-79 species: ~re MP2/aug-cc-pVTZ structure
------------------ INPUT ----------------
Isotopic mass and Gaussian x,y,z coordinates
78.918338 0.509772 -1.135552 0.000000
12.000000 0.004420 0.721206 0.000000
12.000000 -1.459698 0.843297 0.000000
14.003074 -2.612320 0.936697 0.000000
18.998403 0.509772 1.322245 1.079381
18.998403 0.509772 1.322245 -1.079381
Gaussian Electric Field Gradient Tensor
x y z
x 0.996682 -0.126950 0.000000
```

```
y -0.126950 -0.454997 0.000000

z 0.000000 0.000000 -0.541684

Xij = eqQeff*(-qij) where eqQeff = 4.558608

------------------ OUTPUT -------------------

Rotational Constants (MHz)

A = 3480.530397

B = 1745.440399

C = 1459.760694

Atomic coordinates in a,b,c system

a b c

-1.157195 -0.259966 0.000000

0.639445 0.429248 0.000000

1.602932 -0.679914 0.000000

2.359243 -1.554702 0.000000

0.825825 1.192066 1.079381

0.825825 1.192066 -1.079381

efg tensor in a,b,c system

a b c

a 0.172705 -0.730293 0.000000

b -0.730293 0.368980 0.000000

c 0.000000 0.000000 -0.541684

nqcc tensor in a,b,c system

a b c

a -0.787294 3.329121 0.000000

b 3.329121 -1.682036 0.000000

c 0.000000 0.000000 2.469325

-----------------------------------------

Principal efg: qii where i=x,y,z
```

```
xx = -0.466015 yy = -0.541684 zz = 1.007700
Principal nqcc: Xii where i=x,y,z
xx = 2.124381 yy = 2.469325 zz = -4.593710
Eigenvectors, direction cosines
x y z
a 0.752723 0.000000 -0.658337
b 0.658337 0.000000 0.752723
c 0.000000 1.000000 0.000000
Rotation Angles (degrees)
a 41.1732 90.0000 131.1732
b 48.8268 90.0000 41.1732
c 90.0000 0.0000 90.0000
(Xxx-Xyy)/Xzz = 0.075091
------------------- fini ------------------
Br-79
------------------ INPUT ---------------
Isotopic mass and Gaussian x,y,z coordinates
78.918338 0.509772 -1.135552 0.000000
12.000000 0.004420 0.721206 0.000000
12.000000 -1.459698 0.843297 0.000000
14.003074 -2.612320 0.936697 0.000000
18.998403 0.509772 1.322245 1.079381
18.998403 0.509772 1.322245 -1.079381
Gaussian Electric Field Gradient Tensor
x y z
x 3.012683 3.338841 0.000000
y 3.338841 -7.013265 0.000000
z 0.000000 0.000000 4.000582
```

```
Xij = eqQeff*(-qij) where eqQeff = 77.628160
------------------ OUTPUT -------------------
Rotational Constants (MHz)
A = 3480.530397
B = 1745.440399
C = 1459.760694
Atomic coordinates in a,b,c system
a b c
-1.157195 -0.259966 0.000000
0.639445 0.429248 0.000000
1.602932 -0.679914 0.000000
2.359243 -1.554702 0.000000
0.825825 1.192066 1.079381
0.825825 1.192066 -1.079381
efg tensor in a,b,c system
a b c
a -6.696929 -3.770857 0.000000
b -3.770857 2.696347 0.000000
c 0.000000 0.000000 4.000582
nqcc tensor in a,b,c system
a b c
a 519.870243 292.724696 0.000000
b 292.724696 -209.312423 0.000000
c 0.000000 0.000000 -310.557820
-------------------------------------------
Principal efg: qii where i=x,y,z
xx = 4.000582 yy = 4.022812 zz = -8.023394
Principal nqcc: Xii where i=x,y,z
```

```
xx = -310.557820 yy = -312.283479 zz = 622.841299
Eigenvectors, direction cosines
x y z
a 0.000000 -0.331835 0.943337
b 0.000000 0.943337 0.331835
c 1.000000 0.000000 0.000000
Rotation Angles (degrees)
a 90.0000 109.3802 19.3802
b 90.0000 19.3802 70.6198
c 0.0000 90.0000 90.0000
(Xxx-Xyy)/Xzz = 0.002771
------------------- fini ------------------

N-14 in Br-81 species: ~re MP2/aug-cc-pVTZ structure
------------------ INPUT ----------------
Isotopic mass and Gaussian x,y,z coordinates
80.916291 0.509772 -1.135552 0.000000
12.000000 0.004420 0.721206 0.000000
12.000000 -1.459698 0.843297 0.000000
14.003074 -2.612320 0.936697 0.000000
18.998403 0.509772 1.322245 1.079381
18.998403 0.509772 1.322245 -1.079381
Gaussian Electric Field Gradient Tensor
x y z
x 0.996682 -0.126950 0.000000
y -0.126950 -0.454997 0.000000
z 0.000000 0.000000 -0.541684
Xij = eqQeff*(-qij) where eqQeff = 4.558608
```

```
------------------ OUTPUT -------------------
Rotational Constants (MHz)
A = 3477.395277
B = 1729.647114
C = 1448.154349
Atomic coordinates in a,b,c system
a b c
-1.143488 -0.252038 0.000000
0.655921 0.429912 0.000000
1.614919 -0.683135 0.000000
2.367689 -1.560972 0.000000
0.845383 1.191970 1.079381
0.845383 1.191970 -1.079381
efg tensor in a,b,c system
a b c
a 0.166806 -0.729476 0.000000
b -0.729476 0.374879 0.000000
c 0.000000 0.000000 -0.541684
nqcc tensor in a,b,c system
a b c
a -0.760404 3.325397 0.000000
b 3.325397 -1.708925 0.000000
c 0.000000 0.000000 2.469325
--------------------------------------------
Principal efg: qii where i=x,y,z
xx = -0.466015 yy = -0.541684 zz = 1.007700
Principal nqcc: Xii where i=x,y,z
xx = 2.124381 yy = 2.469325 zz = -4.593710
```

```
Eigenvectors, direction cosines
x y z
a 0.755377 0.000000 -0.655290
b 0.655290 0.000000 0.755377
c 0.000000 1.000000 0.000000
Rotation Angles (degrees)
a 40.9417 90.0000 130.9417
b 49.0583 90.0000 40.9417
c 90.0000 0.0000 90.0000
(Xxx-Xyy)/Xzz = 0.075091
------------------- fini ------------------
Br-81
------------------ INPUT ----------------
Isotopic mass and Gaussian x,y,z coordinates
80.916291 0.509772 -1.135552 0.000000
12.000000 0.004420 0.721206 0.000000
12.000000 -1.459698 0.843297 0.000000
14.003074 -2.612320 0.936697 0.000000
18.998403 0.509772 1.322245 1.079381
18.998403 0.509772 1.322245 -1.079381
Gaussian Electric Field Gradient Tensor
x y z
x 3.012683 3.338841 0.000000
y 3.338841 -7.013265 0.000000
z 0.000000 0.000000 4.000582
Xij = eqQeff*(-qij) where eqQeff = 64.856040
------------------ OUTPUT -------------------
Rotational Constants (MHz)
```

```
A = 3477.395277
B = 1729.647114
C = 1448.154349
Atomic coordinates in a,b,c system
a b c
-1.143488 -0.252038 0.000000
0.655921 0.429912 0.000000
1.614919 -0.683135 0.000000
2.367689 -1.560972 0.000000
0.845383 1.191970 1.079381
0.845383 1.191970 -1.079381
efg tensor in a,b,c system
a b c
a -6.727249 -3.732778 0.000000
b -3.732778 2.726667 0.000000
c 0.000000 0.000000 4.000582
nqcc tensor in a,b,c system
a b c
a 436.302743 242.093218 0.000000
b 242.093218 -176.840837 0.000000
c 0.000000 0.000000 -259.461906
-----------------------------------------
Principal efg: qii where i=x,y,z
xx = 4.000582 yy = 4.022812 zz = -8.023394
Principal nqcc: Xii where i=x,y,z
xx = -259.461906 yy = -260.903644 zz = 520.365550
Eigenvectors, direction cosines
x y z
```

```
a 0.000000 -0.328021 0.944670

b 0.000000 0.944670 0.328021

c 1.000000 0.000000 0.000000

Rotation Angles (degrees)

a 90.0000 109.1487 19.1487

b 90.0000 19.1487 70.8513

c 0.0000 90.0000 90.0000

(Xxx-Xyy)/Xzz = 0.002771

------------------- fini ------------------
```

TABLE B.12. Kraitchman Substitution Calculations for Bromodifluoroacetonitrile

```
 ---------------------------------------------------------------------------
|                                                                           |
|    KRA  -  SINGLE ISOTOPIC SUBSTITUTION - Various permutations            |
|            of Kraitchman's equations for symmetric/asymmetric tops        |
|___________________________________________________________________________|
 version 14c.X.2002                                          Zbigniew KISIEL

-----------------------------------------------------------------------------
    Brodiflo Kraitchman
-----------------------------------------------------------------------------


  parent species


Planar calculation will be made from I.a and I.b

-----------------------------------------------------------------------------


  Br81

-----------------------------------------------------------------------------


======>  The common species:

  X,  Y,  Z  =        3464.12100000       1742.53170000       1456.34210000
 dX, dY, dZ  =           0.00100000          0.00030000          0.00030000
```

```
 IX, IY, IZ  =         145.88955467        290.02575391        347.01947434
dIX,dIY,dIZ  =           0.00004211          0.00004993          0.00007148
Mass         =   154.91821650

======>  The isotopic species:

  X,  Y,  Z  =        3460.98220000       1726.80140000       1444.78630000
 dX, dY, dZ  =           0.00040000          0.00030000          0.00020000
 IX, IY, IZ  =         146.02186339        292.66774396        349.79503197
dIX,dIY,dIZ  =           0.00001688          0.00005085          0.00004842
Mass change =     1.99795290
Total mass  =   156.91616940

  KRAITCHMAN'S RESULTS

     PLANAR:    a=   1.15679  +-0.00002    b=   0.26135  +-0.00004
+Costain err.   a=   1.15679  +-0.00130    b=   0.26135  +-0.00574

  NONPLANAR:    a=   1.15693  +-0.00001    b=   0.26198  +-0.00006
                c=   0.01800*i+-0.00086                          R= 1.18609
+Costain err.   a=   1.15693  +-0.00130    b=   0.26198  +-0.00573  +-0.00219
                c=   0.01800*i+-0.08333

--------------------------------------------------------------------------------

  1C13

--------------------------------------------------------------------------------
```

```
======>  The common species:

  X,  Y,  Z  =        3464.12100000       1742.53170000       1456.34210000
 dX, dY, dZ  =           0.00100000          0.00030000          0.00030000
 IX, IY, IZ  =         145.88955467        290.02575391        347.01947434
dIX,dIY,dIZ  =           0.00004211          0.00004993          0.00007148
Mass         =   154.91821650

======>  The isotopic species:

  X,  Y,  Z  =        3459.87600000       1740.24800000       1453.97500000
 dX, dY, dZ  =           0.00600000          0.00200000          0.00100000
 IX, IY, IZ  =         146.06854986        290.40635013        347.58442889
dIX,dIY,dIZ  =           0.00025331          0.00033375          0.00023906
Mass change =     1.00335400
Total mass  =   155.92157050

  KRAITCHMAN'S RESULTS

     PLANAR:    a=   0.61750  +-0.00027    b=   0.42430  +-0.00030
+Costain err.   a=   0.61750  +-0.00244    b=   0.42430  +-0.00355

  NONPLANAR:    a=   0.61967  +-0.00020    b=   0.42748  +-0.00029
                c=   0.05200*i+-0.00239                          R= 0.75101
+Costain err.   a=   0.61967  +-0.00243    b=   0.42748  +-0.00352  +-0.00347
                c=   0.05200*i+-0.02895
```

```
--------------------------------------------------------------------------------

  2C13

--------------------------------------------------------------------------------

======>  The common species:

  X,  Y,  Z  =        3464.12100000       1742.53170000       1456.34210000
 dX, dY, dZ  =           0.00100000          0.00030000          0.00030000
 IX, IY, IZ  =         145.88955467        290.02575391        347.01947434
dIX,dIY,dIZ  =           0.00004211          0.00004993          0.00007148
Mass        =   154.91821650

======>  The isotopic species:

  X,  Y,  Z  =        3453.00000000       1727.07800000       1453.69600000
 dX, dY, dZ  =           0.30000000          0.00500000          0.00600000
 IX, IY, IZ  =         146.35941790        292.62087178        347.65113889
dIX,dIY,dIZ  =           0.01271585          0.00084716          0.00143490
Mass change =     1.00335400
Total mass  =   155.92157050

  KRAITCHMAN'S RESULTS

     PLANAR:    a=   1.61081  +-0.00027    b=   0.69268  +-0.00937
+Costain err.   a=   1.61081  +-0.00097    b=   0.69268  +-0.00962
```

```
  NONPLANAR:     a=    1.17537  +-0.00273    b=    0.86031*i+-0.00369
                 c=    1.10123  +-0.00290                            R= 1.36164
+Costain err.    a=    1.17537  +-0.00302    b=    0.86031*i+-0.00408  +-0.00449
                 c=    1.10123  +-0.00321

--------------------------------------------------------------------------------
--------------------------------------------------------------------------------


   A,   B,   C =           3464.121000         1742.531700         1456.342100
  dA,  dB,  dC =              0.001000            0.000300            0.000300

  IA,  IB,  IC =            145.889536          290.025717          347.019430
 dIA, dIB, dIC =              0.000042            0.000050            0.000071

  PA,  PB,  PC =            245.577806          101.441625           44.447911

Inertial Defect=            -88.895823  +-        0.000097
         Kappa =             -0.714919
      (A+B)/2C =              1.787579
      2A/(B+C) =              2.165838

--------------------------------------------------------------------------------
--------------------------------------------------------------------------------


   A,   B,   C =           3460.982200         1726.801400         1444.786300
  dA,  dB,  dC =              0.000400            0.000300            0.000200
```

```
  IA,  IB,  IC =          146.021845          292.667707          349.794988
dIA, dIB, dIC =            0.000017            0.000051            0.000048

  PA,  PB,  PC =          248.220425          101.574563           44.447282

Inertial Defect=          -88.894564  +-        0.000072
         Kappa =           -0.720250
      (A+B)/2C =            1.795346
      2A/(B+C) =            2.182492

-------------------------------------------------------------------------------
-------------------------------------------------------------------------------


   A,   B,   C =         3459.876000         1727.078000         1442.370000
  dA,  dB,  dC =            0.300000            0.005000            0.006000

  IA,  IB,  IC =          146.068531          292.620835          350.380974
dIA, dIB, dIC =            0.012665            0.000847            0.001458

  PA,  PB,  PC =          248.466639          101.914335           44.154196

Inertial Defect=          -88.308392  +-        0.012777
         Kappa =           -0.717762
      (A+B)/2C =            1.798066
      2A/(B+C) =            2.183267
```

```
--------------------------------------------------------------------------------
--------------------------------------------------------------------------------

   A,   B,   C =          3464.121000        1742.531700        1456.342100
  dA,  dB,  dC =             0.001000           0.000300           0.000300

  IA,  IB,  IC =           145.889536         290.025717         347.019430
 dIA, dIB, dIC =             0.000042           0.000050           0.000071

  PA,  PB,  PC =           245.577806         101.441625          44.447911

Inertial Defect=           -88.895823  +-       0.000097
         Kappa =            -0.714919
      (A+B)/2C =             1.787579
      2A/(B+C) =             2.165838

--------------------------------------------------------------------------------
--------------------------------------------------------------------------------

   A,   B,   C =          3460.982200        1726.801400        1444.786300
  dA,  dB,  dC =             0.000400           0.000300           0.000200

  IA,  IB,  IC =           146.021845         292.667707         349.794988
 dIA, dIB, dIC =             0.000017           0.000051           0.000048

  PA,  PB,  PC =           248.220425         101.574563          44.447282
```

```
Inertial Defect=          -88.894564  +-       0.000072
         Kappa =           -0.720250
      (A+B)/2C =            1.795346
      2A/(B+C) =            2.182492

-------------------------------------------------------------------------------
-------------------------------------------------------------------------------


   A,   B,   C =        3459.876000       1740.248000       1453.975000
  dA,  dB,  dC =           0.006000          0.002000          0.001000

  IA,  IB,  IC =         146.068531        290.406313        347.584385
 dIA, dIB, dIC =           0.000253          0.000334          0.000239

  PA,  PB,  PC =         245.961083        101.623301         44.445230

Inertial Defect=          -88.890460  +-       0.000482
         Kappa =           -0.714569
      (A+B)/2C =            1.788244
      2A/(B+C) =            2.166333

-------------------------------------------------------------------------------
-------------------------------------------------------------------------------


   A,   B,   C =        3453.000000       1727.078000       1443.696000
```

```
  dA,  dB,  dC =          0.100000          0.005000          0.006000

  IA,  IB,  IC =        146.359399        292.620835        350.059158
 dIA, dIB, dIC =          0.004239          0.000847          0.001455

  PA,  PB,  PC =        248.160297        101.898861         44.460538

Inertial Defect=        -88.921076  +-      0.004561
         Kappa =         -0.717930
      (A+B)/2C =          1.794034
      2A/(B+C) =          2.178017
```

```
   A,   B,   C =       3456.400000       1724.436000       1442.370000
  dA,  dB,  dC =          0.300000          0.002000          0.006000

  IA,  IB,  IC =        146.215428        293.069158        350.380974
 dIA, dIB, dIC =          0.012691          0.000340          0.001458

  PA,  PB,  PC =        248.617352        101.763622         44.451806

Inertial Defect=        -88.903612  +-      0.012779
         Kappa =         -0.719899
      (A+B)/2C =          1.795946
      2A/(B+C) =          2.182893
```

```
-------------------------------------------------------------------------------

-------------------------------------------------------------------------------


   A,   B,   C =          3450.200000        1711.405000        1432.154000
  dA,  dB,  dC =             0.100000           0.002000           0.001000

  IA,  IB,  IC =           146.478177         295.300648         352.880351
 dIA, dIB, dIC =             0.004245           0.000345           0.000246

  PA,  PB,  PC =           250.851411         102.028940          44.449237

Inertial Defect=           -88.898474  +-       0.004267
         Kappa =            -0.723246
      (A+B)/2C =             1.802043
      2A/(B+C) =             2.195092

-------------------------------------------------------------------------------
```

APPENDIX C

PIVALOYL CHLORIDE DATA

Table C.1: A Complete Listing of All Pivaloyl Chloride Transitions Measured in MHz.[a]

$J'_{K_aK_c} - J''_{K_aK_c}$	$F' - F''$	^{35}Cl ν_{obs}	^{37}Cl ν_{obs}
2_{11} - 2_{12}	$\frac{7}{2} - \frac{7}{2}$	835.1896	805.1594
5_{23} - 5_{24}	$\frac{7}{2} - \frac{7}{2}$	1204.2143	
	$\frac{13}{2} - \frac{13}{2}$	1204.4850	
	$\frac{9}{2} - \frac{9}{2}$	1205.1622	1115.0558
	$\frac{11}{2} - \frac{11}{2}$	1205.4314	1115.2382
1_{10} - 1_{01}	$\frac{5}{2} - \frac{5}{2}$	1545.1669	1568.5007
2_{11} - 2_{02}	$\frac{1}{2} - \frac{1}{2}$		1872.1942
	$\frac{5}{2} - \frac{3}{2}$	1865.7362	1875.0958
	$\frac{7}{2} - \frac{7}{2}$	1866.0309	1875.4466
	$\frac{5}{2} - \frac{5}{2}$	1871.8123	1879.9876
3_{12} - 3_{03}	$\frac{3}{2} - \frac{3}{2}$		2397.0935
	$\frac{9}{2} - \frac{9}{2}$		2398.4880
1_{01} - 0_{00}	$\frac{3}{2} - \frac{3}{2}$	3132.0656	3068.8066
	$\frac{5}{2} - \frac{3}{2}$	3140.4160	3075.5465
	$\frac{1}{2} - \frac{3}{2}$	3146.9702	3080.8653
2_{12} - 1_{11}	$\frac{7}{2} - \frac{5}{2}$	6000.9546	
3_{03} - 2_{12}	$\frac{9}{2} - \frac{7}{2}$		8007.55
3_{13} - 2_{12}	$\frac{5}{2} - \frac{3}{2}$	8972.65	8796.50
	$\frac{7}{2} - \frac{5}{2}$	8973.05	8796.80
	$\frac{3}{2} - \frac{1}{2}$	8974.80	8798.20
	$\frac{9}{2} - \frac{7}{2}$	8975.15	8798.50

continued

Table 3. continued

$J'_{K_aK_c} - J''_{K_aK_c}$	$F' - F''$	^{35}Cl ν_{obs}	^{37}Cl ν_{obs}
	$\frac{7}{2} - \frac{7}{2}$	8967.45	
	$\frac{5}{2} - \frac{5}{2}$	8976.65	
	$\frac{3}{2} - \frac{3}{2}$	8980.40	
3_{03} - 2_{02}	$\frac{5}{2} - \frac{3}{2}$	9255.85	9076.05
	$\frac{3}{2} - \frac{1}{2}$	9256.10	9076.25
	$\frac{7}{2} - \frac{5}{2}$	9257.85	9077.70
	$\frac{9}{2} - \frac{7}{2}$	9258.05	9077.85
	$\frac{7}{2} - \frac{7}{2}$	9249.40	
	$\frac{5}{2} - \frac{5}{2}$	9261.95	
	$\frac{3}{2} - \frac{3}{2}$	9264.55	
4_{13} - 3_{22}	$\frac{9}{2} - \frac{7}{2}$	9596.50	9216.65
	$\frac{7}{2} - \frac{5}{2}$	9598.50	
	$\frac{11}{2} - \frac{9}{2}$	9602.25	
	$\frac{5}{2} - \frac{3}{2}$	9604.25	
3_{22} - 2_{21}	$\frac{5}{2} - \frac{5}{2}$		9217.7685[b]
	$\frac{7}{2} - \frac{5}{2}$	9410.30	9217.7781[b]
	$\frac{5}{2} - \frac{3}{2}$	9416.25	
	$\frac{9}{2} - \frac{7}{2}$	9418.60	
	$\frac{3}{2} - \frac{1}{2}$	9424.50	
3_{21} - 2_{20}	$\frac{7}{2} - \frac{5}{2}$	9569.05	
	$\frac{5}{2} - \frac{3}{2}$	9574.925	
	$\frac{9}{2} - \frac{7}{2}$	9577.125	
	$\frac{3}{2} - \frac{1}{2}$	9582.95	

continued

Table 3. continued

$J'_{K_aK_c} - J''_{K_aK_c}$	$F' - F''$	^{35}Cl ν_{obs}	^{37}Cl ν_{obs}
3_{12} - 2_{11}	$\frac{7}{2} - \frac{5}{2}$	9805.10	9599.20
	$\frac{5}{2} - \frac{3}{2}$	9805.45	9599.40
	$\frac{9}{2} - \frac{7}{2}$	9807.25	9600.90
	$\frac{3}{2} - \frac{1}{2}$	9807.60	9601.15
	$\frac{7}{2} - \frac{7}{2}$	9802.45	
	$\frac{3}{2} - \frac{3}{2}$	9810.25	
3_{13} - 2_{02}	$\frac{5}{2} - \frac{3}{2}$	10004.30	9867.50
	$\frac{9}{2} - \frac{7}{2}$	10006.00	9868.80
	$\frac{7}{2} - \frac{5}{2}$	10006.70	9869.50
	$\frac{7}{2} - \frac{7}{2}$	9998.275	
	$\frac{3}{2} - \frac{1}{2}$	10003.60	
	$\frac{5}{2} - \frac{5}{2}$	10010.35	
2_{21} - 1_{10}	$\frac{3}{2} - \frac{3}{2}$	10359.50	
	$\frac{1}{2} - \frac{1}{2}$	10361.40	
	$\frac{7}{2} - \frac{5}{2}$	10362.75	10322.35
	$\frac{5}{2} - \frac{3}{2}$	10365.45	10324.70
	$\frac{3}{2} - \frac{1}{2}$	10369.65	
	$\frac{5}{2} - \frac{5}{2}$	10371.05	
2_{20} - 1_{11}	$\frac{7}{2} - \frac{5}{2}$	10681.85	10627.95
	$\frac{5}{2} - \frac{3}{2}$	10687.60	10632.45
	$\frac{5}{2} - \frac{5}{2}$	10690.35	
4_{04} - 3_{13}	$\frac{7}{2} - \frac{5}{2}$	11439.55	11167.30
	$\frac{9}{2} - \frac{7}{2}$	11440.05	11167.70

continued

Table 3. continued

$J'_{K_aK_c} - J''_{K_aK_c}$	$F' - F''$	^{35}Cl ν_{obs}	^{37}Cl ν_{obs}
	$\frac{11}{2} - \frac{9}{2}$	11441.25	11168.70
	$\frac{5}{2} - \frac{3}{2}$	11440.80	
4_{14} - 3_{13}	$\frac{7}{2} - \frac{5}{2}$	11924.80	11692.8681[b]
	$\frac{9}{2} - \frac{7}{2}$	11925.40	11693.3322[b]
	$\frac{5}{2} - \frac{3}{2}$	11925.70	11693.5863[b]
	$\frac{11}{2} - \frac{9}{2}$	11926.30	11694.0507[b]
	$\frac{9}{2} - \frac{9}{2}$	11917.65	
	$\frac{7}{2} - \frac{7}{2}$	11928.45	
4_{04} - 3_{03}	$\frac{7}{2} - \frac{5}{2}$	12188.00	11958.75
	$\frac{5}{2} - \frac{3}{2}$	12188.25	11958.95
	$\frac{9}{2} - \frac{7}{2}$	12188.90	11959.50
	$\frac{11}{2} - \frac{9}{2}$	12189.20	11959.65
4_{23} - 3_{22}	$\frac{9}{2} - \frac{7}{2}$	12520.70	12265.75
	$\frac{7}{2} - \frac{7}{2}$		12266.7050[b]
	$\frac{7}{2} - \frac{5}{2}$	12521.85	12266.7114[b]
	$\frac{11}{2} - \frac{9}{2}$	12524.05	12268.50
	$\frac{5}{2} - \frac{3}{2}$	12525.25	12269.40
4_{31} - 3_{30}	$\frac{9}{2} - \frac{7}{2}$	12644.40	12378.15
	$\frac{11}{2} - \frac{9}{2}$	12651.80	12384.15
	$\frac{7}{2} - \frac{5}{2}$	12648.25	
	$\frac{5}{2} - \frac{3}{2}$	12655.60	
4_{14} - 3_{03}	$\frac{5}{2} - \frac{3}{2}$	12673.15	12484.15
	$\frac{7}{2} - \frac{5}{2}$	12673.25	12484.30

continued

Table 3. continued

$J'_{K_aK_c} - J''_{K_aK_c}$	$F' - F''$	^{35}Cl ν_{obs}	^{37}Cl ν_{obs}
	$\frac{11}{2} - \frac{9}{2}$	12674.20	12485.00
	$\frac{9}{2} - \frac{7}{2}$	12674.30	12485.15
4_{22} - 3_{21}	$\frac{9}{2} - \frac{7}{2}$	12886.70	12603.00
	$\frac{7}{2} - \frac{7}{2}$		12603.80
	$\frac{7}{2} - \frac{5}{2}$	12887.85	12603.95
	$\frac{11}{2} - \frac{9}{2}$	12889.80	12605.55
	$\frac{5}{2} - \frac{3}{2}$	12890.90	12606.45
4_{32} - 3_{31}	$\frac{7}{2} - \frac{5}{2}$	12625.55	
	$\frac{11}{2} - \frac{9}{2}$	12629.15	
	$\frac{5}{2} - \frac{3}{2}$	12632.975	
4_{13} - 3_{12}	$\frac{7}{2} - \frac{5}{2}$	13017.125	12747.90
	$\frac{9}{2} - \frac{7}{2}$	13017.35	12748.10
	$\frac{5}{2} - \frac{3}{2}$	13018.05	12748.60
	$\frac{11}{2} - \frac{9}{2}$	13018.30	12748.85
	$\frac{9}{2} - \frac{9}{2}$	13012.55	
	$\frac{7}{2} - \frac{7}{2}$	13019.35	
	$\frac{5}{2} - \frac{5}{2}$	13022.875	
3_{22} - 2_{11}	$\frac{3}{2} - \frac{1}{2}$	13221.375	13126.75
	$\frac{9}{2} - \frac{7}{2}$	13223.30	13128.3419[b]
	$\frac{7}{2} - \frac{7}{2}$		13128.3419[b]
	$\frac{5}{2} - \frac{3}{2}$	13224.05	13128.9885[b]
	$\frac{3}{2} - \frac{3}{2}$		13128.9995[b]
	$\frac{5}{2} - \frac{5}{2}$		13130.6261[b]

continued

Table 3. continued

$J'_{K_aK_c} - J''_{K_aK_c}$	$F' - F''$	^{35}Cl ν_{obs}	^{37}Cl ν_{obs}
	$\frac{7}{2} - \frac{5}{2}$	13225.975	13130.6261[b]
5_{14} - 4_{23}	$\frac{11}{2} - \frac{9}{2}$	13244.725	
	$\frac{9}{2} - \frac{7}{2}$	13245.30	
	$\frac{13}{2} - \frac{11}{2}$	13247.65	
	$\frac{7}{2} - \frac{5}{2}$	13248.25	
3_{21} - 2_{12}	$\frac{9}{2} - \frac{7}{2}$		14115.95
5_{05} - 4_{14}	$\frac{9}{2} - \frac{7}{2}$		14247.95
	$\frac{11}{2} - \frac{9}{2}$		14248.25
	$\frac{7}{2} - \frac{5}{2}$		14248.45
	$\frac{13}{2} - \frac{11}{2}$		14248.75
5_{05} - 4_{04}	$\frac{9}{2} - \frac{7}{2}$	15051.50	14773.50
	$\frac{7}{2} - \frac{5}{2}$	15051.75	14773.65
	$\frac{11}{2} - \frac{9}{2}$	15052.05	14773.90
	$\frac{13}{2} - \frac{11}{2}$	15052.30	14774.10
5_{15} - 4_{14}	$\frac{9}{2} - \frac{7}{2}$	14851.9691[b]	
	$\frac{11}{2} - \frac{9}{2}$	14852.4262[b]	
	$\frac{7}{2} - \frac{5}{2}$	14852.4603[b]	
	$\frac{13}{2} - \frac{11}{2}$	14852.9189[b]	
	$\frac{9}{2} - \frac{9}{2}$	14855.00	
5_{15} - 4_{04}	$\frac{9}{2} - \frac{7}{2}$		15091.35
	$\frac{7}{2} - \frac{5}{2}$		15091.45
5_{24} - 4_{23}	$\frac{11}{2} - \frac{9}{2}$	15601.55	15287.05
	$\frac{9}{2} - \frac{7}{2}$	15601.85	15287.25

continued

Table 3. continued

$J'_{K_aK_c} - J''_{K_aK_c}$	$F' - F''$	^{35}Cl ν_{obs}	^{37}Cl ν_{obs}
	$\frac{13}{2} - \frac{11}{2}$	15603.275	15288.45
	$\frac{7}{2} - \frac{5}{2}$	15603.55	15288.65
5_{33} - 4_{32}	$\frac{11}{2} - \frac{9}{2}$	15796.825	15466.75
	$\frac{9}{2} - \frac{7}{2}$	15798.10	15467.75
	$\frac{13}{2} - \frac{11}{2}$	15800.55	15469.75
	$\frac{7}{2} - \frac{5}{2}$	15801.80	15470.75
5_{32} - 4_{31}	$\frac{11}{2} - \frac{9}{2}$	15873.60	15533.25
	$\frac{9}{2} - \frac{7}{2}$	15874.85	15534.20
	$\frac{13}{2} - \frac{11}{2}$	15877.25	15536.15
	$\frac{7}{2} - \frac{5}{2}$	15878.475	15537.15
4_{23} - 3_{12}	$\frac{11}{2} - \frac{9}{2}$	15940.10	15795.95
	$\frac{9}{2} - \frac{9}{2}$	15936.75	
	$\frac{5}{2} - \frac{3}{2}$	15939.05	
	$\frac{7}{2} - \frac{5}{2}$	15940.45	
	$\frac{9}{2} - \frac{7}{2}$	15941.55	
	$\frac{7}{2} - \frac{7}{2}$	15942.75	
	$\frac{5}{2} - \frac{5}{2}$	15943.825	
5_{14} - 4_{13}	$\frac{9}{2} - \frac{7}{2}$	16168.65	15842.40
	$\frac{11}{2} - \frac{9}{2}$	16168.90	15842.60
	$\frac{7}{2} - \frac{5}{2}$	16169.20	15842.80
	$\frac{13}{2} - \frac{11}{2}$	16169.45	15843.00
	$\frac{9}{2} - \frac{9}{2}$	16170.70	
	$\frac{7}{2} - \frac{7}{2}$	16174.95	

continued

Table 3. continued

$J'_{K_aK_c} - J''_{K_aK_c}$	$F' - F''$	^{35}Cl ν_{obs}	^{37}Cl ν_{obs}
5_{23} - 4_{22}	$\frac{11}{2} - \frac{9}{2}$	16241.025	15882.30
	$\frac{9}{2} - \frac{7}{2}$	16241.25	15882.50
	$\frac{13}{2} - \frac{11}{2}$	16242.475	15883.50
	$\frac{7}{2} - \frac{5}{2}$	16242.70	15883.70
3_{31} - 2_{20}	$\frac{9}{2} - \frac{7}{2}$	16441.20	16388.45
	$\frac{3}{2} - \frac{1}{2}$	16442.35	16389.40
	$\frac{7}{2} - \frac{5}{2}$		16390.05
	$\frac{5}{2} - \frac{3}{2}$	16444.35	16391.00
3_{30} - 2_{21}	$\frac{9}{2} - \frac{7}{2}$	16486.05	16429.15
	$\frac{7}{2} - \frac{5}{2}$	16488.20	16430.85
	$\frac{3}{2} - \frac{1}{2}$	16487.125	
	$\frac{5}{2} - \frac{3}{2}$	16489.20	
6_{06} - 5_{15}	$\frac{11}{2} - \frac{9}{2}$	17600.70	17238.7517[b]
	$\frac{13}{2} - \frac{11}{2}$	17600.9959[b]	17239.0166[b]
	$\frac{9}{2} - \frac{7}{2}$	17601.0171[b]	17239.0423[b]
	$\frac{15}{2} - \frac{13}{2}$	17601.3530[b]	17239.3067[b]
6_{16} - 5_{15}	$\frac{11}{2} - \frac{9}{2}$	17757.05	17417.6228[b]
	$\frac{9}{2} - \frac{7}{2}$		17417.8686[b]
	$\frac{13}{2} - \frac{11}{2}$		17417.8975[b]
	$\frac{15}{2} - \frac{13}{2}$	17757.75	17418.1451[b]
6_{06} - 5_{05}	$\frac{11}{2} - \frac{9}{2}$	17886.3821[b]	17556.65
	$\frac{13}{2} - \frac{11}{2}$	17886.7485[b]	17556.95
	$\frac{15}{2} - \frac{13}{2}$	17886.9901[b]	17557.10

continued

Table 3. continued

$J'_{K_aK_c} - J''_{K_aK_c}$	$F' - F''$	^{35}Cl ν_{obs}	^{37}Cl ν_{obs}
	$\frac{9}{2} - \frac{7}{2}$	17886.6188[b]	
	$\frac{9}{2} - \frac{9}{2}$	17895.90	
6_{16} - 5_{05}	$\frac{11}{2} - \frac{9}{2}$	18042.774662[b]	
	$\frac{9}{2} - \frac{7}{2}$	18042.972425[b]	
	$\frac{13}{2} - \frac{11}{2}$	18043.150135[b]	
	$\frac{15}{2} - \frac{13}{2}$	18043.352515[b]	
6_{25} - 5_{24}	$\frac{13}{2} - \frac{11}{2}$	18649.7378[b]	18278.3916[b]
	$\frac{11}{2} - \frac{9}{2}$	18649.7504[b]	18278.3995[b]
	$\frac{15}{2} - \frac{13}{2}$	18650.7661[b]	18279.2125[b]
	$\frac{9}{2} - \frac{7}{2}$	18650.7715[b]	18279.2125[b]
5_{24} - 4_{13}	$\frac{13}{2} - \frac{11}{2}$		18335.55
	$\frac{9}{2} - \frac{7}{2}$		18335.70
	$\frac{11}{2} - \frac{9}{2}$		18336.20

[a] Frequency measurements have an estimated uncertainty of ± 1 kHz below 8 GHz and ± 25 kHz above 8 GHz unless otherwise stated.

[b] Frequency measurements have an estimated uncertainty of ± 1 kHz

APPENDIX D

TIN MONOSULFIDE DATA

Supplemental data for SnS referenced table below describes transitions measured with the chirped pulse Fourier transform microwave spectrometer (CP-FTMW) with laser ablation source.

Table D.1: Measured Transition Frequencies for SnS.[a]

Isotopologue	Abund.[b]	$J' - J''$	v	$F' - F''$	Frequency / MHz	Obs-Cal / kHz
$^{112}Sn^{32}S$	0.92%	1 - 0	0		8313.9485	−2.6
$^{114}Sn^{32}S$	0.62%		0		8281.5742	0.1
$^{116}Sn^{32}S$	13.81%	1 - 0	0		8250.2971	−0.8
			1		8219.6225	−3.1
			2		8188.9233	−3.6
			3		8158.2033	1.6
			4		8127.4530	3.0
			5		8096.6709	−1.0
		2 - 1	0		16500.5572	−3.8
			1		16439.2148	−1.6
$^{117}Sn^{32}S$	7.30%	1 - 0	0	$\frac{3}{2} - \frac{1}{2}$	8235.0050	
				HLC[c]	8235.0333	−1.5
				$\frac{1}{2} - \frac{1}{2}$	8235.0900	
			1	$\frac{3}{2} - \frac{1}{2}$	8204.4149	
				HLC[c]	8204.4434	−4.2
				$\frac{1}{2} - \frac{1}{2}$	8204.5005	

continued

SnS Measurements Continued

Isotope	Abund.[b]	$J' - J''$	v	$F' - F''$	Frequency / MHz	Obs-Cal / kHz
$^{118}Sn^{32}S$	23.02%	1 - 0	0		8220.0681	−0.6
			1		8189.5640	−1.0
			2		8159.0355	0.4
			3		8128.4819	3.0
			4		8097.9018	5.3
			5		8067.2901	2.3
			6		8036.6534	0.6
		2 - 1	0		16440.1030	0.2
			1		16379.0921	−3.4
$^{119}Sn^{32}S$	8.16 %	1 - 0	0	$\frac{3}{2} - \frac{1}{2}$	8205.2785	
				HLC[c]	8205.3082	−1.3
				$\frac{1}{2} - \frac{1}{2}$	8205.3677	
$^{120}Sn^{32}S$	30.97%	1 - 0	0		8190.8373	0.0
			1		8160.4967	0.3
			2		8130.1317	2.3
			3		8099.7367	0.3
			4		8069.3194	2.1
			5		8038.8652	−6.9
			6		8008.3989	−2.0
		2 - 1	0		16381.6413	1.0

continued

SnS Measurements Continued

Isotope	Abund.[b]	$J' - J''$	v	$F' - F''$	Frequency / MHz	Obs-Cal / kHz
			1		16320.9566	−2.0
$^{122}Sn^{32}S$	4.40%	1 - 0	0		8162.5573	1.1
			1		8132.3726	0.2
		2 - 1	0		16325.0826	4.3
$^{124}Sn^{32}S$	5.50%	1 - 0	0		8135.1828	2.3
			1		8105.1497	1.0
		2 - 1	0		16270.3328	5.6

[a] Frequency measurements have an estimated uncertainty of ± 5 kHz.

[b] This is the isotopologue abundance.

[c] HLC = hypothetical line center.

APPENDIX E

OPEN-SHELL DIATOMICS AND LASER ABLATION PRODUCT CHEMISTRY DATA

Supplemental data for referenced tables below describes transitions measured with the chirped pulse Fourier transform microwave spectrometer (CP-FTMW) with laser ablation source.

Table E.1: Measured Transition Frequencies for BaS.[a]

Isotopologue	Abund.[b]	$J' - J''$	v	$F' - F''$	Frequency / MHz
$^{138}Ba^{32}S$	68.1%	1 - 0	0		6185.108
			1		6166.163
		2 - 1	0		12370.194
			1		12332.301
			2		12294.305
			3		12256.203
			4		12217.991
			5		12179.666
			6		12141.227
			7		12102.669
		3 - 2	0		18555.236
			1		18498.397
			2		18441.404
			3		18384.248
			4		18326.933
		4 - 3	0		24740.207

continued

BaS Measurements Continued

Isotope	Abund.[b]	$J' - J''$	v	$F' - F''$	Frequency / MHz
$^{137}Ba^{32}S$	10.7%	2 - 1	0	Unassigned	12384.321
				Unassigned	12387.169
				Unassigned	12388.006
		3 - 2		Unassigned	18575.922
				Unassigned	18578.776
				Unassigned	18581.170
$^{136}Ba^{32}S$	7.5%	1 - 0	0		6202.231
		2 - 1	0		12404.438
			1		12366.387
			2		12328.235
			3		12289.972
		3 - 2	0		18606.602
			1		18549.526
$^{135}Ba^{32}S$	6.3%	2 - 1	0	$\frac{5}{2} - \frac{5}{2}$	12416.185
				$\frac{5}{2} - \frac{3}{2}$	12422.457
				$\frac{3}{2} - \frac{3}{2}$	12426.926
			1	Unassigned	12377.540
				Unassigned	12378.359
		3 - 2	0	$\frac{5}{2} - \frac{3}{2}$	18631.563
				$\frac{7}{2} - \frac{5}{2}$	18633.120

continued

BaS Measurements Continued

Isotope	Abund.[b]	$J' - J''$	v	$F' - F''$	Frequency / MHz
$^{134}Ba^{32}S$	2.3%	2 - 1	0		12439.697
			1		12401.487
		3 - 2	0		18659.488
$^{138}Ba^{34}S$	3.07%	2 - 1	0		11780.667
			1		11745.456
		3 -2			17670.952

[a] Frequency measurements have an estimated uncertainty of ± 1 kHz.

[b] This is the isotopologue abundance.

TABLE E.2. A Concise Line Listing of All Transitions Measured for SnCl.

Transition /MHz	Transition /MHz	Transition /MHz	Transition /MHz	Transition /MHz
9518.5974	9916.0668	10070.7006	10248.6723	16715.2794
9687.4966	9927.4189	10072.4985	15840.0010	16834.8716
9724.0114	9931.4349	10073.1954	15892.7310	16838.2863
9787.7526	9931.9351	10139.9322	15950.7086	16839.4148
9807.2020	9941.2080	10144.8553	15967.0322	16855.6299
9812.6263	9953.9415	10147.1800	16016.2959	16893.9055
9821.4525	9965.2887	10156.2469	16269.2289	16894.6964
9838.2850	9970.5991	10166.0952	16540.9395	16895.4833
9843.7508	9985.5772	10169.6224	16556.8552	16898.1271
9846.3072	9993.0985	10173.8416	16557.0904	16899.3146
9852.8209	9999.8525	10178.7971	16576.5751	16902.7336
9856.9230	10000.1482	10184.8054	16579.6698	16903.8529
9864.1670	10000.2537	10186.0440	16586.2331	16906.2814
9876.1453	10015.8362	10204.9583	16587.9205	16943.2106
9883.9094	10020.5229	10208.4817	16588.2855	16965.9492
9893.5635	10022.3570	10212.7071	16643.1231	16967.2651
9895.4965	10024.3578	10218.9846	16649.6862	16969.3695
9902.0410	10029.7109	10226.2315	16651.3722	17213.4524
9912.7721	10065.3805	10245.1493	16708.7410	

All data and calculation outputs for lead monochloride, PbCl. Quantum numbers in table are given as N',p',J', $F' \leftarrow N''$,p'',J'', F'' where p is for parity. Literature values[124] in table are given in cm^{-1} for transitions 1-150. Transitions past 150 are measurements made on the CP-FTMW with laser ablation source.

TABLE E.3. PbCl Transitions from the Literature[124] (in cm^{-1}, transitions 1-150) and Measured (in MHz, transitions 151-173) at the University of North Texas along with the fitted parameters.

	obs	o-c	error	blends o-c	blends wt	Notes
1: 29 -1 30 30 31 1 31 32	8279.54950	0.00108	.00100			
2: 28 1 29 29 30 -1 30 31	8279.60200	0.00123	.00100			
3: 51 -1 52 52 53 1 53 54	8279.61770	-0.00395	.00100			
4: 27 -1 28 28 29 1 29 30	8279.66010	0.00216	.00100			
5: 52 1 53 53 54 -1 54 55	8279.67660	-0.00412	.00100			
6: 26 1 27 27 28 -1 28 29	8279.72210	0.00214	.00100			
7: 25 -1 26 26 27 1 27 28	8279.78920	0.00239	.00100			
8: 24 1 25 25 26 -1 26 27	8279.86100	0.00251	.00100			
9: 23 -1 24 24 25 1 25 26	8279.93700	0.00200	.00100			
10: 56 1 57 57 58 -1 58 59	8279.96130	-0.00420	.00100			
11: 22 1 23 23 24 -1 24 25	8280.01990	0.00355	.00100			
12: 57 -1 58 58 59 1 59 60	8280.04250	-0.00633	.00100			
13: 18 -1 19 19 20 1 20 21	8280.80080	0.00073	.00100			
14: 15 1 16 16 17 -1 17 18	8281.07140	0.00168	.00100			
15: 14 -1 15 15 16 1 16 17	8281.17140	0.00213	.00100			
16: 13 1 14 14 15 -1 15 16	8281.27580	0.00214	.00100			
17: 11 1 12 12 13 -1 13 14	8281.49920	0.00229	.00100			
18: 10 -1 11 11 12 1 12 13	8281.61880	0.00302	.00100			
19: 10 1 11 11 11 -1 11 12	8283.73020	0.00296	.00100			
20: 12 1 13 13 13 -1 13 14	8283.86620	0.00298	.00100			
21: 13 -1 14 14 14 1 14 15	8283.94110	0.00267	.00100			

```
22: 18 -1 19 19   19  1 19 20            8284.00190  0.00472 .00100
23: 14  1 15 15   15 -1 15 16            8284.02060  0.00214 .00100
24: 19  1 20 20   20 -1 20 21            8284.08470  0.00384 .00100
25: 16  1 17 17   17 -1 17 18            8284.19570  0.00272 .00100
26: 17 -1 18 18   18  1 18 19            8284.29000  0.00254 .00100
27: 22 -1 23 23   23  1 23 24            8284.36430  0.00355 .00100
28: 18  1 19 19   19 -1 19 20            8284.38820  0.00144 .00100
29: 23  1 24 24   24 -1 24 25            8284.46710  0.00343 .00100
30: 19 -1 20 20   20  1 20 21            8284.49290  0.00202 .00100
31: 24 -1 25 25   25  1 25 26            8284.57430  0.00290 .00100
32: 20  1 21 21   21 -1 21 22            8284.60080  0.00098 .00100
33: 25  1 26 26   26 -1 26 27            8284.68580  0.00185 .00100
34: 21 -1 22 22   22  1 22 23            8284.71460  0.00102 .00100
35: 22  1 23 23   23 -1 23 24            8284.83350  0.00135 .00100
36: 23 -1 24 24   24  1 24 25            8284.95620  0.00065 .00100
37:  8  1  9  9    8 -1  8  9            8285.00960  0.00601 .00100
38: 24  1 25 25   25 -1 25 26            8285.08450  0.00073 .00100
39: 29  1 30 30   30 -1 30 31            8285.18370  0.00147 .00100
40: 30 -1 31 31   31  1 31 32            8285.32000  0.00118 .00100
41: 26  1 27 27   27 -1 27 28            8285.35500  0.00035 .00100
42: 31  1 32 32   32 -1 32 33            8285.45990 -0.00033 .00100
43: 27 -1 28 28   28  1 28 29            8285.49770  0.00037 .00100
44: 32 -1 33 33   33  1 33 34            8285.60690  0.00046 .00100
45: 11 -1 12 12   11  1 11 12            8285.68260  0.00452 .00100
46: 33  1 34 34   34 -1 34 35            8285.75740 -0.00007 .00100
47: 29 -1 30 30   30  1 30 31            8285.79700 -0.00013 .00100
48: 30  1 31 31   31 -1 31 32            8285.95350 -0.00076 .00100
49: 35  1 36 36   36 -1 36 37            8286.07290 -0.00104 .00100
50: 31 -1 32 32   32  1 32 33            8286.11490 -0.00132 .00100
51: 36 -1 37 37   37  1 37 38            8286.23780 -0.00160 .00100
52: 32  1 33 33   33 -1 33 34            8286.28120 -0.00179 .00100
53: 33 -1 34 34   34  1 34 35            8286.45150 -0.00309 .00100
54: 38 -1 39 39   39  1 39 40            8286.58260 -0.00213 .00100
```

```
55: 34  1 35 35   35 -1 35 36          8286.62830 -0.00270 .00100
56: 15 -1 16 16   15  1 15 16          8286.65010  0.00546 .00100
57: 39  1 40 40   40 -1 40 41          8286.76150 -0.00311 .00100
58: 35 -1 36 36   36  1 36 37          8286.80920 -0.00304 .00100
59: 16  1 17 17   16 -1 16 17          8286.90340  0.00511 .00100
60: 36  1 37 37   37 -1 37 38          8286.99500 -0.00330 .00100
61: 41  1 42 42   42 -1 42 43          8287.13580 -0.00299 .00100
62: 17 -1 18 18   17  1 17 18          8287.16180  0.00507 .00100
63: 37 -1 38 38   38  1 38 39          8287.18530 -0.00388 .00100
64: 42 -1 43 43   43  1 43 44          8287.32960 -0.00350 .00100
65: 38  1 39 39   39 -1 39 40          8287.38120 -0.00368 .00100
66: 18  1 19 19   18 -1 18 19          8287.42370  0.00374 .00100
67: 43  1 44 44   44 -1 44 45          8287.52810 -0.00411 .00100
68: 39 -1 40 40   40  1 40 41          8287.58140 -0.00400 .00100
69: 19 -1 20 20   19  1 19 20          8287.69250  0.00450 .00100
70: 44 -1 45 45   45  1 45 46          8287.73200 -0.00413 .00100
71: 45  1 46 46   46 -1 46 47          8287.94030 -0.00455 .00100
72: 20  1 21 21   20 -1 20 21          8287.96450  0.00367 .00100
73: 41 -1 42 42   42  1 42 43          8287.99640 -0.00451 .00100
74: 46 -1 47 47   47  1 47 48          8288.15410 -0.00429 .00100
75: 42  1 43 43   43 -1 43 44          8288.21180 -0.00411 .00100
76: 21 -1 22 22   21  1 21 22          8288.24230  0.00385 .00100
77: 43 -1 44 44   44  1 44 45          8288.43140 -0.00432 .00100
78: 22  1 23 23   22 -1 22 23          8288.52430  0.00343 .00100
79: 48 -1 49 49   49  1 49 50          8288.59600 -0.00388 .00100
80: 44  1 45 45   45 -1 45 46          8288.65640 -0.00395 .00100
81: 45 -1 46 46   46  1 46 47          8288.88580 -0.00401 .00100
82: 50 -1 51 51   51  1 51 52          8289.05630 -0.00429 .00100
83: 46  1 47 47   47 -1 47 48          8289.12030 -0.00379 .00100
84: 51  1 52 52   52 -1 52 53          8289.29360 -0.00456 .00100
85: 47 -1 48 48   48  1 48 49          8289.35950 -0.00369 .00100
86: 25 -1 26 26   25  1 25 26          8289.39950  0.00264 .00100
87: 52 -1 53 53   53  1 53 54          8289.53610 -0.00444 .00100
```

```
 88: 26  1 27 27   26 -1 26 27            8289.70180  0.00336 .00100
 89: 53  1 54 54   54 -1 54 55            8289.78460 -0.00312 .00100
 90: 49 -1 50 50   50  1 50 51            8289.85190 -0.00397 .00100
 91: 54 -1 55 55   55  1 55 56            8290.03600 -0.00370 .00100
 92: 50  1 51 51   51 -1 51 52            8290.10570 -0.00374 .00100
 93: 55  1 56 56   56 -1 56 57            8290.29270 -0.00380 .00100
 94: 28  1 29 29   28 -1 28 29            8290.31710  0.00114 .00100
 95: 51 -1 52 52   52  1 52 53            8290.36420 -0.00364 .00100
 96: 57  1 58 58   58 -1 58 59            8290.82050 -0.00400 .00100
 97: 30  1 31 31   30 -1 30 31            8290.95360  0.00097 .00100
 98: 58 -1 59 59   59  1 59 60            8291.09230 -0.00341 .00100
 99: 54  1 55 55   55 -1 55 56            8291.16870 -0.00328 .00100
100: 31 -1 32 32   31  1 31 32            8291.27880  0.00066 .00100
101: 59  1 60 60   60 -1 60 61            8291.36880 -0.00292 .00100
102: 55 -1 56 56   56  1 56 57            8291.44610 -0.00357 .00100
103: 32  1 33 33   32 -1 32 33            8291.60890  0.00047 .00100
104: 60 -1 61 61   61  1 61 62            8291.64890 -0.00364 .00100
105: 56  1 57 57   57 -1 57 58            8291.72880 -0.00339 .00100
106: 57 -1 58 58   58  1 58 59            8292.01670 -0.00283 .00100
107: 62 -1 63 63   63  1 63 64            8292.22660 -0.00199 .00100
108: 34  1 35 35   34 -1 34 35            8292.28410  0.00075 .00100
109: 58  1 59 59   59 -1 59 60            8292.30920 -0.00250 .00100
110: 63  1 64 64   64 -1 64 65            8292.52170 -0.00212 .00100
111: 64 -1 65 65   65  1 65 66            8292.82180 -0.00206 .00100
112: 60  1 61 61   61 -1 61 62            8292.90870 -0.00181 .00100
113: 65  1 66 66   66 -1 66 67            8293.12760 -0.00110 .00100
114: 61 -1 62 62   62  1 62 63            8293.21570 -0.00145 .00100
115: 66 -1 67 67   67  1 67 68            8293.43780 -0.00054 .00100
116: 62  1 63 63   63 -1 63 64            8293.52750 -0.00112 .00100
117: 38  1 39 39   38 -1 38 39            8293.68950 -0.00106 .00100
118: 67  1 68 68   68 -1 68 69            8293.75170 -0.00109 .00100
119: 63 -1 64 64   64  1 64 65            8293.84500  0.00008 .00100
120: 39 -1 40 40   39  1 39 40            8294.05370 -0.00060 .00100
```

```
121: 64  1 65 65   65 -1 65 66            8294.16670  0.00066 .00100
122: 69  1 70 70   70 -1 70 71            8294.39820  0.00210 .00100
123: 40  1 41 41   40 -1 40 41            8294.42080 -0.00201 .00100
124: 65 -1 66 66   66  1 66 67            8294.49260  0.00061 .00100
125: 70 -1 71 71   71  1 71 72            8294.72800  0.00304 .00100
126: 41 -1 42 42   41  1 41 42            8294.79380 -0.00230 .00100
127: 66  1 67 67   67 -1 67 68            8294.82430  0.00154 .00100
128: 71  1 72 72   72 -1 72 73            8295.06130  0.00268 .00100
129: 72 -1 73 73   73  1 73 74            8295.40000  0.00292 .00100
130: 68  1 69 69   69 -1 69 70            8295.50230  0.00351 .00100
131: 43 -1 44 44   43  1 43 44            8295.55440 -0.00260 .00100
132: 73  1 74 74   74 -1 74 75            8295.74370  0.00335 .00100
133: 69 -1 70 70   70  1 70 71            8295.84840  0.00436 .00100
134: 44  1 45 45   44 -1 44 45            8295.94230 -0.00230 .00100
135: 74 -1 75 75   75  1 75 76            8296.09460  0.00618 .00100
136: 70  1 71 71   71 -1 71 72            8296.19980  0.00568 .00100
137: 45 -1 46 46   45  1 45 46            8296.33430 -0.00268 .00100
138: 71 -1 72 72   72  1 72 73            8296.55490  0.00587 .00100
139: 46  1 47 47   46 -1 46 47            8296.73140 -0.00272 .00100
140: 76 -1 77 77   77  1 77 78            8296.80700  0.00804 .00100
141: 72  1 73 73   73 -1 73 74            8296.91630  0.00754 .00100
142: 47 -1 48 48   47  1 47 48            8297.13410 -0.00193 .00100
143: 77  1 78 78   78 -1 78 79            8297.17060  0.00916 .00100
144: 73 -1 74 74   74  1 74 75            8297.28160  0.00827 .00100
145: 48  1 49 49   48 -1 48 49            8297.53980 -0.00290 .00100
146: 79  1 80 80   80 -1 80 81            8297.91350  0.01271 .00100
147: 49 -1 50 50   49  1 49 50            8297.95000 -0.00414 .00100
148: 50  1 51 51   50 -1 50 51            8298.36750 -0.00285 .00100
149: 52  1 53 53   52 -1 52 53            8299.21490 -0.00215 .00100
150: 53 -1 54 54   53  1 53 54            8299.64520 -0.00234 .00100
151:  2  1  2  3    1 -1  1  2             7983.0391   0.0062  0.025
152:  2  1  2  2    1 -1  1  1             7984.3868   0.0025  0.025
153:  2  1  2  2    1 -1  1  2             7998.6421  -0.0064  0.025
```

```
 154:  2  1  2  1    1 -1  1  1              8003.1939  -0.0060  0.025
 155:  2  1  2  0    1 -1  1  1              8015.1082   0.0054  0.025
 156:  2 -1  2  1    1  1  1  2              8527.7068   0.0024  0.025
 157:  2 -1  2  2    1  1  1  2              8552.5912   0.0095  0.025
 158:  2 -1  2  3    1  1  1  2              8602.0513  -0.0053  0.025
 159:  2 -1  2  1    1  1  1  1              8622.3875  -0.0013  0.025
 160:  2 -1  2  2    1  1  1  1              8647.2736   0.0074  0.025
 161:  3 -1  3  3    2  1  2  2             13519.2909  -0.0016  0.025
 162:  3 -1  3  4    2  1  2  3             13519.5175   0.0070  0.025
 163:  3 -1  3  1    2  1  2  0             13523.9712  -0.0046  0.025
 164:  3 -1  3  3    2  1  2  3             13534.9085   0.0001  0.025
 165:  3 -1  3  1    2  1  2  1             13535.8789   0.0002  0.025
 166:  3 -1  3  2    2  1  2  3             13554.0005   0.0030  0.025
 167:  3  1  3  3    2 -1  2  3             14093.4862  -0.0080  0.025
 168:  3  1  3  2    2 -1  2  2             14120.0083  -0.0010  0.025
 169:  3  1  3  1    2 -1  2  1             14133.0560  -0.0073  0.025
 170:  3  1  3  4    2 -1  2  3             14133.9476   0.0036  0.025
 171:  3  1  3  3    2 -1  2  2             14142.9721   0.0030  0.025
 172:  3  1  3  1    2 -1  2  0             14143.1827  -0.0024  0.025
 173:  3  1  3  2    2 -1  2  1             14144.8866  -0.0001  0.025
-------------------------------------------------------------------------------
PARAMETERS IN FIT:

         100            B  /MHz         2801.8554(14)                        1
         200            D  /kHz            1.076(14)                        2
    10040000        -.5*p  /MHz          305.4720(55)                        3
    10040100     -0.5*p_D  /MHz            0.000847(15)                      4
    10010000            A  /MHz    248333381.0(40)                          5
    10010100          A_D  /MHz           72.1110(15)                        6
   120040000        -0.5d  /MHz           20.4163(55)                        7
    20010000    a-(b+c)/2  /MHz           30.170(13)                         8
   220010000   1.5eQq(Cl)  /MHz          -37.414(67)                         9
```

```
 MICROWAVE AVG =        0.000278 MHz, IR AVG =        0.00000
 MICROWAVE RMS =        0.004965 MHz, IR RMS =        0.00348
 END OF ITERATION  1 OLD, NEW RMS ERROR=        3.23938         3.23938

  distinct frequency lines in fit:   173
       distinct parameters of fit:     9

 for standard errors previous errors are multiplied by:   3.327078

 PARAMETERS IN FIT WITH STANDARD ERRORS ON THOSE THAT ARE FITTED:

          100            B  /MHz         2801.8554(48)                          1
          200            D  /kHz            1.076(47)                           2
     10040000        -.5*p  /MHz          305.472(18)                           3
     10040100     -0.5*p_D  /MHz            0.000847(49)                        4
     10010000            A  /MHz    248333381.(13)                              5
     10010100          A_D  /MHz           72.1110(50)                          6
    120040000        -0.5d  /MHz           20.416(18)                           7
     20010000    a-(b+c)/2  /MHz           30.170(43)                           8
    220010000   1.5eQq(Cl)  /MHz          -37.41(22)                            9

 CORRELATION COEFFICIENTS, C.ij:

           B        -D       -.5*p    -0.5*p_D A        A_D      -0.5d    a-(b+c)/

B           1.0000
-D         -0.1148   1.0000
-.5*p      -0.0558   0.0045   1.0000
-0.5*p_D    0.1022   0.0103  -0.1291   1.0000
A          -0.3941  -0.1050   0.0112  -0.0520   1.0000
A_D         0.5115   0.0753  -0.0139   0.1911  -0.7819   1.0000
-0.5d      -0.0344  -0.0047   0.3033  -0.0279   0.0042  -0.0024   1.0000
a-(b+c)/2   0.0163   0.0038   0.0162  -0.0044  -0.0006  -0.0004  -0.1425   1.0000
```

```
1.5eQq(Cl) -0.0900   0.0029  -0.0601   0.0071  -0.0035   0.0008  -0.1553   0.1626

           1.5eQq(C

1.5eQq(Cl)  1.0000

 Mean value of |C.ij|, i.ne.j =   0.0999
 Mean value of  C.ij,  i.ne.j =  -0.0208

 Worst fitting lines (obs-calc/error):

   146:  -12.7        143:   -9.2        144:   -8.3        140:   -8.0
   141:   -7.5         12:    6.3        135:   -6.2         37:   -6.0
   138:   -5.9        136:   -5.7         56:   -5.5         59:   -5.1
    62:   -5.1         22:   -4.7         84:    4.6         71:    4.6
    45:   -4.5         73:    4.5         69:   -4.5         87:    4.4
   133:   -4.4         77:    4.3         82:    4.3         74:    4.3
    10:    4.2        147:    4.1         70:    4.1          5:    4.1
    67:    4.1         75:    4.1         81:    4.0         68:    4.0
    96:    4.0         90:    4.0          3:    4.0         80:    4.0
    63:    3.9         79:    3.9         76:   -3.9         24:   -3.8
    93:    3.8         83:    3.8         92:    3.7         66:   -3.7
    91:    3.7         85:    3.7         65:    3.7         72:   -3.7
    95:    3.6        104:    3.6

                                          ------------------------------------
_____________________________________/ SPFIT output reformatted with PIFORM
```

BIBLIOGRAPHY

[1] C. H. Townes and A. L. Schawlow, *Microwave Spectroscopy* (Dover Publications, Inc., New York, 1975).

[2] W. Gordy and R. L. Cook, *Microwave Molecular Spectra; Techniques of Chemistry Vol. XVIII* (Wiley, New York, 1984).

[3] T. J. Balle and W. H. Flygare, *Rev. Scient. Instrum.* **52,** 33 (1981).

[4] K. A. Walker and M. C. L. Gerry, *J. Mol. Spectrosc.* **182,** 178 (1997).

[5] G. G. Brown, B. C. Dian, K. O. Douglass, S. M. Geyer, and B. H. Pate, *J. Mol. Spectrosc.* **238,** 200 (2006).

[6] B. C. Dian, G. G. Brown, K. O. Douglass, and B. H. Pate, *Science* **320,** 924 (2008).

[7] G. G. Brown, B. C. Dian, K. O. Douglass, S. M. Geyer, S. T. Shipman, and B. H. Pate, *Rev. Scient. Instrum.* **79,** 053103 (2008).

[8] J. C. McGurk, T. G. Schmalz, and W. H. Flygare, *J. Chem. Phys.* **60,** 4181 (1974).

[9] J. C. McGurk, T. G. Schmalz, and W. H. Flygare, in *Advances in Chemical Physics*, edited by S. A. Rice and I. Prigogine (Academic, New York, 1974), Vol. 25, p. 1.

[10] G. M. Barrow, *The Structure of Molecules: An Introduction to Molecular Spectroscopy* (W. A. Benjamin, Inc., New York, 1963).

[11] P. Atkins and J. de Paula, *Physical Chemistry*, 7th ed. (W. H. Freeman and Company, New York, 2002).

[12] L. Herzberg and G. Herzberg, *Fundamental Formula's of Physics Vol. 2: Molecular Spectra Chapter* (D. Menzel/Dover, New York, 1960).

[13] B. S. Ray, *Z. Physik.* **78,** 74 (1932).

[14] H. W. Kroto, *Molecular Rotation Spectra* (H. W. Kroto/Dover, Mineola, N.Y., 1992).

[15] K. C. Etchison, C. T. Dewberry, and S. A. Cooke, *Chem. Phys.* **342,** 71 (2007).

[16] J. K. G. Watson, *J. Chem. Phys.* **48,** 4517 (1968).

[17] J. K. G. Watson, *Vibrational Spectra and Structure* **6,** 1 (1977).

[18] J. Kraitchman, *Am. J. Phys.* **21,** 17 (1953).

[19] G. S. Grubbs II and S. A. Cooke, *J. Mol. Struct.* **963,** 87 (2010).

[20] R. A. Frosch and H. M. Foley, *Phys. Rev.* **88,** 1337 (1952).

[21] J. L. Dunham, *Phys. Rev.* **41,** 721 (1932).

[22] J. K. G. Watson, *J. Mol. Spectrosc.* **45,** 99 (1973).

[23] J. K. G. Watson, *J. Mol. Spectrosc.* **80,** 411 (1980).

[24] C. T. Dewberry, K. C. Etchison, G. S. Grubbs II, R. A. Powoski, M. M. Serafin, S. A. Peebles, and S. A. Cooke, *Phys. Chem. Chem. Phys.* (2007).

[25] C. Chen, *System and Signal Analysis* (Saunders College Publishing, New York, N.Y., 1989).

[26] J. Cooley and J. Tuckey, *Math. Comput.* **19,** 297 (1965).

[27] J. Ekkers and W. H. Flygare, *Rev. Scient. Instrum.* **47,** 448 (1976).

[28] G. S. Grubbs II, C. T. Dewberry, K. C. Etchison, K. E. Kerr, and S. A. Cooke, *Rev. Scient. Instrum.* **78,** 096106 (2007).

[29] G. S. Grubbs II, C. T. Dewberry, K. C. Etchison, M. M. Serafin, S. A. Peebles, and S. A. Cooke, *J. Mol. Spectrosc.* **251,** 378 (2008).

[30] G. S. Grubbs II, C. T. Dewberry, K. C. Etchison, M. M. Serafin, S. A. Peebles, and S. A. Cooke, in *The Pure Rotational Spectrum of Pivaloyl Chloride between 800 and 18800 MHz*, 63rd Ohio State University International Symposium on Molecular Spectroscopy (Ohio State University, Columbus, OH, 2008).

[31] C. T. Dewberry, G.S. Grubbs II, and S. A. Cooke, *J. Mol. Spectrosc.* **257,** 66 (2009).

[32] G. S. Grubbs II, C. T. Dewberry, and S. A. Cooke, in *Some effects of successive fluorination on 1-iodopropane*, 64th Ohio State University International Symposium on Molecular Spectroscopy (Ohio State University, Columbus, OH, 2009).

[33] G. S. Grubbs II, W. C. Bailey, and S. A. Cooke, *Chem. Phys. Lett.* **477,** 37 (2009).

[34] G. S. Grubbs II, W. C. Bailey, and S. A. Cooke, *Mol. Phys.* **107,** 221 (2009).

[35] G. S. Grubbs II, B. E. Long, R. A. Powoski, and S. A. Cooke, *J. Mol. Spectrosc.* **258,** 1 (2009).

[36] G. S. Grubbs II and S. A. Cooke, *Chem. Phys. Lett.* **483,** 21 (2009).

[37] R. A. Powoski, G. S. Grubbs II, and S. A. Cooke, *J. Mol. Struct.* **963,** 106 (2009).

[38] G. S. Grubbs II, W. C. Bailey, and S. A. Cooke, *J. Mol. Struct.* **987,** 255 (2011).

[39] C. T. Dewberry, G. S. Grubbs II, K. C. Etchison, and S. A. Cooke, in *Measurement of the Vibrational Population Distribution of Barium Sulfide, Seeded in an Argon Supersonic Expansion, Following Production Through the Reaction of Laser Ablated Barium with Carbonyl Sulfide*, 64th Ohio State University International Symposium on Molecular Spectroscopy (Ohio State University, Columbus, OH, 2009).

[40] J. M. Blackledge, *Digital Signal Processing: Mathematical and Computational Methods, Software Development and Applications* (Horwood Publishing, Sussex, England, 2003).

[41] *AWG710 & AWG710B Arbitrary Waveform Generator User Manual*, Tektronix, P. O. Box 500, Beaverton, OR 97077, 2004.

[42] G. S. Grubbs II and S. A. Cooke, *J. Mol. Spectrosc.* **259,** 120 (2010).

[43] G. S. Grubbs II and S. A. Cooke, in *Chirped Pulse Fourier Transform Microwave Spectroscopy of SnCl*, 65th Ohio State University International Symposium on Molecular Spectroscopy (Ohio State University, Columbus, OH, 2010).

[44] C. T. Dewberry, G. S. Grubbs II, K. C. Etchison, and S. A. Cooke, in *Hyperfine Structure in the Pure Rotational Spectrum of* $^{208}Pb^{35}Cl$, 65th Ohio State University International Symposium on Molecular Spectroscopy (Ohio State University, Columbus, OH, 2010).

[45] T. G. Dietz, M. A. Duncan, D. E. Powers, and R. E. Smalley, *J. Chem. Phys.* **74,** 6511 (1981).

[46] E. J. Campbell, L. W. Buxton, T. J. Balle, M. R. Keenan, and W. H. Flygare, *J. Chem. Phys.* **74,** 829 (1981).

[47] G. S. Grubbs II, R. A. Powoski, D. Jojola, and S. A. Cooke, *J. Phys. Chem. A* **114,** 8009 (2010).

[48] R. D. Chambers, J. Hutchison, R. H. Mobbs, and W. K. R. Musgrave, *Tetrahedron* **20,** 497 (1964).

[49] A. P. Cox, G. Duxbury, J. A. Hardy, and Y. Kawashima, *J. Chem. Soc. Faraday Trans. 2* **76,** 339 (1980).

[50] A. L. Andreassen and S. H. Bauer, *J. Chem. Phys.* **56,** 3802 (1972).

[51] O. Risgin and R. C. Taylor, *Spectrochimica Acta* **15,** 1036 (1959).

[52] S. Eltayeb, G. A. Guirgis, A. R. Fanning, and J. R. Durig, *J. Raman Spectrosc.* **27,** 111 (1996).

[53] Y. Zhao and D. Truhlar, *Theor. Chem. Acc.* **120,** 215 (2008).

[54] Y. Zhao and D. Truhlar, *Acc. Chem. Res.* **41,** 157 (2008).

[55] R. Krishnan, J. S. Binkley, R. Seeger, and J. A. Pople, *J. Chem. Phys.* **72,** 650 (1980).

[56] M. N. Glukhovtsev, A. Pross, M. P. McGrath, and L. Radom, *J. Chem. Phys.* **103,** 1878 (1995).

[57] D. Feller, *J. Comp. Chem* **17,** 1571 (1996).

[58] K. L. Shuschart, B. T. Didier, T. Elsethagen, L. Sun, V. Gurumoorthi, J. Chase, J. Li, and T. L. Windus, *J. Chem. Inf. Model.* **47,** 1045 (2007).

[59] M. W. Schmidt *et al.*, *J. Comput. Chem.* **14,** 1347 (1993).

[60] R. Weast, *CRC Handbook of Chemistry and Physics 67th Edition* (CRC Press, Inc., Boca Raton, Fl., 1986).

[61] Z. Kisiel, PROSPE – Programs for ROtational SPEctroscopy, URL: http://info.ifpan.edu.pl/ kisiel/prospe.htm.

[62] P. Pyykkö, *Mol. Phys.* **106,** 1965 (2008).

[63] H. M. Pickett, *J. Mol. Spectrosc.* **148,** 371 (1991).

[64] Z. Kisiel, L. Pszczolkowski, I. R. Medvedev, M. Winnewisser, F. C. D. Lucia, and C. E. Herbst, *J. Mol. Spectrosc.* **233,** 231 (2005).

[65] W. H. Flygare, *J. Chem. Phys.* **41,** 793 (1964).

[66] D. Boucher, A. Dubrulle, and J. Demaison, *J. Mol. Spectrosc.* **84,** 375 (1980).

[67] J. Gripp and H. Dreizler, *Z. Naturforsch. Teil A* **43,** 971 (1988).

[68] G. Wlodarczak, D. Boucher, R. Bocquet, and J. Demaison, *J. Mol. Spectrosc.* **124,** 53 (1987).

[69] M. Fujitake and M. Hayashi, *J. Mol. Spectrosc.* **127,** 112 (1988).

[70] G. S. Grubbs II, C. T. Dewberry, A. King, W. Lin, W. C. Bailey, and S. A. Cooke, *J. Mol. Spectrosc.* **263,** 127 (2010).

[71] J. A. Fournier, R. K. Bohn, J. J. A. Montgomery, and M. Onda, *J. Phys. Chem. A* **114,** 1118 (2010).

[72] G. S. Grubbs II, C. T. Dewberry, S. A. Cooke, and W. Lin, *J. Mol. Struct.* **973,** 190 (2010).

[73] G. S. Grubbs II, G. Kadiwar, W. C. Bailey, and S. A. Cooke, *J. Chem. Phys.* **132,** 024310 (2010).

[74] G. S. Grubbs II and S. A. Cooke, *Chem. Phys. Lett.* **495,** 182 (2010).

[75] B. P. van Eijck and E. W. Kaleveld, *J. Mol. Struct.* **34,** 161 (1976).

[76] C. W. Bunn and E. R. Howells, *Nature* **174,** 549 (1954).

[77] Y. Xu, W. Jäger, M. C. L. Gerry, and I. Merke, *J. Mol. Spectrosc.* **160,** 258 (1993).

[78] Gaussian 03 Revision D.01, M. J. Frisch, G. W. Trucks, H. B. Schlegel, G. E. Scuseria, M. A. Robb, J. R. Cheeseman, J. A. Montgomery, Jr., T. Vreven, K. N. Kudin, J. C. Burant, J. M. Millam, S. S. Iyengar, J. Tomasi, V. Barone, B. Mennucci, M. Cossi, G. Scalmani, N. Rega, G. A. Petersson, H. Nakatsuji, M. Hada, M. Ehara, K. Toyota, R. Fukuda, J. Hasegawa, M. Ishida, T. Nakajima, Y. Honda, O. Kitao, H. Nakai, M. Klene, X. Li, J. E. Knox, H. P. Hratchian, J. B. Cross, V. Bakken, C. Adamo, J. Jaramillo, R. Gomperts, R. E. Stratmann, O. Yazyev, A. J. Austin, R. Cammi, C. Pomelli, J. W. Ochterski, P. Y. Ayala, K. Morokuma, G. A. Voth, P. Salvador, J. J. Dannenberg, V. G. Zakrzewski, S. Dapprich, A. D. Daniels, M. C. Strain, O. Farkas, D. K. Malick, A. D. Rabuck, K. Raghavachari, J. B. Foresman, J. V. Ortiz, Q. Cui, A.

G. Baboul, S. Clifford, J. Cioslowski, B. B. Stefanov, G. Liu, A. Liashenko, P. Piskorz, I. Komaromi, R. L. Martin, D. J. Fox, T. Keith, M. A. Al-Laham, C. Y. Peng, A. Nanayakkara, M. Challacombe, P. M. W. Gill, B. Johnson, W. Chen, M. W. Wong, C. Gonzalez, J. A. Pople, *Gaussian 03* (Gaussian, Inc., 340 Quinnipiac Street, Building 40, Wallingford, CT, 06492, 2003), copyright © 1994-2003.

[79] W. C. Bailey, Calculation of Nuclear Quadrupole Coupling Constants in Gaseous State Molecules, URL: http://web.mac.com/wcbailey/nqcc/.

[80] A. D. Becke, *J. Chem. Phys.* **104,** 1040 (1996).

[81] C. Adamo and V. Barone, *Chem. Phys. Lett.* **274,** 242 (1977).

[82] A. Schäfer, C. Huber, and R. Ahlrichs, *J. Chem. Phys.* **100,** 5829 (1994).

[83] W. C. Bailey and F. M. Gonzalez, *J. Mol. Struct.* **651,** 689 (2002).

[84] A. D. Becke, *J. Chem. Phys.* **98,** 5648 (1993).

[85] J. P. Perdew and Y. Wang, *Phys. Rev. B* **45,** 13244 (1992).

[86] W. C. Bailey, *Chem. Phys.* **252,** 57 (2000).

[87] C. C. Costain, *Trans. Am. Crystallogr. Assoc.* **2,** 157 (1966).

[88] U. Spoerel, H. Dreizler, and W. Stahl, *Z. Naturforsch. Teil A* **49,** 645 (1994).

[89] C. H. Townes and B. P. Dailey, *J. Chem. Phys.* **17,** 782 (1949).

[90] A. E. Reed, R. B. Weinstock, and F. Weinhold, *J. Chem. Phys.* **83,** 735 (1985).

[91] K. M. Sinnott, *J. Chem. Phys.* **34,** 851 (1961).

[92] H. Karlsson, *J. Mol. Struct.* **33,** 227 (1976).

[93] F. Mata and J. Pérez, *Spectrochimica Acta* **40a,** 109 (1984).

[94] L. P. Thomas, N. S. True, and R. K. Bohn, *J. Phys. Chem.* **82,** 480 (1978).

[95] J. R. Durig, R. Kenton, H. V. Phan, and T. S. Little, *J. Mol. Struct.* **247,** 237 (1991).

[96] J. McMurry, *Organic Chemistry* (Brooks/Cole-Thomson Learning, California, 2004), 6th Edition.

[97] A. M. Ronn and R.C. Woods III, *J. Chem. Phys.* **45,** 3831 (1966).

[98] A. M. Ronn and E. B. Wilson, Jr., *J. Chem. Phys.* **46,** 3262 (1967).

[99] A. P. Cox, A. D. Couch, K. W. Hillig II, M. S. LaBarge, and R. L. Kuczkowski, *J. Chem. Soc. Faraday Trans.* **87,** 2689 (1991).

[100] J. -U. Grabow, W. Stahl, and H. Dreizler, *Rev. Scient. Instrum.* **67,** 4072 (1996).

[101] K. C. Etchison, C. T. Dewberry, K. E. Kerr, D. W. Shoup, and S. A. Cooke, *J. Mol. Spectrosc.* **242,** 39 (2007).

[102] P. Pyykkö, *Mol. Phys.* **99,** 1617 (2001).

[103] J. Hoeft, *Z. Naturforsch. Teil A* **20,** 313 (1965).

[104] J. Hoeft, F. J. Lovas, E. Tiemann, R. Tischer, and T. Törring, *Z. Naturforsch. Teil A* **24,** 1222 (1969).

[105] A. N. Murty and R. F. Curl, Jr., *J. Mol. Spectrosc.* **30,** 102 (1969).

[106] J. Hoeft, F. J. Lovas, E. Tiemann, and T. Törring, *J. Chem. Phys.* **53,** 2736 (1970).

[107] R. Honerjäger and R. Tischer, *Z. Naturforsch. Teil A* **32,** 1 (1977).

[108] A. Laaksonen and R. E. Wasylishen, *J. Am. Chem. Soc.* **117,** 392 (1995).

[109] W. H. Flygare, *Chem. Rev.* **74,** 653 (1974).

[110] C. T. Dewberry, K. C. Etchison, G. S. Grubbs II, R. A. Powoski, M. M. Serafin, S. A. Peebles, and S. A. Cooke, *J. Mol. Spectrosc.* **248,** 20 (2008).

[111] N. F. Ramsey, *Phys. Rev.* **78,** 699 (1950).

[112] T. D. Gierke and W. H. Flygare, *J. Am. Chem. Soc.* **94,** 7277 (1972).

[113] W. H. Flygare and J. Goodisman, *J. Chem. Phys.* **49,** 3122 (1968).

[114] H. S. P. Müller and M. C. L. Gerry, *J. Chem. Phys.* **103,** 577 (1995).

[115] G. H. Fuller, *J. Phys. Chem. Ref. Data* **5,** 835 (1976).

[116] L. Bizzocchi, B. M. Giuliano, M. Hess, and J.-U. Grabow, *J. Chem. Phys.* **126,** 114305 (2007).

[117] R. E. Wasylishen, D. L. Bryce, C. J. Evans, and M. C. L. Gerry, *J. Mol. Spectrosc.* **204,** 184 (2000).

[118] G. Audi, A. H. Wapstra, and C. Thibault, *Nucl. Phys. A* **729,** 337 (2003).

[119] E. Tiemann, H. Arnst, W. U. Stieda, T. Törring, and J. Hoeft, *Chem. Phys.* **67,** 133 (1982).

[120] H. W. Kroto, J. R. Heath, S. C. O'Brien, and R. E. Smalley, .

[121] R. D. Suenram, F. J. Lovas, and K. Matsumura, *Astrophys. J. Lett.* **342,** L103 (1989).

[122] D. A. Helms, M. Winnewisser, and G. Winnewisser, *J. Phys. Chem. A* **84,** 1758 (1980).

[123] N. Bandowski, W. Zyrnicki, and J. Borkowska-Burnecka, *J. Phys. B* **20,** 531 (1987).

[124] K. Ziebarth, K. D. Setzer, O. Shestakov, and E. H. Fink, *J. Mol. Spectrosc.* **191,** 108 (1998).

[125] J. M. Brown, J. T. Hougen, K.-P. Huber, J. W. C. Johns, I. Kopp, H. Lefebvre-Brion, A. J. Merer, D. A. Ramsay, J. Rostas, and R. N. Zare, *J. Mol. Spectrosc.* **55,** 500 (1975).

[126] S. Saito, Y. Endo, and E. Hirota, *J. Mol. Spectrosc.* **94,** 199 (1982).

[127] M. Tanimoto, S. Saito, Y. Endo, and E. Hirota, *J. Mol. Spectrosc.* **103,** 330 (1984).

[128] L. Bizzocchi, D. Esposti, and P. Botschwina, *J. Chem. Phys.* **113,** 1465 (2000).

[129] P. Botschwina, M. Horn, S. Seeger, and J. Flügge, *Mol. Phys.* **78,** 191 (1993).

[130] P. Botschwina and J. Flügge, *Chem. Phys. Lett.* **180,** 589 (1991).

[131] M. Colmont, G. Wlodarczak, D. Priem, H. S. P. Müller, E. H. Tien, R. J. Richards, and M. C. L. Gerry, *J. Mol. Spectrosc.* **181,** 330 (1997).

[132] J. Demaison, G. Wlodarczak, H. Rück, K. H. Wiedenmann, and H. D. Rudolph, *J. Mol. Struct.* **376,** 399 (1996).

[133] M. L. Guennec, G. Wlodarczak, J. Burie, and J. Demaison, *J. Mol. Spectrosc.* **154,** 305 (1992).

[134] M. L. Guennec, J. Demaison, G. Wlodarczak, and C. J. Marsden, *J. Mol. Spectrosc.* **160,** 471 (1993).

[135] H. S. Tam, J.-I. Choe, and M. D. Harmony, *J. Phys. Chem. A* **95,** 9267 (1991).

[136] M. D. Harmony, *J. Chem. Phys.* **93,** 7522 (1990).

[137] P. Botschwina, P. Sebald, M. Bogey, C. Demuynck, and J.-L. Destombes, *J. Mol. Spectrosc.* **153,** 255 (1992).

[138] C. D. Esposti, P. G. Favero, S. Serenellini, and G. Cazzoli, *J. Mol. Struct.* **82,** 221 (1982).

[139] P. Botschwina and S. Seegar, *J. Mol. Struct.* **320,** 243 (1994).

[140] T. Suzuki and E. Hirota, *J. Chem. Phys.* **88,** 6778 (1988).

[141] M. Nakata, K. Kohata, T. Fukuyama, K. Kuchitsu, and C. J. Wilkins, *J. Mol. Struct.* **68,** 271 (1980).

[142] J. Demaison, A. Perrin, and H. Bürger, *J. Mol. Spectrosc.* **221,** 47 (2003).

[143] Y. Kawashima and A. P. Cox, *J. Mol. Spectrosc.* **72,** 423 (1978).

[144] C. Puzzarini, G. Cazzoli, L. Dore, and A. Gambi, *Phys. Chem. Chem. Phys.* **3,** 4189 (2001).

[145] E. Hirota, *J. Mol. Spectrosc.* **71,** 145 (1978).

[146] M. M. Law, J. L. Duncan, and I. M. Mills, *J. Mol. Struct.: THEOCHEM* **260,** 323 (1992).

[147] F. Tamassia, C. D. Esposti, L. Dore, and G. Cazzoli, *J. Mol. Spectrosc.* **174,** 59 (1995).

[148] R. J. Berry and M. D. Harmony, *Struct. Chem.* **1,** 49 (1990).

[149] N. Zvereva-Loëte, J. Demaison, and H. D. Rudolph, *J. Mol. Spectrosc.* **236,** 248 (2006).

[150] R. W. Cavis and M. C. L. Gerry, *J. Mol. Spectrosc.* **109,** 269 (1985).

[151] G. Graner, *J. Mol. Spectrosc.* **90,** 394 (1981).

[152] S. Carter, I. M. Mills, and N. C. Handy, *J. Chem. Phys.* **97,** 1606 (1992).

[153] J. Demaison, G. Wlodarczak, H. Rück, K. H. Wiedenmann, and H. D. Rudolph, *J. Mol. Struct.* **376,** 399 (1996).

[154] M. L. Guennec, G. Wlodarczak, W. D. Chen, R. Bocquet, and J. Demaison, *J. Mol. Spectrosc.* **153,** 117 (1992).

[155] D. Priem, J. Cosléou, J. Demaison, I. Merke, W. Stahl, W. Jerzembeck, and H. Bürger, *J. Mol. Spectrosc.* **191,** 183 (1998).